

Creating a 4D Printing Toolkit by Comparing the Printing Parameters of Print Patterns and Infill Density

A Thesis Submitted for the Degree of Doctor of Philosophy

By

Seokwoo Nam

*Department of Design
College of Engineering, Design and Physical Sciences
Brunel University London*

September 2023

Declaration

I hereby declare that I am the sole author of this thesis. The work in this thesis was carried out following the university's regulations for a Ph.D., and it is the result of my own investigations and evaluations except where otherwise indicated by specific references in the text. I can confirm that this work has not previously been accepted for any degree nor is it currently submitted and under consideration for any other academic award.

Seokwoo Nam

September 2023

Acknowledgements

I would like to express my sincere gratitude to my principal supervisor, Dr Eujin Pei, for his generous support and valuable recommendations. His enduring encouragement and his practical advice have been an inestimable source of support for me during this process. I would also like to thank Dr Busayawan Lam and Dr Timothy Minton for their advice and feedback. Their varied perspectives have helped me strengthen my work.

Thank you to Kim who shared this journey with me. Finally, thank you to all of my Ph.D. colleagues and mentors who gave their time and provided me with insights into their experiences.

Abstract

Four-dimensional printing (4DP) has shown a rapid advancement in AM. 4DP is described by the formula of 3D printing + time. It is an active and dynamic printing system in which shape, structure, colour, etc., can spontaneously deform according to the appropriate environment, materials, and time sequence (Pugliese et al., 2022). These 4DP is a new technology that needs to be developed. Since most scholars' research is focused on scientific theories and more technical aspects, research on print control and the usefulness of extracting effective print is very limited and fragmented. This study identifies the optimal ways in which to control the printing parameters of the material extrusion to ensure the widespread use of 4DP. It establishes a design guideline for 4DP by providing a basis for achieving user-intended shape deformation and restoration or more complex shape deformation. This study aims to achieve the most predictable and accurate shape deformation and restoration, which is achieved by identifying the types and characteristics of the various backgrounds and knowledge related to 4DP as well as the shape-changing behaviours and printing parameters that can be implemented in 4DP through conducting a literature review. Furthermore, various Shape Memory Effects (SMEs) are discovered such as shape recovery time and shape recovery quality through water bath experiments. In addition, based on the numerical data derived for SMEs, this research also proposes a toolkit for controlling systematic 4DP SMEs. This study investigates how polylactic acid, a shape memory polymer, can be programmed by manipulating its parameters in the slicing step. For this purpose, a water bath experiment is used to show the influence of the printing pattern, infill density, and recovery temperature on printed parts' bending shape recovery quality and the shape recovery rates. The printing parameter experiment proves that the shape recovery quality and shape recovery time can be controlled by the material's characteristics and the printing parameters. The printing parameter control method proposed in this thesis can guide the design and application intended by researchers and designers through easy accessibility and usability. In addition, 4DP-related theoretical knowledge, tools, methods and results presented in this research can be utilized to generate new research results or to develop new applications and suggest guidelines for the proper use of 4DP, saving time and money. This discovery allows researchers, designers, and engineers to develop their work using optimal printing parameters with minimal trial and error and expand it to new applications. It can also serve as a cornerstone for the application of these results to many Additive Manufacturing technologies and industries.

Keywords: Additive Manufacturing; 4D Printing; Polylactic acid; Shape-Memory Effect; Printing parameters; Material extrusion

Table of Contents

DECLARATION.....	I
ACKNOWLEDGEMENTS	II
ABSTRACT	III
TABLE OF CONTENTS	IV
LIST OF FIGURES.....	XII
LIST OF TABLES	XV
Chapter 1. Introduction and Overview	13
1.1 Introduction	13
1.2 Research Aims, Questions, and Objectives	15
1.2.1 Research Questions	15
1.2.2 Research Objectives	15
1.3 Thesis Structure	16
1.4 Chapter Summary	20
Chapter 2. Literature Review.....	21
2.1 Introduction	21
2.2 Additive Manufacturing and 4DP	21
2.2.1 An Overview of Additive Manufacturing	21
2.2.2 4DP	22
2.2.3. Using the 4DP Process for Shape-Changing Behaviours.....	23
2.2.4 Current Applications of 4DP	25
2.3 Shape Memory Polymers (SMPs)	30
2.3.1 Overview of SMP	30
2.3.2 Characteristics of SMPs	31
2.3.3 Stimuli and SMEs.....	32
2.3.4 The SME Process in 4DP	33
2.4 Shape Change through 4DP.....	35
2.4.1 Basic Shape-Changing Behaviours	37
2.4.2 Complex Shape-Changing Behaviours.....	42

2.4.3 Combination Shape-Changing Behaviours	44
2.4.4 A Taxonomy of Shape-Changing Behaviours.....	45
2.5 4DP Parameters of the Shape Change Effect	48
2.6 Chapter Summary	51
Chapter 3. Research Methodology.....	52
3.1 Introduction	52
3.2 Research Methods	55
3.2.1 Literature Review	56
3.2.2 Experimental Work 1	56
3.2.3 Experimental Work 2	59
3.2.4 Questionnaires, and Surveys	60
3.2.5 Validation	60
3.3 Chapter Summary.....	60
Chapter 4. Study One: Evaluating Material Selection.....	62
4.1 Introduction	62
4.2 Determining SMEs and Measurement Criteria	62
4.2.1 Determining SMEs	62
4.2.2 Measurement Criteria	63
4.3 Material Selection.....	64
4.3.1 An Overview of the Examination of the Selected Filaments	64
4.3.2 Comparison of the 16 PLA filaments	66
4.3.3 The Recovery Quality of the Filaments.....	70
4.3.4 Recovery Time Results.....	71
4.4 Chapter Summary	75
Chapter 5. Study Two: The 3D-Printed PLA Samples and Parameter Experiment	76
5.1 Introduction	76
5.2 The 3D-Printed PLA Samples	76
5.2.1 An Overview of the Selected Filaments	76
5.2.2 Comparison of the 3D-Printed PLA Samples	77
5.2.3 The 3D-Printed PLA Samples' Recovery Rates	78

5.3 Testing the Printing Parameters.....	79
5.3.1 An Overview of the Printing Parameters Experiment.....	79
5.3.2 Comparison of the Printed Parts.....	80
5.3.3 Comparison of Weight according to Infill Density	85
5.3.4 The Application of Different Properties.....	87
5.4 Chapter Summary.....	89
Chapter 6. Evaluation the influence of print pattern and infill density	91
6.1 Introduction	91
6.2 Print Patterns and Infill Densities.....	92
6.2.1 An Overview of Print Patterns and Infill Densities.....	92
6.2.2 Comparison of the 12 Patterns and five Infill Densities.....	94
6.2.3 Recovery Quality and Recovery Times in Different Print Patterns and Infill Densities	99
6.2.4 The Results and the Development of a 4DP Tool	114
6.2.5 Repeated experiment	115
6.3 Chapter Summary.....	117
Chapter 7. Design and Development of Toolkit.....	119
7.1 Introduction	119
7.2 Graphic Representation of the Results	119
7.3 The Initial 4DP Web Toolkit.....	123
7.3.1 Scenario	123
7.3.2 The 4DP Web Toolkit	125
7.4 The Finalisation of the 4DP Web Toolkit	126
7.4.1 The Questionnaire	126
7.4.2 Results from the Questionnaire	127
7.4.3 Scenario	134
7.4.4 The Final 4DP Web Toolkit	135
7.5 Chapter Summary.....	137
Chapter 8. Conclusion.....	139
8.1 Introduction	139

8.2 Summary of Work to Answer the Research Questions	139
8.3 Contributions of the Research	143
8.4 Limitations of the Research	145
8.5 Recommendations for Further Research	145
References	147
Appendix I. BREO Acceptance Letter	156
Appendix II. Participation Information Sheet.....	157
Appendix III. 4D Printing web toolkit (Final version).....	159
Appendix IV. List of Publications	173

List of Figures

Chapter 1

Figure 1-1. Key research questions and objectives	16
Figure 1-2. The structure of the thesis	19

Chapter 2

Figure 2-1. Definition of 4DP technology	22
Figure 2-2. Fundamental elements of 4DP (Farhang et al., 2017) and the influence of 4DP elements (Nam & Pei, 2019)	23
Figure 2-3. The shape-changing behaviour process in 4DP	24
Figure 2-4. Setting the parameters of slicing software	25
Figure 2-5. General breakdown of the steps and popular applications used in 4DP (Alsheby et al., 2021; Rayate et al., 2018)	26
Figure 2-6. A smart valve created using 4DP (Bakarich et al., 2015).....	27
Figure 2-7. Tracheal fixation stent made of biomedical PLA (Zarek et al., 2017)	27
Figure 2-8. The design of the shape-changing pasta created using 3DP (Wang & Yao, 2017)	28
Figure 2-9. Structures with smart hinges (Farhang et al., 2017; Ge et al, 2014; Tolley et al. 2014).....	28
Figure 2-10. Multiple material tessellations resulting in different shape-shifting materials (Kim et al., 2012; Wu et al., 2016)	29
Figure 2-11. Desolvation-induced flower-shaped grippers using non-active materials (Zhao et al., 2017).....	29
Figure 2-12. Origami of the hollow platonic solids. (a) Tetrahedron; (b) octahedron (Jian et al., 2022).....	30
Figure 2-13. Representation of the types of materials used for 4DP. (Ahmed et al., 2021) ...	32
Figure 2-14. A categorisation of SRMs (Sun et al., 2012)	33
Figure 2-15. Schematic representation of one-way, two-way and multi-way SME.....	34
Figure 2-16. The processes involved in SMEs (Nam & Pei, 2020)	35
Figure 2-17. An example of folding (Tibbits., 2014)	37
Figure 2-18. An example of bending (Wu et al., 2016)	38
Figure 2-19. The difference between folding, bending, rolling, and multiple rolling.....	38
Figure 2-20. An example of rolling (Ge et al., 2013).....	39
Figure 2-21. An example of twisting (Wang & Yao, 2017).....	39
Figure 2-22. The difference between twisting and helixing (Forterre et al, 2011).....	40
Figure 2-23. An example of helixing (Zhang et al., 2016).....	40
Figure 2-24. An example of buckling (van Manen et al., 2018)	41
Figure 2-25. An example of curving (Tibbits, 2014)	41
Figure 2-26. An example of topographic change (Hu et al., 2017).....	41
Figure 2-27. An example of expansion and contraction (Bakarich et al., 2015).....	42
Figure 2-28. An example of waving (Wu et al., 2016).....	42
Figure 2-29. An example of curling (Tibbits, 2014)	43
Figure 2-30. An example of multiple folding (Mao et al., 2015).....	43
Figure 2-31. An example of multiple curving (Tibbits, 2014)	43
Figure 2-32. An example of bending, twisting, and wrinkling (Ge et al., 2013)	44
Figure 2-33. An example of expansion and contraction, twisting, and bending (Teunis et al., 2017).....	44

Figure 2-34. An example of hierarchical structures (Chen et al., 2016)	45
Figure 2-35. A taxonomy of shape-changing behaviours (Nam & Pei, 2019).....	46
Figure 2-36. A matrix of shape-changing behaviours and types of deformations in 4DP.	47
Figure 2-37. The different parameters of 4DP	50
Figure 2-38. The elements of essential shape-changing behaviours in 4DP	51

Chapter 3

Figure 3-1. The initial PLA experiment process	57
Figure 3-2. The experimental facilities	58
Figure 3-3. The process of the water bath experiments.....	59
Figure 3-4. The in-depth PLA experiment process	60

Chapter 4

Figure 4-1. The processes involved in the SME.....	63
Figure 4-2. The filament recovery grade measurement criteria	63
Figure 4-3. The PLA specimen recovery grade measurement criteria	64
Figure 4-4. The processes involved in the SME.....	65
Figure 4-5. The process for the material selection experiment	65
Figure 4-6. The 16 different PLA samples	66
Figure 4-7. The filaments' bending recovery grades and time taken	68
Figure 4-8. The filaments' bending recovery grades.....	70
Figure 4-9. The filaments' recovery times.	72
Figure 4-10. The filaments' recovery rates.	74
Figure 4-11. The recovery rates of D and N.....	74

Chapter 5

Figure 5-1. The experiment setup and prepared 3D printed PLA sample (a) Experiment setup (b) Deformed PLA sample (c) Test the sample	77
Figure 5-2. The process of the PLA sample experiment.	77
Figure 5-3. The 3D-printed PLA samples' bending recovery rates.	78
Figure 5-4. Comparison of material D's and N's bending recovery grades and times.	79
Figure 5-5. The process of the printing parameters experiment.....	80
Figure 5-6. Various infill densities between 5% and 100% (Carino et al.,2018).....	81
Figure 5-7. 0° and 90°build orientation. (a) concentric pattern (b) cross pattern.....	81
Figure 5-8. Recovery quality and time for the quarter cubic pattern	82
Figure 5-9. Recovery quality and time for the line pattern	83
Figure 5-10. Recovery quality and time for the concentric pattern.....	84
Figure 5-11. Recovery quality and time for the cross pattern	85
Figure 5-12 Sample weight measurement equipment according to infill density	86
Figure 5-13. The weight of each printed pattern	86
Figure 5-14. Comparison of fill density by build direction.....	87
Figure 5-15. Application of size, thickness, and proportions.....	87
Figure 5-16. The effects of size, thickness, and proportions on shape recovery quality and time	88

Chapter 6

Figure 6-1. The process for the printing parameters experiment	91
Figure 6.2. Example of variable infill density (Roger & Krawczak., 2015)	92

Figure 6-3. Infill densities from 20% to 100%.....	93
Figure 6-4. The 12 print patterns provided by Qidi Print.....	94
Figure 6-5. The bending recovery rates of 3D-printed PLA using 12 patterns.....	94
Figure 6-6. The process used to derive the SMEs.....	99
Figure 6-7. SMEs with an infill density of 20%.....	100
Figure 6-8. SMEs with an infill density of 40%.....	101
Figure 6-9. SMEs with an infill density of 60%.....	102
Figure 6-10. SMEs with an infill density of 80%.....	103
Figure 6-11. SMEs with an infill density of 100%.....	104
Figure 6-12 Recovery quality results based on temperatures of 65 °C, 70 °C, and 75°C.....	105
Figure 6-13. Recovery times based on temperatures of 65 °C, 70 °C, and 75 °C.....	107
Figure 6-14. The quality recovery rates of the 12 patterns and 5 infill densities at 65 °C, 70 °C, and 75 °C.....	109
Figure 6-15. The recovery times for the 12 patterns and 5 infill densities at 65 °C, 70 °C, and 75 °C.....	111
Figure 6-16. Simple results for the experiment on the 12 patterns and five infill densities..	113
Figure 6-17. The quality of shape recovery and recovery times according to printing parameters.....	115

Chapter 7

Figure 7-1. The results of the experiment on the impact of the 12 patterns and 5 infill densities.....	120
Figure 7-2. The patterns with the highest shape recovery rates.....	120
Figure 7-3. The patterns with intermediate shape recovery rates.....	121
Figure 7-4. The patterns with poor shape recovery rates.....	121
Figure 7-5. The patterns with the shortest recovery times.....	122
Figure 7-6. The patterns with the intermediate recovery times.....	122
Figure 7-7. The patterns with the longest recovery times.....	122
Figure 7-8. The physical version of the 4DP toolkit.....	123
Figure 7-9. Scenario 1: Without using the 4DP toolkit.....	124
Figure 7-10. Scenario 2: Using the 4DP toolkit.....	125
Figure 7-11. The initial version of the 4DP web toolkit.....	126
Figure 7-12. The results for question 1.....	127
Figure 7-13. The results for question 2.....	128
Figure 7-14. The results for question 3.....	128
Figure 7-15. The results for question 4.....	129
Figure 7-16. The results for question 5.....	130
Figure 7-17. The results for question 6.....	131
Figure 7-18 The results for question 7.....	132
Figure 7-19. The results for question 8.....	132
Figure 7-20. The results for question 9.....	133
Figure 7-21. The results for question 10.....	134
Figure 7-22. Final scenario: Using the 4DP web toolkit.....	135
Figure 7-23. The final version of the 4DP web toolkit _ before and after.....	136

Chapter 8

Figure 8-1. A summary of the experiments.....	141
Figure 8-2. The inputs, processes, outputs and outcomes of this research.....	142

Figure 8-3. Class on the Product Design Futures Invitational Lecture Series program (2021) at Bournemouth University in the UK	143
Figure 8-4. Material view with classes and object properties (Dimassi et al., 2021).....	144

List of Tables

Chapter 2

Table 2-1. 4D printing performance parameters	26
Table 2-2. Comparison of SMPs and SMAs (Liu et al., 2007)	30
Table 2-3. Mechanical analysis of each shape deformation (Nam & Pei, 2019)	36

Chapter 3

Table 3-1. Methodology for collecting and analysing the data..	53
--	----

Chapter 5

Table 5-1. Methodology for collecting and analysing the data..	80
--	----

Chapter 6

Table 6-1. Result of SMEs with an infill density of 20%...	100
Table 6-2. Result of SMEs with an infill density of 40%...	101
Table 6-3. Result of SMEs with an infill density of 60%...	102
Table 6-4. Result of SMEs with an infill density of 80%...	103
Table 6-5. Result of SMEs with an infill density of 100%...	104
Table 6-6. 12 sets repeated SMEs test results	117

Chapter 8

Table 7-1. Research questions and objectives defined for this research	139
--	-----

Chapter 1. Introduction and Overview

1.1 Introduction

Additive Manufacturing (AM), also called three-dimensional printing (3DP), is the process of creating a finished 3D object that is usually based on 3D model data by combining materials and adding layers (ISO/ASTM 52900, 2021). This technology continues to be explored in many areas, such as automotive and aerospace industries, engineering, medicine, biological systems, and food supply chains, because of its rapid fabrication, low cost, and ability to print parts with complex geometries. Recently, many countries have regarded AM technology as the fifth industrial revolution and put much effort into the development of AM (Gao et al., 2015; Li et al., 2022). As such, AM is recognised as an innovative technology that can be used in advanced manufacturing systems of the future. AM technology has made significant strides in processing a wide variety of materials, machines, and new applications that have the potential to change society, from everyday life to the global economy. AM has shown many advantages over traditional manufacturing strategies, including providing a wide range of design possibilities as well as minimal material consumption and personalisation when creating 3D objects (Queiroz et al., 2019).

In recent years, four-dimensional printing (4DP) has attracted attention as a new technology that can overcome the limitations of 3DP, and many studies are being attempted on this topic. According to Lee et al. (2017), the rapid development of AM and Shape Memory Materials (SMMs) has fuelled the growth of 4DP. 4D-printed parts can change their shape over time or when arbitrary environmental conditions are satisfied (Teoh et al., 2017). Current 3DP and one-way 4DP need human interaction in the programming stage. However, human interference will ultimately become obsolete in reversible or two-way 4DP as the programming stage will be substituted with another stimulus (Hernandez-Munoz et al., 2015). This means that the need for human interaction, sensors, and batteries will be eliminated, and, by using 4DP, more complex devices and parts can be produced through the correct external stimuli. In addition, since the understanding of SMMs and the design of AM has improved, it has recently been demonstrated that 4DP is feasible (Lee et al., 2017), and it offers a wide range of opportunities, such as self-assembly without the need to assemble separate parts. According to Choi (2022), even complex layout structures can be successfully fabricated without assembly requirements that are impossible with conventional manufacturing methods, and many applications are possible.

4D-printed parts can enable the construction of complex actuation devices and moving components, thereby eliminating sensors, mechanical parts, and batteries. The process of 4DP requires the use of smart materials, including shape memory alloys (SMAs) and shape memory polymers (SMPs). However, organic materials such as wood and paper can also be adapted as stimuli-responsive bio-composites (Nkomo, 2018). These SMMs can be programmed in a temporary form and then returned to their original shape by environmental stimuli without human involvement (Lei et al., 2019). In other words, combining smart materials with AM, known as 4DP, offers opportunities for the design and building of smart and active structures (Wu et al., 2016). Among AM materials, polymers in particular have been considered the most

common materials for AM technology due to their advantages, which include being their lightweight and corrosion resistant as well as having achievable mechanical, thermal, electrical, and fire resistance as well as biocompatibility properties (Tan et al., 2020). The shape memory polymer market size was USD 450.4 million in 2021 and will grow at a CAGR of 26.9% from 2022 to 2030, driven by increasing product demand in the automotive and aerospace sectors (Global market insights., 2022). With the development of 4DP technology, 4DP applications in the product design industry are expected to increase. In addition to medical, construction, and robotic applications of 4DP, many changes and developments can be expected in industrial design that could not be achieved with AM.

Moreover, due to the benefits of a simple manufacturing process and controllable Shape Memory Effects (SMEs), printed SMP parts have significant potential in 4DP applications (Wu et al., 2016). This thesis will focus on SMPs as they are more advantageous than SMAs because current technologies have made polymeric materials lighter and cheaper as well as providing them with a better recoverable strain than SMAs (Hornat et al., 2017; Lan et al., 2009). It is also expected that the widespread adoption of SMPs is more achievable than the adoption of SMAs, which typically involve more complex processes. Since SMPs are lightweight, they can be used for automobile, aerospace, and other applications, and they have a recoverable strain of up to 400% higher than SMAs (Hornat et al., 2017). This research provides answers to the research questions, and to contribute to new knowledge of the transformation of 4D Printed parts that can be achieved using SMPs. For example, using 4DP, different structures can be printed and activated at a certain time by external stimuli in order to transform them into fully deployed functional assemblies. To this end, in the design stage, designers and engineers need to recognise and understand the various shape change effects of 4DP parts. The selection of appropriate process parameters has a significant impact on the 3DP process. However, most of the related studies focus on the effect of process parameters on the mechanical properties of components, such as the tensile strength of parts as well as using chemical treatments, machining, heat treatment, and technical studies to improve quality. There are few studies on the effect of process parameters on SMEs. Therefore, this research provides a design direction that can predict the effect of shape change through a review of the bending deformation of 4DP parts when using polylactic acid (PLA) by combining appropriate printing parameters. This study proves that SMEs can be controlled, controlled and predicted by extracting data from various experiments, classifying it by charting and graphing it, and analyzing it. The main experimental method used in this study is water bath experiments, which are used to evaluate the influence of the printing patterns, infill density, and recovery temperature on the shape-recovery quality and shape-recovery time of 3D-printed PLA. This study also addresses bending shape-changing behaviours, the structure that can be achieved through 4DP, and the ways in which to control the shape-changing effects using printing parameters. This research gives designers and engineers an understanding of the potential of formative behaviours that can be realised using 4DP. This knowledge will allow designers and engineers to better implement appropriate design strategies in order to control configuration change behaviour through mechanical analysis. In addition, it can reduce time and cost, thereby ensuring more specific results.

1.2 Research Aims, Questions, and Objectives

This research aims to propose method for designing effective 4DP parts. It also focuses on deepening the understanding of the ways in which SMEs can be influenced through material extrusion print patterns, infill densities, and temperature. Raviv et al. (2014) found that a careful design process for control of slicing parameters can improve the accuracy of 4D-printed parts. In addition, suitably chosen build parameters can improve the printing characteristics of the components and the related functions that have been created. Therefore, applying optimal parameters is important when designing 4D-printed parts (Türk et al., 2017). However, most of 4D printing research focus on the influence of process parameters on the mechanical properties of components, such as chemical treatment, machining, heat treatment, and technical studies for quality improvement, as well as studies on the tensile strength of parts. There are few guidelines to study printing parameters to control the SMEs and apply it to effective 4DP part design. Moreover, there are insufficient studies on the tuneable printing parameter factors and the SMEs of various factor combinations. Therefore, this research will specifically investigate, in multiple experiments, the ways in which SMPs' printing parameters can be programmed to control the expected SMEs. Figure 1-1 shows the research questions of this study and the research objectives.

1.2.1 Research Questions

The application of printing parameters to control the SMEs starts with detailing the technical knowledge of 4DP and then moves to an analysis of the SMP status, the types of shape-changing behaviours that can be implemented using the SMEs of SMPs, the various types of printing parameters, and the shape analysis of the parameters affecting the SMEs. Therefore, the three key aspects to be investigated in this study are as follows:

- 4DP and SMPs;
- Shape-changing behaviours; and
- Printing parameters.

Each research question aims to provide overall 4DP knowledge to increase the accessibility and usability of 4DP and is an important question element necessary to expand into SME control methods, such as guidelines for designing desired 4DP designs. Based on these three key aspects, the research questions for this study are as follows:

- Q1) What is the status of the use of SMP in 4DP?
- Q2) What AM processes and materials are suitable for using SMPs to enable 4DP?
- Q3) What types of shape-changing behaviours can be achieved using SMPs for 4DP?
- Q4) What SMP is suitable for shape-changing behaviours that are achieved through altering the printing parameters?
- Q5) How are the SMEs affected by the printing parameters?
- Q6) How can the printing parameters be controlled in order to ensure effective 4DP and shape-changing behaviours?

1.2.2 Research Objectives

- 1) To analyse the present state and technology of 4DP.

- 2) To analyse the present state of 4D-printed SMPs.
- 3) To understand how shape-changing behaviours can be achieved through printing parameters, and to examine and classify the different types of shape-changing behaviours of 4DP parts in the form of a taxonomy.
- 4) To compare the different types of PLA and determine the suitable PLA and printing parameters for 4DP parts.
- 5) To compare and combine different SMEs by controlling the printing parameters.
- 6) To propose methods for controlling suitable shape-changing effects, such as printing parameters, so as to design effective 4D-printed parts.

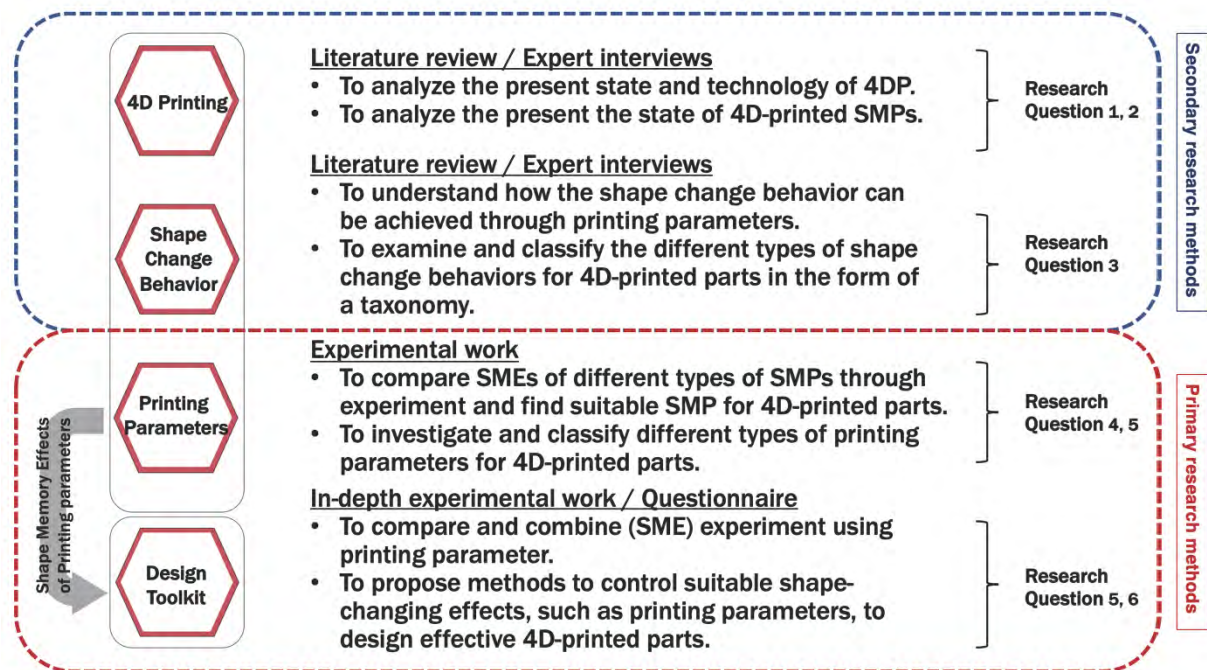


Figure 1-1. Key research questions and objectives.

1.3 Thesis Structure

This thesis is formatted in a manuscript and consists of seven chapters that are divided into four research phases: (1) research exploration and review; (2) experimental work; (3) development, revision, and evaluation; and (4) the conclusion.

(1) Research exploration and review

The research exploration and review phase consists of Chapters 1, 2, and 3, and it begins with collecting the theoretical knowledge about 4DP technology and processes, SMPs' characteristics and SMEs' processes, printing parameters and shape-changing behaviours that is contained in the literature such as published in academic journals including Scopus and Elsevier. These collected data will be used for the initial stage of analysis.

- Chapter 1. Introduction: In Chapter 1, the background, purpose, research questions, and rationale for this study are explained in detail. It also identifies the challenges facing current 4DP research and details the purpose of the research in the form of a flow chart.
- Chapter 2. Literature review: Chapter 2 provides an in-depth understanding of 4DP technology, SMPs, shape-changing behaviours, and printing parameters, which are the key

aspects of this research. This chapter details the current theoretical knowledge on 4DP technologies and processes, SMPs' characteristics and SMEs' processes, printing parameters, and shape-changing behaviours. In addition, the types of shape-changing behaviours that can be implemented by 4DP will be identified. Various types of shape-changing behaviours in 4DP parts will be investigated and classified in the form of taxonomy analysis.

- Chapter 3. Research methodology: Chapter 3 explains the methodological approach of the research, including the details of each study component and contribution to the research aim.

(2) Experimental work

The experimental work phase is explained in Chapters 4 and 5 and begins with investigating the SMEs of PLA using numerical data obtained through a water bath experiment. After this, the collected SMEs are analysed in order to provide an in-depth understanding of the research.

- Chapter 4. Study One: Evaluating material selection: Chapter 4 discusses how research objectives 4 and 5 will be achieved. The ways in which the materials used in the experiment are selected is explained, and the results of the shape-recovery effect according to the printing parameters are derived and analysed. Shape recovery data obtained through altering various printing parameters in water bath experiments are derived as numerical data. These numerical data are then applied to the developed criteria in order to prove the objectivity of the results.
- Chapter 5. Study Two: The 3D-Printed PLA samples and parameter experiment: In this chapter, an in-depth understanding of the study and the initial data obtained is detailed based on the results derived from the previous experiments. The results from the application of the selected materials and printing parameters on shape-recovery effects are analysed. This data is presented in a graph in order to improve access to the numerical information derived from the experiments.

(3) Development, revision, and evaluation

As an extension of Chapter 6 and Chapter 7 discusses the results obtained from a review of the literature, and it contains the development, results, evaluation, and conclusions.

- Chapter 6. Evaluating the influence of print pattern and infill density: In Chapter 6, aims to compare and combine various small and medium-sized enterprises by controlling the printing parameters selected based on previous experimental data and to propose a method to control appropriate shape change effects such as printing parameters to design effective 4D printed parts. Using the results derived from previous experiments, it performed detailed investigations on the main areas of this study to derive numerical data for various shape memory effects (SMEs).
- Chapter 7. Design and development of toolkit: In Chapter 7, a 4DP physical version of the 4DP toolkit and web toolkit is developed, modified, and evaluated in order to access the experimental results obtained in Chapter 6 and the information contained in the graph. This will also allow it to be used more extensively by an increased number of participants.

(4) Conclusion

- Chapter 8. Conclusion: Chapter 8 concludes the thesis by summarising the work and how the research objectives were met. This chapter also highlights each chapter's contribution to the field's knowledge, describes the research limitations, and suggests future avenues of research. This chapter concludes the research by comparing the key research findings against the aims and objectives. Figure 1-2 details the thesis's structure in detail.

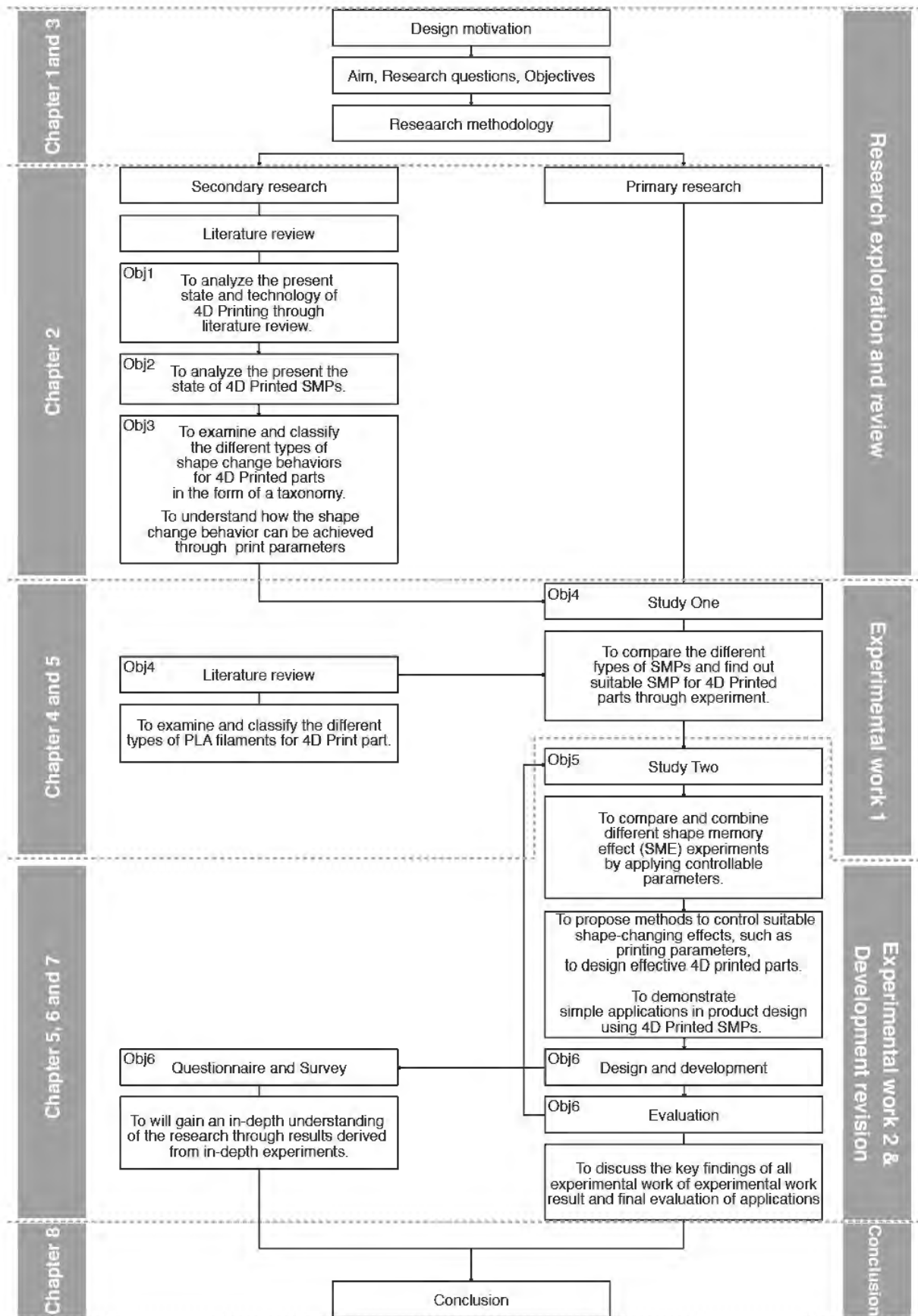


Figure 1-2. The structure of the thesis.

1.4 Chapter Summary

In this chapter, the background, aim, research questions, objectives, and rationale for this study were explained in detail. It also focused on material extrusion using SMP to derive the result of shape memory effect according to printing parameters and identified the challenges facing current 4DP research. The existing literature focuses on the processing parameters of the mechanical properties associated with 4DP technology. Recently, much research has been conducted to apply SMEs to objects by controlling printing parameters, such as that of Choi (2022) and Loh (2022). However, there are not on focusing on how to control the printing parameters. One of the challenges facing 4DP is the need for design and usability reference guidelines and a broad understanding of users' 4DP-related knowledge when designing effective 4D-printed parts. In order to solve this problem, systematic knowledge of shape changes, shape change effects according to shape change operations, and the direction that can affect the range of shape change effects is urgently needed.

The methods adopted in this study to answer the research questions and objectives were also discussed in this chapter. It also outlined the overall structure and outline of the thesis. The next chapter provides an overview of the classification, and it confirms the diversity of shape-changing behaviours by exploring and analysing 4DP technologies and processes, SMPs' properties and SMEs' processes, shape-changing behaviours, and printing parameters. This discussion includes the theoretical knowledge of these key aspects.

Chapter 2. Literature Review

2.1 Introduction

This study covers the vast and complex topics of four-dimensional printing (4DP) and material properties, shape-changing behaviours, and printing parameters. Since each of these concepts has been understood and developed through various academics' and practitioners' theories and experiences, it is essential to review the meaning and function of each concept in the form of a theoretical investigation and definition setting in a literature review. This literature review aims to achieve research objectives 1, 2, and 3. This chapter comprises four main parts. Section 2.2 reviews the working process of 4DP in order to identify comprehensive 4DP technologies, and it also lists the various applications of 4DP. Section 2.3 reviews the characteristics and provides an overview of shape memory polymers (SMPs) and stimuli in order to identify Shape Memory Effects (SMEs), and it also details the SME process that SMPs undergo in response to stimuli. Section 2.4 examines the shape changes identified in 4DP studies in order to comprehensively review the deformable shapes and structures achievable with 4DP, and it analyses the identified shape transformation behaviours and redefines them. This includes an explanation of the perceptions and influence of components on the shape-changing behaviours of 4D-printed parts, such as bending, twisting, folding, and the like, as well as an identification of the characteristics of the shape changes so as to provide an overview of SMPs and their various shape-changing behaviours. Lastly, Section 2.5 discusses the various parameters applicable to the various shape-changing methods. For example, in 4DP programming, the use of different printing patterns, building processes, and layering methods, such as the basic elements of 4DP, can affect the SMEs of 4D-printed parts.

2.2 Additive Manufacturing and 4DP

2.2.1 An Overview of Additive Manufacturing

Additive Manufacturing (AM) positively impacts technology-intensive industries, such as electronics, aviation, automobile, medical care, and education. In addition, it allows the creation of a collaborative culture that produces creative results online or in public production spaces. AM, which has been widely applied in this manner, is used to produce raw materials, parts, and products for manufacturing industries through the use of three-dimensional printing (3DP) technology. AM uses high-density heat sources to stack 3D computer-aided design (CAD) data into 3D geometric layers. In addition, AM is a technology that can produce low-cost and high-efficiency products compared to the existing manufacturing methods. AM uses methods such as directed energy deposition (DED), material extrusion (MEX), material jetting (MJT), power bed fusion (PBF), binder jetting (BJT), vat photopolymerization (VPP), and sheet lamination (SHL) to build solid 3D structures through the controlled deposition of materials in a series of successive layers (Han & Lee, 2020; ISO/ASTM 52900, 2021). Early AM technologies were developed by printing single parts as 3D objects and assembling them. Most AM processes today allow for the production of mechanically stable parts that are robust and static, which can be used to achieve the intended results. As a result, most of these parts are not designed to move or deform. Objects that require assembly are comprised of multiple

parts that are put together after production. Post-processing of separate parts requires certain tolerances and time to assemble them. However, 3D-printed objects have become more complex, and improved functional performance is being increasingly demanded due to the development of 4DP technology. By integrating disparate parts into a single product, objects with a wide range of properties and functions (e.g., mechanical, electrical, medical) can be rapidly manufactured (Mitchell et al., 2018).

2.2.2 4DP

4DP technology takes advantage of the rapid development of smart materials such as SMPs within the free-form, digital manufacturing process. 3DP technology and 4DP structures made of smart materials that used in 4DP have the property of restoring their original shape to stimuli such as heat, pressure, electrical activation, light, pH, and magnetic fields (Ali et al., 2019). Moreover, 4DP incorporates the concept of time. In other words, an object may change over a period of time depending on environmental stimuli (Figure 2-1). In AM, most machine build sizes must accommodate the surface area and volume of the part. However, this limitation does not apply to 4DP as large parts can be ‘folded’ or ‘compressed’, so that they can be printed according to the constraints of the machine bed. These shape changes are due to the mechanisms of AM technology and various actions that are dictated by the characteristics of smart materials. Therefore, it is necessary to understand the mechanisms in order to ensure the effective use of 4DP.

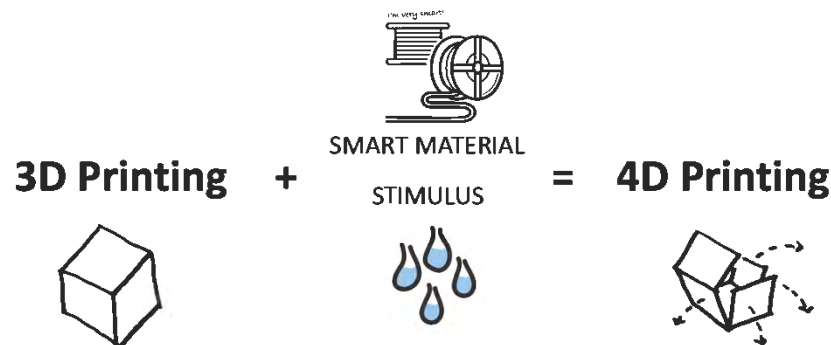


Figure 2-1. Definition of 4DP technology.

According to Farhang et al. (2017), the five fundamental elements of 4DP include the AM process, the stimuli, the stimuli-responsive materials (SRMs), CAD modelling, and the interaction mechanism. Figure 2-2 describes the fundamental elements of 4DP and the influence of 4DP elements. The first element, the AM process, can be defined as the initial stage of designing all or part of the 4D structure by considering smart materials and appropriate stimuli. This process is required for the production of freeform parts. The second element, the stimuli, is required to trigger the alterations in a 4D-printed structure’s shape, properties, functionality, and specifications. The stimuli used in 4DP to date include water, heat, ultraviolet (UV) radiation, pH levels, magnets, a combination of heat and light, a combination of water and heat, and more (Alsheby et al., 2021). Various types of stimuli can be used to initiate physical, chemical, or biological changes in a structure. For example, physical stimuli include light, magnetic fields, moisture, electrical energy, and temperature, while chemical stimuli

include changes in pH levels or the use of oxidizing or reducing agents. Biological stimuli, on the other hand, can be enzymes or glucose. When a stimulus is introduced, the resulting physical or chemical changes in the structure can lead to deformation, such as the relaxation of stress or the motion of molecules, or a phase change (Ahmed et al., 2021). In this study, the focus is on the physical stimulation of PLA, a smart material that responds to heat or temperature changes. The shape change in these materials upon thermal stimulation is primarily due to two mechanisms: the shape change effect (SCE) and the shape memory effect (SME) (Zhou et al., 2015). The third element is SRMs, which are able to return to their initial shape from a deformed state. It also refers to a reversible material that can spontaneously change its shape when stimuli are applied and that can restore its original shape when removed (Zhou & Sheiko, 2016). CAD modelling is the fourth element and is necessary for 4DP as it used to design the material distribution and structure, achieving the desired changes in shape, properties, or functionality. CAD modelling is needed to establish the connections between the four core elements of material structure, its desired final shape and material properties, and the stimuli. The last element, the interaction mechanism, is the programming process in which the material is deformed into a temporary shape. This includes the mechanisms of one-way SMEs using one shape recovery, two-way SMEs that recover shape after automatic shape changes, and multiple SMEs capable of multiple shape changes (Sienkiewicz and Szmeczyk, 2020). These five fundamental elements of 4DP greatly influence the properties of 4D-printed structures. A 4DP effect can be described in terms of the shape-changing behaviours, the resultant position, and the object's behavioural change over time. Shape-changing behaviours are the most basic condition of 4DP and are affected by all five elements of 4DP. Regardless of any type of 4DP, the shape-changing behaviours should be the first effect to be considered. The resultant recovery position can be further described as its deformation sequence and recovery quality. Time can be further divided into the SMEs' durations and the speeds of the change. The carefully calculated CAD modelling and print settings have a large influence on the time of SMEs. These three elements (i.e., shape-changing behaviours, position, and time) are expanded on in Farhang et al.'s (2017) study, which is described in Figure 2-2.

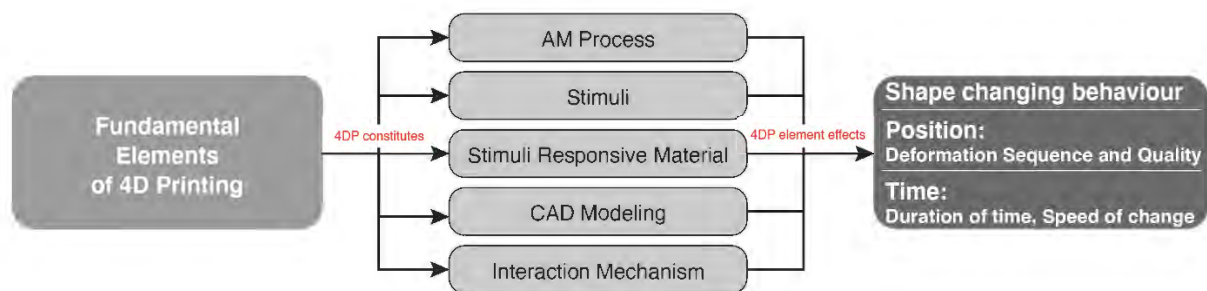


Figure 2-2. Fundamental elements of 4DP (Farhang et al., 2017) and the influence of 4DP elements (Nam & Pei, 2019).

2.2.3. Using the 4DP Process for Shape-Changing Behaviours

AM technology was developed in 1983 and has since seen rapid and wide-ranging applications. AM takes a digital 3D model and turns it into a physical object using CAD (Mitchell et al.,

2018). Single layers are successively added until the 3D structure is completed. This printed physical object is characterised by its inability to change its rigidity and shape like ordinary metal or plastic parts. ISO/ASTM52900, 2021 defines seven categories of the AM process: material extrusion, vat photopolymerisation, powder bed fusion, MJ, BJ, sheet lamination, and directed energy deposition. The technologies used in most 3DP enthusiasts' and consumer-focused products in the 2010s included fused filament fabrication (FFF) and FDM, also known as material extrusion. They demonstrate incredible benefits, such as rapid prototyping, low costs, high efficiency, flexibility, and sustainable manufacturing practices (Kumar et al., 2022). Therefore, this chapter describes the printing process and focuses on material extrusion technology, the process of which includes digital modelling, slicing, transmission to a 3D printer, and printing. The 4DP process is similar to the conventional AM process detailed in the workflow as it uses the same 3D printer, and the computer runs the same program to continuously deposit heated material in layers until a complete 3D structure is formed. However, the 4DP process is divided into seven steps (see Figure 2-3). The first step is the CAD modelling phase, which requires using 3D CAD software such as Solidworks and includes a consideration of the the geometry and the structural design. The second step entails saving the completed model in an STL file format as this as the standard file format recognised by most 3D printers. Thirdly, slicing software is required for the necessary machine specifications to be provided to the 3D printer in order to create a machine toolpath and its operating parameters. At this stage, care settings are required because the various parameters, such as print pattern, infill density, and temperature, can greatly influence shape-changing behaviours. As shown in Figure 2-4, the main parameters include infill density, print pattern, speed, and temperature. The fourth step in the 4DP process is saving the model that has been saved in a G-code file format, which provides the machine commands to the 3D printer in order to allow it to produce the object. The fifth step is sending the G-code file to the 3D printer together with a suitable SMPs material in order to start the printing process. In the sixth step, the physical object is printed and post-processed by, for example, removing support structures. Finally, the component is subjected to an external stimulus to change its shape. The printed object can change its shape into a different one according to the user's intention. An object whose shape has been changed will return to its original shape again due to an external stimulus.

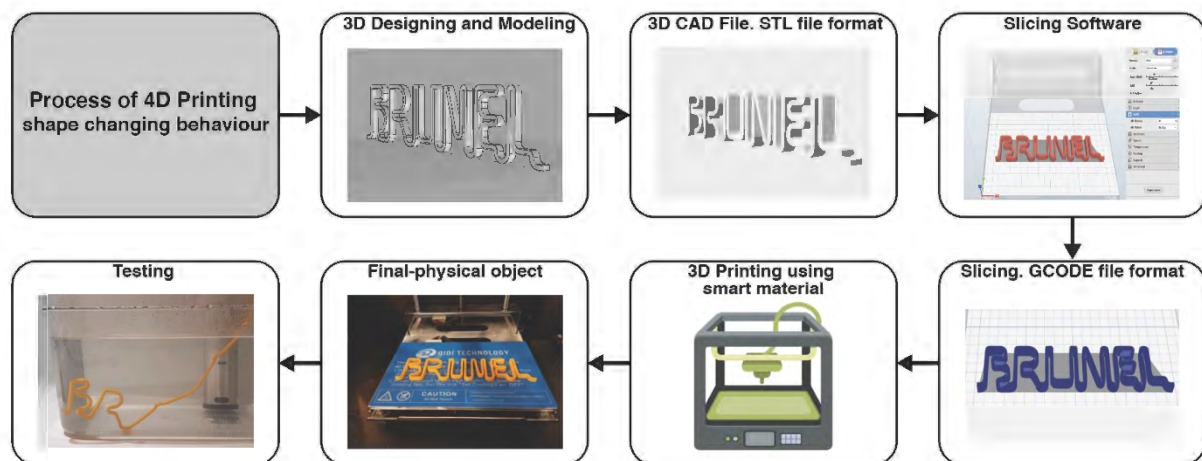


Figure 2-3. The shape-changing behaviour process in 4DP.

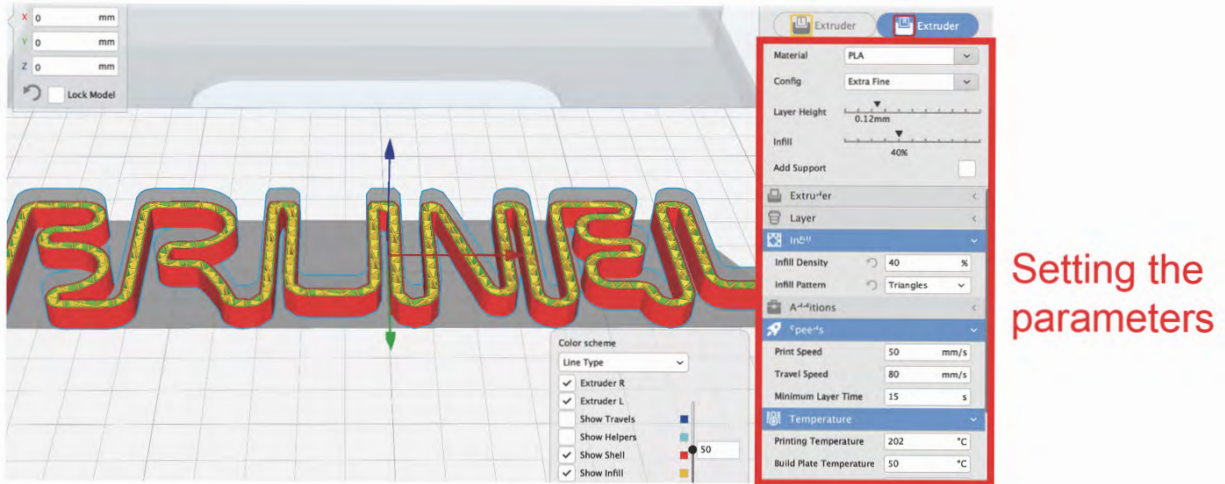


Figure 2-4. Setting the parameters of slicing software.

2.2.4 Current Applications of 4DP

For 4DP to be realized, printing methods, materials, stimuli, and SME actuation must be applied (Alshehly et al., 2021). There may also be some mathematical basis underlying the shape-changing effect. This interaction mechanism exposes the 4D printed structures to external stimuli, which can be shown based on mathematical modelling (Rayate et al., 2018). The printing methods, materials, and stimuli included in Figure 2-5 are not representative of all factors. In particular, less popular or expensive printing techniques and smart materials such as selective laser sintering (SLS), selective laser melting (SLM), layered object modelling (LOM), and direct energy deposition (DED) have not been presented. The choice of smart materials is endless, but the materials mentioned are the design's active parts or actuator parts. In addition, mathematical modelling in 4DP can be accompanied by several mathematical foundations to design essential changes in shape, final product properties or function, and distribution and propagation of different materials in a printed structure (Zhou et al., 2015). However, it can be used in many fields, even by applying some of the elements presented among all elements for 4DP implementation. In other words, 4DP has the potential to be applied in many applications due to its high manufacturing freedom and the use of SME materials. In particular, 4DP can be widely used in many industries that require a lot of technological advancements, such as biomedical, engineering, biomimicry, food and applied industries (XIA et al., 2021; Mallakpour et al., 2021; Mitchell et al., 2018; Mu et al., 2018; Baker et al., 2019). Figure 2-5 shows the five fundamentals of 4DP and their applications properly divided into five categories: biomedical, engineering, biomimicry, food and applied industries. A careful selection of options for each of the five main components can be applied and developed. In recent years, there have been advancements in 4DP applications, but there is still limited research on this topic. This section presents the reported applications of 4DP and the applicable printing structures.

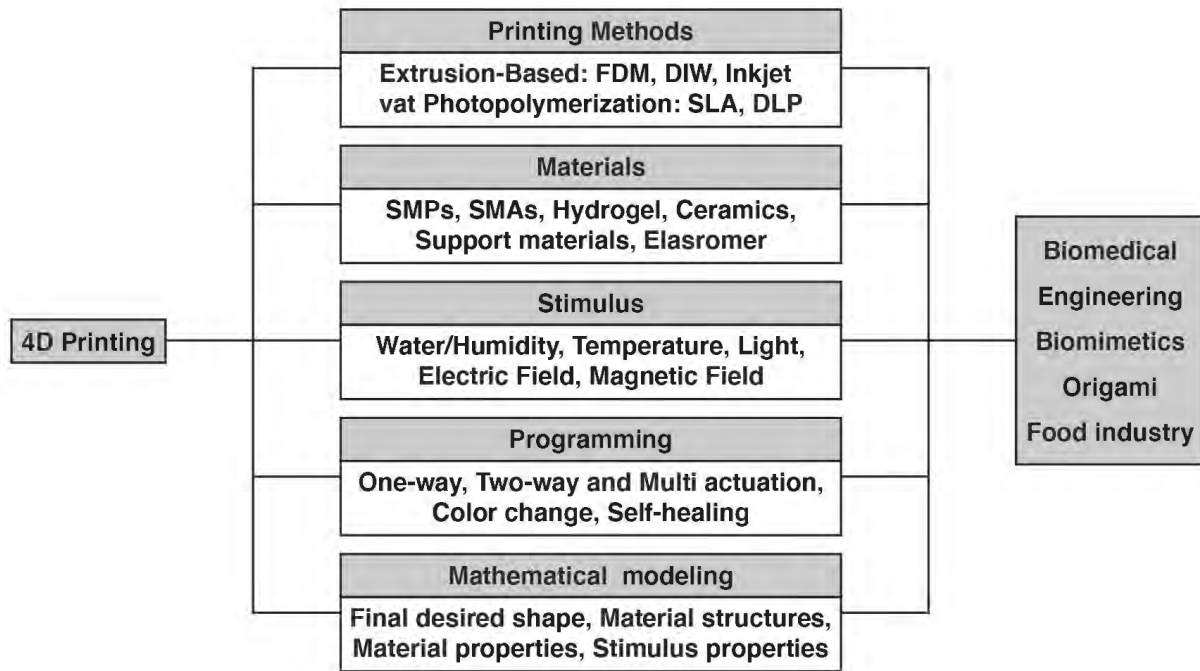


Figure 2-5. General breakdown of the steps and popular applications used in 4DP (Alsheblly et al., 2021; Rayate et al., 2018).

Table 2-1 below also specifies some factors that can affect 4DP in terms of performance parameters. 4DP performance parameters for 4D printing performance, quality, high practicality, and efficient shape change effect include time response, load response, and material durability. Some studies based on performance parameter aspects show the applicability of improved 4DP.

Table 2-1. 4D printing performance parameters.

Performance parameters	Literature paper	Finding
Time responses	Melocchi et al., 2019 Xin et al., 2020 Kim et al., 2021	‘Time response is an important factor in achieving the expansion of objects and changes in properties. In particular, the element of time was considered potentially important for changes in the properties of bulky objects.’
Loading responses	Monzón et al., 2017 Namvar et al., 2022 Serjouei et al., 2022 Xin et al., 2022	‘According to ASTM D790-07, the stress on the external surface can vary depending on the object's proportions. When the same displacement occurs, the load response of the specimen is significantly lower than that of the sample manufactured under high-temperature conditions, resulting in poor mechanical performance.’
Material durability	Senatov et al., 2016 Zhang et al., 2018 Maveas et al., 2022	‘The durability of 4D printing materials is enhanced through advances in stereolithography, chemical/structural modifications, fused deposition modelling, and digital liquid processing for multilayer/reinforcement applications. The

		durability dilemma and practical limitations of SMP development and application can be partially offset by the performance capabilities, quality, efficiency, and advantages of 4D printing over traditional manufacturing technologies.'
--	--	---

The team from the Australian Research Centre's Centre of Excellence for Electromaterials Science explained that shape memory materials (SMMs) can be transformed from their original form into other forms and can be adapted for use in a variety of engineering applications. Figure 2-6 shows a 4D-printed smart valve (Bakarich et al., 2015). The valve automatically closes when exposed to hot water, reducing flow by 95%, and it opens for cold water. With SMMs and CAD modelling, this 4DP technology can be easily extended to creating other types of moving structures.



Figure 2-6. A smart valve created using 4DP (Bakarich et al., 2015).

Figure 2-7 shows a tracheal fixation stent (Zarek et al., 2017). This stent was developed from polylactic acid (PLA) for biomedical use, and it is hard and soft and does not damage surrounding organs. It is inserted and fixed to the required structure through shape change and plays a role in expanding the organ (Alshehly et al., 2021). This structure can be easily and conveniently customised to the individual. Thus, 4DP has many possibilities in biomedicine.

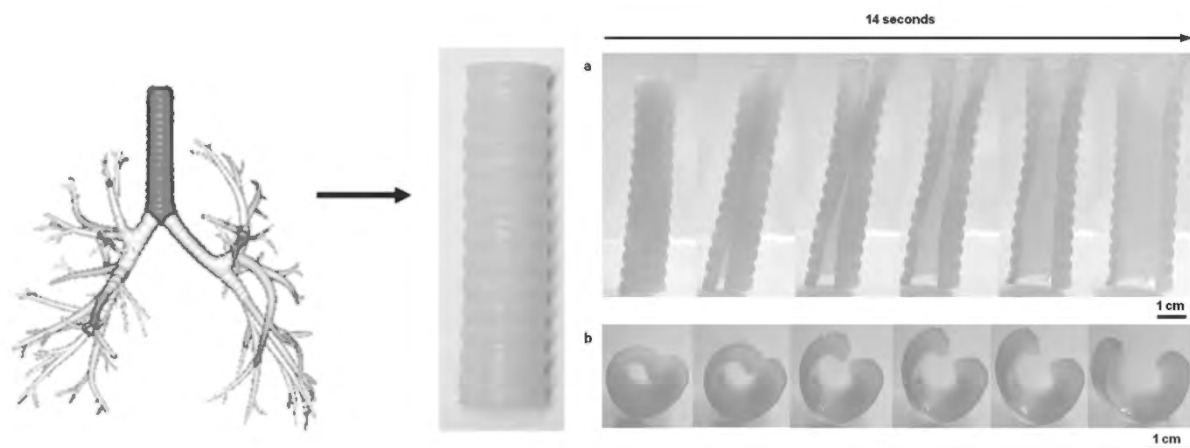


Figure 2-7. Tracheal fixation stent made of biomedical PLA (Zarek et al., 2017).

Attempts to use 4DP have also been made in the food industry. Shape transformations from two dimensions (2D) to 3D have provided methods for facilitating interactions with food.

Figure 2-8 shows that the Massachusetts Institute of Technology's (MIT's) Tangible Media Group has developed a new pasta that reacts in various ways, such as folding, when brought into contact with heat and water. Printed pasta is flat and can be shaped into various forms through many processes, including bending, folding, and drying, when boiled. To achieve this effect, Wang and Yao (2017) 3D-printed pieces of edible cellulose onto a layer of gelatine. This application of 3DP can save shipping costs and storage space as well as provide a new dining experience.

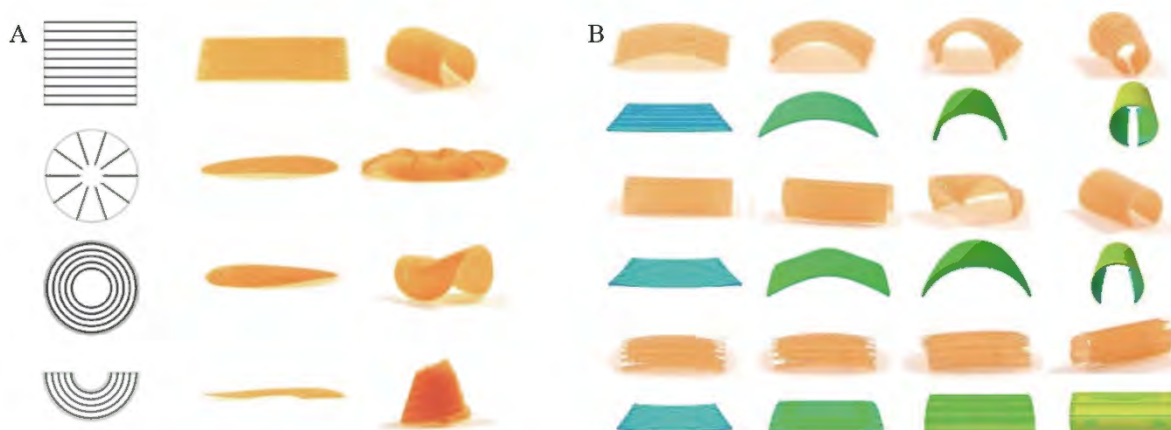


Figure 2-8. The design of the shape-changing pasta created using 3DP (Wang & Yao, 2017).

Mathematical modelling processes are associated with the overall design created by CAD models and their parts. Several scholars and researchers have shown that shape-memory behaviour might be possible by incorporating targeted smart hinges inside structures (Farhang et al., 2017; Ge et al., 2014; Tolly et al., 2014). The hinges are made of non-reactive or smart materials (Figure 2-9).

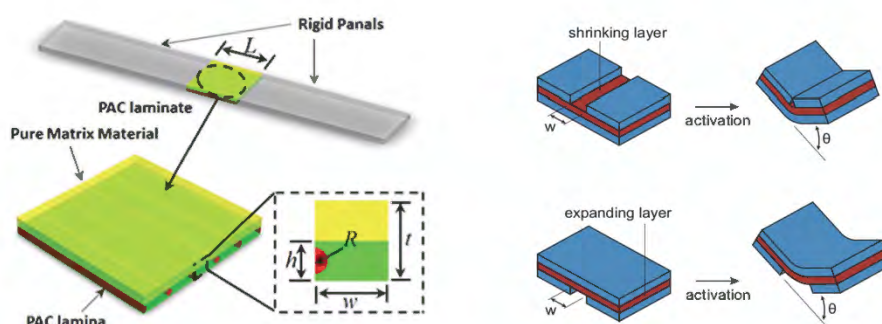


Figure 2-9. Structures with smart hinges (Farhang et al., 2017; Ge et al, 2014; Tolley et al. 2014).

Instead of stacking uniform layers to exhibit various dimensional changes and shape changes in response to stimuli, SMMs can be arranged in controlled amounts, positions, and patterns, so that, upon activation, other effects, such as the rate of expansion, can be produced. Figure 2-10 shows the material results when different swelling rates are achieved (Kim et al., 2012; Wu et al., 2016).

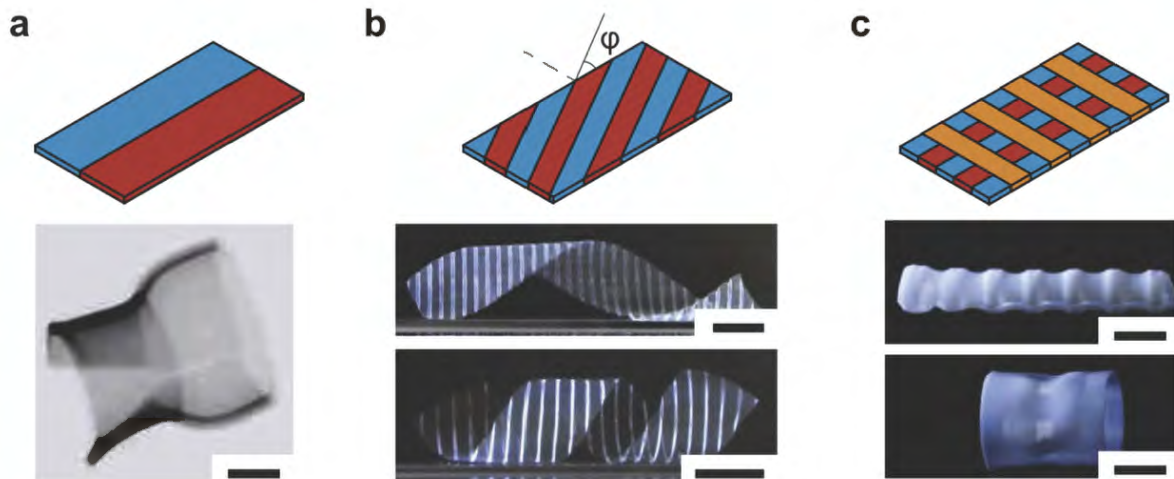


Figure 2-10. Multiple material tessellations resulting in different shape-shifting materials (Kim et al., 2012; Wu et al., 2016).

This is similar to the self-folding structure, such as a hinge, but it can change shape due to environmental reactions. Figure 2-11 shows a flower-shaped gripper that folds into a flower shape through the desolvation of acetone (Zhao et al., 2017). The sample containing acetone maintains its flat shape, but the acetone volatilises and shrinks in shape. 4DP technology can also be used for environmental applications.

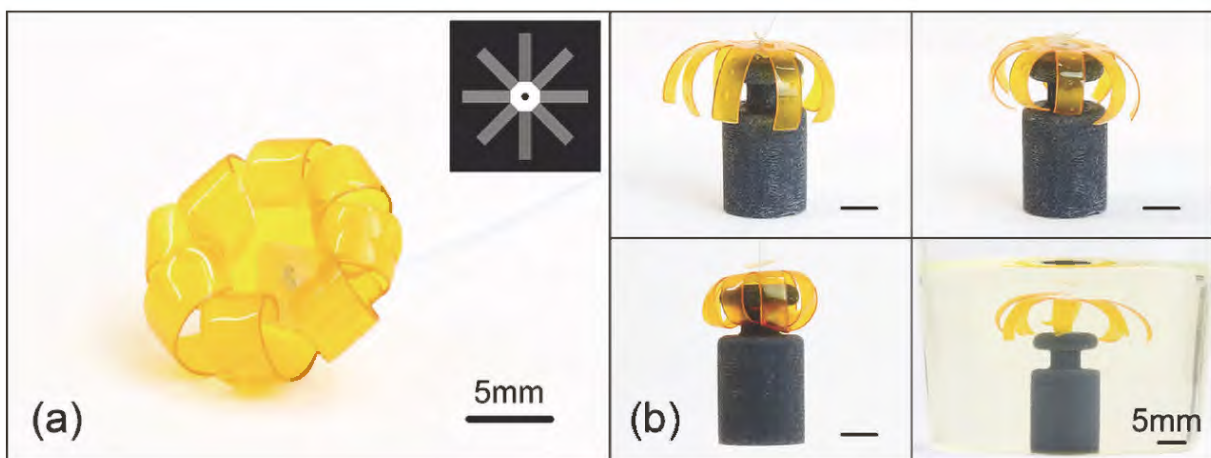


Figure 2-11. Desolvation-induced flower-shaped grippers using non-active materials (Zhao et al., 2017).

Figure 2-12 is a hollow platonic solid using origami (Jian et al., 2022). The flat printed structure is reacted by heat and activated as a hollow 3D structure. With the surge of interest in microrobots and wearable electronics, this activated 3D structure has proposed a way to embed electronic components without damaging the surface as an approach to more general structures. This process was tested using a thermodynamic mechanism and PLA.



Figure 2-12. Origami of the hollow platonic solids. (a) Tetrahedron; (b) octahedron (Jian et al., 2022).

2.3 Shape Memory Polymers (SMPs)

2.3.1 Overview of SMPs

Smart materials have multi-shape functions as they remember one or more temporary shapes, thereby transforming objects into different shapes or returning them to their original shape when exposed to appropriate stimuli (Jia et al., 2021). Smart materials include shape memory and self-healing materials, such as SMPs, shape memory alloys (SMAs), shape memory ceramics (SMCRs), shape memory composites (SMCs), and shape memory hybrids (SMHs) (Ryan et al., 2021). Among them, 4D printed SMP is the most used for 4DP and shows excellent properties (Subash et al., 2020). These SRMs are classified as shown in Figures 2-10. However, among the various smart materials, SMAs and SMPs are the most commonly used materials for 4D-printed parts. SMAs can generally be used to fabricate larger structures that have wider operating temperature ranges with higher tensile strength than SMPs (Alshehly et al., 2021). However, SMAs' high costs and densities, more complex programming, and low biocompatibility and biodegradability efficiency limit its usability within 4DP. As a result, within 4DP, SMAs have shown lower performance than SMPs in the literature. In contrast, SMPs offer several advantages over other smart materials such as metals and ceramics, including low costs and low densities, simple processing, chemical stability, and high recovery strains (Li et al., 2020). Table 2-2 compares the characteristics of SMPs and SMAs. SMPs have lower stresses for deformation and stresses upon recovery compared to SMAs, but, depending on the application, SMPs have advantages and disadvantages. However, SMPs have the potential to achieve shape recovery properties of up to 800% plastic strain, whereas SMAs' recovery properties are around 7–8%. There is also a very large price difference between the two. Nevertheless, SMPs have a similar glass transition temperature (T_g) of -10 – 100 °C. SMAs are considered to be less favourable than SMPs due to their complex production requirements, high costs, and limited recovery rates. Therefore, SMPs are preferred over SMAs; SMPs are the most studied and applied material in 4DP because of their excellent properties and applicability.

Table 2-2. Comparison of SMPs and SMAs (Liu et al., 2007).

Property	Shape memory polymers	Shape memory alloys
Density (g/cm^3)	0.9–1.2	6–8
Extent of deformation (%)	Up to 800	< 8
Required stress for deformation (MPa)	1–3	50–200
Stress generated upon recovery (MPa)	1–3	150–300

Transition temperature (°C)	-10–100	-10–100
Recovery time	1 sec to min	< 1 sec
Processing condition	< 200 °C; low pressure	> 1000 °C; high pressure
Cost	< \$10/lb (£7.5/lb)	Appx. \$250/lb (£189/lb)

2.3.2 Characteristics of SMPs

The concept of SMPs was developed in 1984 at Nippon Zeon when polynorbornene-based SMPs were created. Materials used in 4D printing are commonly referred to as smart materials because of their ability to change properties over time (Mohammad et al., 2013). Material scientists developed an SMP with a wider range of Tg through a series of tests, and it can be deformed from a single shape to multiple shapes in a short period (Shahinpoor, 2020). SMPs have two mechanisms: They can maintain their temporarily deformed shape, and they can recover their original shape according when exposed to certain stimuli (Huang et al., 2010). Temporary deformation results in a temporary shape that is achieved through a Tg between different liquid crystalline phases through bonding, such as the Diels-Alder reaction that is thermoreversible. Restorative deformation entails creating a force capable of restoring its original shape, which is achieved through interpenetrating networks between constant temperature, chemical crosslinking, and crystalline phases of the material (Meng & Li, 2013). The operating mechanism of SMPs is characterised by its Tg, which is the temperature at which a hard vitrified polymer changes into an elastic polymer that changes its shape or the set temperature that is set to activate the materials' SMEs. This temperature point is set externally, so that the shape change of the substrate occurs (Westbrook et al., 2011). Other stimuli-response methods, such as conversion by redox reaction, can also be applied. The shape-changing mechanism of SMPs is usually achieved through thermal transfer, thermal reactivity, and chemical reactivity. Thermal transfer in SMPs is due to a molecular switch or the net point, which is a physical and chemical cross-link. Phase-separated morphology and formation are the basic mechanisms of changing states of matter. In thermosets, the network chains between the net points are made up of switch segments of chemical cross-linking. Shape memory conversion is achieved through the thermal transfer of polymer segments. Because thermosets exhibit less creep, they exhibit less irreversible change during deformation when compared to thermoplastics, and they also exhibit better shape as well as mechanical and thermal memory than thermoplastics (Leng et al., 2011). For thermally reactive SMPs, a dual-component system is used for thermally excited polymers. The matrix remains elastic, and the fibres reversibly change in terms of material stiffness (Ratna & Karger-Kocsis, 2008). Thermally reactive SMPs use the glass temperature to transition, or they use the melting point. In the case of chemically reactive SMPs, immersion in chemicals stimulates the plasticising effect of polymers (Roos & Karel, 1991). This effect often lowers the material's Tg and requires heating the material above the Tg. Due to this chemical reactivity, there are alternatives for morphology recovery, such as ionic strength, pH value, or concentration of the agent (Lu et al., 2013). Thermally reactive SMPs are best suited for 4DP parts, followed by chemically reactive SMPs that specifically use hydration. Methods that can be used to print thermally reactive SMPs include material extrusion, MJ, and STL. For chemically reactive SMPs, hydrogels are usually used, and bio-extrusion is the most common manufacturing method. PLA is the most studied and widely used

material in 4DP due to its high applicability and excellent properties (Ng et al., 2020), and thermoplastics are widely used to operate SMEs. The types of materials used in 4D printing are shown in Figure 2-13 (Ahmed et al., 2021).

4D Printing Materials	Thermo-responsive
	Materials responsive towards heat or temperature
Hydrogels	Photo-responsive
Materials responsive towards moisture	Materials responsive towards light
Electro-responsive	Magneto-responsive
Materials responsive towards electric energy	Materials responsive towards energy
Piezoelectric	pH-responsive
Materials responsive towards mechanical stress	Materials responsive towards pH change

Figure 2-13. Representation of the types of materials used for 4DP. (Ahmed et al., 2021).

2.3.3 Stimuli and SMEs

Material extrusion is known as FFF or FDM. Various materials can be extruded from AM, the most popular of which include thermoplastics such as Acrylonitrile butadiene styrene (ABS), Thermoplastic polyurethane (TPU), PLA, High-impact polystyrene (HIPS), Aliphatic polyamides (PA), also known as nylon, and more recent high-performance plastics such as polyether ether ketone (PEEK) or polyetherimide (PEI) (Chu et al., 2020). Materials that react to environmental conditions and that can change their configurations are often chosen for 4DP (Rastogi & Kandasubramanian, 2019). The global deformation of materials can be achieved by exposing them to external stimuli, such as water and temperature, which are commonly used as activation stimuli, as well as magnetic forces, light, and pH, which are less commonly used. These materials demonstrate how smarter devices can be designed. The materials' geometric designs and reactivities affect their rates of movement. The number of shapes that can be retained in any given material's memory depends on the network elasticity. Smart materials or SRMs are functional material classifications that are characterised by their ability to remember SMEs, which are triggered through stimuli such as water, heat, solvents, and the like. Combining these materials with 3DP techniques can facilitate extensive research on the various applications of 4DP through design transformations. Materials that exhibit feature memory characteristics include shape memory hydrogels, SMCrs, SMAs, shape memory complex, and SMPs, of which SMPs are the most studied. SRMs are smarter than regular materials, and they are one of the most critical components of 4DP. SRMs are classified into several sub-categories, largely divided into physical and chemical properties, as shown in Figure 2-14 below (Sun et al., 2012). In terms of physical properties, SCMs and SMMs are divided according to shape, with SMMs containing SMAs, SMPs, SMHs, and SMCrs. SMAs and SMPs are widely used in 4DP (Sun et al., 2012), and SRMs are an important component of 4DP. In particular, SMPs

can create products that automatically respond to the environment without having to use complex, heavy, and expensive electronic operating systems.

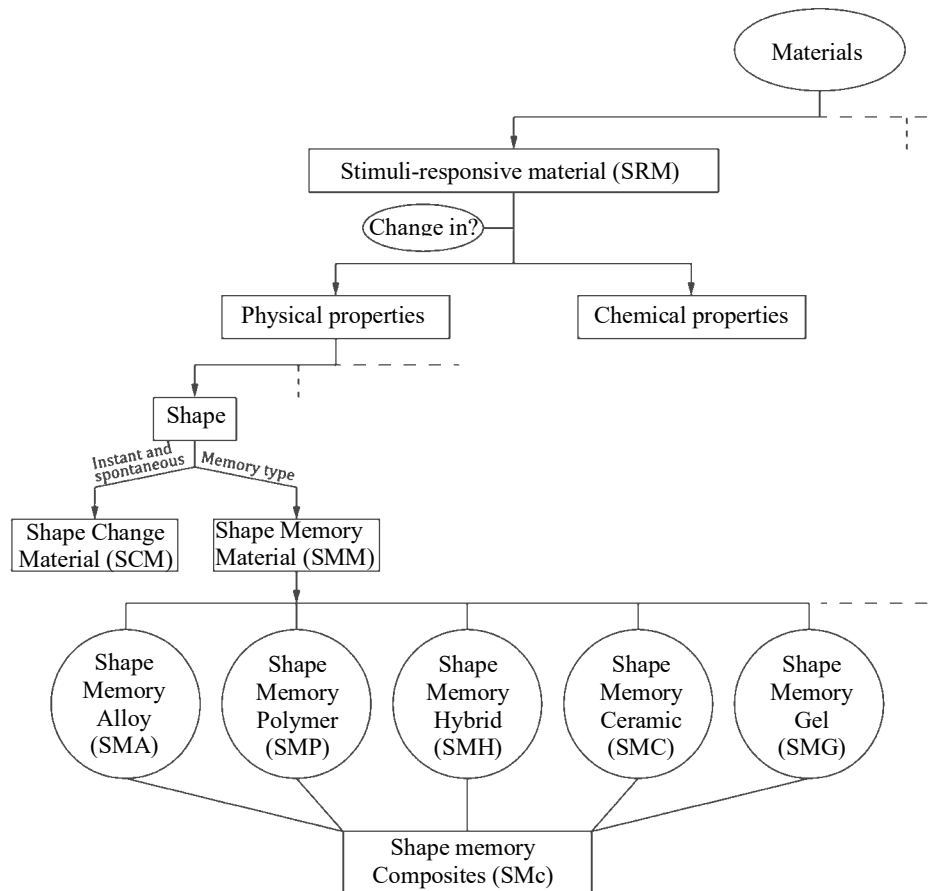


Figure 2-14. A categorisation of SRMs (Sun et al., 2012).

2.3.4 The SME Process in 4DP

In order for materials to be deformed by stimuli, a series of transformation processes by external forces needs to occur. SMEs can be occurred one-way, two-way, or multi-way. The most basic procedure for the polymer shape memory effect is illustrated in Figure 2-15. First, the SMP is heated to its transition or strain temperature (T_d) to soften the material. Second, a strain (i.e. load or stress) is applied to the SMP. The unidirectional SME requires human intervention. Moreover, the SMP, which has undergone the cooling process, has the load removed, and the deformed shape is fixed, a temporary shape. After shape fixation, shape recovery is obtained by reheating the temporarily formed SMP to the recovery temperature (T_r) in the unstressed state (Erkeçoğlu et al., 2016). Moreover, it is restored to the SMP's original (permanent) shape. Two-way SMEs have an SME that can change back and forth from a temporary shape back to a permanent shape (Xie, 2011). Two-way SMEs are performed in a similar way to one-way. Bidirectional SMEs can change back from temporary to permanent by remembering two different shapes. It goes through a cyclic or reversible SME with two low and high fixed temperatures (Zare et al., 2019). Multidirectional SMEs also have an original permanent shape and two metastable shapes. They consist of independent programming steps for two different transitions, including multi-step programming and recovery cycles (Strzelec et al., 2020).

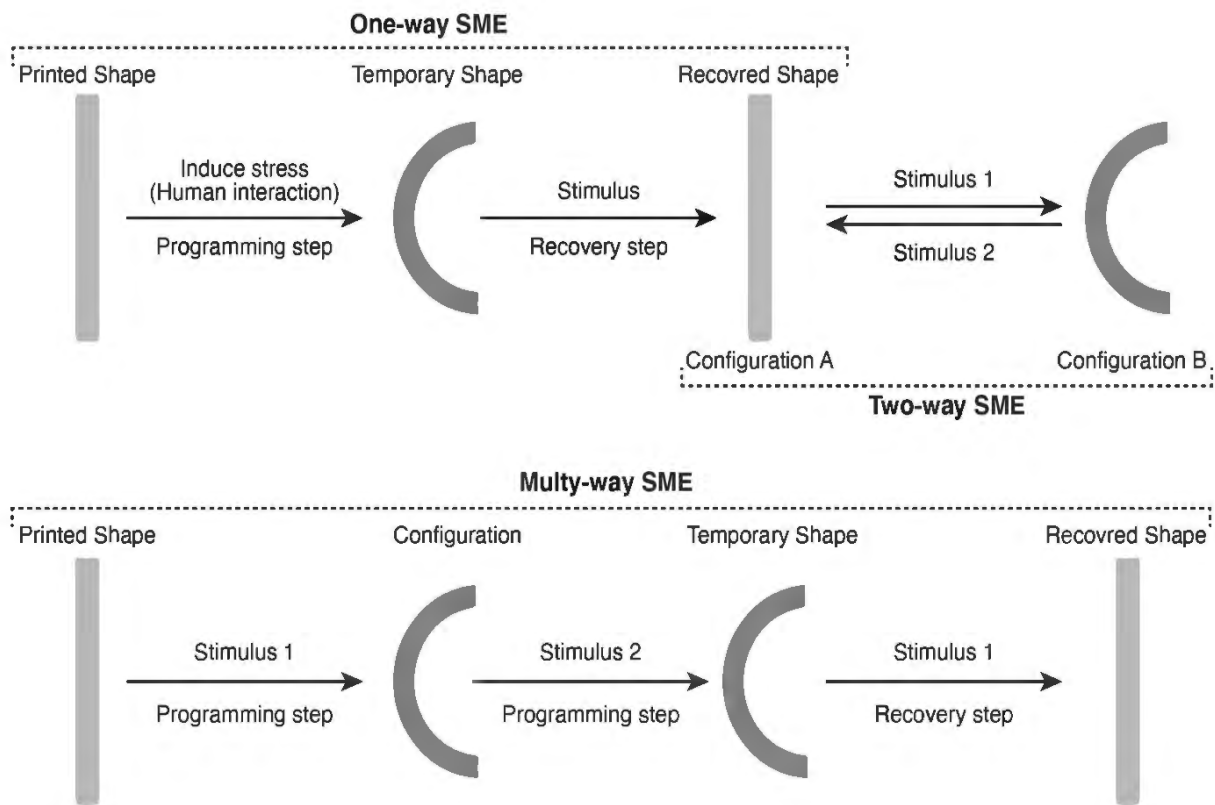


Figure 2-15. Schematic representation of one-way, two-way and multi-way SME

SME process comprises two steps: The first is the programming step, and the second is the recovery step. The programming step produces the deformation caused by an external force, and the recovery step entails returning the programmed or deformed object to its original shape. Therefore, this process results in the original printed shape, the deformed shape, and the recovered shape. A visual summary of the SME process is shown in Figure 2-16, which explains the systematic steps of programming, heating, cooling, triggering stimuli, and recovery. In the programming stage, the printed object is ‘activated’ by a specific trigger that is introduced through human involvement, which results in the 3D-printed component changing its shape rapidly (see Figure 2-16). This trigger is usually temperature. Thus, a component stimulated at a defined temperature will become soft when it reaches its T_g , and the part can then be shaped manually or using a flexural device. The shape is temporarily created, and, when it hardens, it retains its deformed shape, known as the temporary or programmed shape. This shape largely remains stable in temperature variations, such as cooling to room temperature and then being heated again. In the second stage, the part automatically returns to its original shape when it is subjected to the stimuli (heat). This is called the SME, which is the result of the programming that determines the extent of the change and the desired shape when external stimuli are applied (Monzon et al., 2016). The SME of the T_g can be exploited in order to distort the shape using stimuli, and the material can be permanently restored to its original shape when heated again (Mao et al., 2016). The SME of the material is determined by many factors, such as the material composition, applied shape-changing behaviours, deformation rate, deformation temperature, and recovery temperature

(Figure 2-16). As a result, the transformation between a printed shape and a recovered shape is simple and direct and can be achieved with complex geometrical components that have high fidelity. A material's geometric design and reactivity affect the conversion rate from one form to another. The amount of shape a material can hold depends on the network elasticity. The strain recovery rate (R_r) and strain fixity rate (R_f) determine the 'intensity' of an SME. R_r is a material's ability to remember its permanent shape, and the R_f describes a switching segment's ability to correct a mechanical deformation. Most SMPs are limited to near-unidirectional memory, which means that they require reprogramming each time they are restored (Erkeçoğlu et al., 2016).

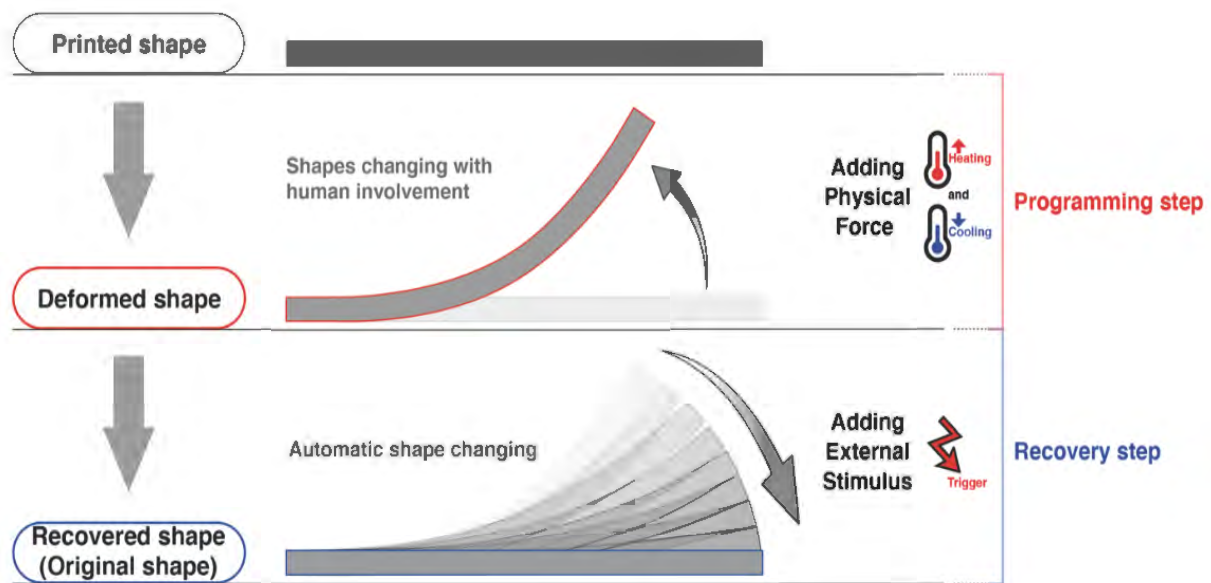













Figure 2-16. The processes involved in SMEs (Nam & Pei, 2020).

2.4 Shape Change through 4DP

In order to implement effective 4DP, it is required to understand the types and definitions of clear and objective change behaviours. Many researcher studying 4DP apply various types of shape-changing behaviours, from the most basic folding to complex shapes, in their experiments. Most of them focus on the process and result of applying the intended shape change. Alternatively, many studies are conducted from a consequential perspective according to the application of various materials, stimuli, AM techniques and CAD, such as those of Wang et al. (2019) and Mallakpour et al., (2021). In other words, few papers organize the types and definitions of form change behaviour. Therefore, it is possible to classify the types and definitions of the form change behavior clearly and objectively, and apply various form change behaviors. Table 2-3 shows the shape change operation that can be implemented with 4DP. It summarized by finding, defining, and listing the various types of shape-changing motions that the researchers applied to the 4DP experiment.

Table 2-3. Mechanical analysis of each shape deformation (Nam & Pei, 2019).

Shape-changing behaviours		Mechanical analysis
	Folding - Raviv et al., 2014 - Tibbits, 2014 - Ionov, 2013	'Folding deformation is created due to the stress mismatch between the rigid and active materials. Also can be convertible to various expansion ratios' (Farhang et al., 2017).
	Bending - Gladman et al., 2016 - Wu et al., 2016 - Zhang et al., 2016	'Bending strain is an area expansion/contraction mismatch in response to an activating stimulus, and maintaining the same strain can lead to different types of strain' (Cendula et al., 2009).
	Rolling - Ge et al., 2013 - Gladman et al., 2016	'Rolling deformation is a dilatation mismatch and thickness-dependent normalized curvature, which is a non-linear relationship between the rolling radius of one hand and the rate of expansion and the sample thickness' (Byun et al., 2013).
	Twisting - Wang & Yao, 2017 - Zhang et al., 2016	'Twist deformation is a proposed specific angle of extension/contraction mismatch, and the final twist angle can be changed by adjusting the angle of the active stimulus' (Zhang et al., 2016).
	Helixing - Zhang et al., 2016 - Ionov, 2013	'Helixing deformation is created by the uniaxial expansion/contraction active layer for a non-zero angle between the principal strain direction of the active layer and the major axis of the bilayer strip' (Janbaz et al., 2016).
	Buckling - van Manen et al., 2018 - Sharon and Efrati, 2010	'Buckling deformation causes out-of-plane buckling of planar structures when compressive stresses in different directions exceed certain critical values' (van Manen et al., 2018).
	Curving - Tibbits, 2014	'Based on the luminous intensity gradient with the thickness of the material, a stress gradient can be created, which causes the structure to spontaneously warp after separation from the substrate' (Zhao et al., 2017).
	Topographical change - Hu et al., 2017 - Tibbits, 2014	'Features of mountains and valleys can be created in concentric circles with the right stimulus. Surface topography refers to the local deviation of a surface from a plane. These features typically occur under compressive loading conditions' (Wang & Yao, 2017).
	Expansion and contraction - Bakarich et al., 2015 - Raviv et al., 2014 - Yu et al., 2015	'This mechanism is driven by the variable expansion ratios between active and rigid substances, which consist of scalable hydrophobic active and rigid substances' (Bakarich et al., 2015).
	Waving - Wu et al., 2016	'Waveform deformation can occur in bilayers with similar stiffness and layer thickness through expansion/contraction mismatch in response to activation stimuli' (Cendula et al., 2009).
	Curling - Tibbits, 2014	'Curling deformation is possible due to stress mismatch between hard and active materials due to different swelling properties' (Tibbits, 2014).

Most of them are based on 11 types of shape-changing behaviours: folding, bending, rolling, twisting, helixing, buckling, curving, topographical change, expansion and contraction, waving, and curling. The listed 4DP shape change behaviours are diversely distributed, from simple to complex shape changes. The most basic shape-changing behaviours, such as folding and bending, are programmed to be fixed to one part and have a single shape-change part. In addition, a shape change operation that causes various shape changes by being complexly programmed in one part and several parts were also discovered. Multiple shape change behaviours refer to an action in which multiple parts are programmed for shape change, and it has a deformed part in various parts, or a single shape change is repeated several times. In addition, several shape-changing behaviours may be combined in a complex manner. These features can be programmed over time to go through a specified set of sequences, sometimes referred to as ‘sequential’ shape shifts (van Manen et al., 2018). In terms of mathematical analysis, all shape variants are the result of different stresses along the plane, and they are affected by various strains and their geometry. The following sections describe and classify a set of examples of reshaping actions that fall into three categories: basic, compound, and combined reshaping actions.

2.4.1 Basic Shape-Changing Behaviours

Basic shape-changing behaviours result in a single deformation, meaning the shape is transformed in one step. Shape-changing behaviours are defined by the way in which the shape change occurs. The nine basic shape-changing behaviours include folding, curving, rolling, twisting, helixing, buckling, bending, buckling, topographical change, and expanding and contracting.

- Folding

Folding is a deformation in which the intra-surface distance between two distinct points of a sheet is maintained without needing self-intersection (Demaine, 2001). Folding is a sharp curvature caused by deformation along a crease, and it is a localised deformation of a material that uses sharp angles to highlight narrow hinged areas (Ryu et al., 2012). Tibbits (2014) generated a 4DP structure that can be folded into precisely truncated octahedrons. The components were printed using a MK technique, and water was used as a stimulus (Figure 2-17), which created an angled 3D object from a flat object through folding.



Figure 2-17. An example of folding (Tibbits, 2014).

- Bending

Bending is the distributed deformation of material along the deflected area that creates the curvature (Ahmed et al., 2013). Wu et al. (2016) produced such an actuation behaviour in which

two segments were linked in the middle and the orientation of the fibre remained parallel to the direction of the bending force. Figure 2-18 illustrates this bending behaviour. If an array of the segments are arranged by altering the materials and position of fibres, a ‘wave’ can be achieved, which is a complex shape.

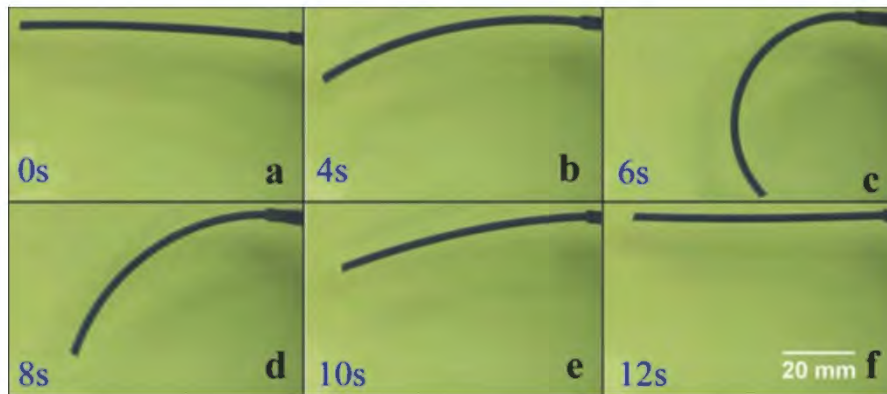


Figure 2-18. An example of bending (Wu et al., 2016).

The difference between folding, bending, and rolling is subtle: Folding is a localised deformation considered to be a sharp angle occurring in a narrow hinge region; bending is a global deformation associated with a softer curvature (Ryu et al., 2012); and rolling occurs when a continuous force is applied to bending. The biggest difference between bending and rolling is the angle of inclination after deformation, which is the difference in curvature. Bending has two positive and two negative slopes, while rolling has varying slopes (see Figure 2-19).

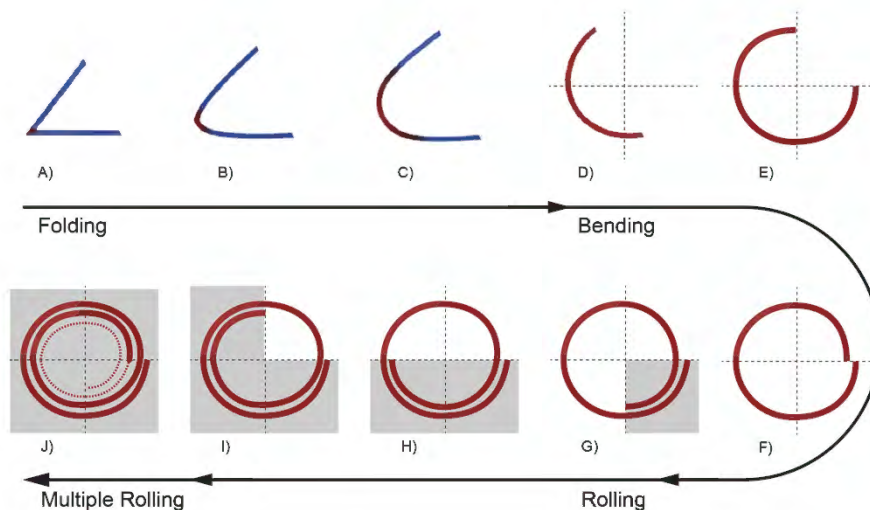


Figure 2-19. The difference between folding, bending, rolling, and multiple rolling.

- Rolling

Rolling is the movement of a shape by rotating it around its own axis. This deformation process allows the component to maintain a constant cross-section throughout the deformation process. This shape-changing behaviour is triggered by the heat of a typical shape-memory cycle that

Twisting or helixing is the dominant mode of deformation without dimensions. The torsional mode is dominated by in-plane stretching, and bending dominates in the spiral layer. Increasing the width of a self-twisted sample increases the stretching energy very rapidly, whereas the bending energy of the helical structure is only linearly related to the sample width. Also, the main difference between torsion and a helix is that the axis of the torsion is centred, whereas the helix has different axes (see Figure 2-22).

Figure 2-21. An example of twisting (Wang & Yao, 2017).



- Twisting
Twisting is dominated by in-plane stretching (Armon et al., 2014). It is possible to combine two anisotropically active layers of a similar type with first-order strain directions that are perpendicular to each other in order to create self-twisting strips (Figure 2-21). Increasing the width of torsion sharply increases the stretching energy. In contrast, the bending energy of a helical structure is only linearly related to the width of the part. Torsion favours small widths for shape change (Armon et al., 2014). An example of a twist can be seen in the twisted pasta shape produced by MIT (Wang & Yao, 2017).

Figure 2-20. An example of rolling (Ge et al., 2013).



includes programming and recovery steps (Farhang et al., 2017). Figure 2-20 an example of rolling contained in Ge et al.'s (2013) study. The image on the left is the original shape of the strip before rolling occurred, and the image on the right shows the result of the rolling. In general, the amount of curvature depends on design variables such as composition, geometry, mechanical load, thermal history, and properties (Ge et al., 2013).

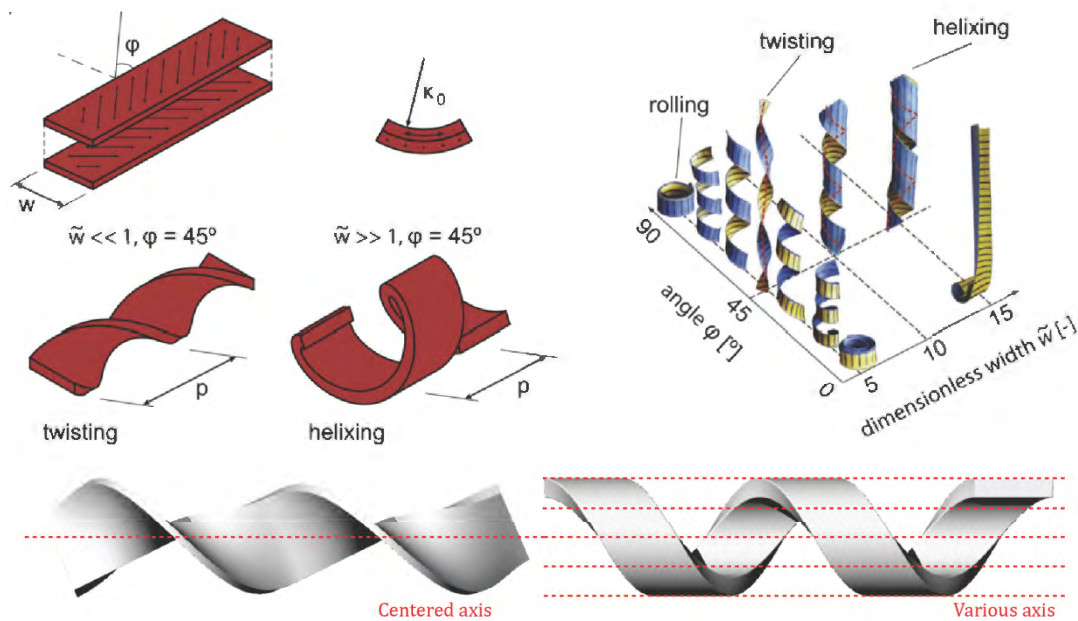


Figure 2-22. The difference between twisting and helixing (Forterre et al., 2011).
Note. w = the strip width; t = the the double layer thickness; k_0 = the reference curvature.

- Helixing

A helix is a type of smooth spatial deformation in which curves occur in 3D space. Zhang et al. (2016) experimented with helical structures with various spiral angle patterns by twisting 2D sheets into 3D shapes (Figure 2-23). They used specific angles to print the fibres so as to induce twists. By adjusting the print angle of the active fibre, it was possible to change the torsional behaviour of the helix.

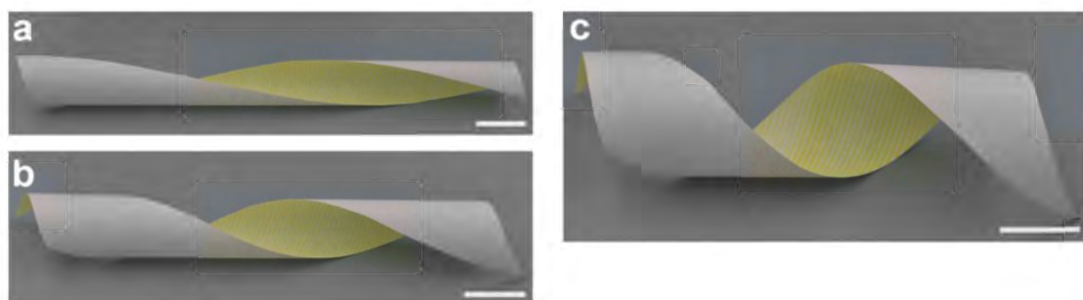


Figure 2-23. An example of helixing (Zhang et al., 2016).

- Buckling

Buckling is characterised by a sudden lateral failure of structural members under high compressive stress on opposite sides. An example of buckling behaviour can be seen in van Manen et al.'s (2018) work (see Figure 2-24). The magnitude of the stretching energy is generally linear to the material thickness, whereas the bending behaviour exhibits a third-order dependence on the thickness. Programming the planar layouts of various active and passive elements allows them to generate the desired compressive stress when activated. Externally generated compressive forces are also used on the passive material layer in order to induce non-planar buckles. It is implemented with various modelling materials.

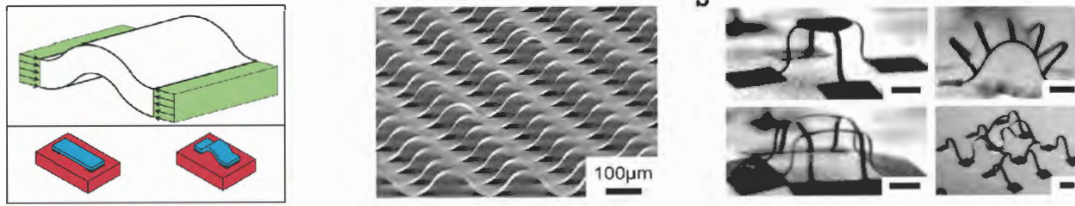


Figure 2-24. An example of buckling (van Manen et al., 2018).

- Curving

A curve is the extent to which the surface of a geometric object deviates from its plane. In Tibbits' (2014) experiment, features of mountains and valleys were generated in concentric circles with appropriate stimuli (Figure 2-25). This shape-changing behaviour was possible due to the stress mismatch between the hard and active materials' different expansion properties when put into contact with water.

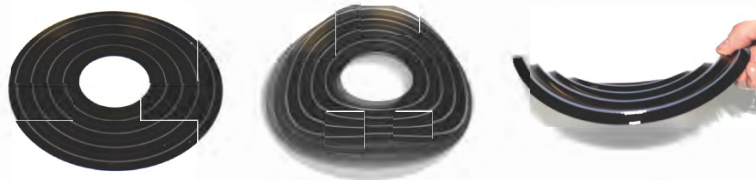


Figure 2-25. An example of curving (Tibbits, 2014).

- Topographical change

Topographical change creates distorted shapes that resemble the physical features of mountains. The image on the left shows shells with different curvatures near and away from the central vertex. The hypotenuse is perfectly straight near the vertex but becomes more curved as it moves away from the vertex, and the edges bend into the shell (Figure 2-26).

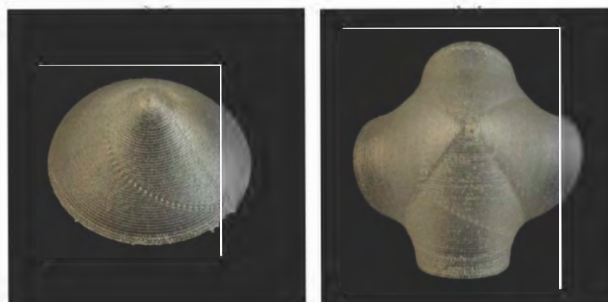


Figure 2-26. An example of topographic change (Hu et al., 2017).

- Expansion and contraction

In general, many materials, including thermoplastics, expand when heated and contract when cooled. As the temperature changes, the material's shape, volume, and area change. Expansion and contraction shape-changing behaviours are based on a shape memory cycle that includes the usual programming and recovery steps for thermally responsive SMPs. Bakarich et al. (2015) showed the expansion and contraction behaviours of linear free expansion as well as the contraction of thermally responsive hydrogels in cold and hot water (Figure 2-27).

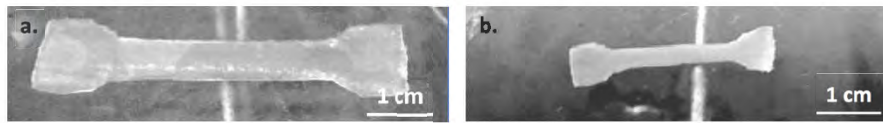


Figure 2-27. An example of expansion and contraction (Bakarich et al., 2015).

2.4.2 Complex Shape-Changing Behaviours

Complex shape-changing behaviours are defined as multiple transform reshaping actions that can be derived from either an extension of the initial shape of a basic reshaping action or a fully multifaceted shape. The characteristics of this multi-deformation shape change are shown by superimposing shape transformations on each other. This means that one or more variations can occur. For example, multiple folding, bending, rolling, twisting, helixing, buckling, topographical change, and curvature changes are extensions of the basic form. Other complex structures include waving and curling.

- Waving

Waving creates a shape with undulating features (wavy up-and-down shapes). Wu et al. (2016) conducted an experiment that resulted in an active ‘wave’ shape when immersed in hot water (Figure 2-28). This sample was designed with a structure in which the position of the material was separated into two parts: upper and lower. Typically, wavy patterns are made from strips patterned with SMP and non-smart material laminate segments (Wu et al., 2016). This flat three-layer component deforms into a curved, wavy shape when heated. Various waveform transformations are possible by changing the position and material of each layer.



Figure 2-28. An example of waving (Wu et al., 2016).

- Curling

As an alternative to bending and rolling, surface curling can be used to create a continuous surface. Curling is characterised by non-uniform shape changes in addition to multiple continuous deformations. A larger surface provides uniform expansion and generally makes the effect of curling much more noticeable. Figure 2-29 shows examples of curling behaviour (Tibbits, 2014).



Figure 2-29. An example of curling (Tibbits, 2014).

- Multiple folding

Mao et al. (2015) demonstrated a series of self-folding operations when transforming a 2D strip into a 3D shape (see Figure 2-30). The folding action was thermally induced in several shape memory cycles that included programming and recovery steps. Multiple folding actions can also be programmed to be precisely timed so that the action effects can occur simultaneously or sequentially.

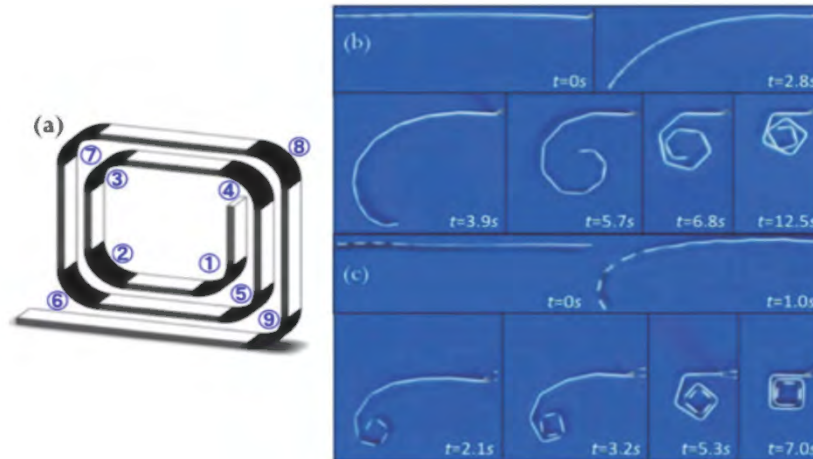


Figure 2-30. An example of multiple folding (Mao et al., 2015).

- Multiple curving

Tibbits (2014) showed surface topography changes (see Figure 2-31). Three shapes evolved, in which the creation of a sinusoidal shape (continuous wave) was manifested through varying the rates of expansion of the rigid and active materials. It is worth noting that the material concentration along the edges was different from the centre. Continuous curving was demonstrated as being dependent on the concentration of the material.



Figure 2-31. An example of multiple curving (Tibbits, 2014).

2.4.3 Combination Shape-Changing Behaviours

Combination shape-changing behaviours are defined as shape actions that combine different types of reshaping actions. For example, combining two or more shape-changing actions, such as combining bending and twisting in one object or combining folding, buckling, and helixing to create various shape transformations.

- Bending, twisting, and wrinkling

Ge et al. (2016) demonstrated the possibility of combining twisting and bending. Figure 2-32 shows an object that was bent and crumpled in various directions and angles. This shape-changing behaviour uses heat as a typical shape memory cycle stimulus with predefined programming and recovery steps. The merged reshaping may have different timing of action depending on the design.



Figure 2-32. An example of bending, twisting, and wrinkling (Ge et al., 2013).

- Expansion and contraction

Teunis et al. (2017) showed the combination of expansion and contraction using expansion, contraction, twisting, and bending behaviours (see Figure 2-33). A single-layer self-rolling element was produced using a parallel arrangement of expansion and contraction strips. In a separate experiment, arranging the strips at a 45° angle to the longitudinal direction produced a self-torsional structure.

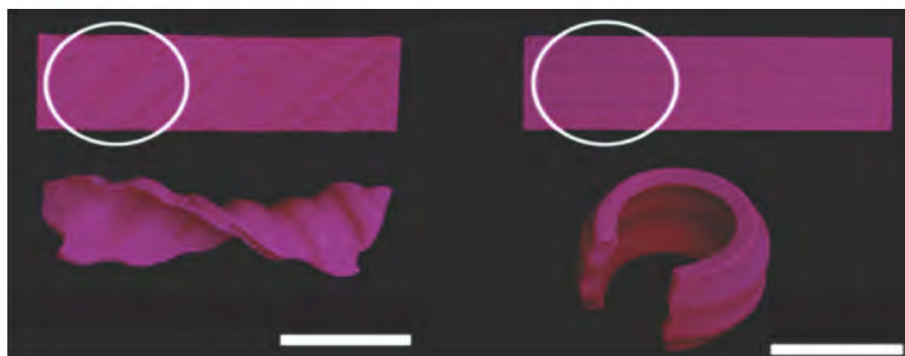


Figure 2-33. An example of expansion and contraction, twisting, and bending (Teunis et al., 2017).

- Hierarchical structures

Hierarchies combine different types of shape-changing components into a system. Chen et al. (2016) produced a single actuator (A, B) as a unit (C, D), after which the unit was co-coupled into a system (E, F) and later acted as a system (G, H). C, D were the four actuators connected in series. In particular, the bracket's shape was the same as the pin's shape. E, F was the global joint that connected the tetrahedral module and the member. G, H showed the tiling of multiple

tetrahedral units in order to show the arrangement of the spatial frame. All three edges of the upper tetrahedron were connected to the highest points of all three lower counterparts (see Figure 2-34).

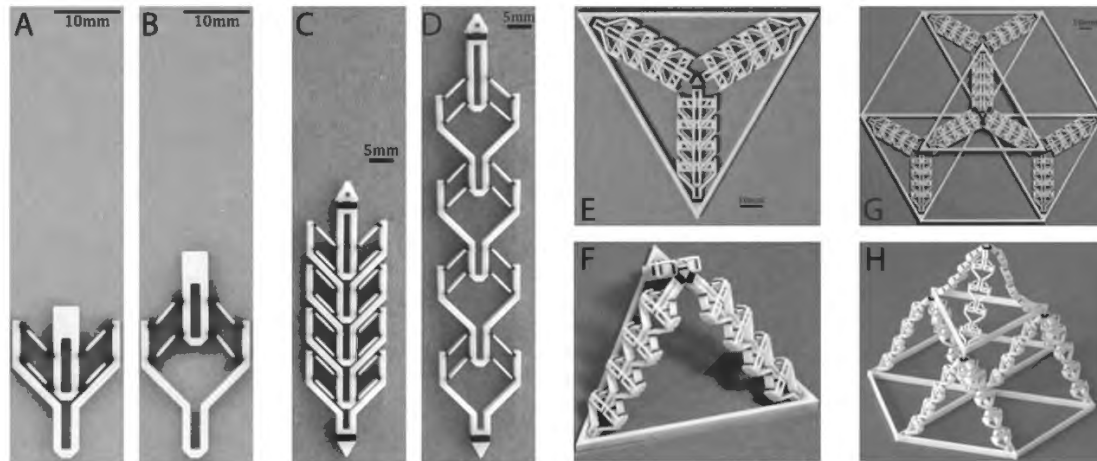


Figure 2-34. An example of hierarchical structures (Chen et al., 2016).

2.4.4 A Taxonomy of Shape-Changing Behaviours

4DP allows many different shape variations for specific applications. According to the literature on the existing shape-changing behaviours, three major shape-changing behaviours were classified (see Figure 2-35): basic, complex, and a combination of shape-changing behaviours. Basic shape-changing behaviours are classified as a single transformation that occurs in a single step or process. It is the most basic motion of shape deformation, and it occurs in a single part. The red highlights in the images of different shape-changing behaviours contained in Figure 2-35 show where the shape change operations take place. In complex shape-changing behaviours, the shape deformation occurs in a single stage or multiple stages. A process that includes two or more shape-changing deformations is also referred to as a sequential shape-shifting process in which certain changes occur at specific points. Complex shape-changing behaviours denote either an initial shape extension of a basic reshaping operation or multiple reshaping operations derived from a fully multifaceted shape. The characteristics of this multi-deformation shape change are displayed by superimposing the shape deformation on the original shape. Figure 2-35 demonstrates that there are several red areas in which shape transformations occur. Complex shape-changing behaviours include multiple folding, bending, rolling, twisting, helixing, buckling, topographical changes, and curvature-changing basic form extensions. Other much more complex structures include waving and curling. Lastly, combination shape-changing behaviours allow two or more construction behaviours to be programmed to occur within a component.

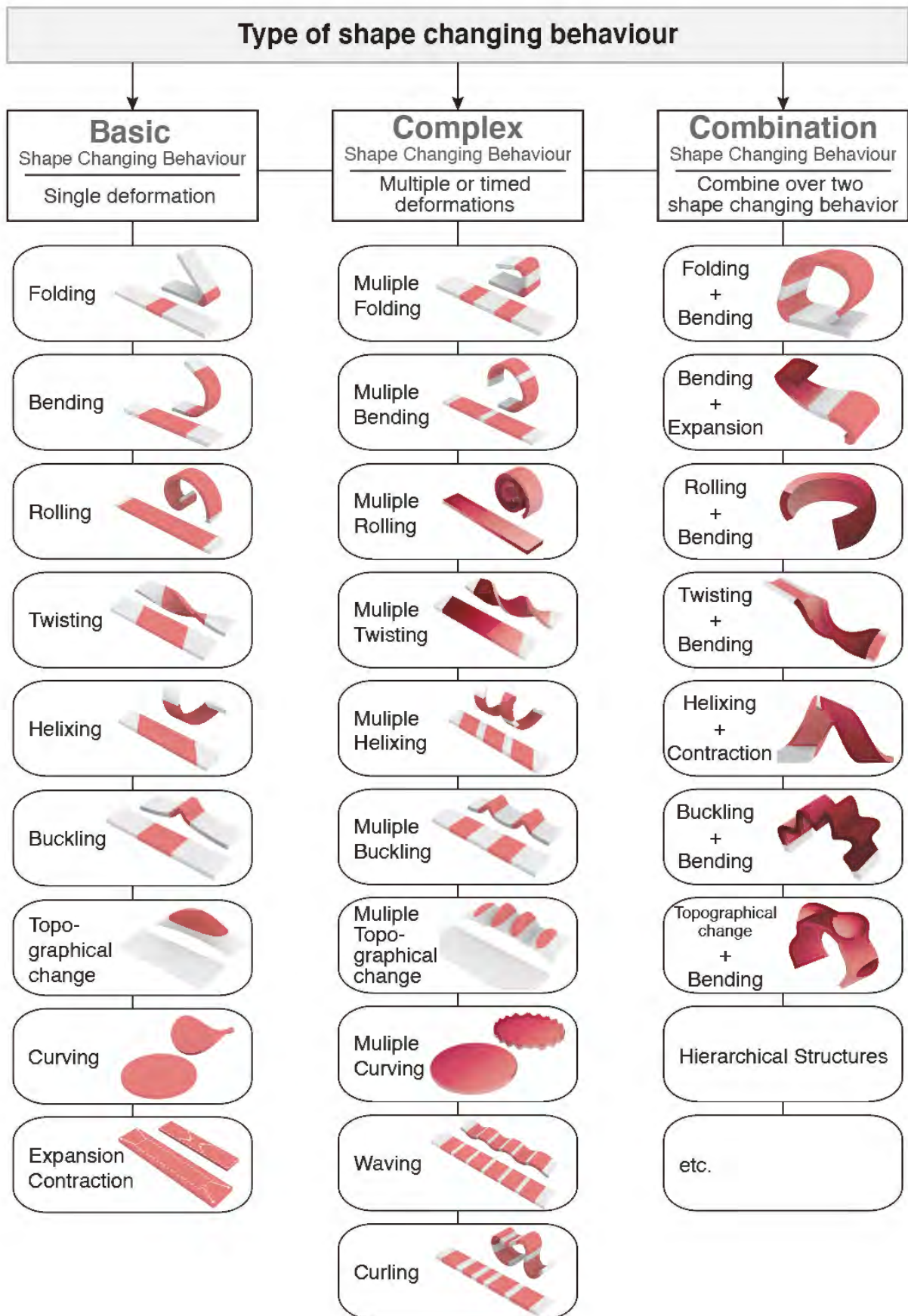


Figure 2-35. A taxonomy of shape-changing behaviours (Nam & Pei, 2019).

Taking it one step further, Figure 2-36 illustrates the different shape-changing behaviours as a matrix. Based on the taxonomy of the shape-changing behaviours in Figure 2-35, the complexity and simplicity as well as the severity of single change and multiple changes were measured according to the area and number of shape changes that are marked in red. The basic shape-changing behaviours, located at the bottom of the matrix, are often limited to a single transformation step in which the changes occur simultaneously. Among the single shape-changing behaviours, the most basic forms are folding and bending. Multiple deformations or sequential shape movement processes can be programmed to occur for more complex shape-changing behaviours, as shown in the upper-right corner of the matrix. The result is complex shape-changing behaviours that incorporate multiple deformation steps into a design, and they include and extend combination shape-changing behaviours.

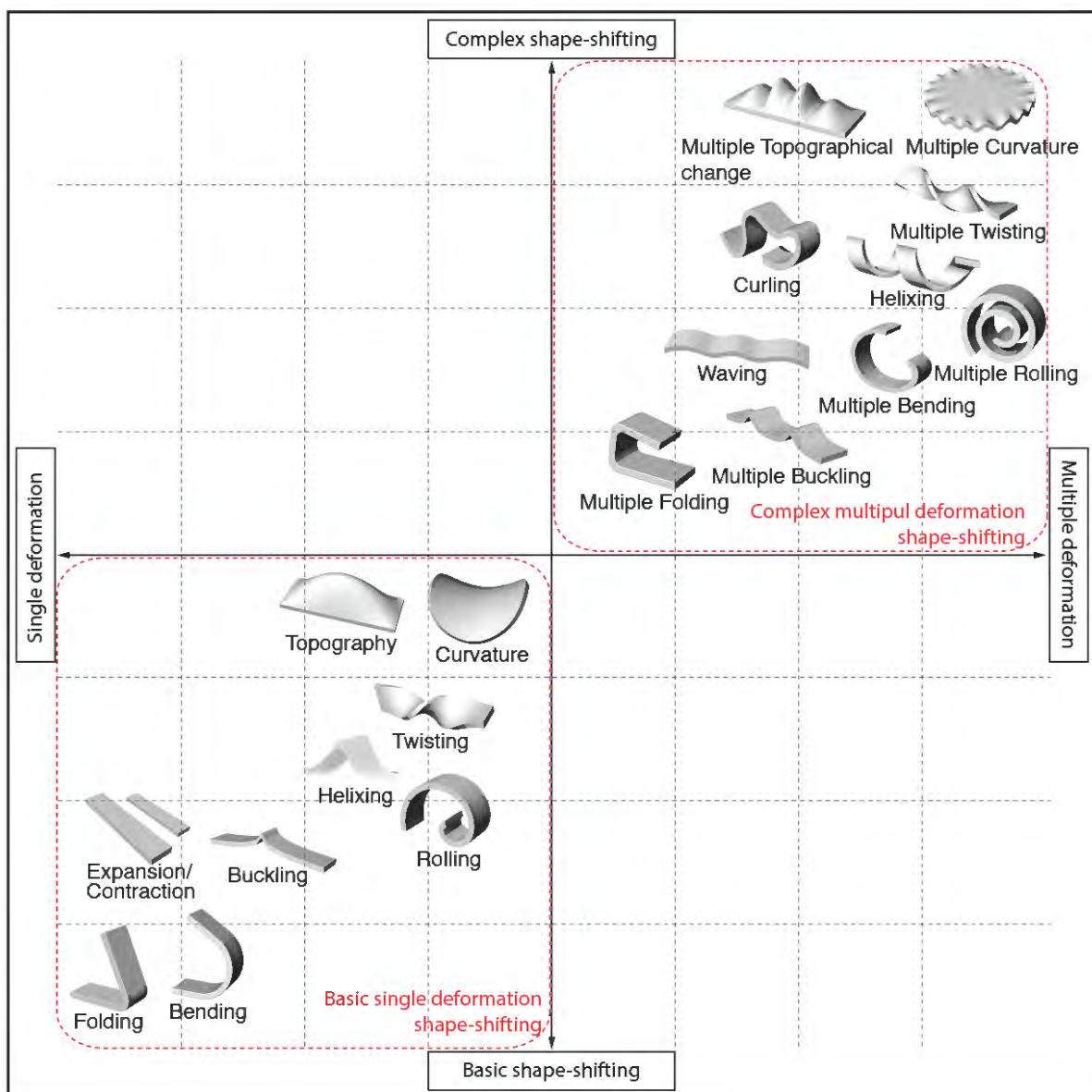


Figure 2-36. A matrix of shape-changing behaviours and types of deformations in 4DP.

2.5 4DP Parameters of the Shape Change Effect

4DP piqued researchers' interest in innovations in the printing field, and many research papers soon appeared from several areas of 4DP, including the next level of AM (the transition to 4DP), processing, materials, SMEs, stimulation, CAD modelling, parameters, applications, and the market for 4D-printed products. However, no research has clearly delineated the 4DP parameters of shape change effects. Therefore, it is necessary to organise the different parameters contained in 4DP research. Figure 2-37 below specifies the factors that can affect 4DP. The types of 4DP parameters for efficient shape change effects can be largely divided into 3D modelling and print slicing stages. According to the literature, parameters that can affect shape changes in the 3D modelling stage include the thickness, the structure of the object to be printed, and the composition according to the material properties. That is, the 3D modelling step entails designing and constructing the objects through 3DP using software such as Solidworks or Rhino, and the design can directly influence the shape-changing effects. The thickness can also be used to adjust the activation time because it takes more time for thicker panels to reach T_g and go into the soft glassy state (van Manen et al., 2017). Therefore, the printing process, including nozzle temperature (T_p), nozzle height (L_p), geometric thickness (H_p), fill factor, and fill angle (θ_f), affects shape memory performance (Wang et al., 2019). Wang et al. (2019) showed an experiment of sequentially blooming petals blooming by applying printing parameters such as sample thickness, nozzle temperature, and layer thickness to show the effect of printing parameters. After the digital 3D object is modelled, print slicing is essential. According to several studies, various influences can be exerted on the shape-changing effects in the print slicing stage (Tanveer et al., 2019; Goo et al., 2020). Parameters that can affect the shape change in this print slicing step include control of the print pattern, angle, infill density, print speed, layer thickness, and build orientation of the modelled object. The slicing step is a process for controlling the G-code used to print the designed 3D object, and it can more precisely specify the 4DP structure. It can greatly influence the shape-changing effects according to the specified design. For example, the printing path orientation determines the shrinking direction, and the printing layer thickness also affects the shrinkage ratio as the filament material property significantly changes according to different shrinkage ratios (Yu et al., 2020). Additionally, the bending angle can be programmed by controlling the print pattern and number of layers (Zolfagharian et al., 2018). The 3D modelling and print slicing steps can be integrated into CAD, which is required for designing the material distribution and structure needed to achieve the desired shape, characteristics, or functional changes in 4DP. More theories and numerical models need to be developed in order to connect the four key elements of material structure, desired final form, material properties, and irritating properties. 4DP requires a more accurate mathematical process than 3DP. 4DP can also be exposed to external stimuli through interaction mechanisms, and mathematical CAD modelling programs can be used to properly manage this process. According to Gladman et al. (2016), mathematical modelling in 4DP printing can be divided into two categories, which are defined as two main problems: forward and reverse. A forward problem considers the material structure, material properties, and stimulation characteristics needed to determine the final desired shape, while an inverse problem ultimately determines the CAD and print slicing parameters according to the final desired shape, material properties, and stimulus properties. 4DP printing studies that

include inverse problems are application-driven in that the focus is on achieving the desired function or shape. Therefore, to control the effective shape change effect, a strategy can be devised to properly apply elements of the two categories of 4DP parameters. There are important elements in applying CAD modelling to the 4DP process. The first is the printing pattern, which are different patterns that are applied depending on the shape deformation required. Moreover, the printing pattern can have a direct impact on the printing time, hardness or softness, and stretch force (Wu et al., 2018). The second is the build structure, which affects overall features such as angle, thickness, and size (Wang et al., 2019). Just like the printing pattern, this element can directly impact time, hardness, and stretch force. Lastly, the number of layers can be limited according to the required shape deformation. As with the printing patterns, different patterns can be applied depending on the required shape deformation. These elements of CAD modelling of 4DP can be used to create various shape deformations and shape change positions and can be used to control the shape changing sequence.

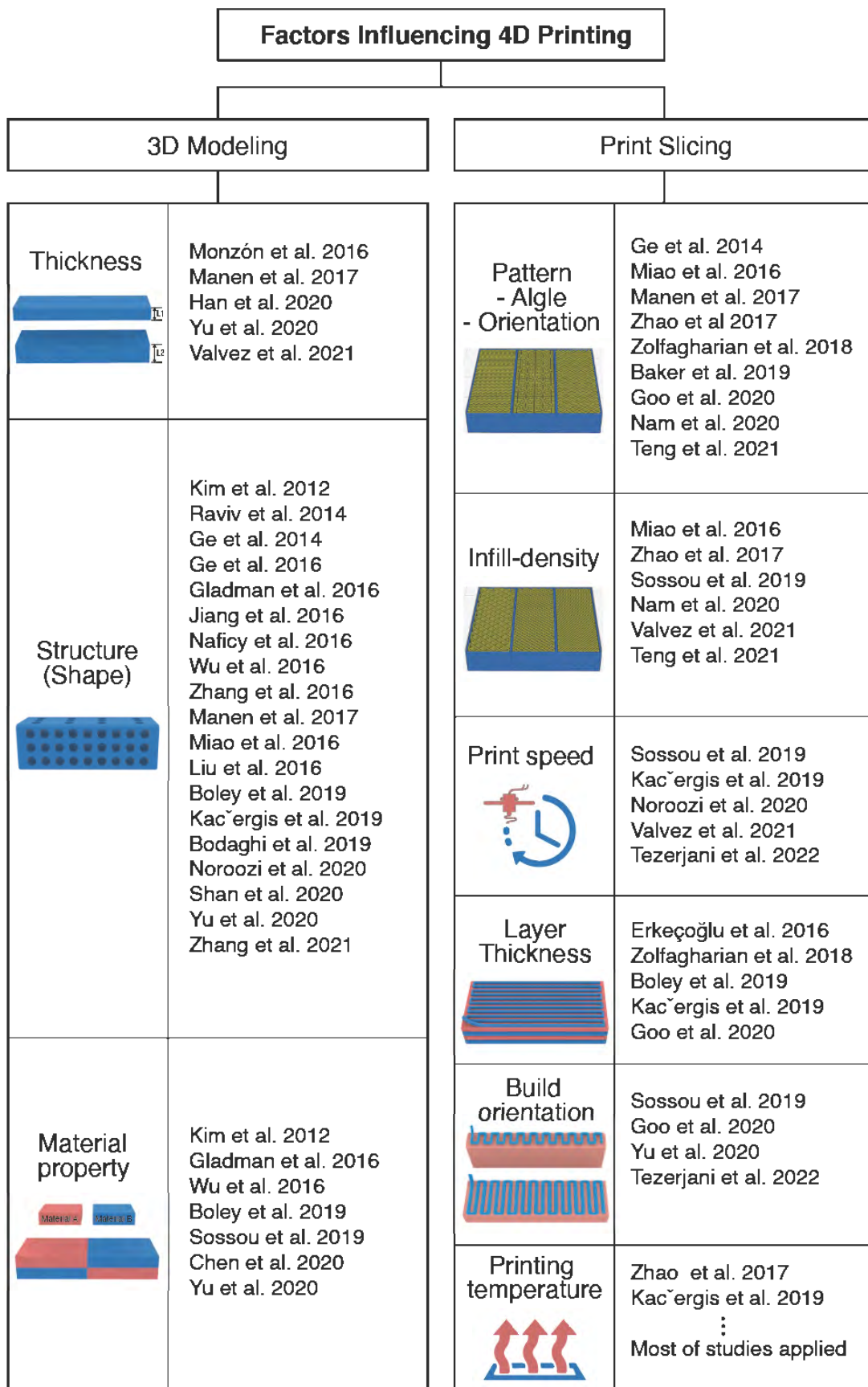


Figure 2-37. The different parameters of 4DP.

2.6 Chapter Summary

This chapter provided a general overview of the fundamental elements of 4DP, including the relationship between the AM processes, stimuli, stimuli-responsive material, interaction mechanisms, and CAD modelling. Against this background, a comprehensive review of shape-changing behaviours in 4D-printed parts that can be achieved using SMPs and an overview of the various shape-changing behaviours were provided. In addition, shape change behaviour, the main contribution of this chapter, is defined as single shape change behaviour, complex shape change behaviour, and combination shape change behaviour. These three major shape change behaviours were summarized as a taxonomy. This chapter also provided an understanding of the essential elements of 4DP and their impact on the characteristics of 4DP structures and shapes. Designing features of 4DP components allows for the creation of simple structures with complex parts before they are activated. When enabled, 4DP components can be returned to their original shapes. One of the most important factors in 4DP is understanding the effectiveness of shape changes according to three main factors: parameters, types of smart materials, and CAD modelling. Figure 2-38 illustrates the impact that CAD modelling, parameters, and SRMs have on 4DP shape-changing behaviours based on the 4D print shape change process.

The following chapter introduces the methodology applied in this study and explains why various research methods were selected. Furthermore, it presents a research plan with specific descriptions of the various studies, including the details of each research component and their contribution to the research objectives, and it also details the research strategies and techniques employed at different stages.

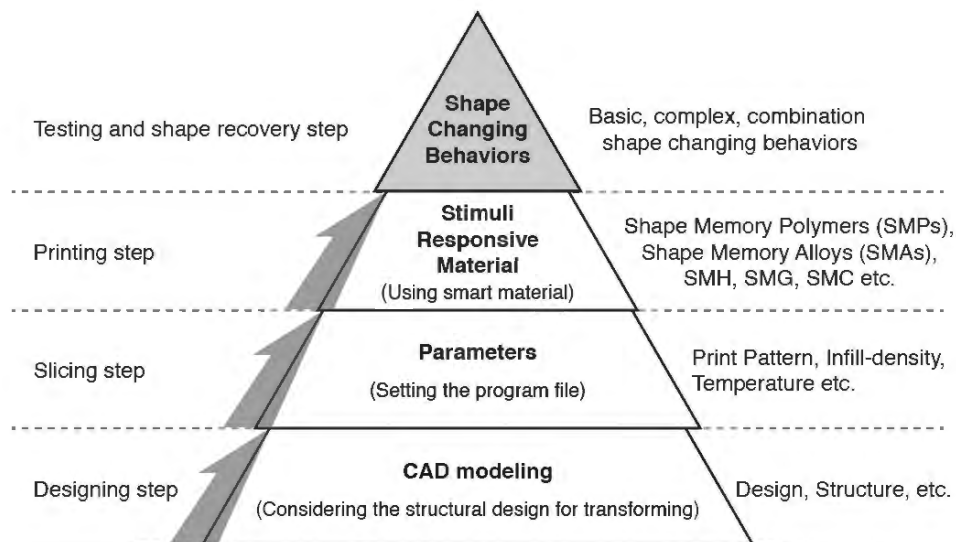


Figure 2-38. The elements of essential shape-changing behaviours in 4DP.

Chapter 3. Research Methodology

3.1 Introduction

This chapter describes research methods to provide a review of the research questions and objectives. Introduces the research methodology adopted by the study to find the answer to the research question. This study used quantitative secondary research and qualitative primary methodologies to achieve the objectives. Table 3-1 describes the research methods adopted to attain the research results, and it also details the research process, from problem identification to research evaluation.

In the initial stage of this study, quantitative data collection methods were mainly used to attain an in-depth understanding of the research topic in order to ascertain the related theories. A qualitative method was then used to determine and generate hypotheses and ideas for the research. In addition, quantitative data collection methods were used to verify the research results in the form of numerical and data analyses of the direct experiments. The quantitative data were collected using a literature review, experiments, questionnaires, and a survey. Chapter 1 provided an overview of four-dimensional printing (4DP), shape memory polymers (SMP), and shape-changing behaviours in 4DP, and it included a literature review on the current problems and solutions in the field in order to contribute to the understanding of the current research.

The perceptions and knowledge about the components as well as their influence on the in-depth exploration of the research topic and the classification of shape-changing behaviours of 4D-printed parts, such as bending, twisting, folding, and the like, were collected as quantitative data, which are detailed in Chapter 2. These data were then used to inform the subsequent literature review and interviews, which were used to derive the analyse the data. An overview of SMPs and their various shape-changing behaviours is also provided.

Based on the collected data, the effect of various smart materials and printing parameters on the Shape Memory Effects (SMEs) was discovered through experimentation. In addition, suitable materials and parameters that were used in the in-depth experiments in this study were derived from numerical data, and the experiment used a deductive approach.

The results derived from the in-depth investigation and initial data output were classified according to the results derived from the experiments detailed in Chapter 4. These results provided an in-depth understanding of the ways in which to control the SME through the use of printing parameters and how these parameters can affect the SME. 4DP tools that can influence SMEs through classified printing parameters were created and tested to yield quantitative data. The ways in which to more effectively control SMEs is then discussed, which includes developing tools created by the results of the experiments. This knowledge will help users gain an in-depth understanding of how to control printing parameters and how they affect them. Finally, the conclusion ends the study with a review of the main findings. The contributions made by and the limitations of this research are also discussed, and suggestions for future research are made. Quantitative data was analyzed in different approaches to clarify research answers and refine research findings. Each data derived from the experiment was

simplified by selecting and categorizing. And then using Excel, the evidence was organized into text, matrix, graph and chart format and displayed for calculation and analysis.

Table 3-1. Methodology for collecting and analysing the data.

Table of contents	Methodology used	Research phase
Chapter 1. Introduction		Research exploration and review
1.1 Introduction	Literature review	Chapter 1 provides an overview of the research and uses the literature to identify the problems. The overall structure of the thesis is also explained.
1.2 Research Aims, Questions, and Objectives	Literature review	
1.3 Thesis Structure	N/A	
1.4 Chapter Summary		
Chapter 2. Literature Review		
2.1 Introduction	Literature review	Chapter 2 details the theoretical knowledge of 4DP technologies and processes, SMP properties and SME processes, printing parameters, and shape-changing behaviours. The types of shape-changing behaviours that can be achieved with 4DP are also identified.
2.2 Additive Manufacturing and 4DP	Literature review	
2.2.1 An Overview of Additive Manufacturing		
2.2.2 4DP		
2.2.3 Using the 4DP Process for Shape-Changing Behaviours		
2.2.4 Current Application of 4DP		
2.3 Shape Memory Polymers (SMPs)	Literature review	
2.3.1 Overview of SMPs		
2.3.2 Characteristics of SMPs		
2.3.3 Stimuli and SMEs		
2.3.4 The SME Process in 4DP		
2.4 Shape Change through 4DP	Literature review	
2.4.1 Basic Shape-Changing Behaviours		
2.4.2 Complex Shape-Changing Behaviours		
2.4.3 Combination Shape-Changing Behaviours		
2.4.4 A Taxonomy of Shape-Changing Behaviours		
2.5 4DP Parameters of the Shape Change Effect	Literature review	
2.6 Chapter Summary		
Chapter 3. Research Methodology		
3.1 Introduction	Literature review	Chapter 3 explains the methodological approach used in this research and the various research methods that were adopted.
3.2 Research Methods	N/A	
3.2.1 Literature Review	N/A	
3.2.2 Experimental Work 1		
3.2.3 Experimental Work 2		
3.2.4 Questionnaires, and Surveys		
3.2.5 Validation		
3.3 Chapter Summary		
Chapter 4. Study One: Evaluating. Material Selection		
4.1 Introduction	Literature review	Chapter 4 discusses how research goals 4 and 5 were achieved. PLA materials were

Chapter 7. Design and Development of Toolkit		Development, revision, and evaluation
7.1 Introduction 7.2 A Graphic Representation of the toolkit 7.3 The Initial 4DP Web Toolkit 7.3.1 Scenario 7.3.2 The 4DP Web Toolkit 7.4 The Finalisation of the 4DP Web Toolkit 7.4.1 Questionnaire 7.4.2 Results from the Questionnaire 7.4.3 Scenario 7.4.4 The Final 4DP Web Toolkit 7.5 Validation 7.6 Chapter Summary	Literature review Questionnaire and survey Experiments	Chapter 7 describes the processes necessary for developing the graphical and physical shape recovery control table developed physical version of the into the web version. It details the development, modification, and evaluation of the experimental results from which SMEs can be derived using selected materials and printing parameters.
Chapter 8. Conclusion		Conclusion
8.1 Introduction 8.2 Summary of work to answer the reserch questions 8.3 Contributions of the Research 8.4 Limitations of the Study 8.5 Recommendations for Further Research		Chapter 8 concludes the thesis by comparing the key research findings against the aim and objectives. The contributions and limitations of the research are also discussed, and avenues for future study are identified.

3.2 Research Methods

This section begins with an explanation of the method most used in this study: individual experiments. This study used individual experiments because the topic being studied requires detailed and complex explanations and analysis aimed at understanding the problems of the given phenomena. Collecting numerical data was of paramount importance in this study as the amount of numerical data could have reduced the experimental variables. Therefore, quantitative research methods in the form of direct experiments were mainly used to attain more numerical results. Analysis of many quantitative studies affects a small number of variables (predetermined dependent or independent measures) (Damico et al., 1999). In addition, based on the collected numerical data, participants for evaluation were subjected to a process of experiencing and evaluating the entire process. Most participants had the opportunity to respond with more elaborate and detailed responses than they would have in usual methods (Ragin, 1987).

Inclusive data was collected through secondary research methods, and the findings were used to provide a better understanding of the research topic and to form the detailed primary research plan by using it to determine the scope of knowledge and the framework in this study. Primary research was crucial for exploring the effects of shape change through printing parameter design within product design and the effects of shape change through SMPs when 4DP parts. Since the shape change behaviour that can be implemented by 4D Printing has been mentioned individually in several papers, it is necessary to classify and classify the shape change behaviour. Therefore, it is derived through data research and expert interviews to organize the types and definitions of shape-changing behaviour that can be implemented with 4D Printing and the recorded shape memory shape. In addition, the types and definitions of print parameters that can affect the shape recovery effect were classified, and the SMEs was derived through

direct experiments. The experiment was conducted as a water bath experiment, and detailed procedures and explanations are mentioned in 3.2.2.

And also quantitative research was used to develop a 4DP tool that can be programmed using the technology contained within the components. Primary research was used to discover and develop the key factors required to improve the guidelines for efficient printing parameter programming when designing 4D-printed parts. Quantitative methods were used for the data collection and analysis processes as qualitative methods provide more insightful and practical information by providing specific results. Thus, this study primarily investigated the effect of shape changes by applying appropriate printing parameters. This was done by conducting a review of 4D-printed parts' bending transformations that can be achieved using SMPs, particularly polylactic acid (PLA). It also provides design directions that can be used to predict shape changes through appropriate printing parameter design.

3.2.1 Literature Review

The main purpose of this literature review is to provide an in-depth understanding of the research context by providing an overview of 4DP, the SMPs, the shape-changing behaviours in the 4DP process, and the printing parameters. In other words, the four major sections of the literature review are as follows: (1) an overview of 4DP studies in order to identify the comprehensive Additive Manufacturing (AM) and 4DP technology, which includes a description of the 4DP process, the fundamental elements of 4DP, and the influence of 4DP elements; (2) an analysis of the differences and similarities between SMPs and smart materials, such as shape memory alloys (SMAs), as well as a detailed overview of the shape-shifting effect, the stimulus that induces shape-shifting, and the general process from the stimulus to the recovery of the shape; (3) an investigation of shape-changing behaviours in 4DP in order to provide a comprehensive review of transformational shapes and structures that can be achieved in 4DP, the influences thereof, and the existing studies. Identifying the different types of shape changes that can occur in 4DP is important for experimental research as it increases the possibility of future research conducted to identify the various shape-changing behaviours; and (4) a discussion on the ways in which to understand and apply the various printing parameters. For example, the use of different printing patterns and different building-process and layer-construction methods could influence the shape change effect in 4D-printed parts.

3.2.2 Experimental Work 1

The experimental work comprises four parts. Figure 3-1 shows the PLA experiment process, which details the steps necessary for performing an experiment 2 based on the results from the first to third experiments. Experiment 1 reviewed PLA material selection tests in order to compare different types of PLA filaments and determine the suitable PLA material needed for 4D-printed parts through a water bath experiment (Chapter 4). Experiment 2 compared the three-dimensional (3D)-printed PLA samples to the selected PLA samples from Experiment 1. These selected PLA components were printed directly, and the suitable PLA for 4D-printed parts was determined through a water bath experiment (Chapter 5). Experiment 3 reviewed the 3D-printed PLA samples of various printing parameter tests in order to determine the characteristics of printing parameters and to compare each parameter's SMEs. The printing

parameters included print orientation, print speed, print thickness, infill density, and print pattern (Chapter 5).

Lastly, Experiment 4 reviewed 12 3D-printed PLA patterns and conducted an infill density test to determine and compare the different patterns' and infill densities' SMEs (Chapter 6). All four parts of the experiment were conducted using a water bath experiment. These experiments discussed and validated the effect of printing parameters on shape recovery. For example, in 4DP programming, the use of different print patterns, building processes, and infill densities (layer composition) can affect different areas of design and engineering by controlling 4D-printed parts' recovery rates and recovery states.

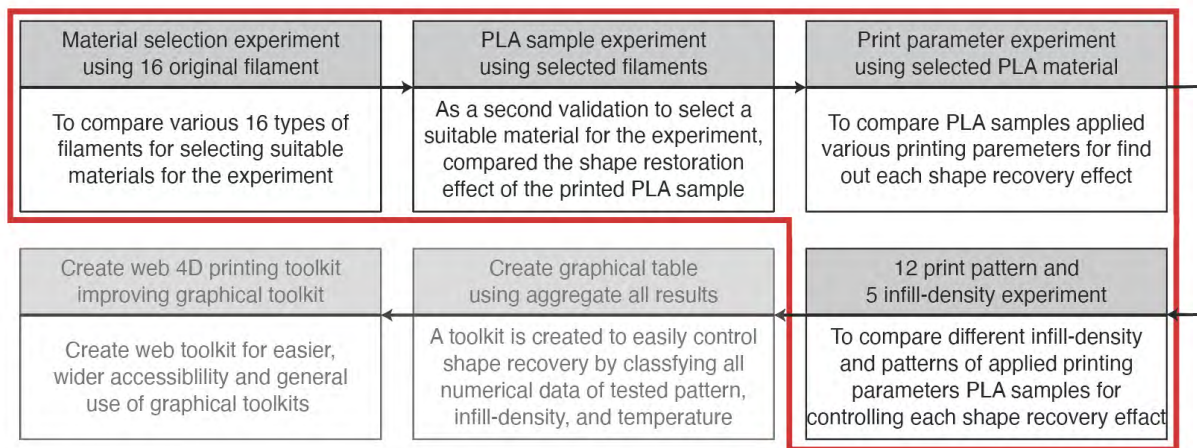


Figure 3-1. The initial PLA experiment process.

- Main experimental facilities

The experimental facilities in this study were based on a total of three experimental processes: sampling through 3D printing (3DP), programming of samples, and testing for results. Firstly, the use of 3DP is inevitable when implementing 3D samples. This study focuses on material extrusion (MEX) types was selected as the 3D printer. MEX printers extrude plastic filaments layer by layer onto a build platform. It has the advantage of being able to create a physical model at a low cost easily. Since the purpose of this study is to determine a method of 4DP that anyone can easily access, the low-cost Qidi X-Pro 3D printer, which can be easily obtained, was used in this study. Shape memory materials (SMMs) were also required. In particular, this study focuses on low-cost PLA, which is easily available in the market. In the material selection experiment, a total of 16 different filaments were used, and a filament for sampling was selected and used throughout the experiment. Secondly, particular software was required, which was provided by 3D Print and used to adjust the numerical values of each parameter. The application used for parameter adjustment was Qidi Print Slicer, which was provided with the Qidi X-Pro 3D printer, although other third-party programs such as Cura and Simplify3D are also compatible. Finally, a water bath experiment was performed to confirm the SMEs of the original filament and the sampled object. For the testing, the sample's deformation temperature and recovery temperature had to be measured. Since it was important to keep the temperature constant, an infusion heater was used to maintain the deformation and recovery temperatures consistent (see Figure 3-2). The same topwater was used for uniformity and

objectivity in all experiments. In addition, experiments were conducted in the same experiment space and time to establish a similar environment for all experiments.

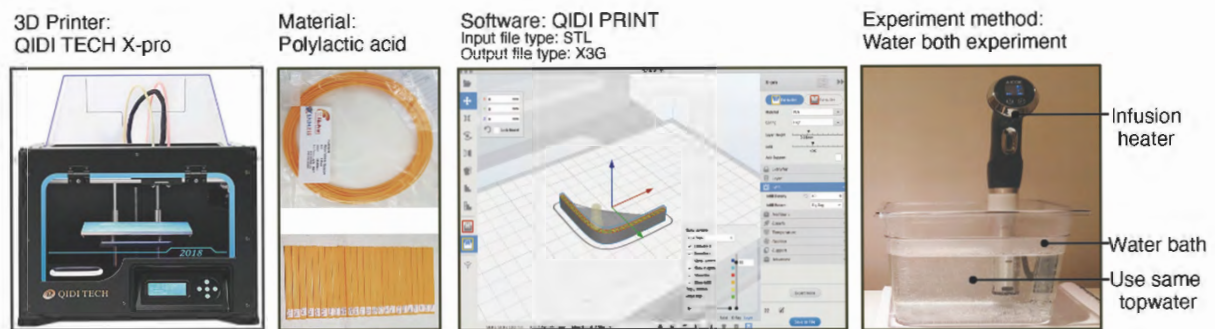


Figure 3-2. The experimental facilities.

- The process for the water bath experiments

Water bath experiments such as the work of Loh. (2022); Teoh et al. (2018); Spiegel et al. (2022), are commonly used for shape change and recovery of 4D Printing parts. In the water bath experiments, the infusion heater is used to precisely control the water temperature in the water bath to maintain a constant temperature so that accurate experimental results can be measured. This water bath experiment included the filament selection experiment from the experimental work 1 and 2. There were four main steps to this water bath experiment through sampling. Step 1 was using the Qidi X-Pro printer to produce PLA samples, which included creating structured samples by converting and sending them to 3DP applications that use various 3D modelling programs, such as Solidworks, CATIA, Rhino, Inventor, 3D MAX, Sketch UP, and Blender. Step 2 was the programming phase, which entailed placing the PLA sample in a water bath for 1 minute and then deforming its shape. This is because PLA samples exposed to high temperatures change their ductile properties and can be deformed into desired shapes. Stage 3 was the cooling stage in which the deformed PLA sample was cooled at room temperature for 1 minute. PLA samples that had changed their intended shape due to their ductile nature gradually became brittle at room temperature. Stage 4 was the recovery stage in which the bath temperature was set to the recovery temperature, and the deformed PLA sample was placed into the water bath. Samples with brittle properties that were hardened become ductile again through high temperatures and returned to their original shape. The final step was analysing and recording the shape recovery results of the PLA samples. A video camera was used to document the entire process of the water bath experiment (see Figure 3-3).

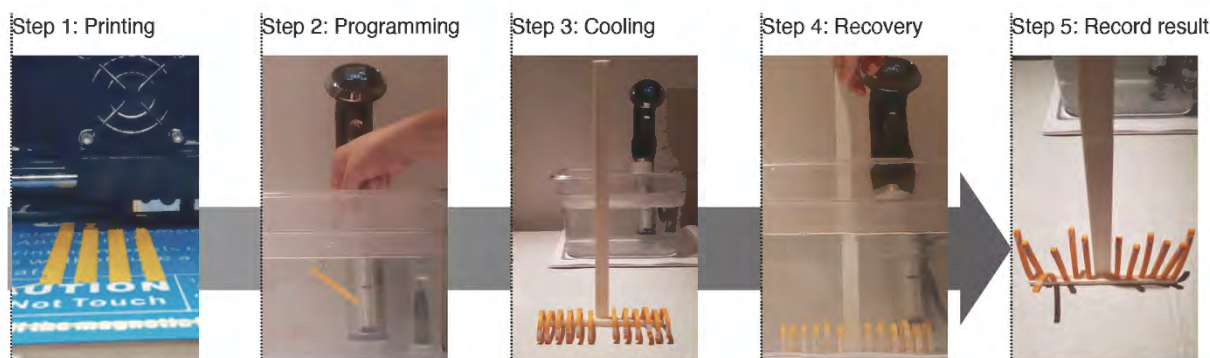


Figure 3-3. The process of the water bath experiments.

3.2.3 Experimental Work 2

The main purpose of experimental work is to gain an in-depth understanding of the topic of study through the results derived from the experiment (Chapter 6 and 7). The results of the water bath experiments, including material selection tests for bending deformation, 3D-printed PLA sample tests, and various printing parameters tests, provided a better understanding of the scope of this research. However, early experimental studies have limitations. Due to the limited number and quality of samples used to provide these results, further study of the trends identified in this study is required. Therefore, it was necessary to analyse the experiment 2 for more accurate predictions and applications of in-depth printing parameters for 3D-printed parts. For example, the determination of the optimal parameters through applying the maximum number of cases to each pattern, infill density, and recovery temperature can significantly impact shape recovery control. A parametric control strategy in 4DP programming was important for creating various samples efficiently. The number of cases could be obtained from various experimental data and was also important for intelligent computer-aided design. Thus, it determined which printing parameters were effective for shape deformation and recovery rate. In addition, it was applied to a simple sample through the collected data, and, based on the data, a guideline for designing 4DP parts using SMP was created. To fulfil this important purpose, this study used the collected data to assist designers when designing 4D-printed parts, develop guidelines for demonstrating printing parameter control programs in product design using 4DP SMPs, and conduct further extensive experimental studies. From design concept to prototype, this study directly impacts the 3D modelling of various programmed methods in terms of shape change and recovery effects. Moreover, it can also be used to create a framework for the design of 4D-printed parts.

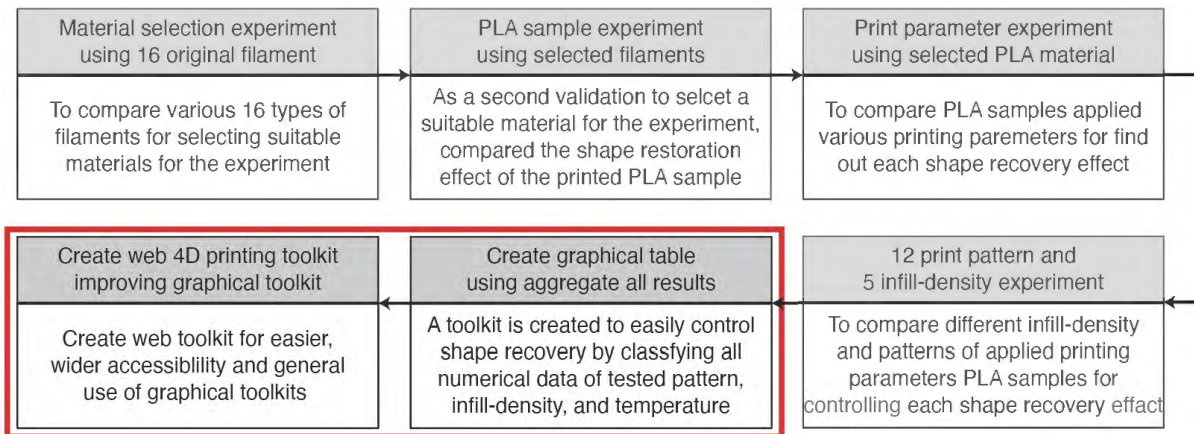


Figure 3-4. The in-depth PLA experiment process.

3.2.4 Questionnaires, and Surveys

Questionnaires are a simple and direct research method. This study needed this direct methodology because applying printing parameters could have easily resulted in various methods of shape change and making more closed results by reducing time and profit, and it required accurate programming. The aim of the Questionnaire is to analyze design direction which can predict effect of shape change though appropriate controlling shape recovery design. It can also be used to determine the printing parameters that are effective for various methods of shape recovery and change. Moreover, it can be used to understand and predict the application of specific products, such as flat packing, through using the collected data to create a guideline for designing 4D-printed parts using SMPs. They were also used to conduct experimental testing and evaluate the outcome of this research by ensuring feedback and modifying the programmed designs according to the results. The participants who completed the questionnaire were experts in various fields of 4DP.

3.2.5 Validation

In order to verify the results of each experiment, samples were made and tested by applying the results derived from each experiment. A simple 4DP sample was created and verified in a water bath experiment. For example, the infill density and pattern experiment in Experiment 4 yielded various SMEs for the pattern and infill densities. These derived patterns and infill densities were then combined into one sample and re-verified to determine whether they were similar to the data for the existing SME. This validation thereby comparing the results derived through the experiment with the extended sample to which each derived result is applied, the accuracy of the experimental results or the limitations of the experiment are determined and discovered.

3.3 Chapter Summary

In this chapter, the research methodology was explained, and the rationale for choosing this methodology was presented. It also detailed the research plan by providing specific descriptions of the various studies, including details of each research component and their contribution to the research objectives, and it also presented the research strategies and

techniques employed at different stages. The research methods selected were literature reviews, expert interviews, questionnaires and surveys, experiments 1, experiments 2, and evaluations, all of which allowed reliable and valid data to be collected. This aim of this review was to determine the deformation shapes and structures that CAD can achieve for 4DP and design modelling of 4D-printed parts. Little research has been conducted to determine and implement strategies that use shape-changing behaviours. The print slicing factors that affect reshaping behaviour include print pattern, infill density, print speed, and direction. Therefore, in the next chapter, SMEs (recovery quality and time) are identified by focusing on parameters that can affect the SMEs of 4DP.

Chapter 4. Study One: Evaluating Material Selection

4.1 Introduction

This section aims to fulfil research objective 4. This chapter will provide an understanding of the key areas of this research through discussing the results derived from the experiments. This chapter has the main focus: Conducting an experiment to select suitable material for this study. Section 4.2 details the material selection criteria used to select the shape memory polymers (SMPs) that were used for the experiment. These criteria were used to record the SMEs of the SMPs as numerical data and same applied in all experiments. The criteria include the SMPs' recovery quality, and recovery time, which were measured based on the numerical data for the SMEs according to applied deformation, deformation rate, deformation temperature, and recovery temperature. Section 4.3 reviews the polylactic acid (PLA) material selection tests used to compare different types of PLA filaments and to determine the suitable PLA materials needed for four-dimensional printing (4DP) through a water bath experiment. For material selection, 16 different filaments were selected, and the SMEs of the original filament test were compared.

4.2 Determining SMEs and Measurement Criteria

4.2.1 Determining SMEs

SME experiments were performed using material extrusion printed PLA samples according to the SME experimental process for PLAs employed by Wu et al. (2017). The SME experimental process using PLA (see Figure 4-1). Shape-memory functionalisation can be realised for polymer-based materials with an appropriate morphology by applying a specific shape-memory creation procedure. A material's SMEs are affected by many factors, including composition, applied deformation, deformation rate, deformation temperature, and recovery temperature (Wu et al., 2017). Therefore, this experimental process included programming, cooling, and recovery. Programming the PLA filaments and 4D-printed sample began with changing the temperature of the water. The water bath was heated to the deformation temperature using an immersion circulator. The PLA samples were placed in a water bath for 1 minute and then deformed to the bent shape using a flexural device. The deformed PLA samples were allowed to cool for 1 minute at room temperature after fixing the flexural device, and the recovery of the PLA restored its original permanent shape. After the PLA samples were completely cooled down and programmed, the water bath temperature was set to the recovery temperature. The deformed PLA samples were then placed in a water bath, and shape recovery experiments were recorded using a camera. A visual summary of the SME process is shown in Figure 4-1.

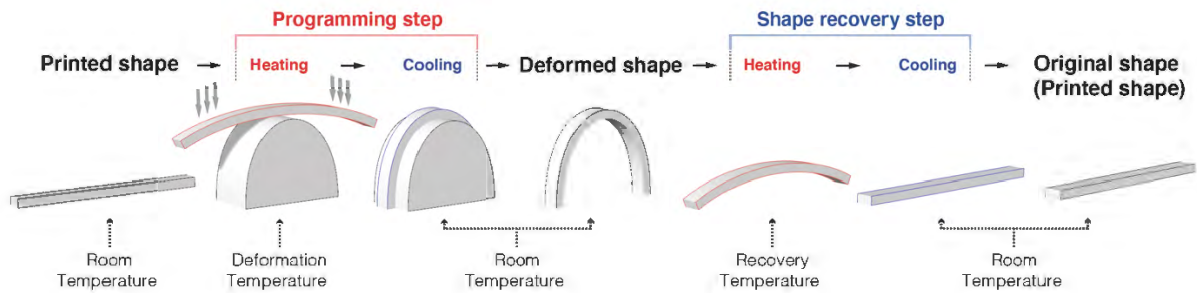


Figure 4-1. The processes involved in the SME.

4.2.2 Measurement Criteria

In order to derive more accurate results, the criteria for measuring the shape-memory recovery rate needed to be applied. The shape recovery rate measurement was compared by measuring the recovery quality and recovery time. Two methods were used to ensure consistent results. Firstly, since the experiment for filament selection tested the original filament, the recovery rate needed to be measured according to the inherent thickness of the filament. Since the thickness of the filament was 1.75 mm, it was measured based on the bending part of the filament to measure the detailed bending curvature. Therefore, in this experiment, the recovery effect was applied and measured to position the curved line upward (see Figure 4-2). It was divided into nine grades, starting with grade 1, which had the highest SME, and ending with grade 9, which had the lowest SME. All filaments were cut to the same size. More details will be mentioned in sections 4.3.1.

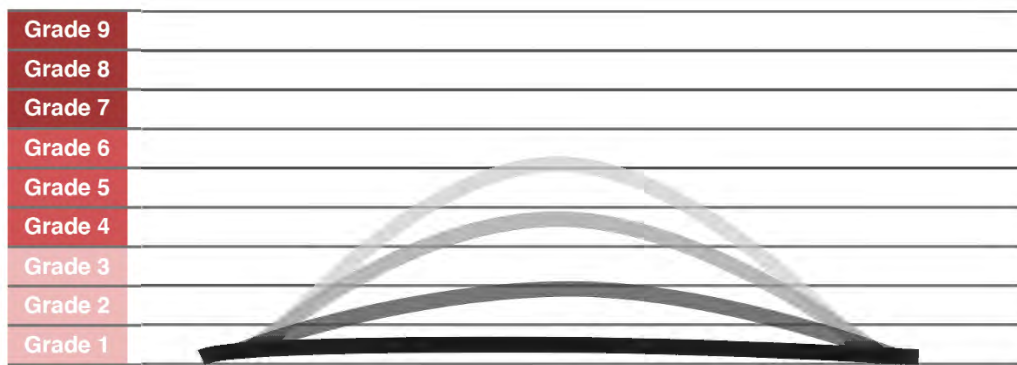
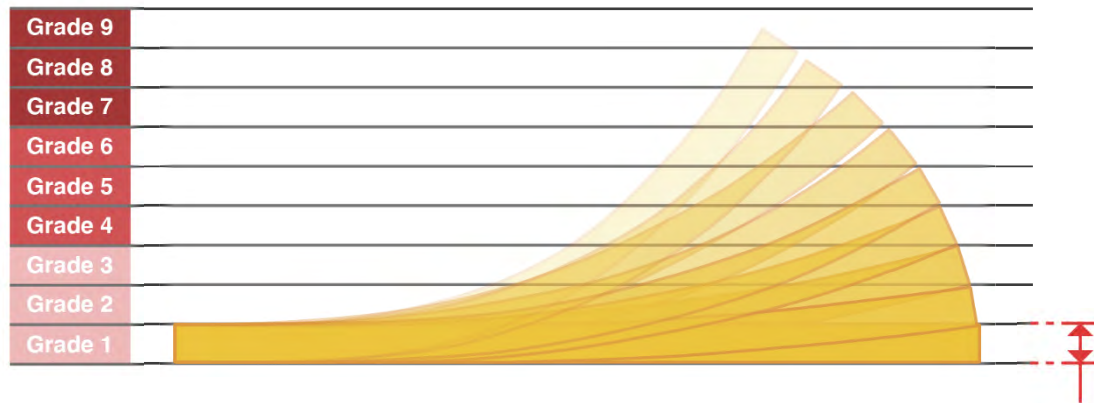


Figure 4-2. The filament recovery grade measurement criteria.

Secondly, the 4D-printed samples were graded sequentially according to their thickness when they were in bar form, and the slope of the restored curve was measured. The thickness of the printed bar form sample was 3 mm, so it was measured based on the angle of curvature. Grade 1 recovery quality equalled the thickness of a flat 4D-printed sample that was recovered. This experiment was evaluated by applying the measurement criteria shown in Figure 4-3. Like the filament test, it was divided into nine stages, from grade 1, which denoted a high shape-recovery effect, to grade 9, which denoted a low shape-recovery effect. All of the 4D-printed samples were the same size.



Recovery quality grade 1 equals the thickness of a flat 4D printed sample

Figure 4-3. The PLA specimen recovery grade measurement criteria.

To record and grade the shape-recovery effect, a grading system was devised: Grade 1 represented excellent recovery, indicating a return to its original shape; and grade 9 represented no recovery. Therefore, a grade 1 rating indicated the best achievable recovery quality. This was an important step in quantifying the SMEs.

The above two methods are methods that were used to attain consistent results in terms of measuring the slope of the restored curved shape. However, when the measurements were applied to the same location, the accuracy in measuring the thickness of the sample was lowered, and two measurement methods were considered according to the thickness of the samples. The latter measurement method was applied to all subsequent experiments.

4.3 Material Selection

4.3.1 An Overview of the Examination of the Selected Filaments

As mentioned in Chapter 3, one of the essential elements of 4DP is a material that responds to stimuli. These materials are often expensive and are difficult to use or develop directly. This can limit the accessibility and potential of 4DP. Therefore, access to a wide range of materials that can be obtained easily and inexpensively is important. The Qidi X-Pro 3D printer used in this research recommended 1.75mm filament. There is also a wider range of accessible materials, and many proprietary filaments ranges made only for 1.75mm, adopting 1.75mm filament, which is readily available and has the advantages of faster print speed and better control over the amount of filament. The first experiment consisted of a material selection protocol that was used to compare 16 types of commercially available PLA materials and select suitable PLA filaments. Figure 4-4 defines the SME process identified through material experiments. The shape recovery rate and time taken for the shape-changing process of the specific filaments and their return to their original shapes were determined, and the experiments were repeated for more accurate results. Figure 4-5 details the filament experiment.

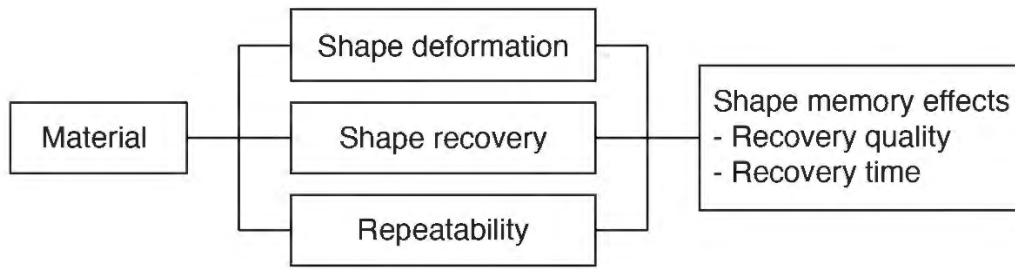


Figure 4-4. The processes involved in the SME.

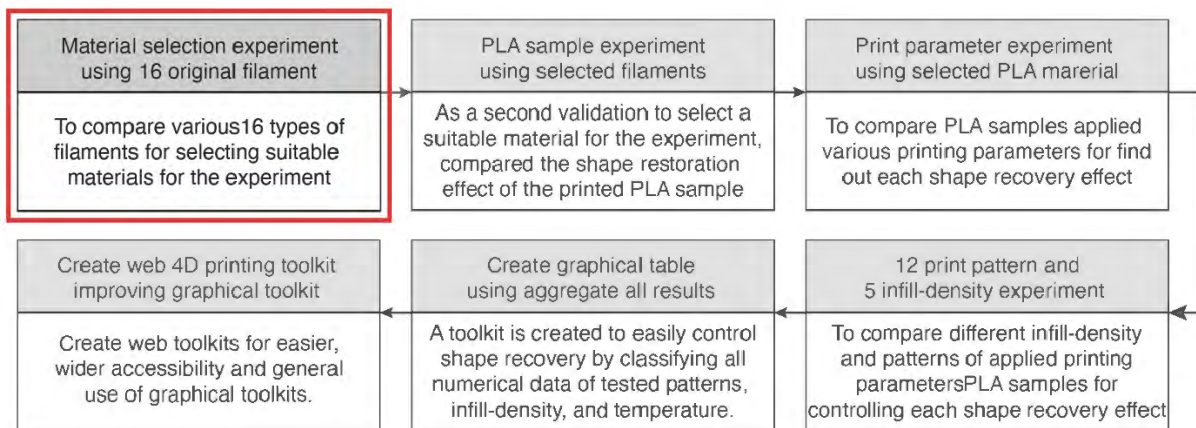


Figure 4-5. The process for the material selection experiment.

As shown in Figure 4-6, 16 types of PLA were purchased from different material suppliers and were labelled as A through to P. As the number of filament manufacturers increases, the price is also considerably lower due to competition from manufacturers to sell popular filaments. 3D printer materials, such as powder and metal materials, require a high cost of more than \$500 for the same amount. However normally, PLA filament can expect \$10 – \$40 per kg of spool. It has a wide range of prices from expensive filaments with special finishing to low-cost filaments with basic colors, but overall high cost is not required. These materials were universal branded materials that anyone can easily purchase. The prices were also low without much difference between them, so the materials were easily available. This research used filaments priced at ±\$40. Notably, 1.75 mm filaments were used, and they had a melting point of 180–210 °C when used in the printing. To ensure consistency in the test results, each reel of material was cut into 80 mm-long strips. The recovery quality and recovery time were simultaneously measured in order to determine the shape-recovery effect.

















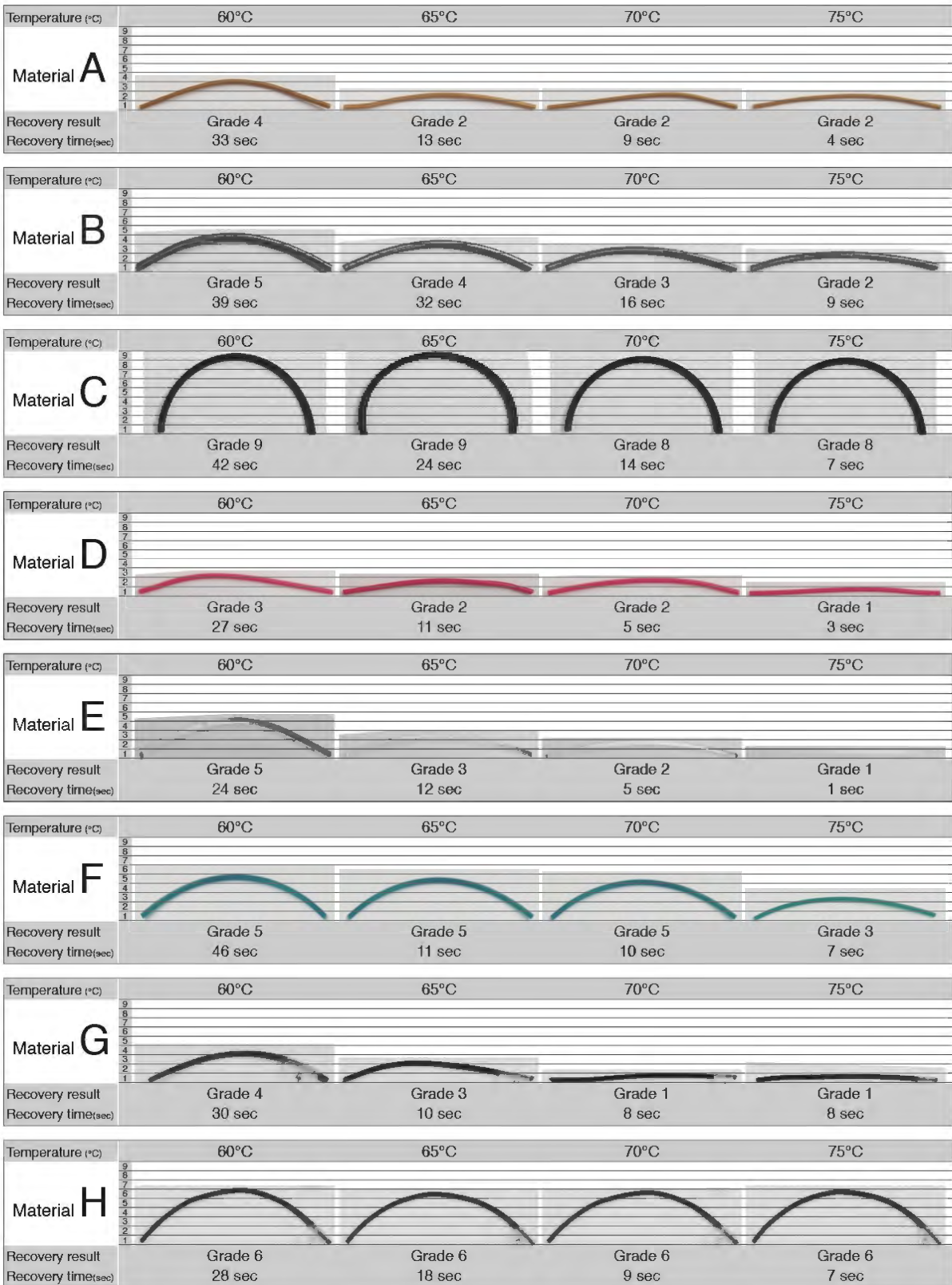
No.	16 Filaments	Manufacturers	Printing Temperature	Image
1	Material A	Filament PM	200–220 °C	
2	Material B	3D JAKE	195–215 °C	
3	Material C	ColorFabb	195–220 °C	
4	Material D	Bq	200–220 °C	
5	Material E	Kyoraku	195–220 °C	
6	Material F	Dremel	180–230 °C	
7	Material G	FlashForge	195–220 °C	
8	Material H	AMZ3D	180–210 °C	
9	Material I	Pxmalion	190–210 °C	
10	Material J	Prusa research	190–210 °C	
11	Material K	FilaPrint	180–210 °C	
12	Material L	Utsaline 3D	190–210 °C	
13	Material M	Fiberlogy	200–210 °C	
14	Material N	Fillamentum	190–210 °C	
15	Material O	3Dom	195–210 °C	
16	Material P	Qidi tech	180–220 °C	

Figure 4-6. The 16 different PLA samples.

4.3.2 Comparison of the 16 PLA filaments

This experiment referenced the procedures described in Wang et al. (2018) and Wang et al. (2019). For a more accurate experiment, a simple test was conducted to set the recovery temperature of the filament before the full-scale experiment. It was found that the shape recovery was not performed well at a low temperature of 60° or less. And it was difficult to measure the recovery time at too high a temperature above 80° due to too a fast shape recovery. Therefore, the experiment was conducted by setting a recovery temperature of between 60 °C and 75 °C, which was judged to be suitable for the experiment. In the water bath experiments, hot water was used to trigger the filaments and the 3D-printed samples used in this experiment. The programming of PLA filaments started with changing the temperature of the water. Most of PLA filament specimens achieved a rubbery state at 80 °C and could be easily and effectively fixed into programmed bending shape. Therefore, the water bath was heated to the shape deforming temperature (Td) of 80°C using an immersion circulator. Sixteen different PLA filaments that were cut to 80 mm in length were placed in a water bath for 1 minute and manually deformed into a bent form using a bending device. The modified PLA filaments were fixed by natural cooling at room temperature for 1 minute. After that, the temperature of the water bath was changed the recovery temperature in order to restore the shape of the fixed filaments. Four recovery temperatures of 60 °C, 65 °C, 70 °C, and 75 °C, determined by the glass transition temperature (Tg) of the PLAs used in this experiment, were tested, meaning that there were four samples of each material in order to test each recovery temperature for a total of 64 PLA filaments. As shown in Figure 4-7, more than 64 instances of numerical data were collected for the various properties of the 16 PLA filaments, and the four recovery temperatures were analysed and mapped based on the recovery quality and recovery time. All temperatures were maintained for a maximum of 2 minutes in order to determine the recovery

effect and classify the highest recovery rates from grade 1 to grade 9. The shape-recovery grade was determined by the difference between the original and recovery deformation. It is an important characteristic for the quantification of SMEs. A flat shape indicates good recovery quality. This section evaluates the recovery quality and time of recovery through analysing the different characteristics of various PLA filaments and the recovery temperatures of the PLA filaments. The deformed PLA filaments were placed in a water bath, and shape recovery experiments were recorded using a video camera mounted on a tripod. Efforts were made to ensure that the tests performed were consistent across all of the samples.



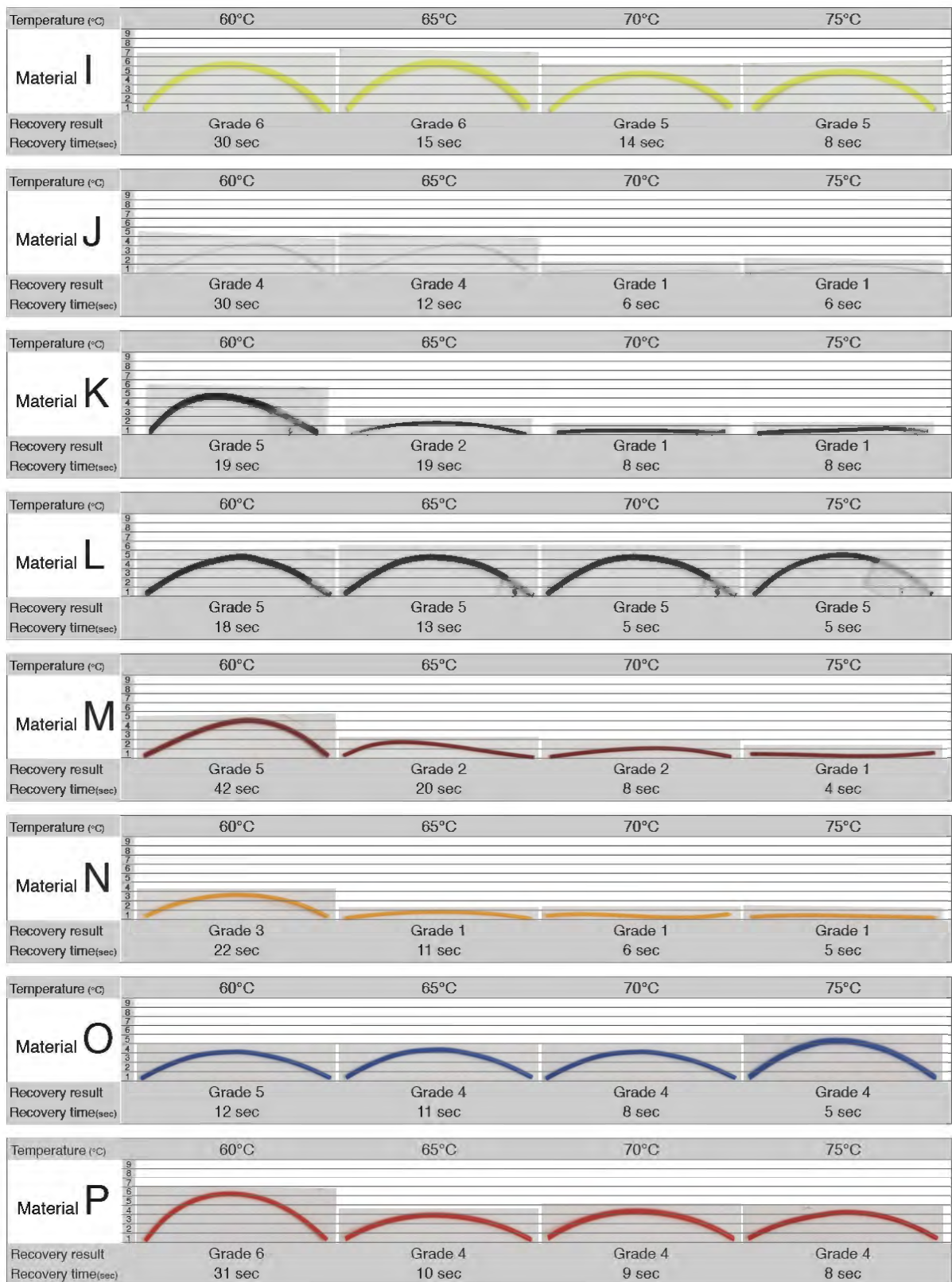
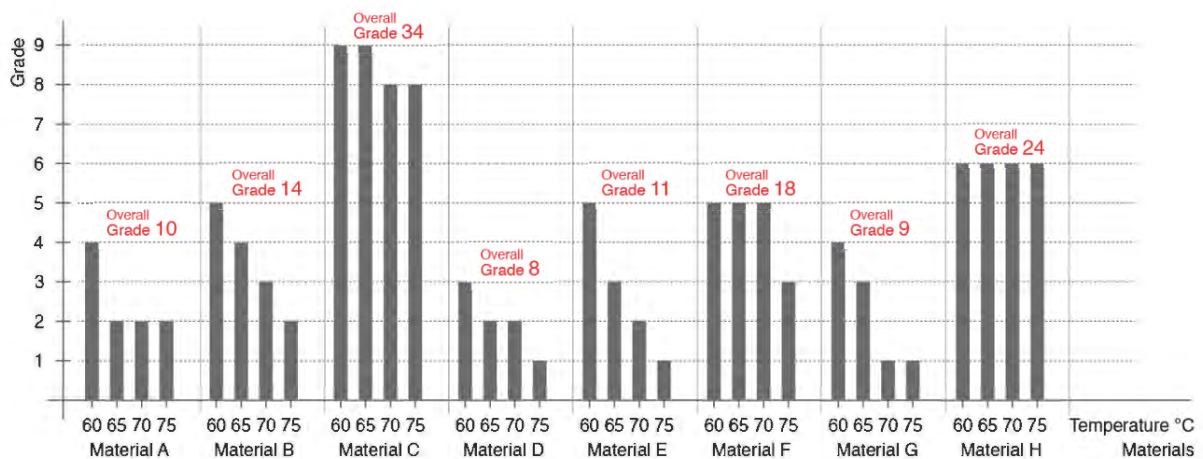


Figure 4-7. The filaments' bending recovery grades and time taken.

4.3.3 The Recovery Quality of the Filaments

Using the bending recovery data for the filaments, a study was conducted on the effects of the 16 filaments' properties and recovery temperatures on the shape recovery quality and maximum shape recovery grade. The filaments' recovery qualities are shown in Figure 4-8. The materials with the highest recovery qualities at 60 °C were N and D. Most of the materials attained grade 5 or grade 6 recovery rates, and C showed the lowest recovery quality at grade 9. The water bath at 65 °C resulted in mostly higher recovery quality than the water bath at 60 °C. The materials that produced good recovery quality with temperature were J, K, and M, and C, H, I, L, and O were not significantly affected by temperature. For accurate measurements, the filaments' recovery qualities at different temperatures were combined. The overall grade was determined as the sum of the results for each temperature. Better recovery results were seen at 65 °C and 75 °C. D and N attained good quality recovery grades, and C attained bad quality recovery grades. As indicated by the red box in Figure 4-8, N showed the highest recovery grade, with an overall recovery grade of 6, which was followed by D with an overall recovery grade of 8. However, material C had the lowest recovery grade with overall grade of 34. The results show the following: $N > D > G = K > A = J = M > E > B > O > F = P > L > I > H > C$. A high recovery temperature indicates a high recovery quality. This is clear evidence that recovery quality can vary depending on the nature of the material. However, to utilize more diverse and distinct filaments, it needs to understand why some materials work better than others through additional testing, such as applying a wider variety of filaments or comparing filaments from different brands.



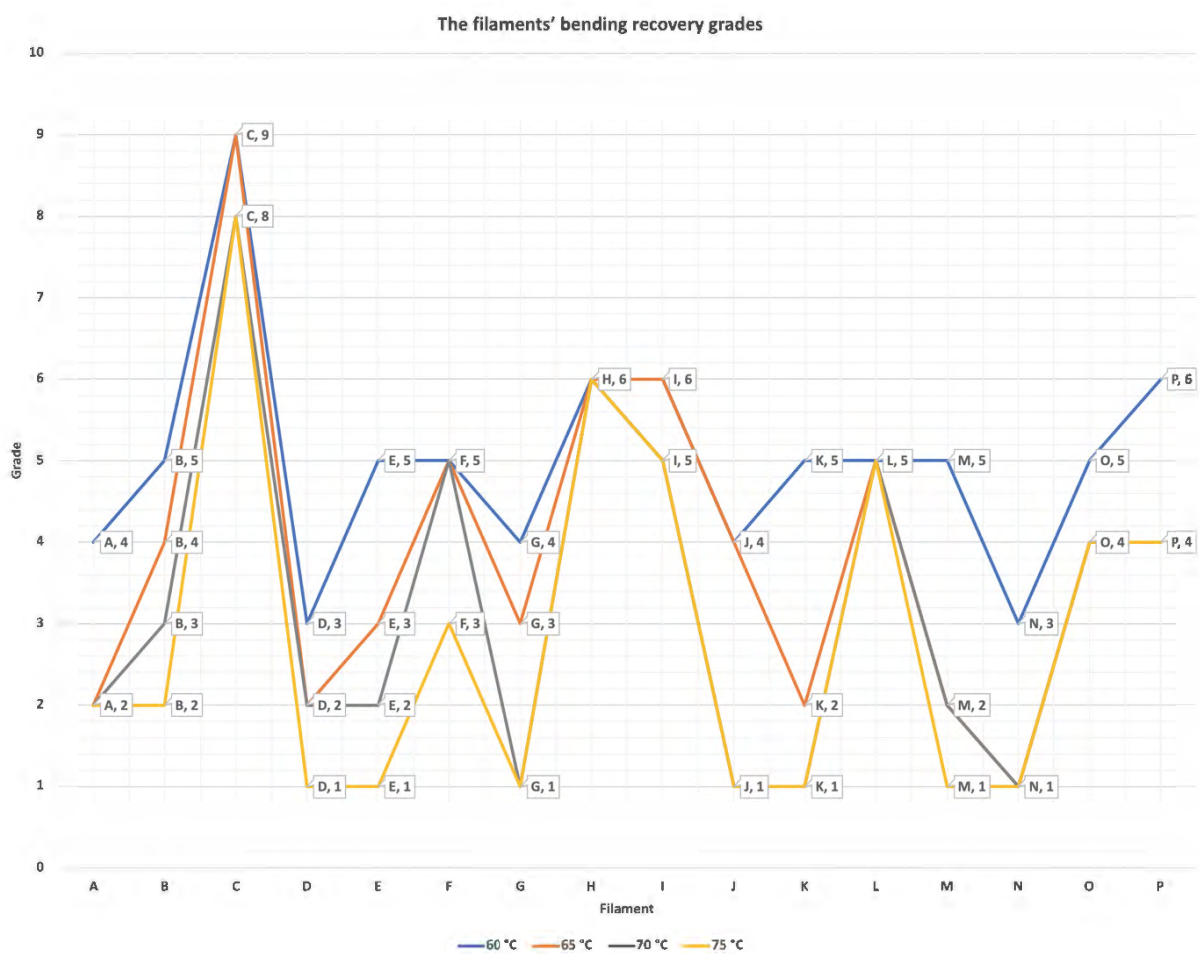
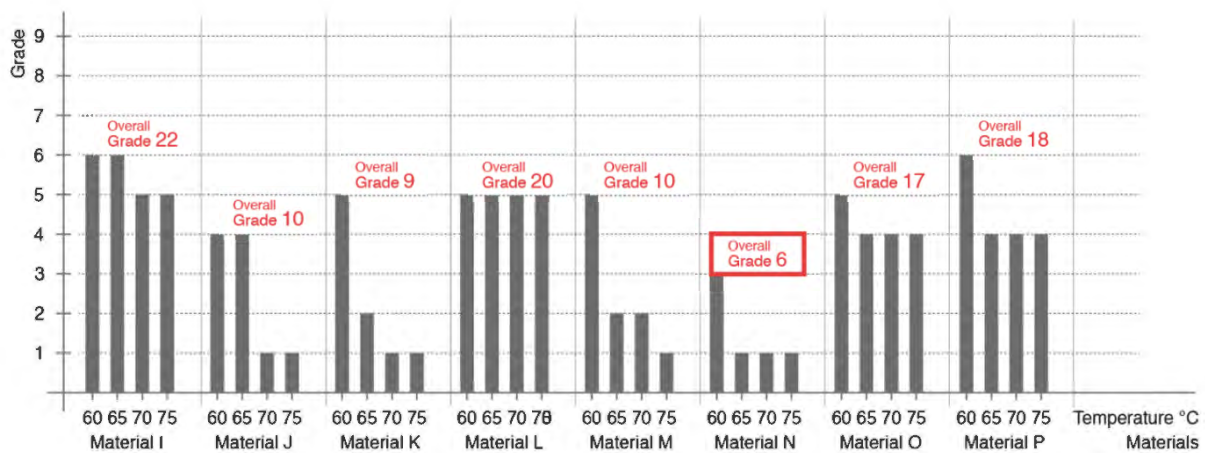
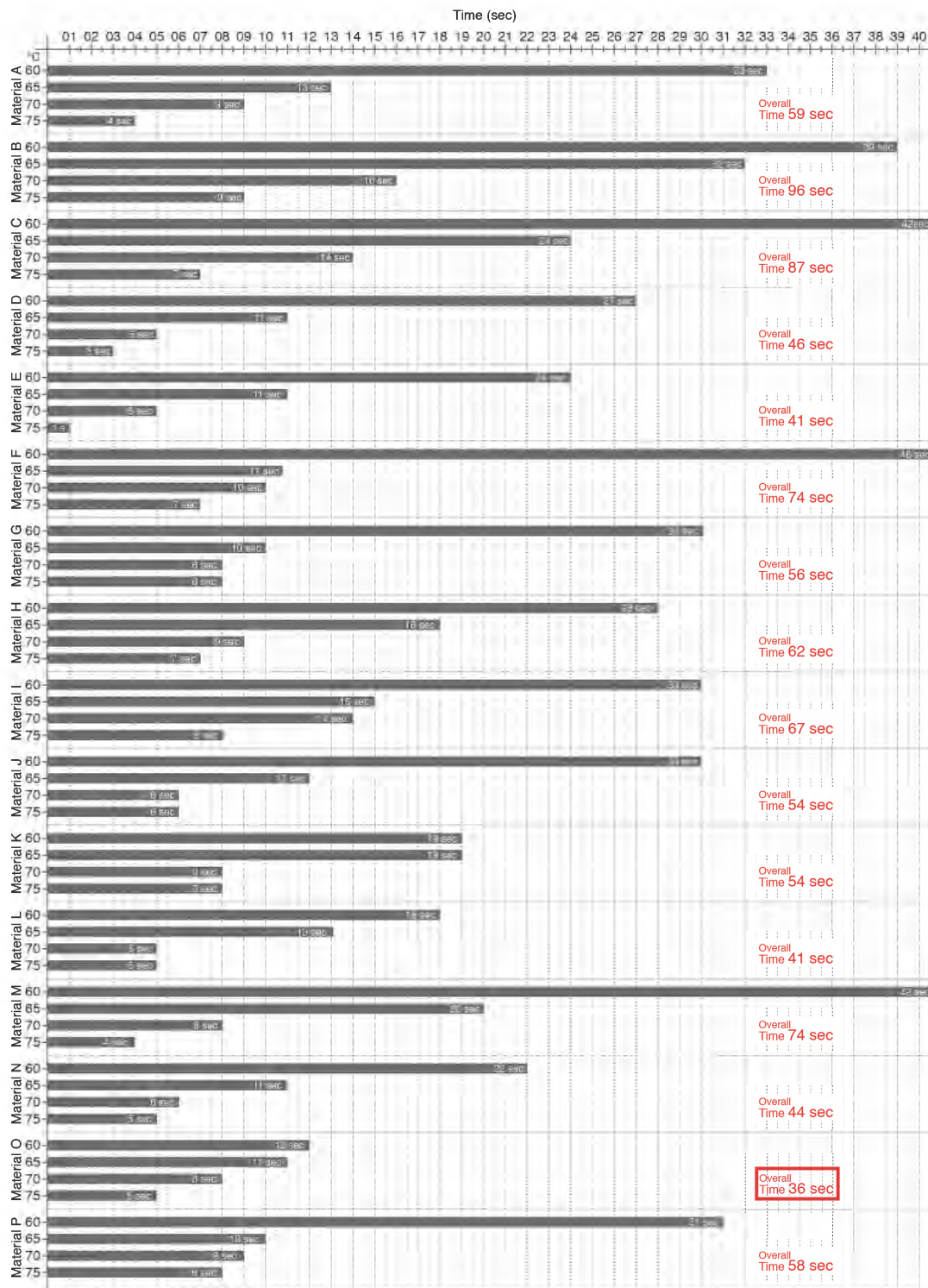


Figure 4-8. The filaments' bending recovery grades.

4.3.4 Recovery Time Results

A study was also conducted on the effect of the filaments' different characteristics and the recovery temperature on the shape recovery rate through the recovery time test. The shape change of all filaments occurred within 2 minutes. However, in order to confirm the correct recovery effect, all temperatures were set to a maximum of 2 minutes. Therefore, each material was measured for up to 2 minutes to determine the moment at which there was no further shape

change. As shown in Figure 4-9, all recovery times had a large effect on the temperature difference. For accurate measurements, the filaments' recovery speeds at each temperature were combined, with higher temperatures showing faster speeds. The results for the shape-recovery time experiment are listed in Figure 4-9. O had the fastest recovery (36 seconds), L and E both had the second fastest recovery (41 seconds), and N had the third fastest recovery (44 seconds). The results show the following: $O > L = E > N > D > J > K > G > P > A = B > H > I > M > F > C$.



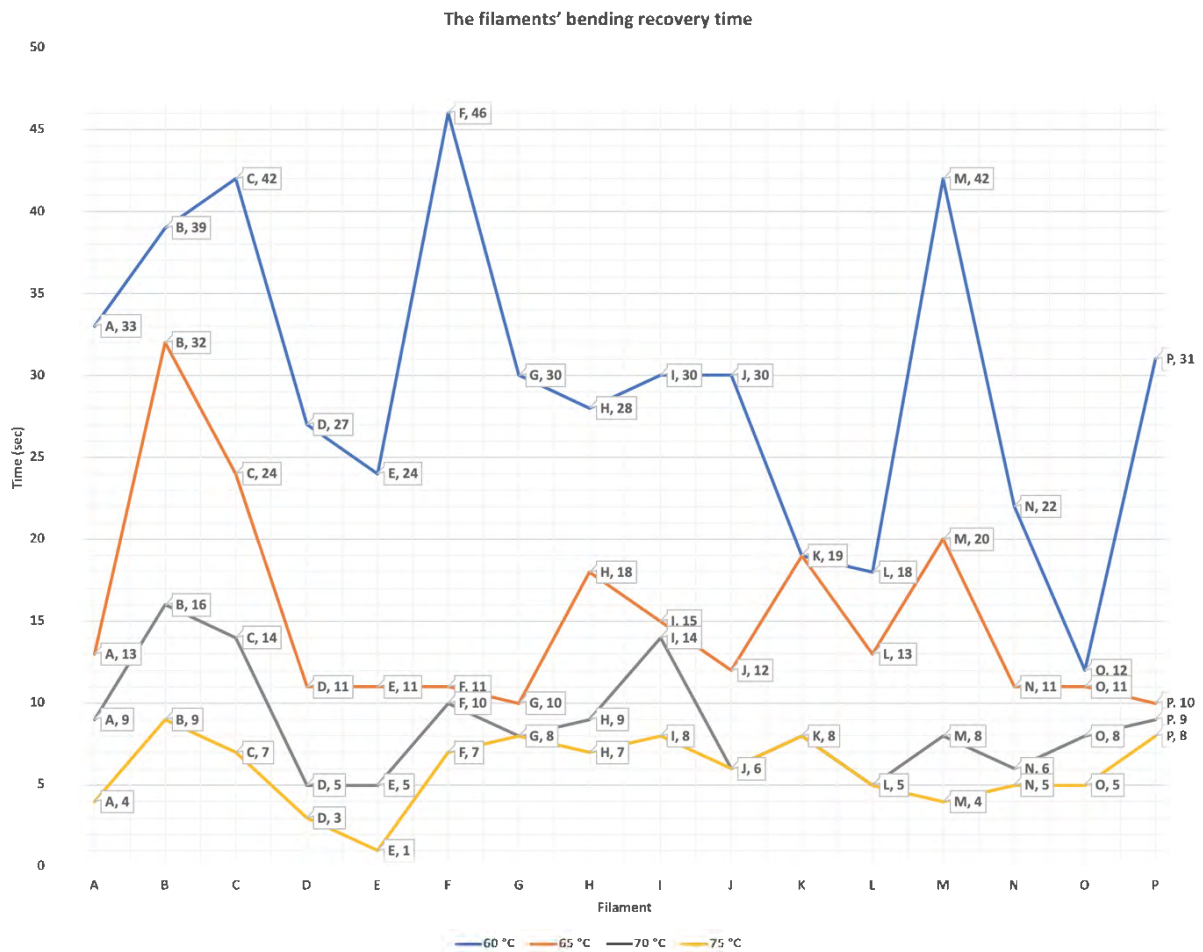


Figure 4-9. The filaments' recovery time.

Following this, the recovery quality and recovery time results were synthesised and quantitatively compared through histograms. Based on the four temperatures (60°, 65°, 70° and 75°) included in these experiments, the four samples per material were rated in order to determine the highest overall recovery results. In the graph Figure 4-10, the derived results are superimposed and the summed results can be compared. For example, calculating recovery quality of material N as 3 + 1 + 1 + 1 gave a total score of 6, which was the lowest grade and the highest recovery score. Material N showed the highest shape recovery with overall grade 6. The material with the second highest shape recovery was overall grade 8, material D. On the other hand, Material C showed the lowest shape recovery with overall grade 34. It was also shown that better recovery results were achieved between 65 °C and 75 °C. The recovery time was determined (see Figure 4-10), and the sum of the 16 filaments with different temperatures was calculated. In general, the results show that, the higher the water temperature, the faster the response. The material that achieved the fastest recovery was O at 36 seconds. L and E then achieved the second fastest recovery at 41 seconds, and N achieved the third fastest recovery at 44 seconds. Each material is the same PLA material. However, differences in the properties of each material may occur depending on the different environments and technologies of each manufacturing process. The decision to include D and N in the shortlist was based on aspects such as the achieved performance, availability, and the cost of PLA filaments. In order to find

out the reason for the difference in shape recovery for each material, additional experiments focusing on material properties are needed, but this study does not cover them.

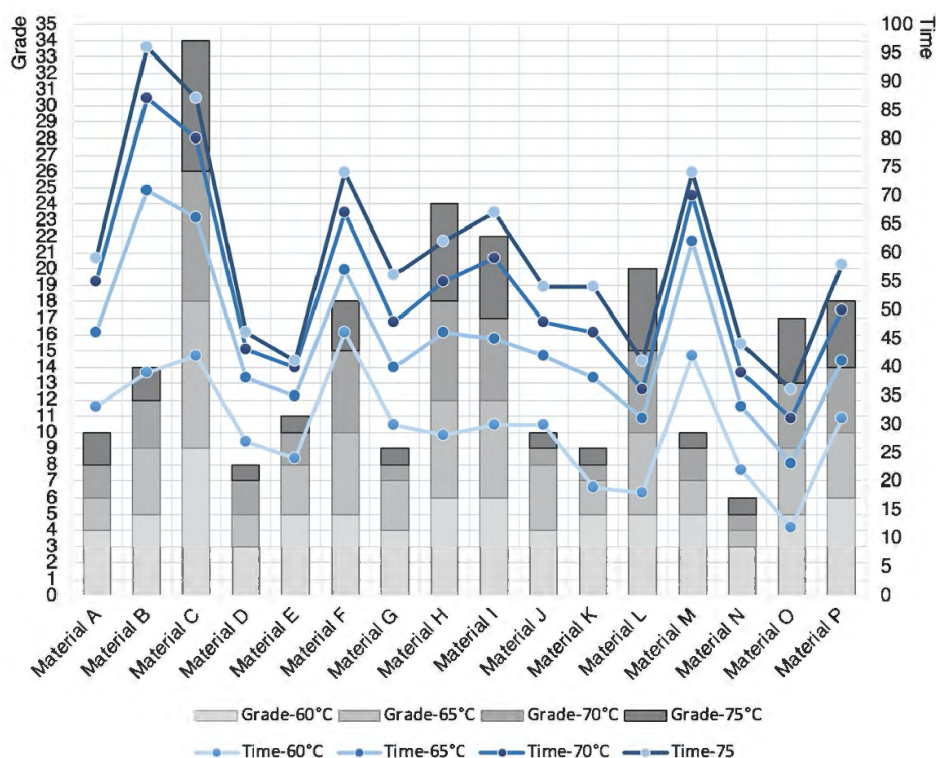


Figure 4-10. The filaments’ recovery rates.

The results of the first experiments were systematically documented, and the results for these PLA filaments were placed on a grade card. As mentioned in Figures 4-2 and 4-3, the filaments were rated from 1, indicating the highest recovery quality, to 9, indicating the lowest recovery. Figure 4-11 shows the SMEs of D and N according to the four recovery temperatures. There was a difference in shape recovery depending on the filaments’ properties. D and N were further compared because, of the 16 selected materials, they showed the highest recovery results. The experiment also recorded the time taken to return the filaments to their original shapes. N had a grade 1 recovery at 65 °C, 70 °C, and 75 °C but not at 60 °C, and D had a grade 1 recovery at only 75 °C. Therefore, it was determined that N exhibited a better shape recovery rate than D.

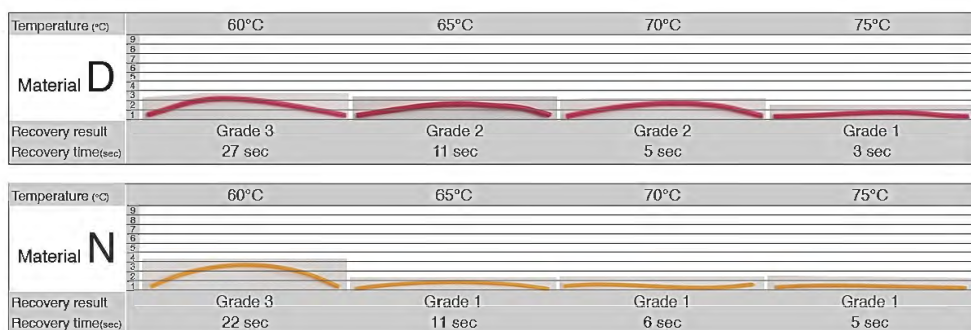


Figure 4-11. The recovery rates of D and N.

4.4 Chapter Summary

In this chapter, the shape memory effect of PLA of 16 different filaments was derived and analyzed, and then the most suitable filament was explored for application in the experiments of this paper. These experiments show that even when the same type of PLA filament is used in the same environment, different SMEs occur depending on the material properties of PLA. Due to time and cost constraints, minimising the number of cases applicable to this study is inevitable. Therefore, this study set out to find suitable filaments and identify printing parameters that can significantly impact small and medium-sized SMEs. The following chapters explore which printing parameters could have a greater impact on the SMEs using a variety of printing parameters, including print orientation, print speed, print thickness, temperature, infill density, and print pattern. Results are converted into numerical data and analyzed through graphs.

Chapter 5. Study Two: The 3D-Printed PLA Samples and Parameter Experiment

5.1 Introduction

This section aims to fulfil research objective 4. This chapter will provide an understanding of the key areas of this research through discussing the results derived from the experiments. This chapter has the main focus: Conducting an experiment to select parameters that can greatly influence Shape Memory Effects (SMEs). Section 5.2 details the three-dimensional (3D)-printed PLA samples test that was used to compare the PLA filaments selected from the experiment discussed in Section 4.3. For more detailed measurements, the two most suitable filaments from the 16 types of PLA filaments were 4D-printed and compared again. These selected PLAs were printed directly and were found to be suitable for 4DP through a water bath experiment. The experiment used to identify the printing parameters that significantly impact SMEs is described in Section 5.3. The identified parameters were then used for the experiments 2. This section discusses the various printing parameters that were applied to 3D-printed PLA, and the characteristics of the parameters and the SME of each parameter were investigated through a water bath experiment. These experiments demonstrate the influence of printing parameters. For example, the use of different printing patterns, building process methods, and infill density (layer construction) as fundamental elements of 4DP, such as programming 4D-printed parts and various printing parameters, influence the SMEs of 4D-printed parts.

5.2 The 3D-Printed PLA Samples

5.2.1 An Overview of the Selected Filaments

D and N were compared in a 3D-printed PLA sample test. This was because there may have been a difference between the original materials' recovery rates and the recovery rates of the materials that had been deformed through the printing process. This experiment led to the selection of suitable materials for this study.

The 3D-printed PLA sample test had the same experimental procedure as detailed in Section 4.3 as it included programming, cooling, and recovery. The programming of PLA samples began with changing the temperature of the water. The water bath was heated to the strain temperatures (55 °C, 60 °C, 65 °C, 70 °C, and 75 °C). using an immersion circulator. The PLA samples were placed in a water bath for 1 minute and then deformed into a bent shape using a bending device. The deformed PLA samples were allowed to cool for 1 minute at room temperature after being fixed on the bending device. Moreover, the PLA samples were restored to their original permanent forms. After the PLA samples were fully cooled and programmed, the water bath temperature was set to the recovery temperature. This experiment differed from the previous one by adding a strain temperature of 55 °C in order to obtain a wider range of data. The deformed PLA samples were placed in a water bath, and the shape recovery experiments were recorded using a camera. Figure 4-12 shows a 3D-printed PLA sample and experimental setup. And experiments were carried out on the prepared settings.

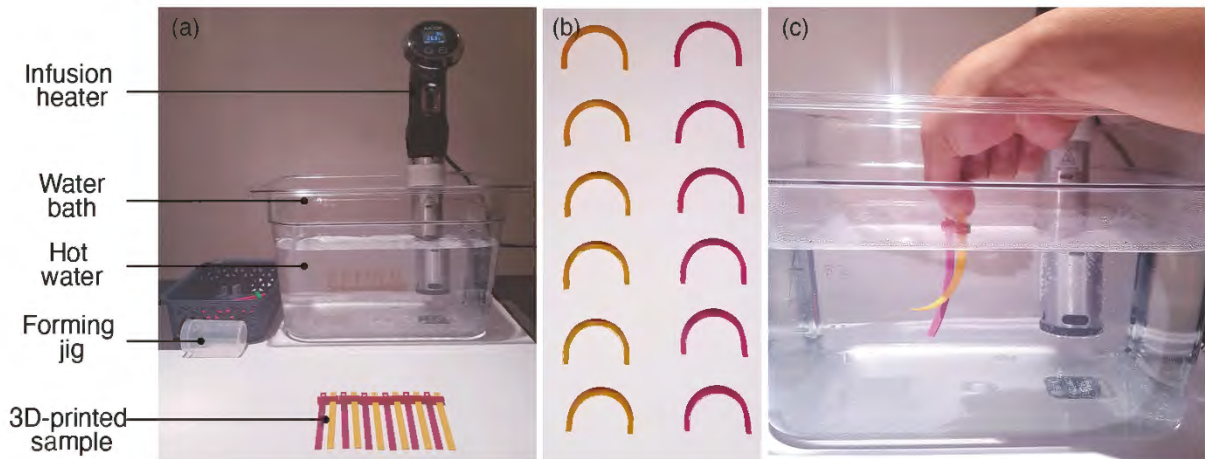


Figure 5-1. The experiment setup and prepared 3D printed PLA sample (a) Experiment setup (b) Deformed PLA sample (c) Test the sample

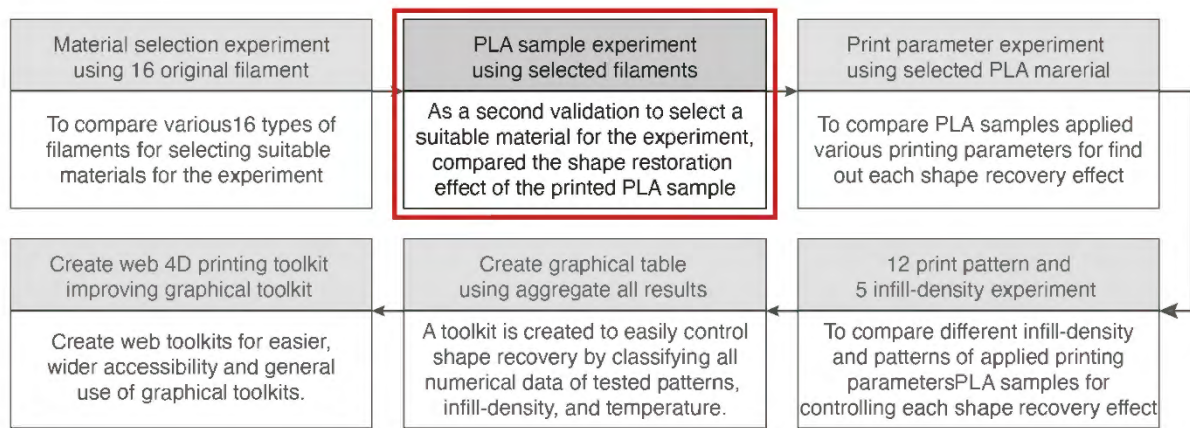


Figure 5-2. The process of the PLA sample experiment.

5.2.2 Comparison of the 3D-Printed PLA Samples

The two 3D-printed PLA samples examined in this section, N and D, were original materials with excellent recoverability rates and recovery times (Figure 4-14). Their recovery qualities, recovery temperatures, and recovery time were compared. These PLA samples were fabricated using the Qidi X-Pro printer. The extruder temperature was set at 210 °C, the printing speed was set at 50 mm/s, the retraction speed was set at 30 mm/min, the retraction distance was set at 1.5 mm, and the infill density was set at 100%. Shape-recovery experiments were conducted using rectangular samples measuring 80 mm × 6 mm × 3 mm. To derive objective results, the printer's standard settings for nozzle thickness and pattern were applied. In addition, to create the same environment for the entire experiment, the printing parameters such as extruder temperature, printing speed, retraction speed, retraction distance, and infill density were applied with the same parameters. The PLA samples were programmed for 60 seconds using a deformation temperature of 80 °C, and they were bent using the same deformation device. For secure deformation, a T_g of 80 °C was selected, which was higher than each PLA sample's T_g in this experiment. According to the T_g and the possible applications of the PLA used in this experiment, the recovery temperature for the filaments was tested five times by setting five

different recovery temperatures (55 °C, 60 °C, 65 °C, 70 °C, and 75 °C). To understand the recovery rate at the lowest temperature, a recovery temperature of 55 °C was added to the research design. The samples spent a maximum of 2 minutes in the water bath in order to determine their bending rates and recovery grades from 1 to 9. The shape-recovery grade was measured as the difference between the original deformation and the recovery deformation, with a flat shape indicating good recovery quality. This is important for the quantification of SMEs.

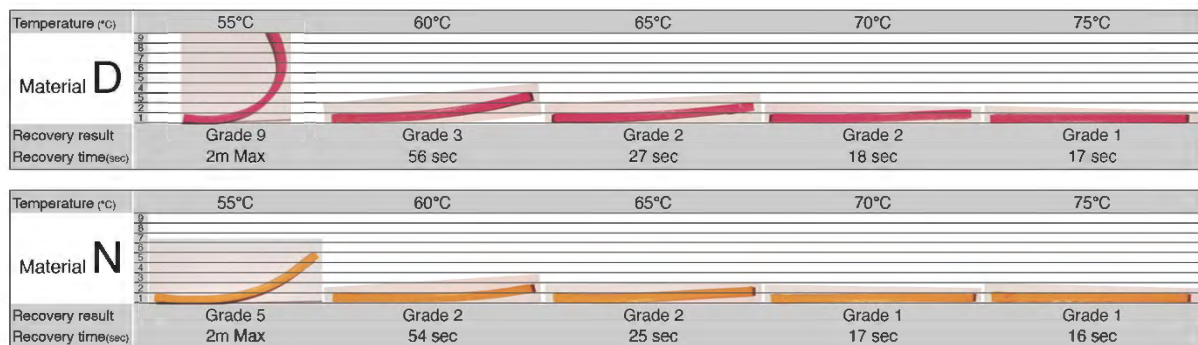


Figure 5-3. The 3D-printed PLA samples' bending recovery rates.

5.2.3 The 3D-Printed PLA Samples' Recovery Rates

Show Figure 4-15, the second experiment was performed using the materials D and N selected in the first experiment. In order to obtain more accurate results, repeated experiments were carried out and two materials were selected. D and N were chosen for this experiment because they showed excellent recovery time and recovery rates. The results of this experiment demonstrated the different recovery qualities and recovery rates due to the different properties of the two selected PLA filament samples. For recovery quality, D and N showed the same recovery results at 75 °C. However, at temperatures other than 75 °C, N showed better recovery quality. At a recovery temperature of 55°C, D hardly recovered its shape, thereby showing a low recovery rate. This means that the lower the temperature, the greater the difference in recovery quality. Moreover, in terms of speed, N showed faster shape recovery than D at all temperatures. In terms of recovery time, D and N were slightly different. The results show that, the higher the temperature, the faster the recovery time of both materials. It was demonstrated that high temperatures can result in better recovery quality and better recovery time. As N showed better recovery quality and faster recovery rates, N was used as the sample for the third experiment: testing the printing parameters.

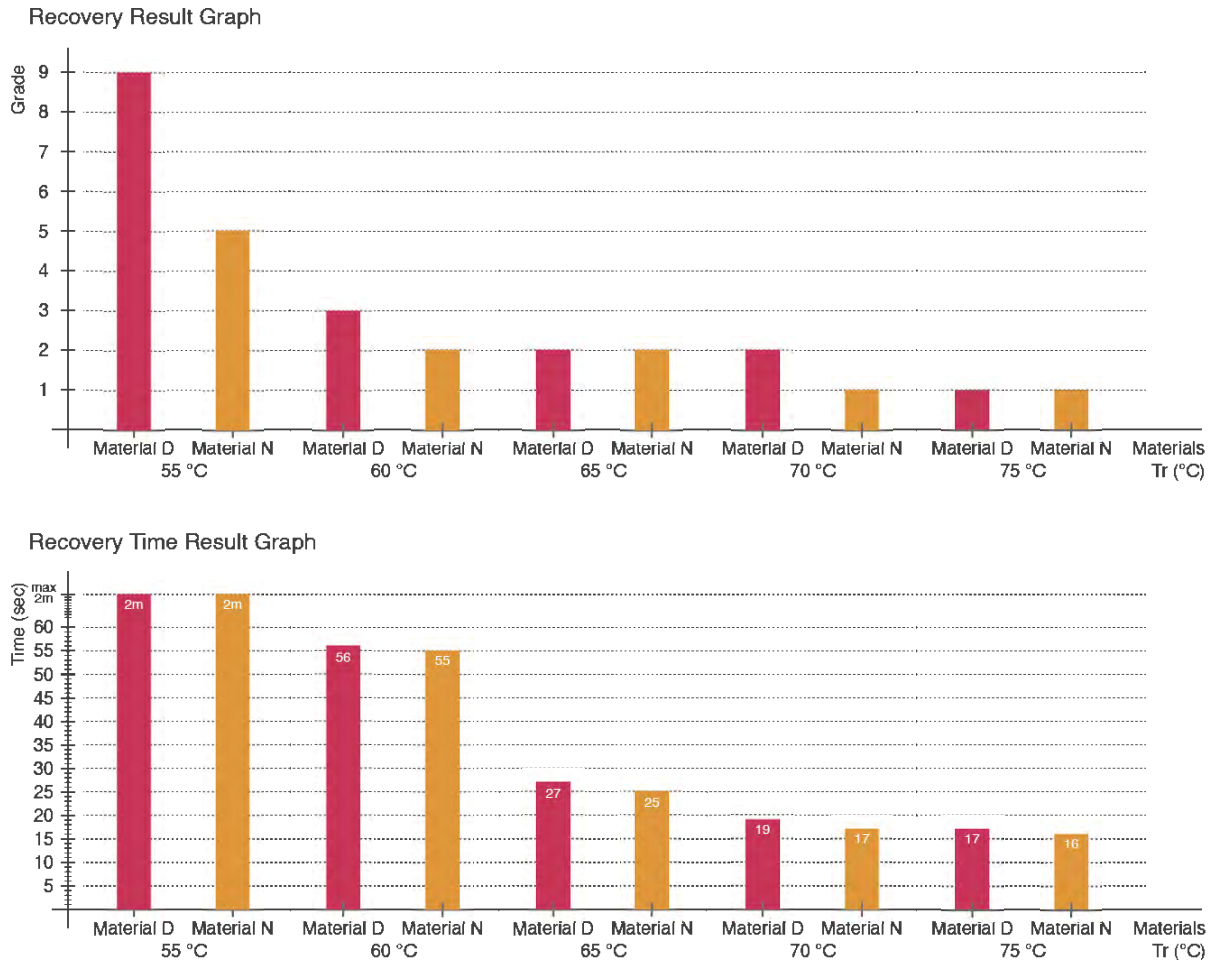


Figure 5-4. Comparison of material D's and N's bending recovery grades and times.

5.3 Testing the Printing Parameters

5.3.1 An Overview of the Printing Parameters Experiment

The previous experiment selected a material judged suitable for the study after testing the PLA sample. Various printing parameters discussed in Section 2.5 of Chapter 2 can affect the effect of shape deformation. However, in this research, it was necessary to select suitable parameters for the efficiency of the study because incorporating a wide range of experiments was not feasible due to the time constraints. In addition, selecting the correct parameters that greatly affect the shape-change effect was important for maximising the usability and efficiency of the study. Therefore, this experiment aimed to determine the printing parameters that greatly influence the shape deformation effect, which will allow for more in-depth experiments on these parameters. This experiment consisted of four parts. Section 5.3.2 details the experiment conducted to compare the SMEs by applying various printing parameters through a water bath experiment. These printing parameters include print orientation, print speed, print thickness, infill density, and print pattern (see Figure 2-37). Section 5.3.3 compares and analyses the weight results according to infill density in order to determine the difference in SMEs due to the weight of the experimental samples based on the results from Section 5.3.2. Section 5.3.4 details the experiment conducted to compare the SMEs by applying various other properties through a water bath experiment. These properties include differences in size, thickness, and

proportions of the printed samples. All these experiments were performed using water baths. The various printing parameters and differences in the properties of the print samples is discussed herein. For example, in programming a 4D-printed part, the use of various printing parameters, such as the basic elements of 4DP, can affect how a 4D-printed part changes shape.

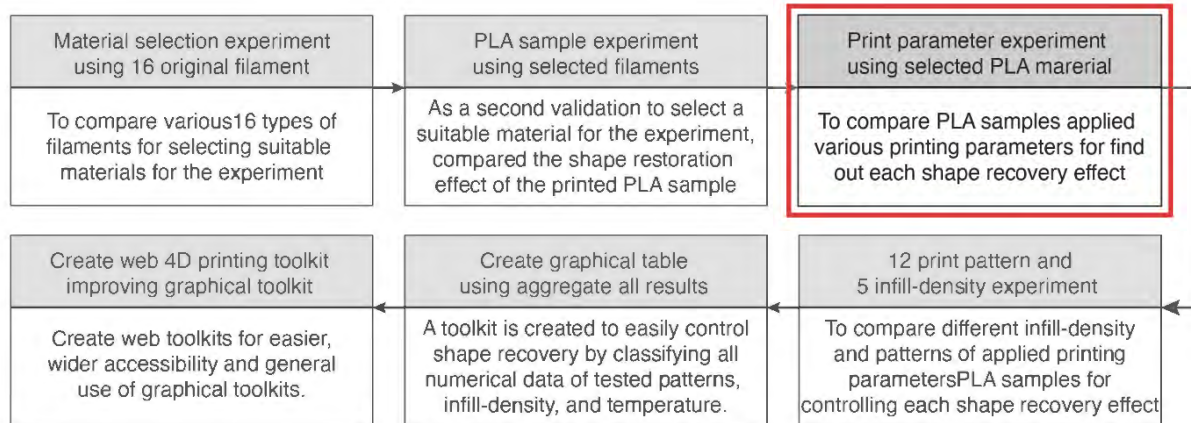


Figure 5-5. The process of the printing parameters experiment.

5.3.2 Comparison of the Printed Parts

Applying a number of printing parameters in all cases to the experiment can lead to a more accurate and wide range of results. However, it was necessary to find a printing parameter that could more effectively act on the SMEs due to the time constraint and cost of the experiment. Therefore, the printing parameters of the slicing stage were mainly selected and applied among various printing parameters. In detail, the value of the difference between the printing pattern and the infill density layer thickness was applied with a large deviation in order to understand the definite deviation value. For example, it can be difficult to compare the result values of 95% and 100% infill densities because they are similar. However, the results of the SMEs of 20% and 100% infill densities are easy to compare. Therefore, four different patterns (quarter cubic, line, concentric, and cross), three print speeds (50 mm/s, 100 mm/s, and 140 mm/s), two infill densities (20% and 100%), two layer thicknesses (0.08 mm and 0.2 mm), the recovery qualities, and recovery time were compared by combining all aspects in two different printing orientations (0° and 90°) shown table 5-1.

Table 5-1. Print parameters and type for selecting printing parameters of the slicing stage

Print parameter	Type
Patterns	Quarter cubic, Line, Concentric, and Cross
Print speeds	50 mm/s, 100 mm/s, and 140 mm/s
infill densities	20% and 100%
Layer thicknesses	0.08 mm and 0.2 mm
Shape memory effects	Recovery qualities, and Recovery time
Printing orientations	0° and 90°

Infill density is one of the 3D printing parameters and is the fill of the model inside the shell. The infill amount can be set as a percentage, with 0% indicating no fill and 100% indicating the object volume is filled. Figure 5-6 shows the filling density from 10% to 100%. Figures 5-7 show the infill densities of the build orientation at 0° and 90°. It shows that even with the same infill density of the same pattern, the infill density can be different depending on the difference in the build orientation.

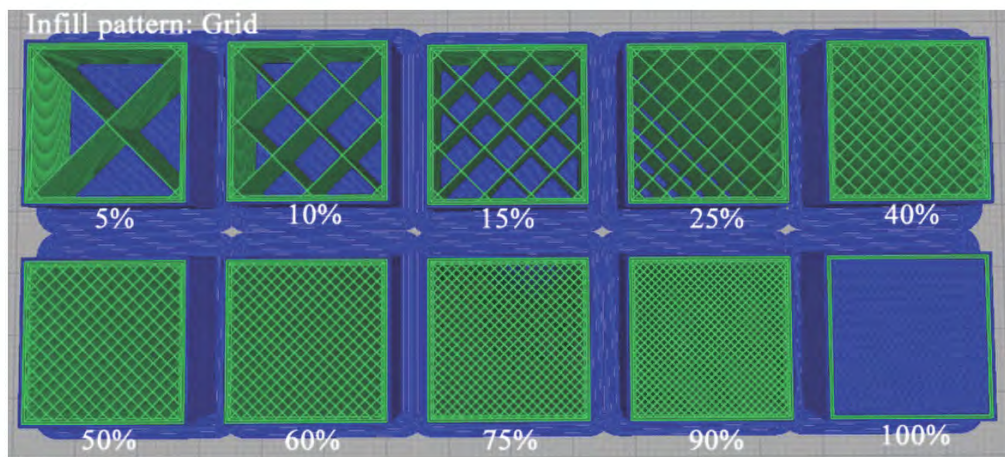


Figure 5-6. Various infill densities between 5% and 100% (Carino et al.,2018).

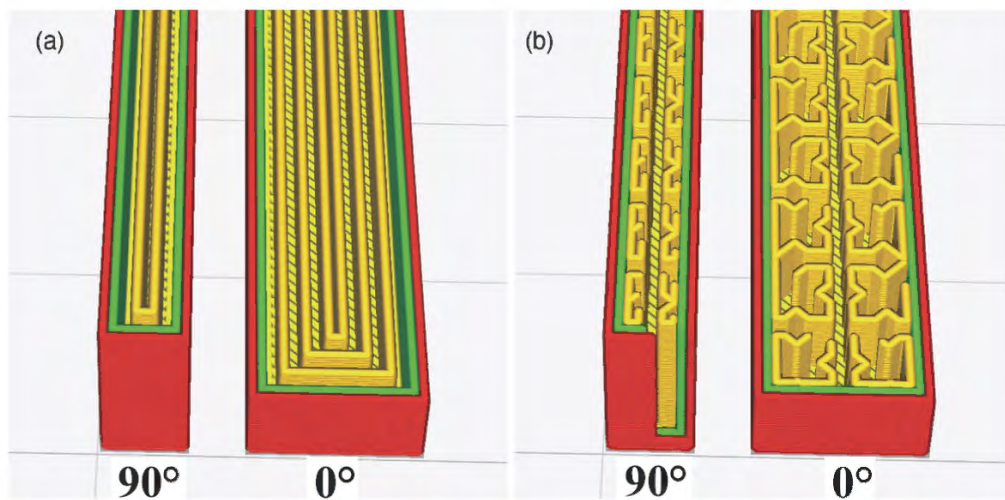


Figure 5-7. 0° and 90° build orientation. (a) concentric pattern (b) cross pattern

The 3D-printed PLA samples selected for this experiment were of the same materials used in the previous experiments, and the experiment was performed in the same way as the previous experiments. This comparison examined the effect of the parameters on shape recovery. Depending on the Tg of the PLA samples used in this experiment and their possible applications, the filament test was performed three times by setting the recovery temperature at 75 °C. All samples spent a maximum of 2 minutes in the water bath in order to check the SMEs. Figures 5-8 and 5-9 detail the results, the most striking of which is for the quarter cubic pattern in which the infill density affected the recovery time. Layer thickness, print speed, and build orientation show similar recovery rates, but this is not the case for infill density. The line

pattern also showed similar results to the quarter cubic pattern in that a lower infill density resulted in faster recovery rate. On the other hand, as shown in Figures 5-10 and 5-11, the concentric and cross patterns had different results. When the same build orientation was applied, there were similar recovery times, but different recovery times were obtained when a different build orientation was applied. Therefore, the build orientation affected the recovery time of the concentric pattern and cross patterns in that a 90° orientation resulted in faster recovery rates than a 0° orientation. Although recovery quality and recovery time were derived through the experiment, recovery quality showed similar results to the previous experiment, which was not discussed in this thesis.

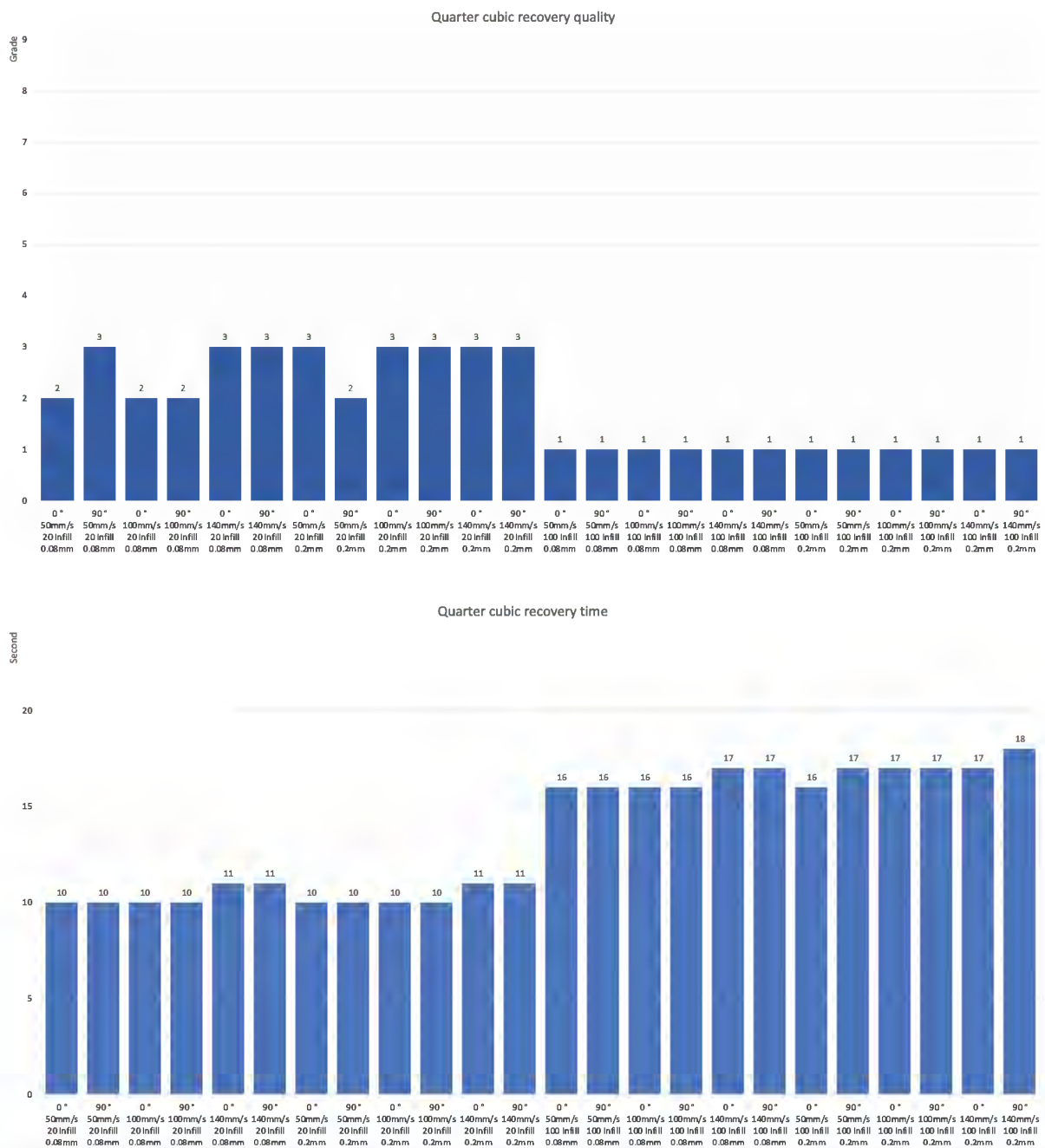


Figure 5-8. Recovery quality and time for the quarter cubic pattern.

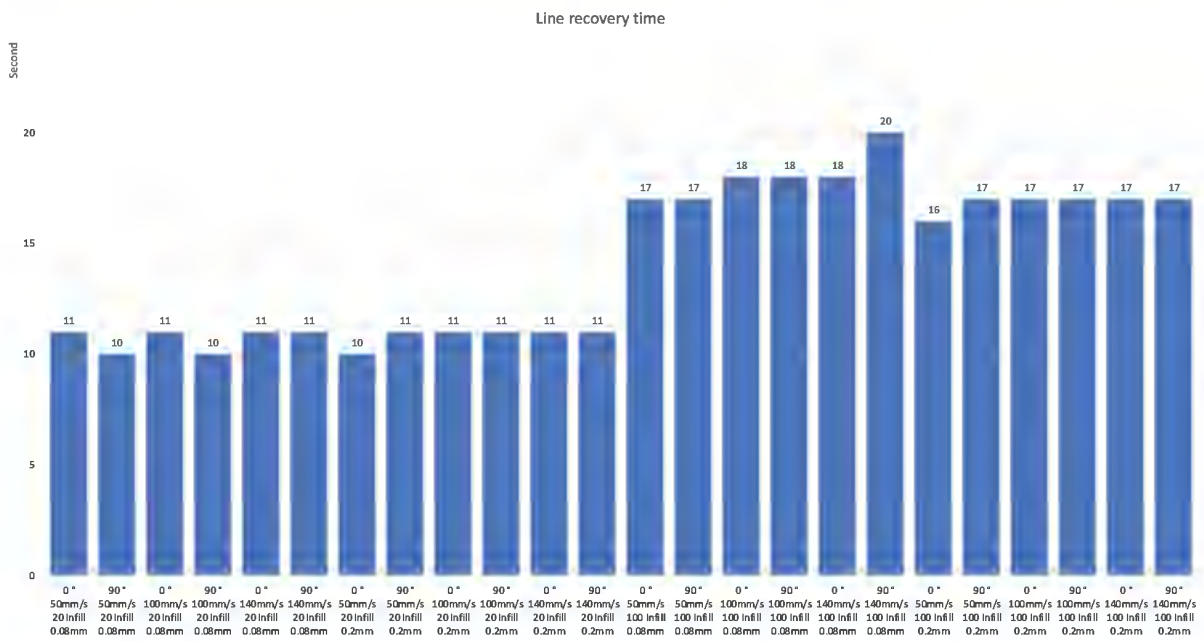
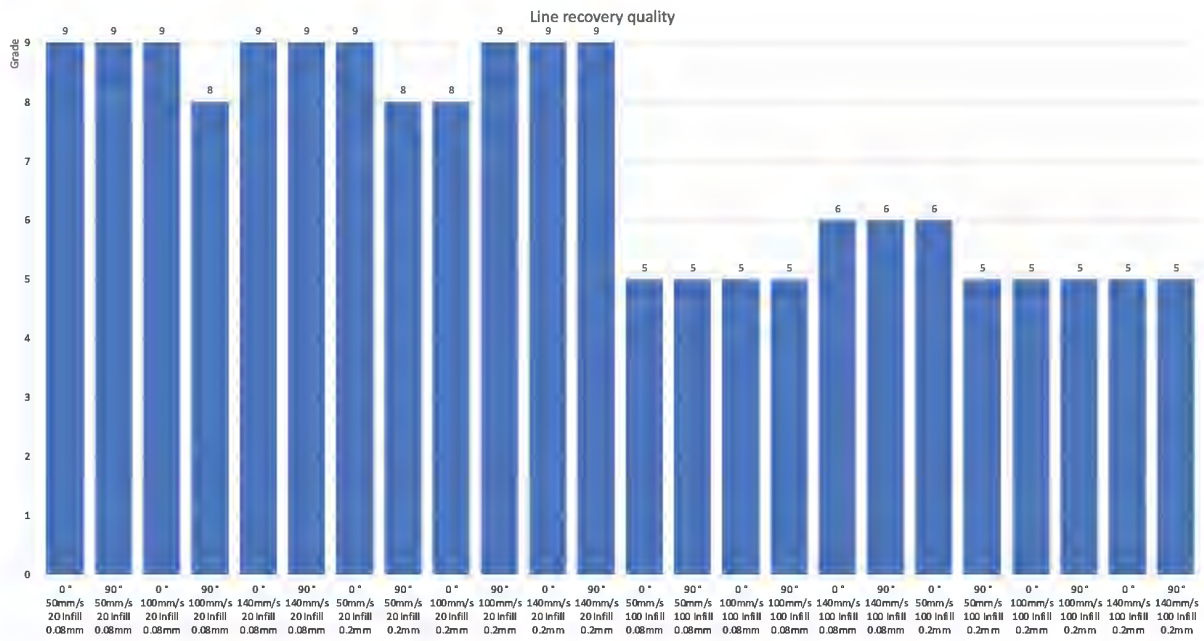


Figure 5-9. Recovery quality and time for the line pattern.

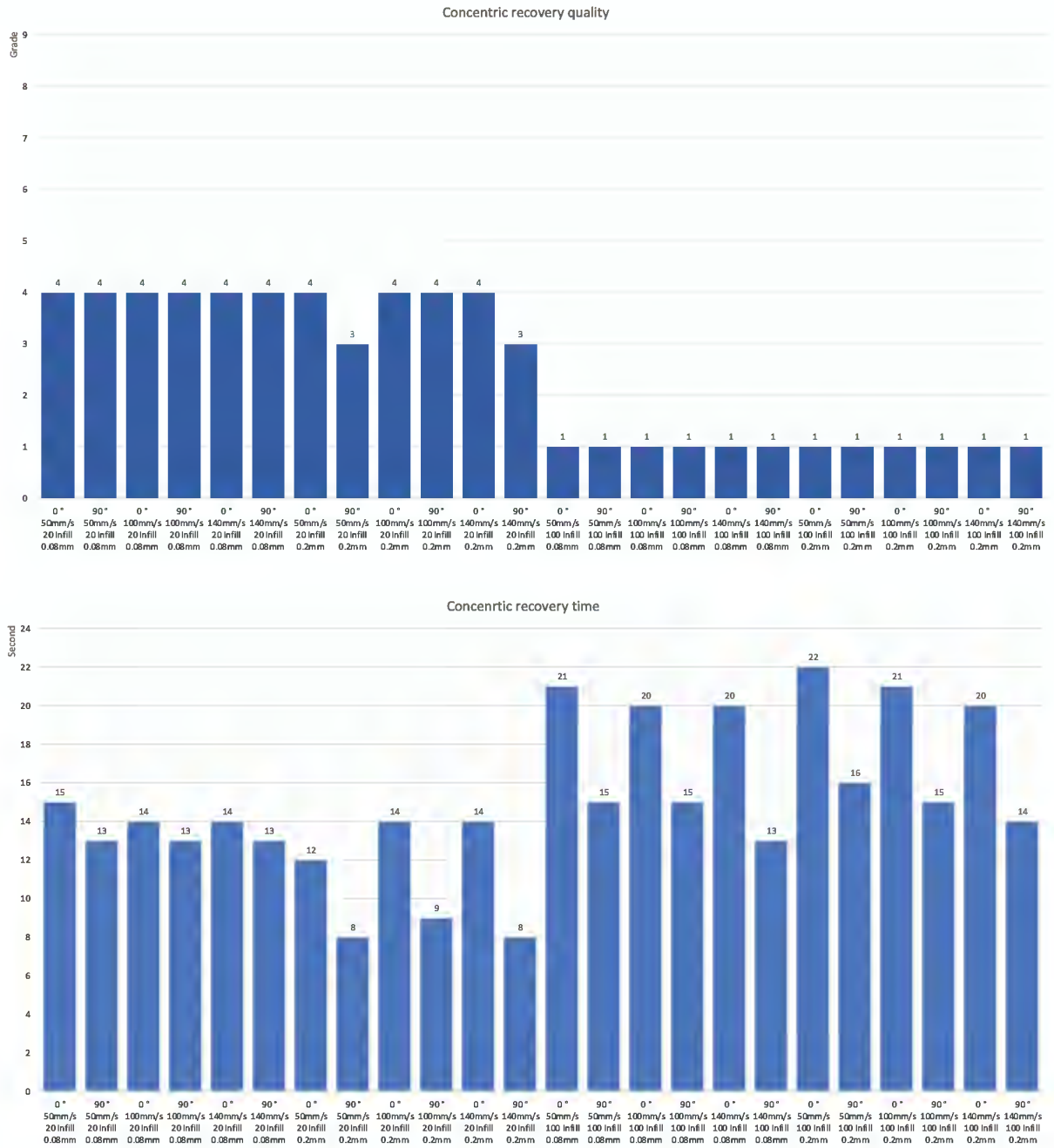


Figure 5-10. Recovery quality and time for the concentric pattern.

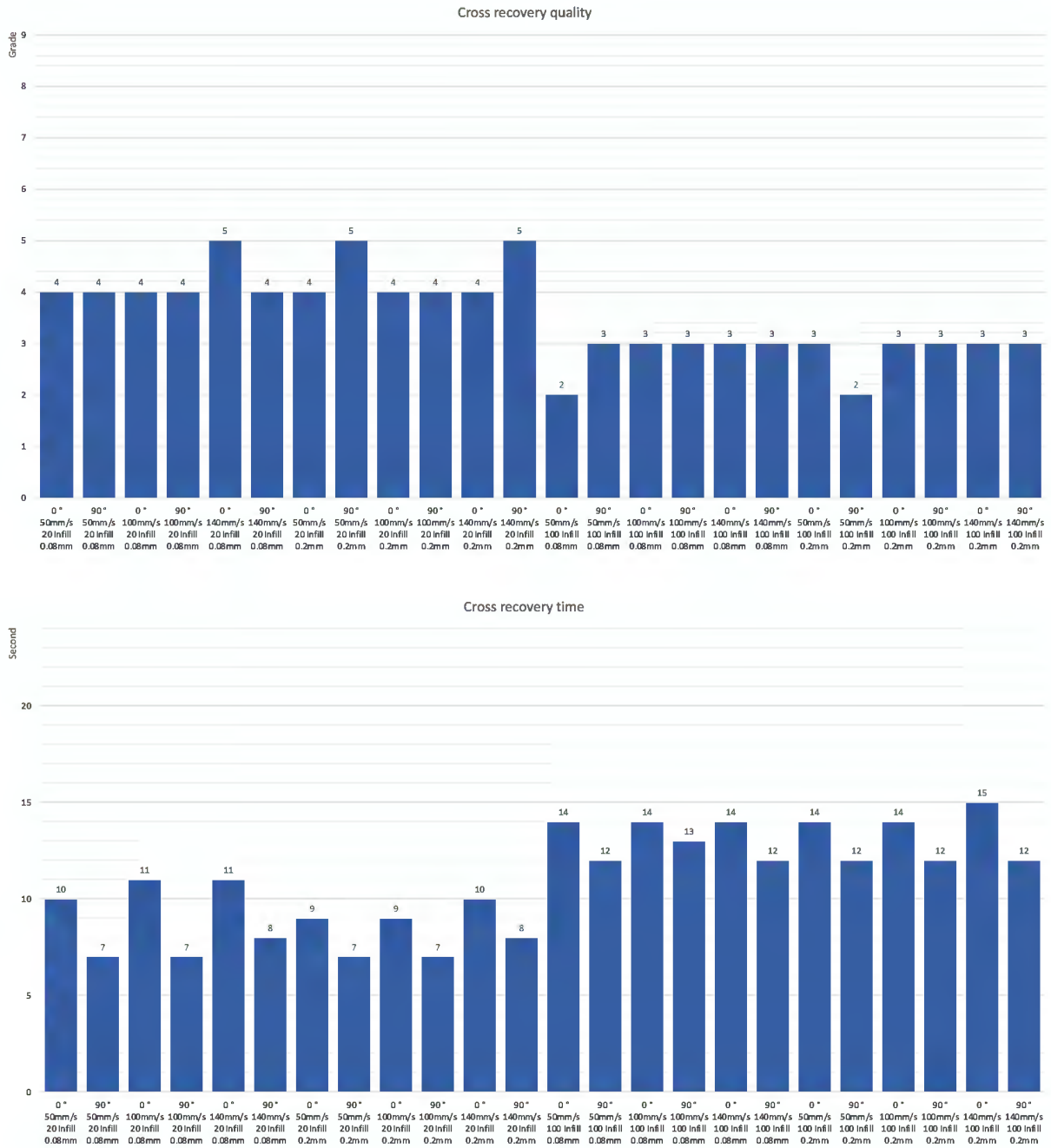


Figure 5-11. Recovery quality and time for the cross pattern.

5.3.3 Comparison of Weight according to Infill Density

Although it is standard practice to weigh the specimen before testing, we measured the weight of the specimen after testing because changes in the sample after testing can explain differences in SME. The previous experiments show that the SMEs differed at the same infill density, depending on the pattern. To analyse this more closely, samples from each pattern and build orientation with the same infill density were weighed using an accurate scale. Due to the small volume of the sample, a high-precision balance capable of weighing even 0.001 g was used to obtain an accurate reading (see Fig. 5-12). This was used to confirm the volume differences in the samples according to the pattern and build direction in order to determine their relationship

with the recovery rate. As shown in Figure 5-13, the weight of the quarter cubic and line patterns in different build orientations (0° and 90°) was 1.649 g and 1.684 g, so there was a difference of 35 g. However 35g volume difference had not a significant effect on the recovery time and recovery quality. On the contrary, the weights of the concentric and cross patterns differed significantly according to the build orientation. Therefore, the patterns' volumes differed according to the printing direction, with both patterns suggesting that they can be filled well when the build orientation is 0° . Figure 5-14 shows that the infill density of each pattern can be different depending on the build direction. A uniform pattern that does not have a certain shape, such as quarter cubic and line, can have a constant infill density regardless of the build direction. On the other hand, for patterns made based on shapes such as concentric and cross, the infill density can have a large effect on the build orientation.



Figure 5-12. Sample weight measurement equipment according to infill density.





Patter	Orientation	Weight	Weight difference
Quarter cubic 	0°	1.649g	$0^\circ < 90^\circ$
	90°	1.684g	0.035g
Line 	0°	1.648g	$0^\circ < 90^\circ$
	90°	1.684g	0.036g
Concentric 	0°	1.677g	$0^\circ > 90^\circ$
	90°	1.509g	0.168g
Cross 	0°	1.543g	$0^\circ > 90^\circ$
	90°	1.454g	0.099g

Figure 5-13. The weight of each printed pattern.

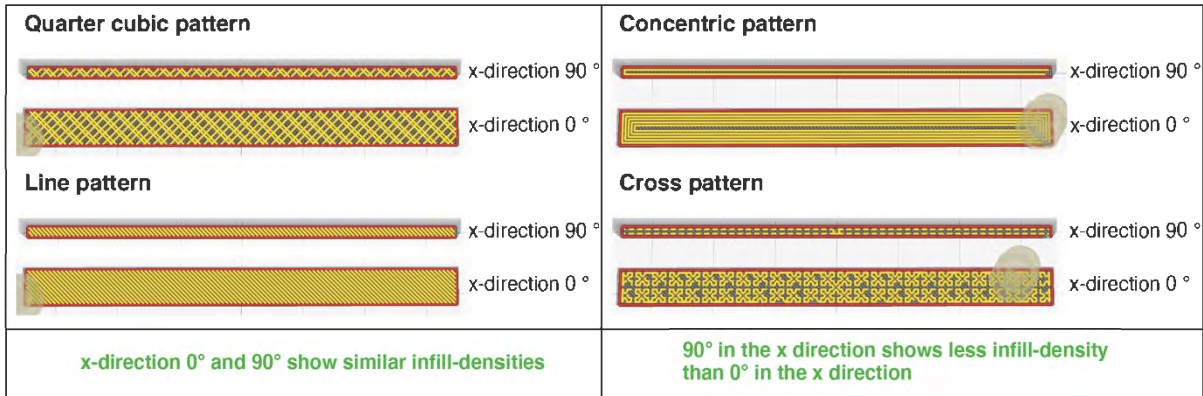


Figure 5-14. Comparison of fill density by build direction.

5.3.4 The Application of Different Properties

This experiment was conducted to measure and classify shape recovery quality and shape recovery rate through various factors such as patterns and thicknesses, sizes, sample proportions, and different materials. It allowed for a wide range of measurements by combining the quality and time of recovery in the properties of the printed samples (Figure 5-15). When comparing the quarter cubic pattern to the line pattern, the former showed excellent recovery quality and quick recovery times for both materials (N and P). Therefore, quarter cubic patterns of any material exhibit higher recovery rates and faster recovery rates than line patterns. The larger the sample size, the worse the recovery quality and the longer the recovery time. The overall volume had a greater effect on the recovery quality and recovery time than the thickness of one side. Therefore, high capacity is inversely proportional to good recovery quality and time (Figure 5-16).

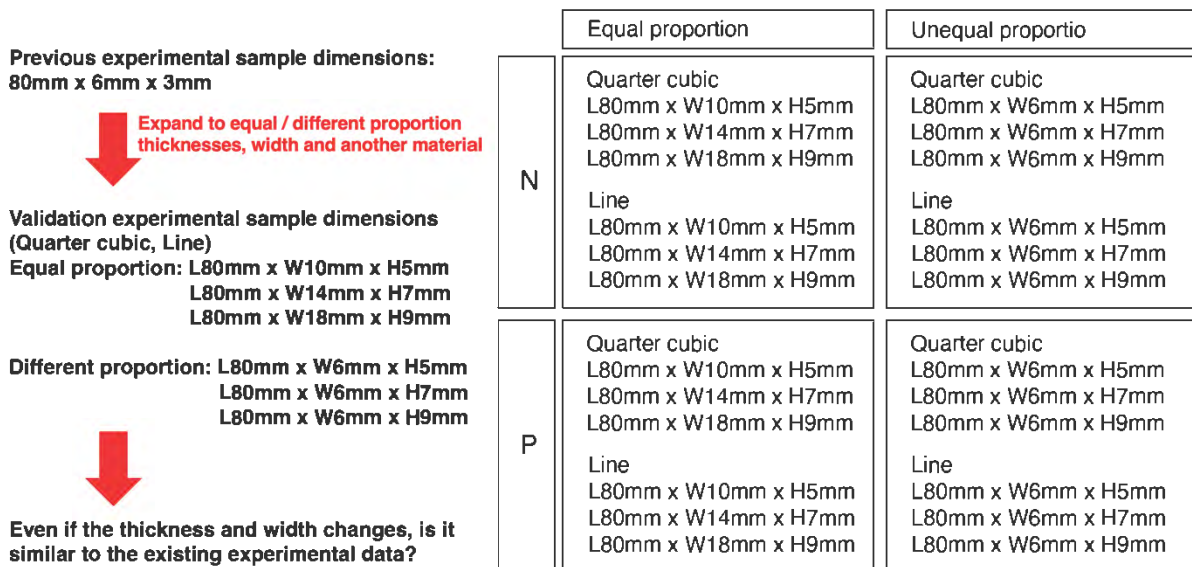


Figure 5-15. Application of size, thickness, and proportions.


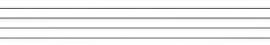
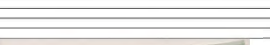

Material N

Pattern: Quarter cubic, Line
Layer thickness: 0.08mm (Extra fine config)
Infill density: 100% Infill density
Print speed: 50mm/s
Temperature: 75°
Build orientation: x-direction 0°





Dimensions of equal proportion:
 L80mm x W10mm x H5mm
 L80mm x W14mm x H7mm
 L80mm x W18mm x H9mm

Dimensions of different proportion:
 L80mm x W6mm x H5mm
 L80mm x W6mm x H7mm
 L80mm x W6mm x H9mm





Equal proportion (W=2H)

Dimensions(mm)	L80mm x W10mm x H5mm	L80mm x W14mm x H7mm	L80mm x W18mm x H9mm
			
Quarter Cubic	Grade 1	Grade 2	Grade 3
Recovery result	38sec	1min 16sec	1min 57sec
Recovery time(sec)			




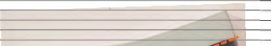
Unequal proportio (Thickness change)

Dimensions(mm)	L80mm x W6mm x H5mm	L80mm x W6mm x H7mm	L80mm x W6mm x H9mm
			
Quarter Cubic	Grade 1	Grade 1	Grade 3
Recovery result	25sec	50sec	56sec
Recovery time(sec)			

Equal proportion (W=2H)

Dimensions(mm)	L80mm x W10mm x H5mm	L80mm x W14mm x H7mm	L80mm x W18mm x H9mm
			
Line	Grade 4	Grade 5	Grade 6
Recovery result	47sec	1min 21 sec	2min 7sec
Recovery time(sec)			

Unequal proportio (Thickness change)

Dimensions(mm)	L80mm x W6mm x H5mm	L80mm x W6mm x H7mm	L80mm x W6mm x H9mm
			
Line	Grade 4	Grade 5	Grade 5
Recovery result	30sec	55sec	1min 5sec
Recovery time(sec)			

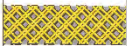


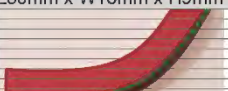
Material P

Pattern: Quarter cubic, Line
Layer thickness: 0.08mm (Extra fine config)
Infill density: 100% Infill density
Print speed: 50mm/s
Temperature: 75°
Build orientation: x-direction 0°



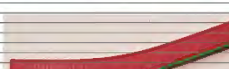
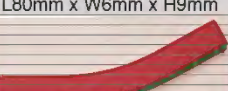
Dimensions of equal proportion:
 L80mm x W10mm x H5mm
 L80mm x W14mm x H7mm
 L80mm x W18mm x H9mm

Dimensions of different proportion:
 L80mm x W6mm x H5mm
 L80mm x W6mm x H7mm
 L80mm x W6mm x H9mm



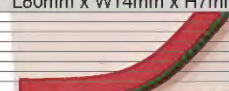
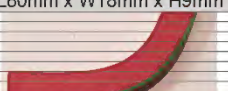
Equal proportion (W=2H)

Dimensions(mm)	L80mm x W10mm x H5mm	L80mm x W14mm x H7mm	L80mm x W18mm x H9mm
			
Recovery result	Grade 4	Grade 6	Grade 9
Recovery time(sec)	45sec	1min 20sec	2min 30sec

Unequal proportio (Thickness change)

Dimensions(mm)	L80mm x W6mm x H5mm	L80mm x W6mm x H7mm	L80mm x W6mm x H9mm
			
Recovery result	Grade 4	Grade 5	Grade 7
Recovery time(sec)	33sec	1min 2sec	1min 28sec

Equal proportion (W=2H)

Dimensions(mm)	L80mm x W10mm x H5mm	L80mm x W14mm x H7mm	L80mm x W18mm x H9mm
			
Recovery result	Grade 5	Grade 9	Grade 9
Recovery time(sec)	57sec	1min 35sec	2min 34sec

Unequal proportio (Thickness change)




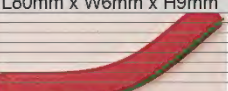
Dimensions(mm)	L80mm x W6mm x H5mm	L80mm x W6mm x H7mm	L80mm x W6mm x H9mm
			
Recovery result	Grade 4	Grade 6	Grade 9
Recovery time(sec)	42sec	1min 14sec	1min 40sec

Figure 5-16. The effects of size, thickness, and proportions on shape recovery quality and time.

5.4 Chapter Summary

In this chapter, the shape memory effect of selected PLA filaments was derived and analyzed and then explored which printing parameters could have a greater impact on the SMEs using a variety of printing parameters, including print orientation, print speed, print thickness, temperature, infill density, and print pattern. Moreover, the SMEs resulting from the samples' different properties, including size, thickness, and the samples' properties, were determined. These experiments show that using different printing parameters and applying different print properties result in different SMEs. However, it was found through experiments that the printing parameters rather than the print properties had a major impact on SMEs. For example, the build direction among printing parameters affects the infill density. Therefore, when the build orientation changes, the infill density changes, and the difference in infill density affects shape recovery and development recovery time. Also, according to the recovery temperature and pattern, SMEs showed a significant difference. However, the difference in print properties, such as print speed and thickness scaled at the same rate, did not significantly impact SMEs. In conclusion, this experiment indicates that print pattern and infill density have a significant

effect on SMEs compared to the other parameters of build orientation, print speed, and thickness. In addition, the quarter cubic pattern and the line pattern were compared, and the quarter cubic pattern showed excellent recovery quality and recovery time for both materials. It was also demonstrated that, the larger the sample size, the worse the recovery quality and the longer the recovery time. The difference in overall volume had a greater effect on the recovery quality and recovery time than the thickness of one side. Therefore, high capacity was inversely proportional to good recovery quality and time. Applying a wider variety of materials and printing parameters can result in a wider range of SMEs. However, due to time and cost constraints, it is inevitable to minimize the number of cases applicable to this study. Therefore, this study went through the process of finding suitable filaments and identifying print parameters that could have a significant impact on SMEs. In the next chapter, recovery quality and recovery time for all cases are determined by focusing on the parameters that had a large impact on the SMEs of 4D-printed parts, including infill density, printing pattern, and temperature, in order to determine the recovery rate and recovery time. The results are converted into numerical data and analysed through graphs.

Chapter 6. Evaluating the influence of print pattern and infill density

6.1 Introduction

This section aims to achieve research objectives 5: To compare and combine different SMEs by controlling the printing parameters and 6: To propose methods for controlling suitable shape-changing effects, such as printing parameters, so as to design effective 4D-printed parts. Using the results derived from the previous experiments, detailed experiments were conducted on the main areas of this study in order to derive numerical data for many Shape Memory Effects (SMEs). All of these experiments used water baths.

Figure 6-1 illustrates that the previous experiments focused on deriving filaments suitable for the experiments, identifying parameters that significantly impacted SMEs, and applying them directly to PLA samples. The shape, size, and shape transformation method applied to the sample adopted the same bar shape as the previous experiment, measuring 80 mm × 6 mm × 3 mm, and bending deformation to derive consistent results. These included infill density, print pattern, and temperature. The results of this section were derived from the results of the first three experiments. All 12 patterns provided by the 3D printer were applied. The infill density of 20%, 40%, 60%, 80%, and the highest 100% that can be realized with the printer was applied to various experiments. Due to the small size of the samples, infill densities of less than 20% were not applied due to difficulties in printing. This chapter consists of four parts. Section 6.2 details the experiment conducted to compare the SMEs of 12 patterns and five infill densities in a water bath experiment, which was conducted in order to determine the number of all SMEs (recovery quality and recovery time) by applying each pattern and infill density. The results are compared and analysed in graphs by converting the recovery rate and recovery time into numerical data. Section 5.3 provides a table showing the results of Section 6.2. The shape recovery rate and recovery time data derived from the experiment were incorporated into the shape control table and the physical four-dimensional printing (4DP) toolkit in order to ensure accessibility and ease of use. Section 5.4 details the experiments conducted to validate the plotted graphics and toolkit samples. The first goal of this section is to verify that the numerical data for recovery rates and recovery times can be reproduced by the physical 4DP toolkit, and the second goal is to determine the ways in which to improve the 4DP printing toolkit.

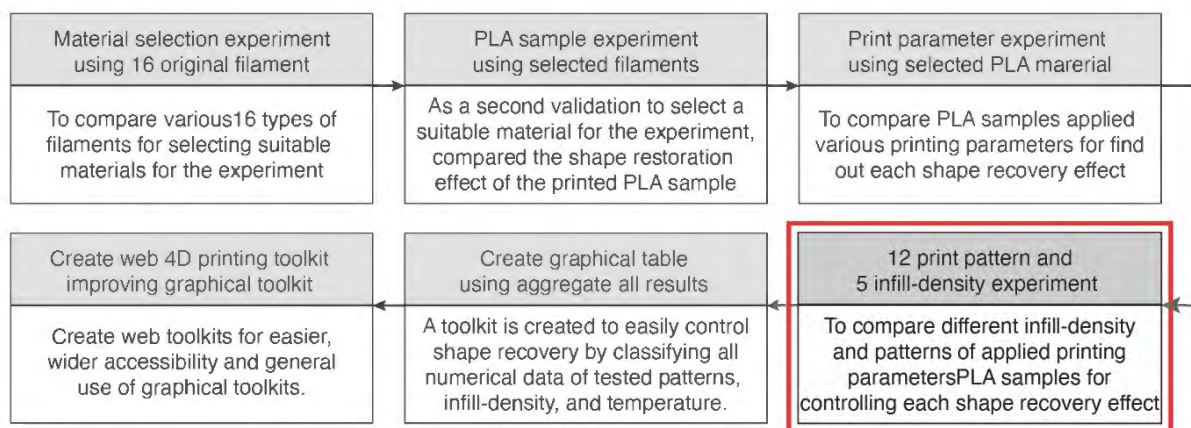


Figure 6-1. The process for the printing parameters experiment.

6.2 Print Patterns and Infill Densities

6.2.1 An Overview of Print Patterns and Infill Densities

Infill density refers to the settings on the inside of an object excluding the outer walls, and, in 4DP, it plays an important role in a part's strength, structure, and weight. Unlike many manufacturing technologies, 4DP allows careful control of wall line count and infill density. Infill density greatly impacts a part's strength, weight, buoyancy, and overall structure. The infill density of a part can be set in the printer slicer when the 3D model is converted to G-code. In slicers, infill density is defined as a percentage between 0 and 100%. 0% means the inside of the printed object is empty, and 100% means that it is completely solid. An object created with a 100% infill density represents 100% of the object's density. There are many levels in between, and adjusting these values is useful for accommodating different features. Infill density can affect the print strength, flexibility, and the amount of material used. The higher the infill density, the higher the strength, weight, printing time, and material consumption. Also, the higher the infill density, the less flexible and buoyant the part. The higher the percentage of the filling process, the harder the object is due to being made with more material, resulting in a longer time taken to produce it. In contrast, a lower proportion of infill results in lighter objects and faster production (Yarwindran et al., 2016). 4DP printed structures with different infill patterns could influence the relaxation behaviour to guide the load path at constant strain (Cadete et al., 2022). Printers generally recommend an infill density percentage of 20–50% so as to ensure standard print times, material consumption, and moderate strength. However, the user can control the infill density for functional printing and research. Some slicers allow different infill densities within the same part. This is called variable infill density, and certain settings in the slicing program allow users to specify the desired densities for different substrate areas (Roger & Krawczak., 2015; Tanveer et al., 2019) (Figure 6-2).

This chapter used infill densities of 20–50%, defined as standard infill densities, to identify a wide range of SMEs through infill densities. Infill densities of up to 100% were also experimented with in order to grasp the effect of the combination of various parameters on SMEs. The infill densities applied in this experiment were 20%, 40%, 60%, 80%, and 100%. This was because these infill densities could be sufficiently deduced from SMEs between 20% and 100% depending on the continuity of the numerical values. Figure 6-3 provides a visual example of infill density.

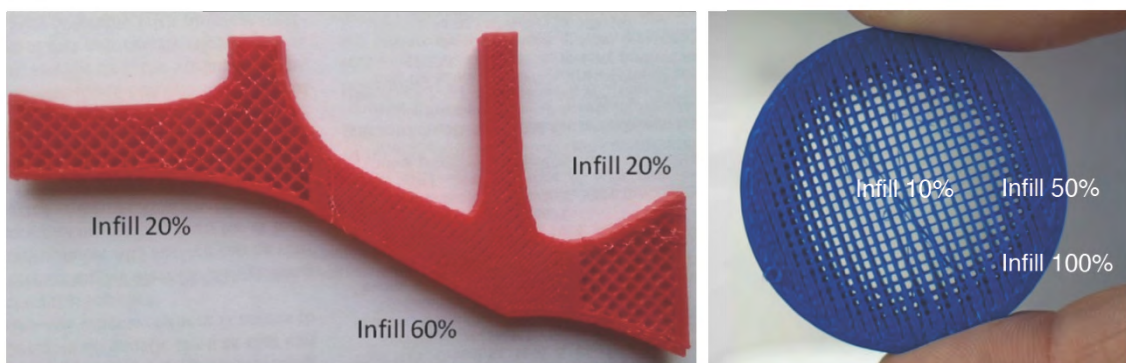


Figure 6-2. Example of variable infill density (Roger & Krawczak., 2015).

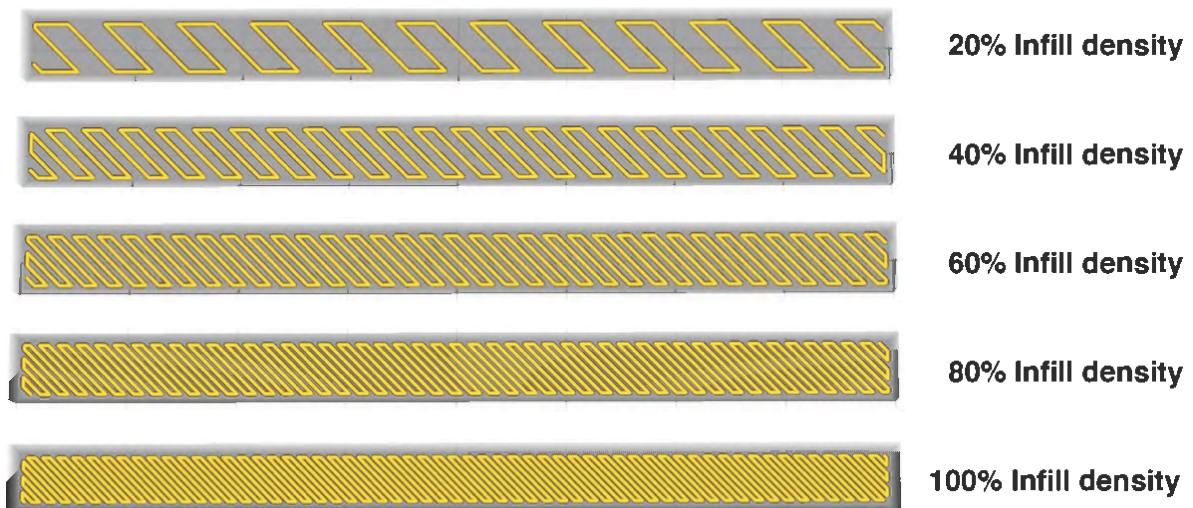


Figure 6-3. Infill densities from 20% to 100%.

The 12 print patterns applied prior to the experiment were patterns that are typically provided by the slicer software (Qudi tech V5.3.2) for the Qidi X-Pro material extrusion printer. These patterns are also compatible with third-party programs such as Cura and Simplify3D. There are 12 predefined patterns, including concentric circles, crosses, cubes, cube subdivisions, grids, gyroids, lines, octets, quarter cubes, triangles, tri-hexagons, and zigzags (see Figure 6-4). In general, each pattern has its characteristics and different uses. In particular, a pattern's characteristics can be distinguished by the strength difference. Lines and zigzags are the most popular patterns because three-dimensional printing (3DP) with polylactic acid (PLA) is not typically used to fabricate objects that will be subjected to heavy handling or high-intensity stress. Line and zigzag patterns are generally available with low infill densities of 0–15%. The patterns that can support higher stresses include grids, triangles, and tri-hexagons. In general, an infill density of 15–50% is recommended. In particular, since triangle and tri-hexagon patterns are stacked in a triangular mesh structure, they have high strength when a load is applied perpendicular to the object's surface. The difference between triangle and tri-hexagon patterns is the presence of a dense mesh. Tri-hexagon patterns have shorter lines connecting each side, so there are fewer warping problems due to poor printing cooling, resulting in their being stronger. The printing time of these patterns is 25% more than that of line patterns. In general, the patterns that provide the most strength are cubes, cubic subdivisions, quarter cubes, octets, and gyroids. These patterns are stacked in a 3D pattern in order to obtain prints with the same high levels of stiffness in multiple directions. Therefore, this infill pattern can support stress in multiple directions. These patterns' characteristics affect the printed part's strength, flexibility, and print speed (Zolfagharian et al., 2018). The bending angle of a 4DP actuator can be significantly affected by the pattern type and number of layers. Therefore, Material Extrusion build parameters, such as print pattern and layer height, can affect SMEs.

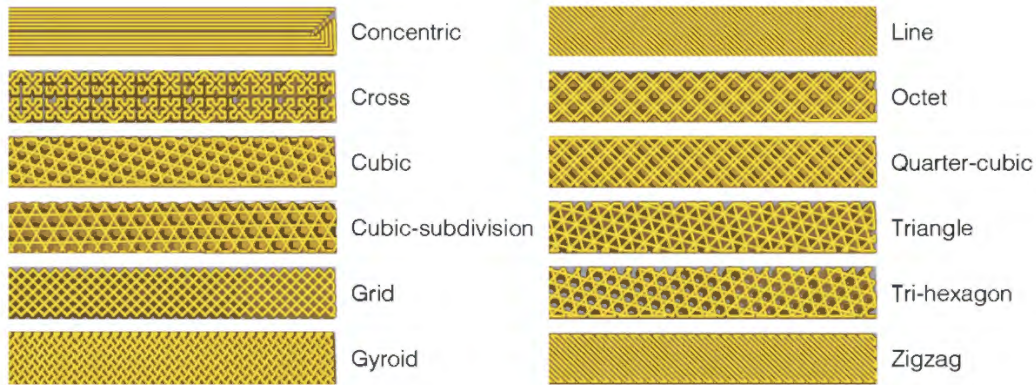








Figure 6-4. The 12 print patterns provided by Qidi Print.







6.2.2 Comparison of the 12 Patterns and Five Infill Densities

This experiment used 12 patterns and five infill densities of 20%, 40%, 60%, 80%, and 100% for N. The same procedure performed in previous experiments was carried out in this experiment. Figure 6-5 shows the selected 3D-printed PLA sample of N. This filament was used here as it was an original material with excellent recoverability and recovery time. This 3D-printed PLA sample was used to evaluate the characteristics of the 12 patterns and five infill densities. The patterns and fill densities were applied to N when fabricating the PLA sample. The application of the print pattern and fill density to the PLA sample led to determining the recovery quality and recovery time. In order to produce accurate and wide-ranging results, these patterns and infill densities were applied in three repetitions of the experiment. The PLA sample was produced with the same Qidi X-Pro printer as the previous experiment, and the parameters were the same as for the previous experiment: The extruder temperature was set at 210 °C, the printing speed was set at 50 mm/s, the retraction speed was set at 30 mm/min, and the retraction distance was set at 1.5 mm. Shape-recovery experiments were conducted using rectangular samples measuring 80 mm × 6 mm × 3 mm. For secure deformation, a glass transition temperature (T_g) of 80 °C was selected, which was higher than each PLA sample's T_g . According to the T_g and the use of the PLA in this experiment, the recovery temperature for the filament test was performed three times by setting three different recovery temperatures (65 °C, 70 °C, and 75 °C). All temperatures were maintained for 2 minutes in order to determine the bending rating. The SME quality was then rated from 1 (the highest grade) to 9 (the lowest grade). The shape-recovery grade was defined as the difference between the original and recovery deformation, with a flat shape indicating good recovery quality.







Temperature 65°C

Infill density (%)	20%	40%	60%	80%	100%
					
Concentric					
Recovery result	Grade 7	Grade 7	Grade 6	Grade 6	Grade 4
Recovery time(sec)	21 sec	25 sec	28 sec	29 sec	29 sec




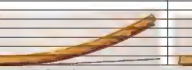

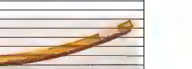
Temperature 70°C

Infill density (%)	20%	40%	60%	80%	100%
					
Concentric					
Recovery result	Grade 4	Grade 4	Grade 3	Grade 3	Grade 2
Recovery time(sec)	16 sec	22 sec	23 sec	24 sec	26 sec







Temperature 75°C

Infill density (%)	20%	40%	60%	80%	100%
					
Concentric					
Recovery result	Grade 4	Grade 3	Grade 3	Grade 2	Grade 1
Recovery time(sec)	16 sec	17 sec	18 sec	22 sec	24 sec







Temperature 65°C

Infill density (%)	20%	40%	60%	80%	100%
					
Cross					
Recovery result	Grade 7	Grade 6	Grade 6	Grade 5	Grade 5
Recovery time(sec)	14 sec	16 sec	17 sec	19 sec	22 sec







Temperature 70°C

Infill density (%)	20%	40%	60%	80%	100%
					
Cross					
Recovery result	Grade 4	Grade 4	Grade 4	Grade 4	Grade 4
Recovery time(sec)	11 sec	13 sec	14 sec	15 sec	18 sec







Temperature 75°C

Infill density (%)	20%	40%	60%	80%	100%
					
Cross					
Recovery result	Grade 4	Grade 4	Grade 3	Grade 3	Grade 3
Recovery time(sec)	9 sec	10 sec	12 sec	12 sec	13 sec







Temperature 65°C

Infill density (%)	20%	40%	60%	80%	100%
					
Cubic					
Recovery result	Grade 5	Grade 5	Grade 5	Grade 4	Grade 4
Recovery time(sec)	15 sec	17 sec	23 sec	23 sec	24 sec


Temperature 70°C

Infill density (%)	20%	40%	60%	80%	100%
					
Cubic					
Recovery result	Grade 3	Grade 3	Grade 3	Grade 3	Grade 2
Recovery time(sec)	9 sec	14 sec	16 sec	18 sec	19 sec


Temperature 75°C

Infill density (%)	20%	40%	60%	80%	100%
					
Cubic					
Recovery result	Grade 3	Grade 3	Grade 2	Grade 2	Grade 1
Recovery time(sec)	8 sec	13 sec	14 sec	16 sec	17 sec


Temperature 65°C

Infill density (%)	20%	40%	60%	80%	100%
					
Cubic-subdivision					
Recovery result	Grade 3	Grade 4	Grade 5	Grade 7	Grade 8
Recovery time(sec)	11 sec	14 sec	17 sec	19 sec	19 sec


Temperature 70°C

Infill density (%)	20%	40%	60%	80%	100%
					
Cubic-subdivision					
Recovery result	Grade 2	Grade 3	Grade 4	Grade 4	Grade 4
Recovery time(sec)	8 sec	13 sec	15 sec	16 sec	17 sec


Temperature 75°C

Infill density (%)	20%	40%	60%	80%	100%
					
Cubic-subdivision					
Recovery result	Grade 2	Grade 3	Grade 3	Grade 3	Grade 4
Recovery time(sec)	6 sec	11 sec	12 sec	13 sec	13 sec


Temperature 65°C

Infill density (%)	20%	40%	60%	80%	100%
					
Grid					
Recovery result	Grade 5	Grade 5	Grade 5	Grade 5	Grade 3
Recovery time(sec)	12 sec	14 sec	19 sec	20 sec	21 sec


Temperature 70°C

Infill density (%)	20%	40%	60%	80%	100%
					
Grid					
Recovery result	Grade 4	Grade 4	Grade 3	Grade 3	Grade 2
Recovery time(sec)	10 sec	12 sec	15 sec	16 sec	16 sec


Temperature 75°C

Infill density (%)	20%	40%	60%	80%	100%
					
Grid					
Recovery result	Grade 3	Grade 3	Grade 3	Grade 2	Grade 1
Recovery time(sec)	9 sec	11 sec	12 sec	14 sec	14 sec


Temperature 65°C

Infill density (%)	20%	40%	60%	80%	100%
					
Gyroid					
Recovery result	Grade 4	Grade 4	Grade 4	Grade 3	Grade 3
Recovery time(sec)	14 sec	17 sec	21 sec	22 sec	22 sec

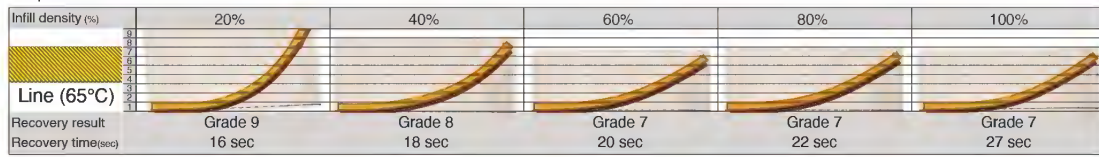
Temperature 70°C

Infill density (%)	20%	40%	60%	80%	100%
					
Gyroid					
Recovery result	Grade 3	Grade 3	Grade 3	Grade 3	Grade 3
Recovery time(sec)	11 sec	15 sec	17 sec	19 sec	20 sec

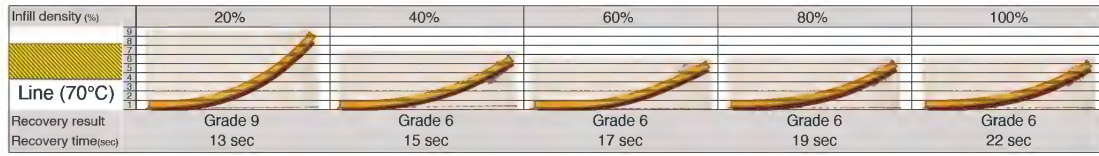
Temperature 75°C

Infill density (%)	20%	40%	60%	80%	100%
					
Gyroid					
Recovery result	Grade 3	Grade 3	Grade 3	Grade 3	Grade 2
Recovery time(sec)	7 sec	10 sec	12 sec	13 sec	15 sec

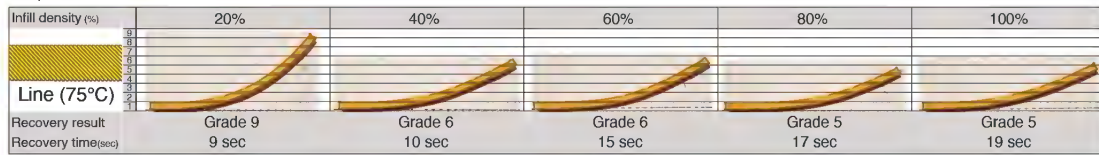
Temperature 65°C



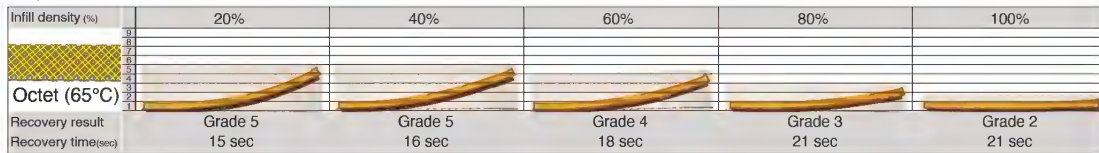
Temperature 70°C



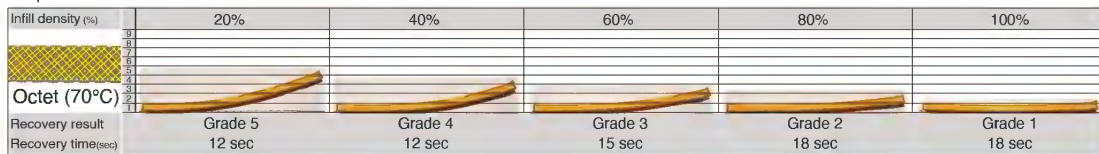
Temperature 75°C



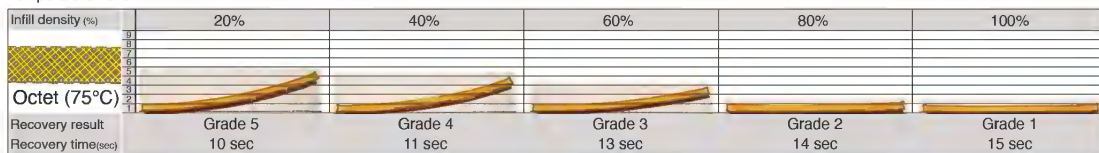
Temperature 65°C



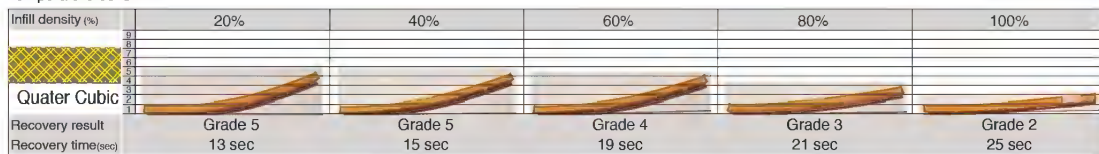
Temperature 70°C



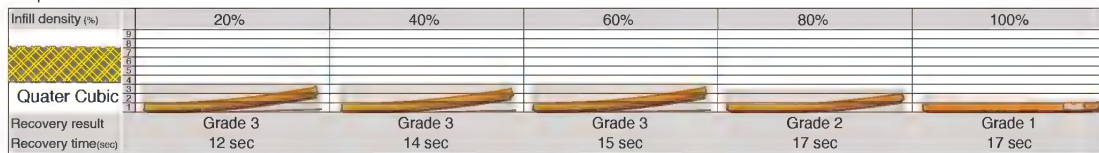
Temperature 75°C



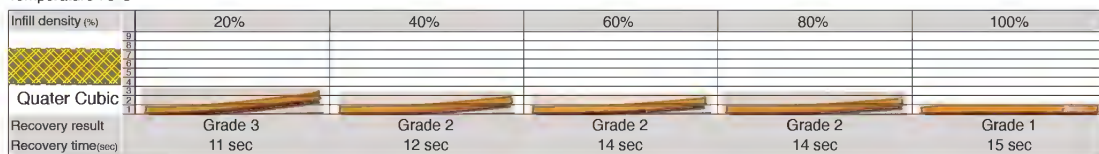
Temperature 65°C



Temperature 70°C



Temperature 75°C



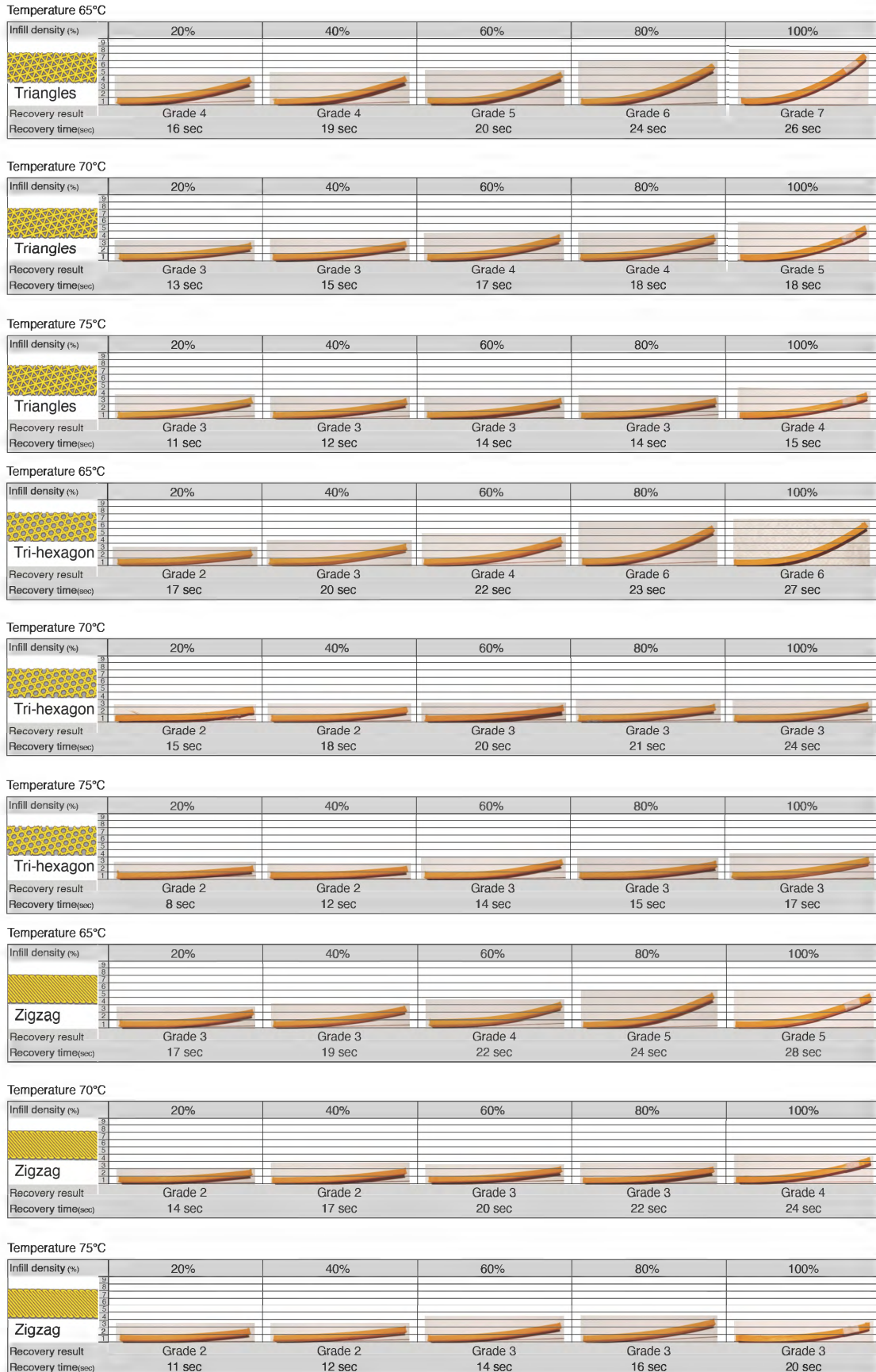


Figure 6-5. The bending recovery rates of 3D-printed PLA using 12 patterns.

6.2.3 Recovery Quality and Recovery Times in Different Print Patterns and Infill Densities

The effects of the patterns and infill densities used were expanded on by combining recovery quality and time; Recovery grade and recovery time were the result of one shape recovery. A high-quality recovery and a fast recovery rate do not indicate the merit of that parameter. This result can be used in various designs of printed objects regardless of the deviation of the recovery effect, and it can increase the dependence of the print design.

In order to more accurately identify the derived data, the results were divided into graphs, according to the patterns, infill densities, recovery temperatures, and recovery results such as recovery grade and time. The recovery quality was measured by applying the criteria specified in Chapter 4, section 4.2. Measurement Criteria in order to ensure consistency in the results. In order to ensure more accurate results, the experiment was repeated twelve times. In addition, the temperature and humidity of the printing and testing areas were kept as constant as possible in order to avoid possible errors from environmental influences. As shown in Figures 6-7 through 6-11, all 12 patterns and 5 infill densities led to different SME results. Detailed repeated experimental results will be discussed at the end of the chapter to demonstrate clarity and accuracy.

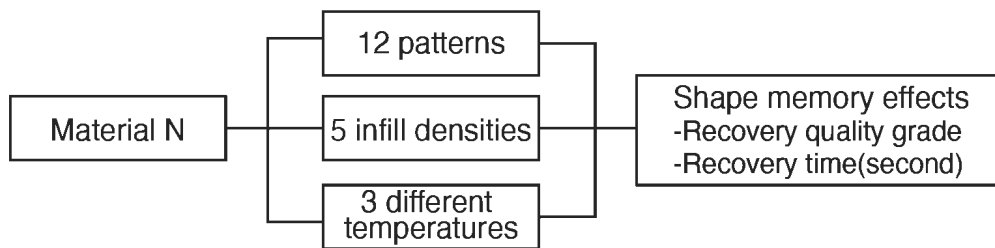


Figure 6-6. The process used to derive the SMEs.

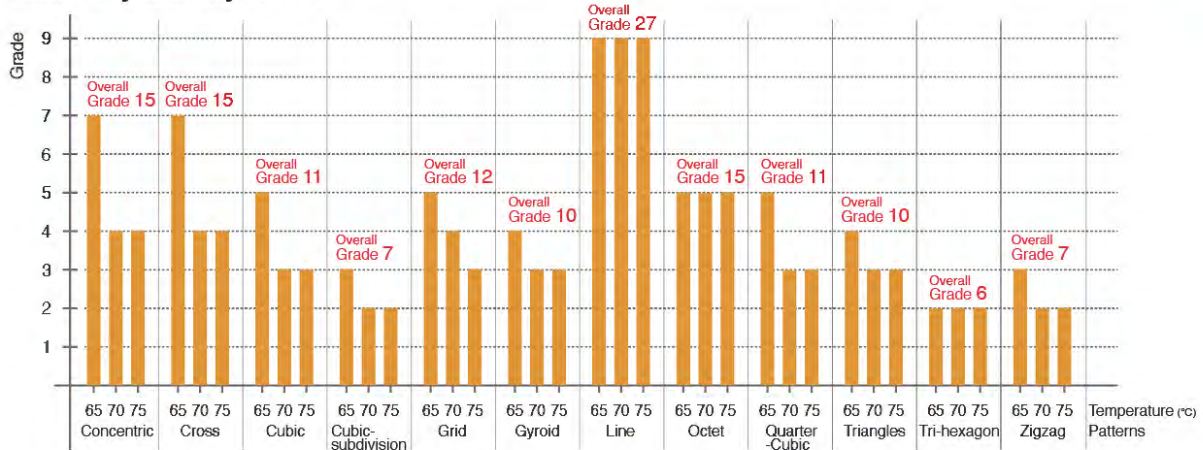
Figures 6-7 to 6-11 compare the results of the different infill densities for each division. Table 6-1 and Figure 6-7 shows the recovery grades and recovery times for 20% infill density, with the data demonstrating that the grade 2 tri-hexagon pattern produced the highest recovery results at 65 °C, 70 °C, and 75 °C. Moreover, the line pattern in each grade produced the lowest recovery results. An infill density of 20% meant that the material did not receive sufficient heat because there were too many empty spaces inside the sample. Therefore, this infill density may not be suitable for printing objects that need a high recovery rate. The line pattern, which was characterised by a straight repeating pattern, had different amounts of pattern filling in the sample compared to the tri-hexagon pattern, which was filled in in the form of a dense mesh. Therefore, even with the same infill density of 20%, the amount of material to be filled varies according to the pattern used, and the volume of the internal structure that can accommodate heat can differ. Thus, the shape recovery rate differed between each pattern. In terms of time, the cubic-subdivision pattern provided the shortest duration of 6 seconds at 75 °C, and the concentric pattern provided the longest duration of 21 seconds at 65 °C.

Table 6-1. Result of SMEs with an infill density of 20%.

20% infill density recovery quality and time result

Pattern (°C)	Concentric	Cross	Cubic	Cubic-subdivision	Grid	Gyroid	Line	Octet	Quarter-cubic	Triangles	Tri-hexagon	Zigzag
65°C	21 sec / 7	14 sec / 7	15 sec / 5	11 sec / 3	12 sec / 5	14 sec / 4	16 sec / 9	15 sec / 5	13 sec / 5	16 sec / 4	17 sec / 2	17 sec / 3
70°C	16 sec / 4	11 sec / 4	09 sec / 3	08 sec / 2	10 sec / 4	11 sec / 3	13 sec / 9	12 sec / 5	12 sec / 3	13 sec / 3	15 sec / 2	14 sec / 2
75°C	16 sec / 4	09 sec / 4	08 sec / 3	06 sec / 2	09 sec / 3	07 sec / 3	09 sec / 9	10 sec / 5	11 sec / 3	11 sec / 3	08 sec / 2	11 sec / 2

Recovery Quality Grade



Recovery Time Result

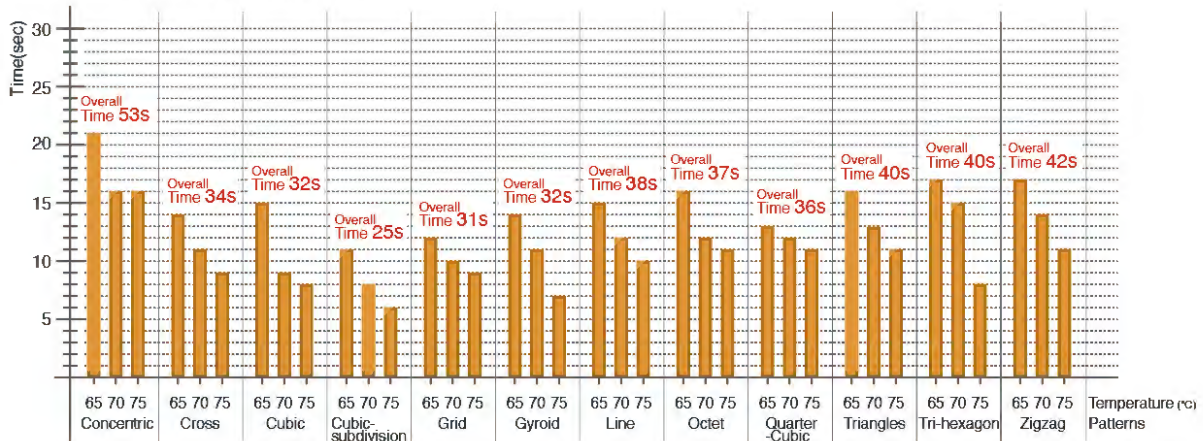


Figure 6-7. SMEs with an infill density of 20%.

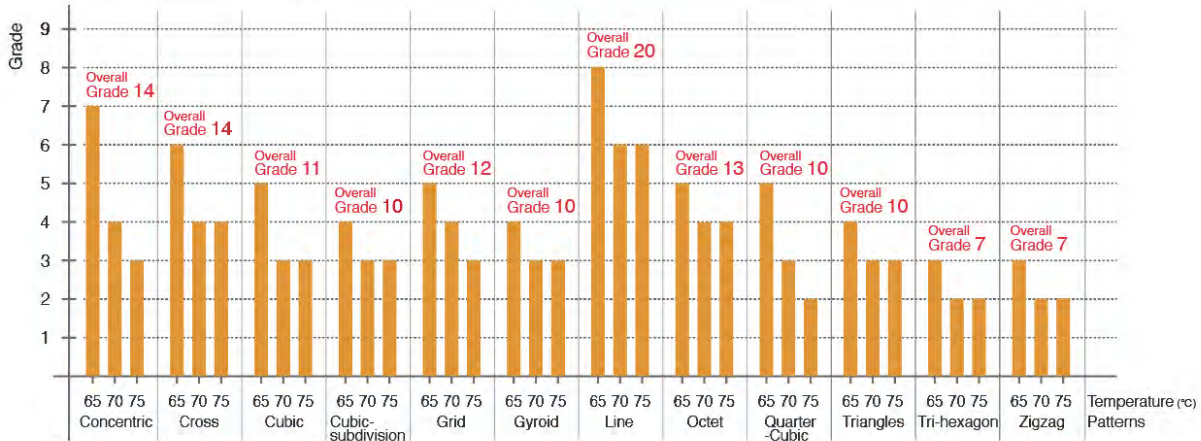
Table 6-2 and Figure 6-8 shows the object’s recovery grades and recovery times at 40% infill density. 75 °C produced the highest recovery results for grade 2 quarter-cubic, tri-hexagon, and zigzag patterns. At 65°C, a grade 8 line pattern produced the lowest recovery results. Regarding time, the cross, gyroid, and line patterns provided the shortest duration of 10 seconds at 75 °C. The concentric pattern provided the longest duration of 25 seconds at 65 °C. Therefore, the 40% infill density showed a good overall recovery rate compared to the 20% infill density. However, it showed a slower shape recovery rate than the 20% infill density.

Table 6-2. Result of SMEs with an infill density of 40%.

40% infill density recovery quality and time result

Pattern (°C)	Concentric	Cross	Cubic	Cubic-subdivision	Grid	Gyroid	Line	Octet	Quarter-cubic	Triangles	Tri-hexagon	Zigzag
65°C	25 sec / 7	16 sec / 6	17 sec / 5	14 sec / 4	14 sec / 5	17 sec / 4	18 sec / 8	16 sec / 5	15 sec / 5	19 sec / 4	20 sec / 3	19 sec / 3
70°C	22 sec / 4	13 sec / 4	14 sec / 3	13 sec / 3	12 sec / 4	15 sec / 3	15 sec / 6	12 sec / 4	14 sec / 3	15 sec / 3	18 sec / 2	17 sec / 2
75°C	17 sec / 3	10 sec / 4	13 sec / 3	11 sec / 3	11 sec / 3	10 sec / 3	10 sec / 6	11 sec / 4	12 sec / 2	12 sec / 3	12 sec / 2	12 sec / 2

Recovery Quality Grade



Recovery Time Result

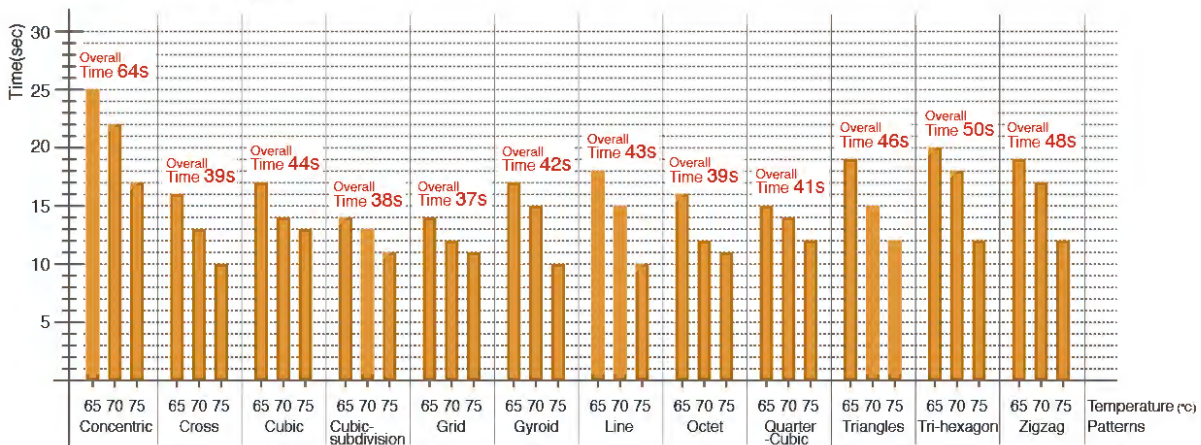


Figure 6-8. SMEs with an infill density of 40%.

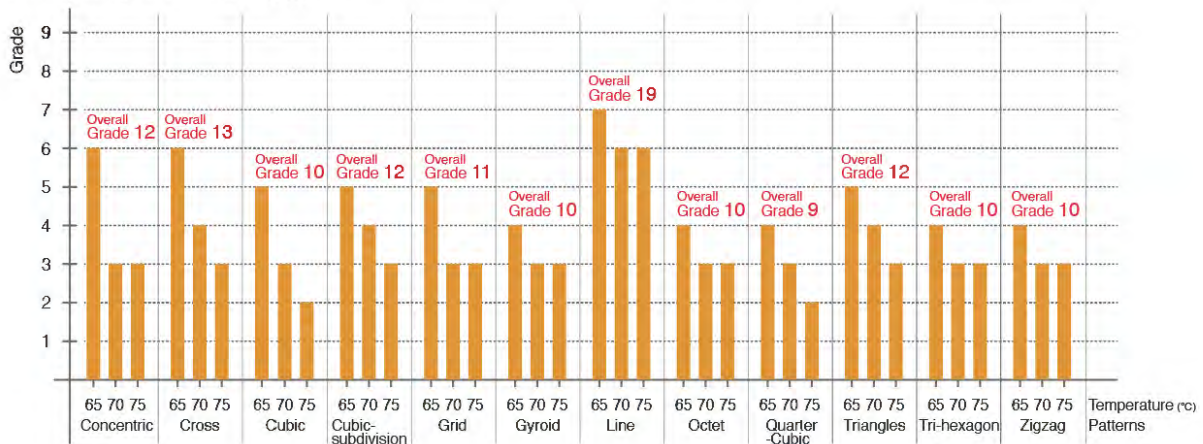
Table 6-3 and Figure 6-9 shows the recovery grades and recovery times for 60% infill density. 75 °C produced the highest recovery results for grade 2 cube and quarter cubic patterns. Moreover, 65 °C showed the lowest shape recovery results of the grade 7 line pattern. In addition, the line pattern had the lowest recovery rates at each temperature. When adding the shape recovery grades at each temperature to derive an average, the quarter cubic pattern showed the highest recovery rates, with an overall grade of 9, and the line pattern showed the lowest recovery rate, with an overall grade of 19. In terms of time, the cubic subdivision, cross, grid, and gyroid patterns provided the shortest duration of 12 seconds at 75 °C. The concentric circle pattern provided the longest duration of 28 seconds at 65 °C. Compared to the recovery times for 20% and 40% infill densities, the recovery time gradually slowed.

Table 6-3. Result of SMEs with an infill density of 60%.

60% infill density recovery quality and time result

Pattern (°C)	Concentric	Cross	Cubic	Cubic- sub-division	Grid	Gyroid	Line	Octet	Quarter- cubic	Triangles	Tri- hexagon	Zigzag
65°C	28 sec / 6	17 sec / 6	23 sec / 5	17 sec / 5	19 sec / 5	21 sec / 4	20 sec / 7	18 sec / 4	19 sec / 4	20 sec / 5	22 sec / 4	21 sec / 4
70°C	23 sec / 3	14 sec / 4	16 sec / 3	15 sec / 4	15 sec / 3	17 sec / 3	17 sec / 6	15 sec / 3	15 sec / 3	17 sec / 4	20 sec / 3	20 sec / 3
75°C	18 sec / 3	12 sec / 3	14 sec / 2	12 sec / 3	12 sec / 3	12 sec / 3	15 sec / 6	13 sec / 3	14 sec / 2	14 sec / 3	14 sec / 3	14 sec / 3

Recovery Quality Grade



Recovery Time Result

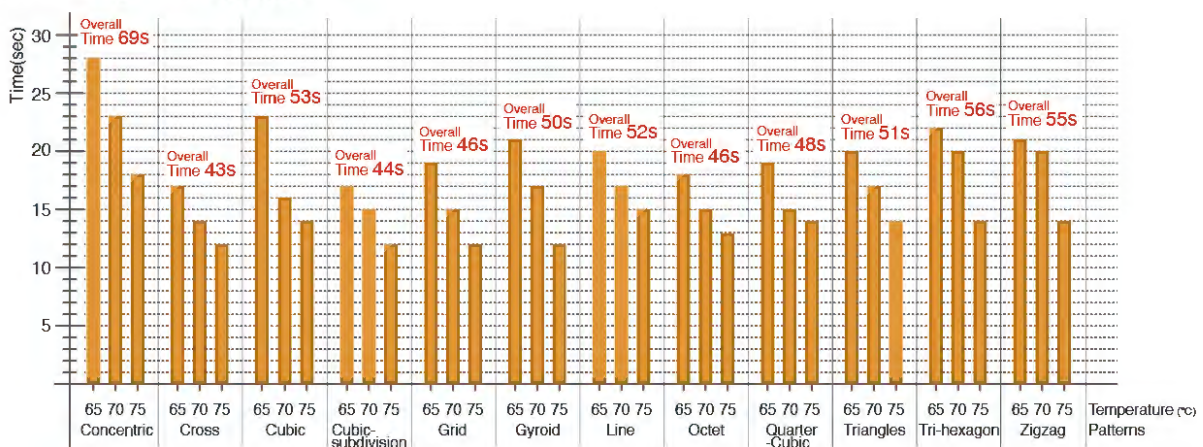


Figure 6-9. SMEs with an infill density of 60%.

Table 6-4 and Figure 6-10 shows the recovery grades and recovery times for 80% infill density. This infill density produced the highest recovery results for the grid and quarter cubic patterns with a grade of 1 at 75 °C. Moreover, at 65 °C, a grade 7 cubic-sub-division and line pattern produced the lowest shape recovery grade. The overall grade also showed the highest recovery rate with the quarter cubic pattern, which was labelled as having a grade 6 recovery rate. Regarding time, the cross pattern provided the shortest duration of 12 seconds at 75 °C, and the concentric pattern provided the longest duration of 29 seconds at 65 °C. A fill density of

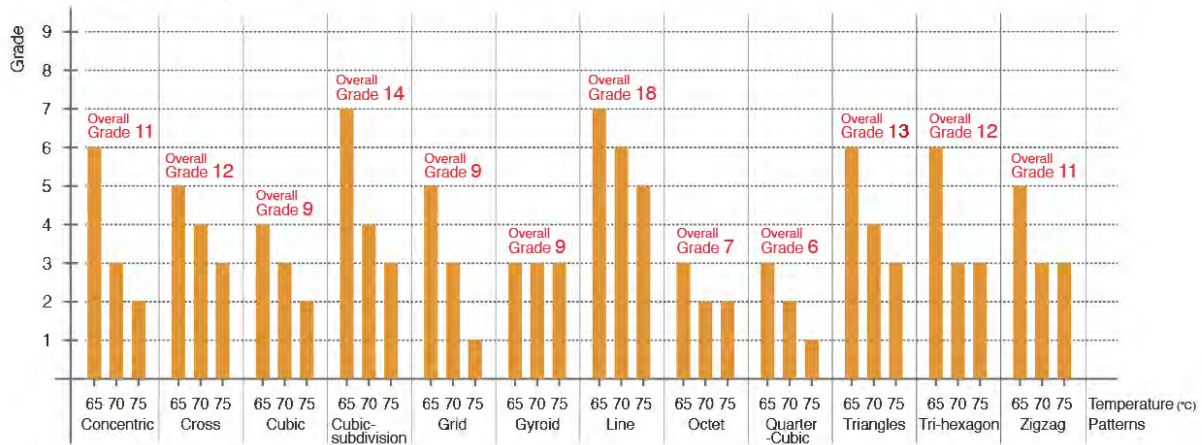
80% did not show a significant difference in overall recovery grade and time when compared to a infill density of 60%. The thresholds for 60% and 80% infill densities were very close.

Table 6-4. Result of SMEs with an infill density of 80%.

80% infill density recovery quality and time result

Pattern (°C)	Concentric	Cross	Cubic	Cubic- sub-division	Grid	Gyroid	Line	Octet	Quarter- cubic	Triangles	Tri- hexagon	Zigzag
65°C	29 sec / 6	19 sec / 5	23 sec / 4	19 sec / 7	20 sec / 5	22 sec / 3	22 sec / 7	21 sec / 3	21 sec / 3	24 sec / 6	23 sec / 6	24 sec / 5
70°C	24 sec / 3	15 sec / 4	18 sec / 3	16 sec / 4	16 sec / 3	19 sec / 3	19 sec / 6	18 sec / 2	17 sec / 2	18 sec / 4	21 sec / 3	22 sec / 3
75°C	22 sec / 2	12 sec / 3	16 sec / 2	13 sec / 3	14 sec / 1	13 sec / 3	17 sec / 5	14 sec / 2	14 sec / 1	14 sec / 3	15 sec / 3	16 sec / 3

Recovery Quality Grade



Recovery Time Result

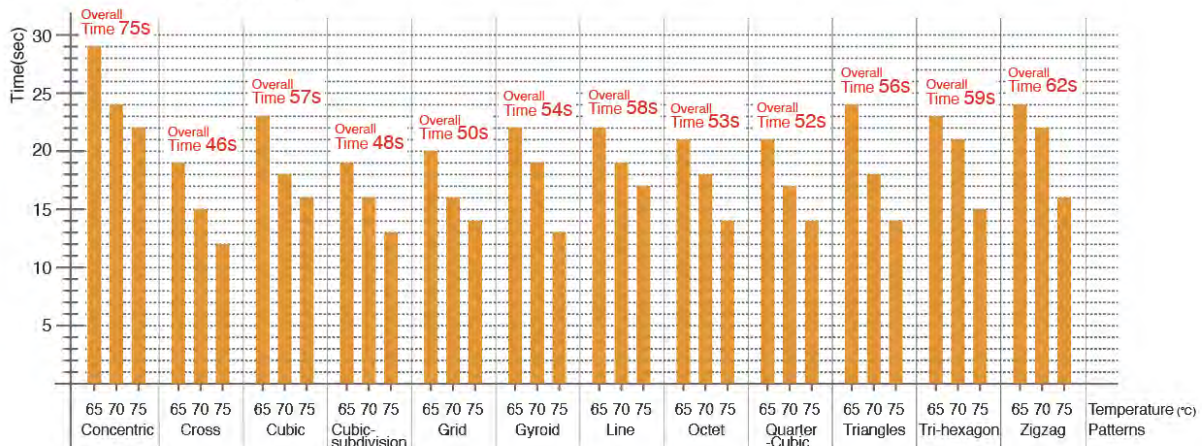


Figure 6-10. SMEs with an infill density of 80%.

Table 6-5 and Figure 6-11 shows the recovery grades and recovery times for 100% infill density. The highest recovery results were in the octet and quarter-cubic patterns at 70 °C and 75 °C with a grade of 1. Moreover, 65 °C resulted in the lowest outcomes for a grade 8 cubic-sub-division pattern. As for the overall grade, octet and quarter-cubic patterns showed similar shape recovery rates with a grade of 4, while the line pattern showed the lowest shape recovery rate, with a grade of 18. In terms of time, the concentric pattern provided the longest shape

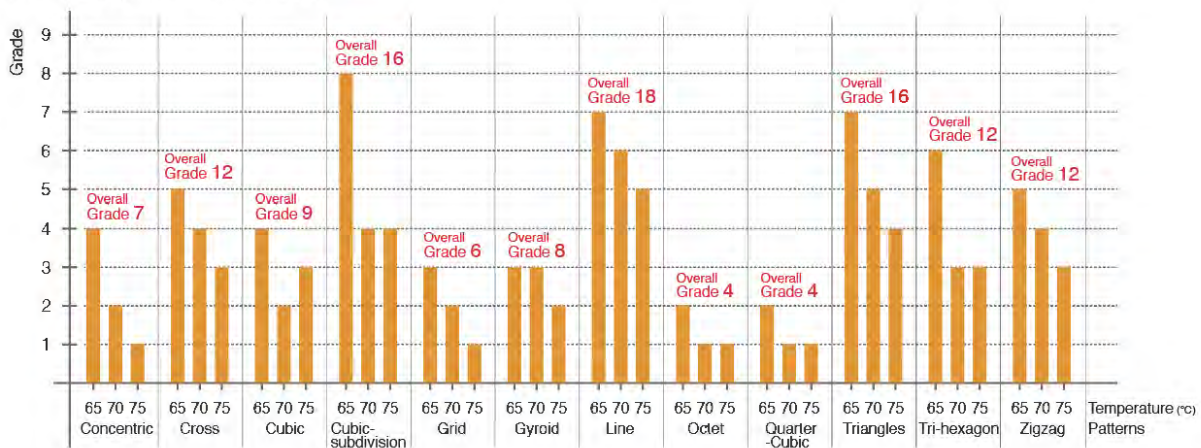
recovery duration of 29 seconds at 65 °C. Overall, the recovery rate gradually improved compared to the other infill densities. On the other hand, the recovery rate of all patterns significantly decreased.

Table 6-5. Result of SMEs with an infill density of 100%.

100% infill density recovery quality and time result

Pattern (°C)	Concentric	Cross	Cubic	Cubic-subdivision	Grid	Gyroid	Line	Octet	Quarter-cubic	Triangles	Tri-hexagon	Zigzag
65°C	29 sec / 4	22 sec / 5	24 sec / 4	19 sec / 8	21 sec / 3	22 sec / 3	27 sec / 7	21 sec / 2	25 sec / 2	26 sec / 7	27 sec / 6	28 sec / 5
70°C	26 sec / 2	18 sec / 4	19 sec / 2	17 sec / 4	16 sec / 2	20 sec / 3	22 sec / 6	18 sec / 1	17 sec / 1	18 sec / 5	24 sec / 3	24 sec / 4
75°C	24 sec / 1	13 sec / 3	17 sec / 3	13 sec / 4	14 sec / 1	15 sec / 2	19 sec / 5	15 sec / 1	15 sec / 1	15 sec / 4	17 sec / 3	20 sec / 3

Recovery Quality Grade



Recovery Time Result

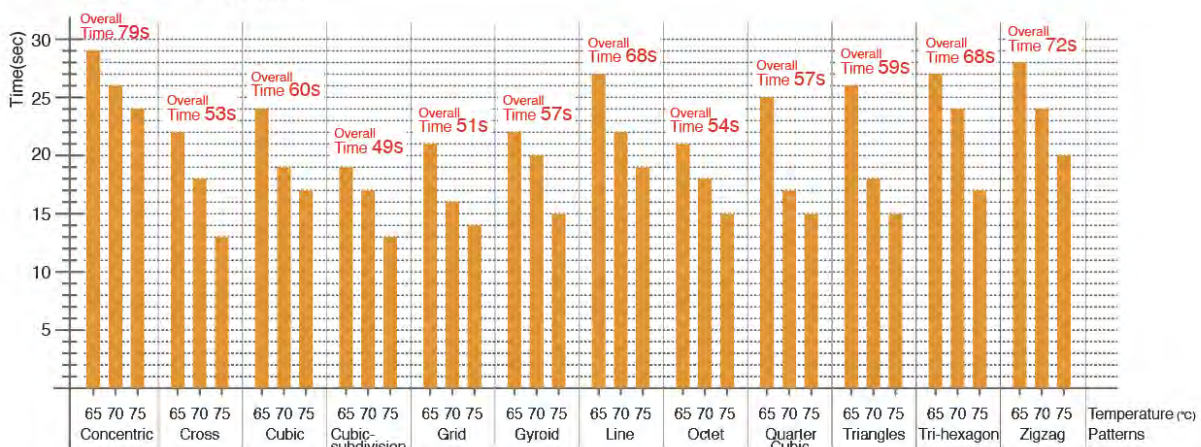
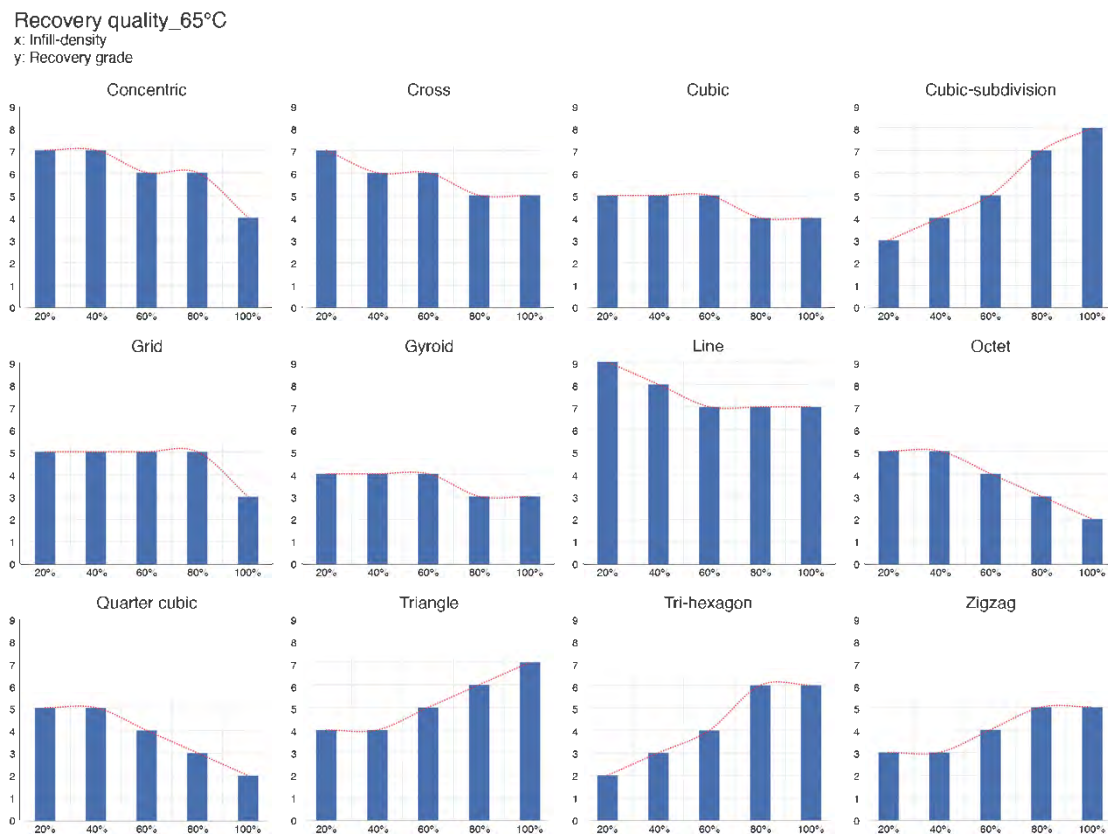


Figure 6-11. SMEs with an infill density of 100%.

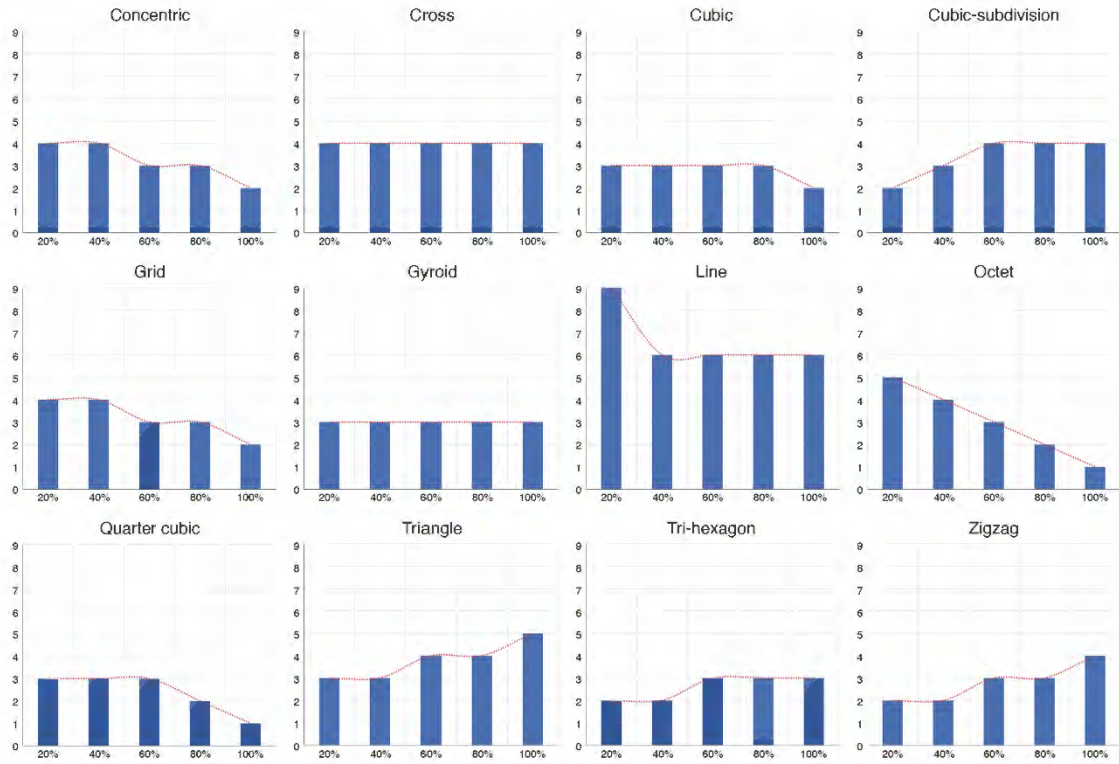
Figures 6-12 and 6-13 compare each shape recovery result in terms of temperature. Figure 6-12 shows the shape recovery grades according to temperatures of 65 °C, 70 °C, and 75°C, and Figure 6-13 shows the shape recovery times at different temperatures. Figure 6-12 shows that the higher the infill density, the closer the grade is to 1 in most of the patterns. Moreover, the recovery rate of the cubic-subdivision, triangle, tri-hexagon, and zigzag patterns decreased as

the infill density increased. The experiment was repeated, and the results were similar. It can be seen that the patterns with lower recovery due to higher infill densities are those with inherent high mass characteristics. The tri-hexagon pattern, which showed the highest recovery rate at an infill density of 20%, significantly deteriorated as the infill density increased. This could be used to disprove that a perfectly solid object (100% infill) can be accompanied by high shape recovery. In particular, what should be focused on in this graph is the result of shape recovery according to temperature. Without a single variable, all patterns showed higher shape recovery results at higher temperatures. It can also be seen that there is a difference between the shape recovery rates at 65 °C and 70 °C and the shape recovery rates at 70 °C and 75 °C. The patterns that had low shape recovery rates at a recovery temperature of 65 °C showed significantly higher shape recovery at 70 °C. On the other hand, the recovery temperatures of 70 °C and 75 °C showed less shape recovery. Thus, 70°C is the threshold for the critical point of shape recovery .



Recovery quality_70°C

x: Infill-density
y: Recovery grade



Recovery quality_75°C

x: Infill-density
y: Recovery grade

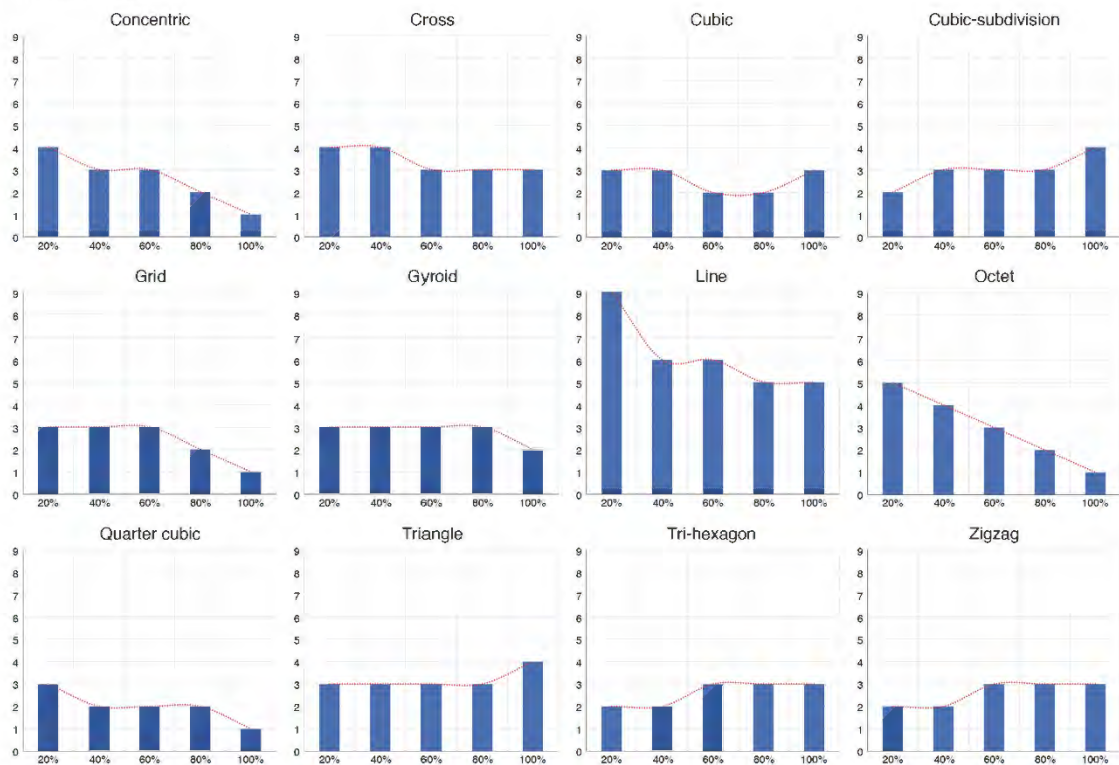
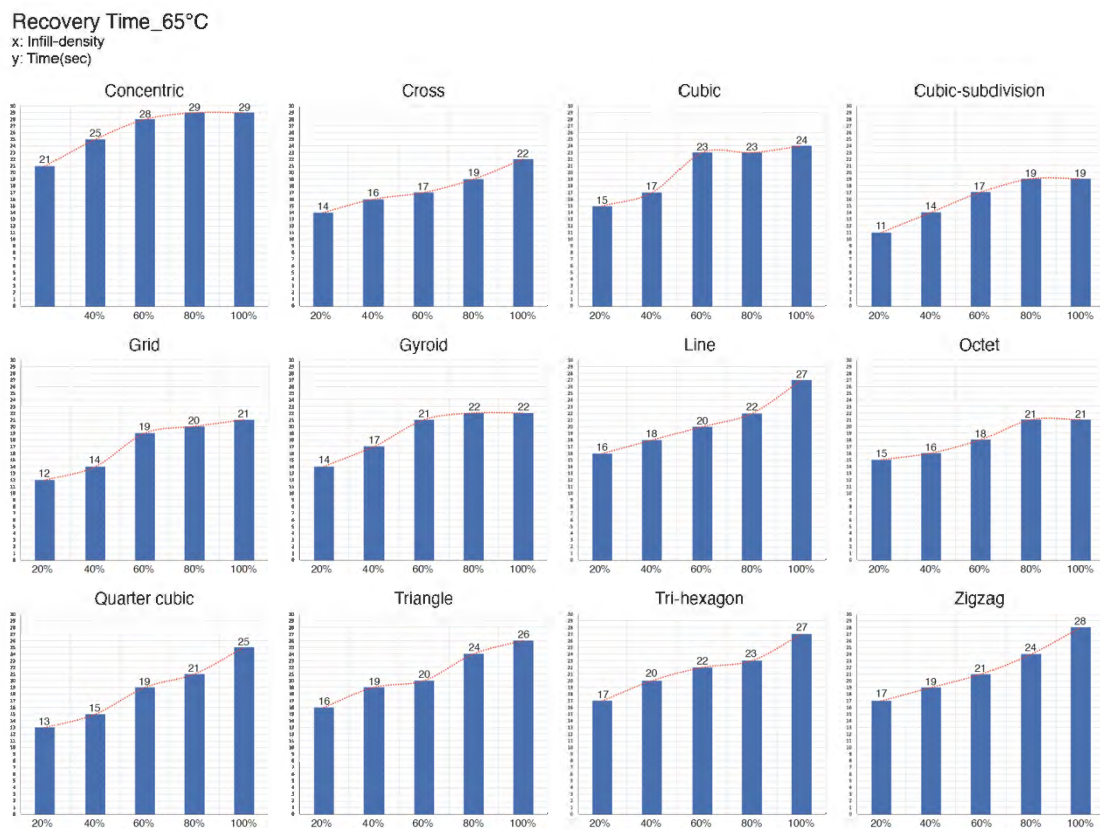
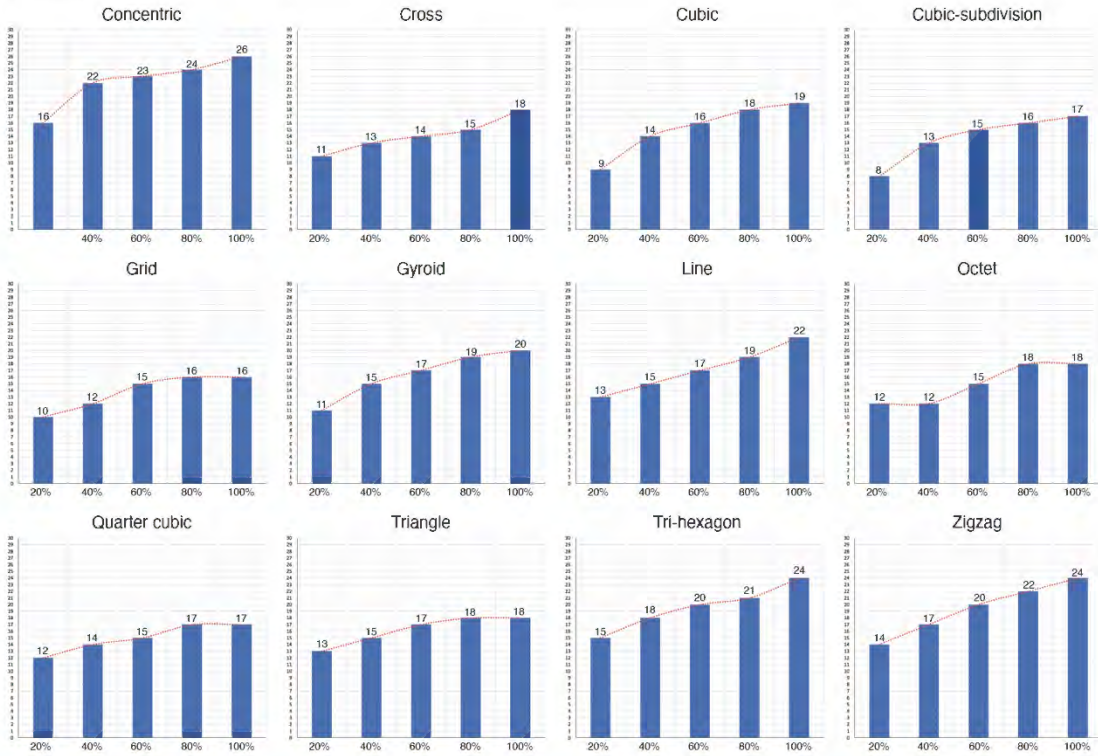


Figure 6-12. Recovery quality results based on temperatures of 65 °C, 70 °C, and 75 °C.

Figure 6-13 shows the shape recovery time according to different temperatures. At a glance, the graphs of all patterns show a line that gradually rises. This undoubtedly means that the higher the infill density for all patterns, the longer the shape recovery will be. High heat results in high recovery rates and fast recovery. Moreover, the high-density material accumulates a lot of recovery energy. Therefore, the higher the infill density, the higher the recovery rate. However, high-density materials that have accumulated a lot of heat have increased recovery times as the recovery mass is greater than the recovery energy. A material with a high mass (i.e., a material that absorbs a lot of heat) takes a longer time to recover its shape because the volume that needs to be recovered is large. Regardless of the infill density, high temperatures result in faster shape recovery rates at the same infill density.



Recovery Time_70°C
 x: Infill-density
 y: Time(sec)



Recovery Time_75°C
 x: Infill-density
 y: Time(sec)

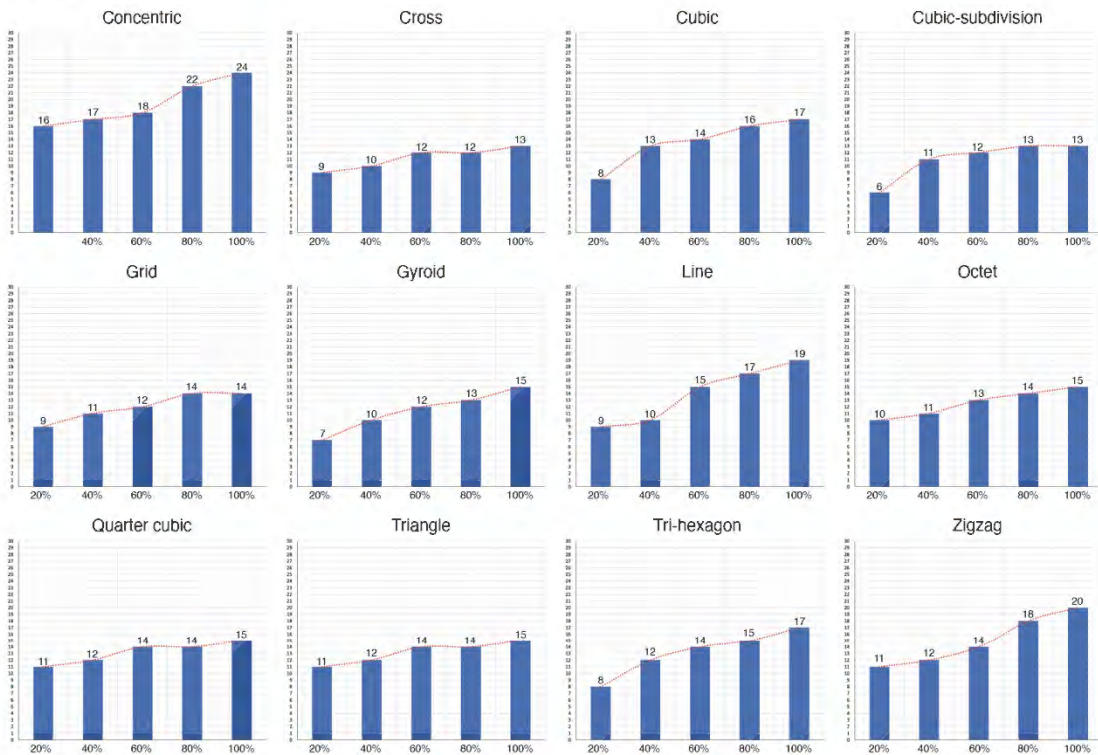
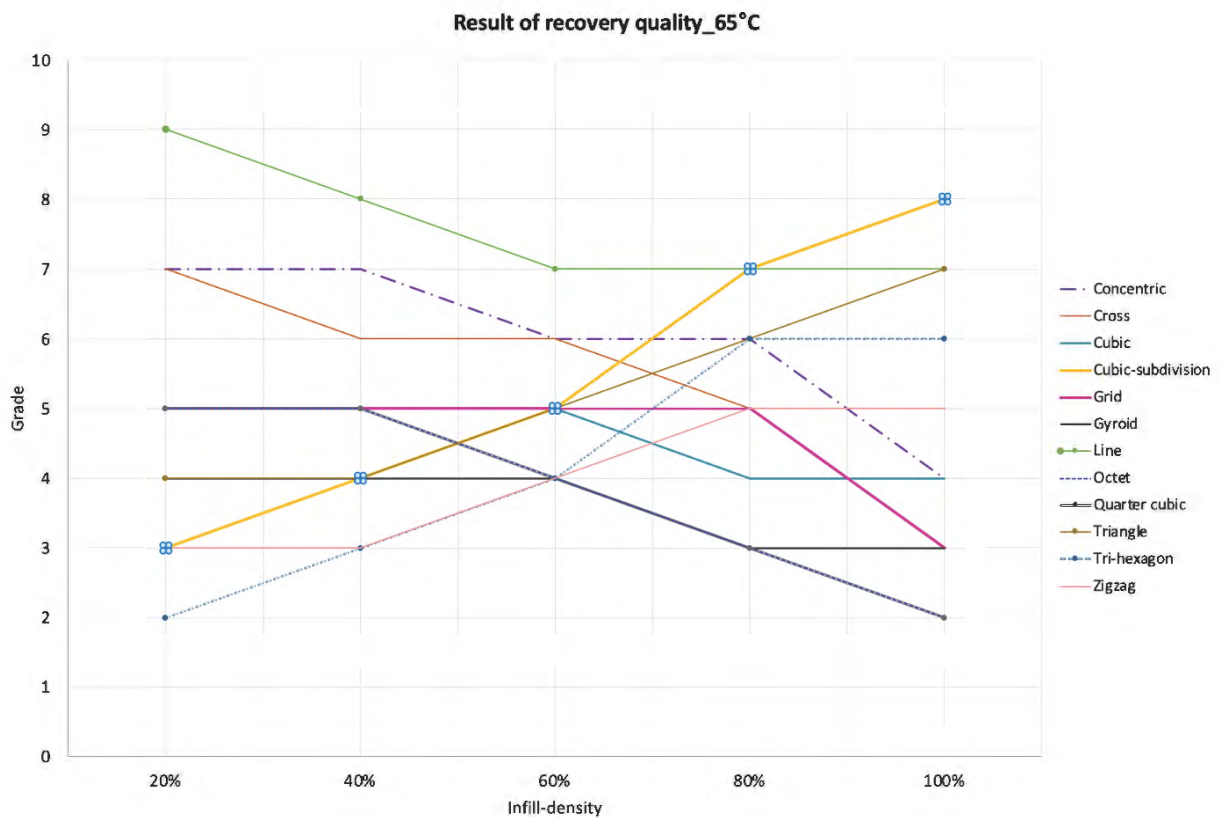


Figure 6-13. Recovery times based on temperatures of 65 °C, 70 °C, and 75 °C.

Figures 6-14 and 6-15 display the shape recovery rates of the different printing patterns. Figure 6-14 shows the results of the same recovery grade but focuses on the printing pattern. In order to easily identify the shape recovery rate of each pattern, different colours and lines were used. A line pattern with 20% infill density showed a grade 9 shape recovery rate, which gradually increased as the fill density increased to 100%. The patterns that showed the highest recovery rates were the octet and quarter-cubic patterns, and the higher the infill density, the higher the shape recovery. At a recovery temperature of 65 °C, the cubic subdivisions and triangle patterns (indicated by the yellow and brown lines, respectively) showed lower recovery rates as the infill density increased. However, as the temperature increased, most of the patterns' grades (except for the line pattern's grade) start to decrease. Therefore, high temperature greatly affects shape recovery.

The numerical data were recorded at infill densities of 20%, 40%, 60%, 80% and 100%. However, the infill density results that were excluded from the experiment can be inferred by the rising and falling lines in the graph. For example, a line pattern with a 50% infill density can yield a recovery rate of 7.5°.



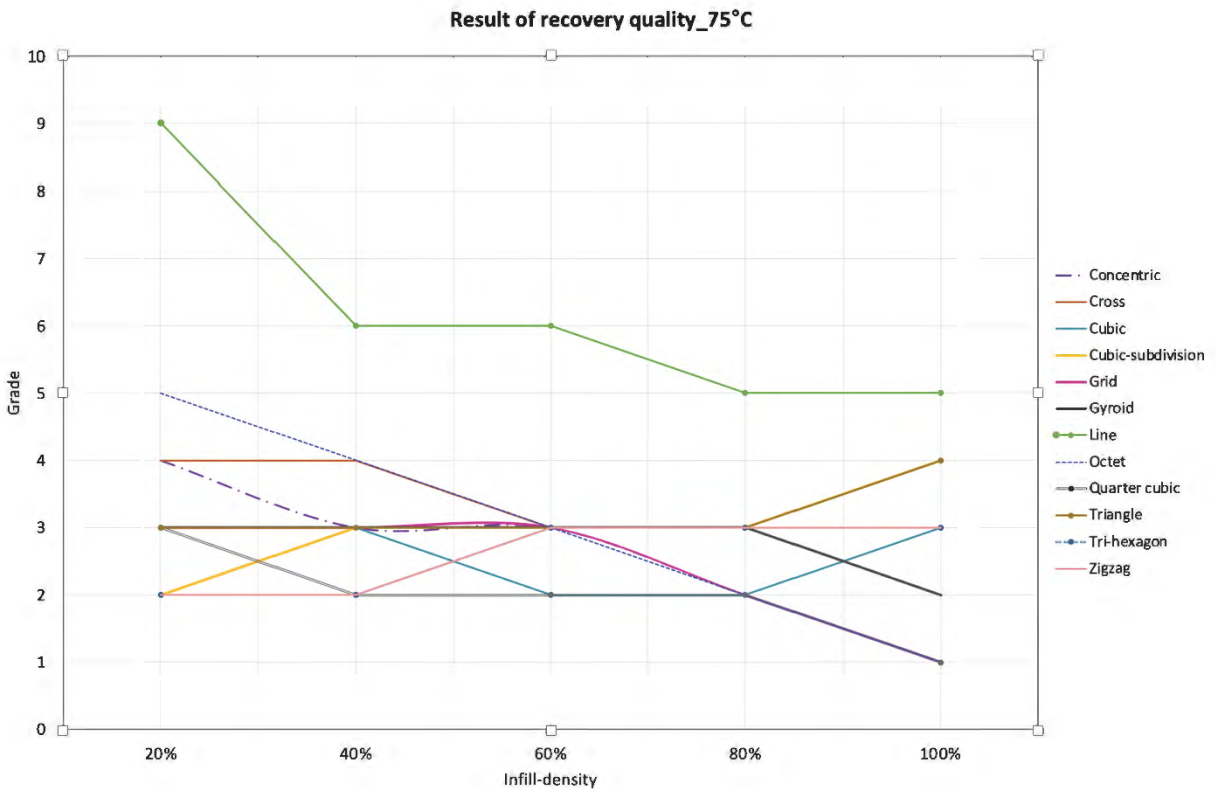
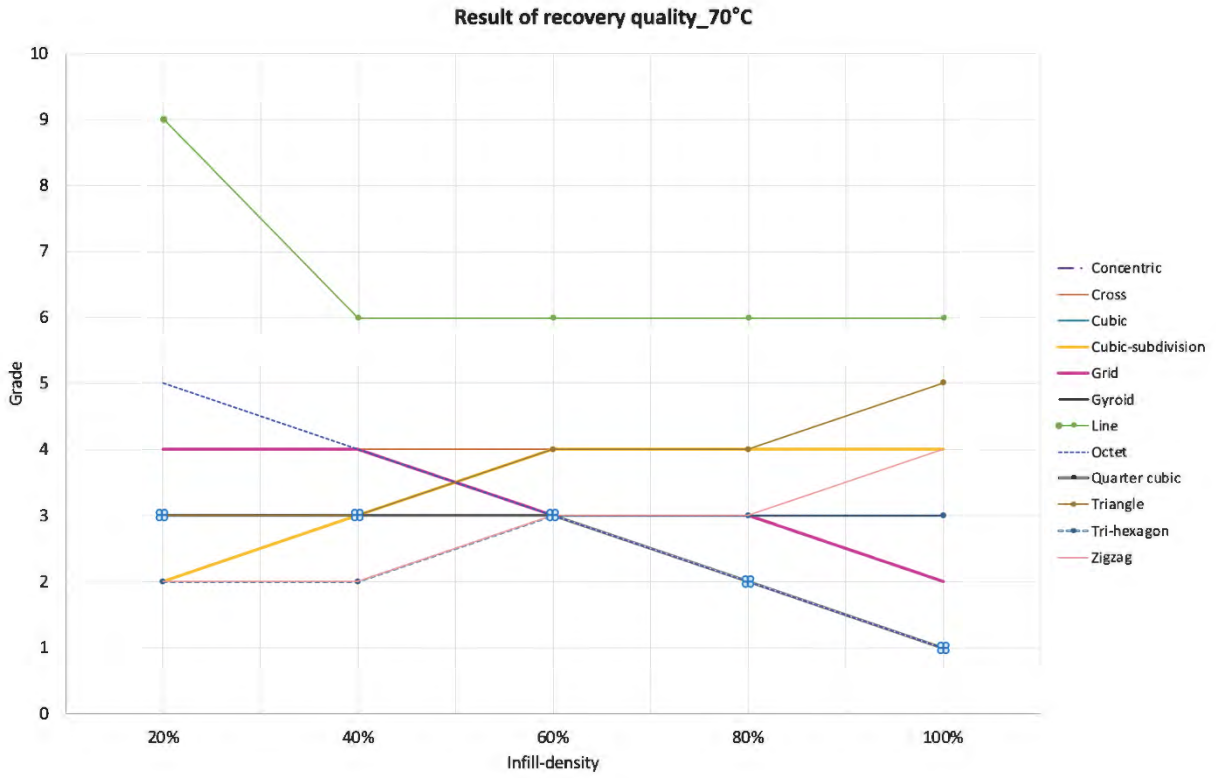
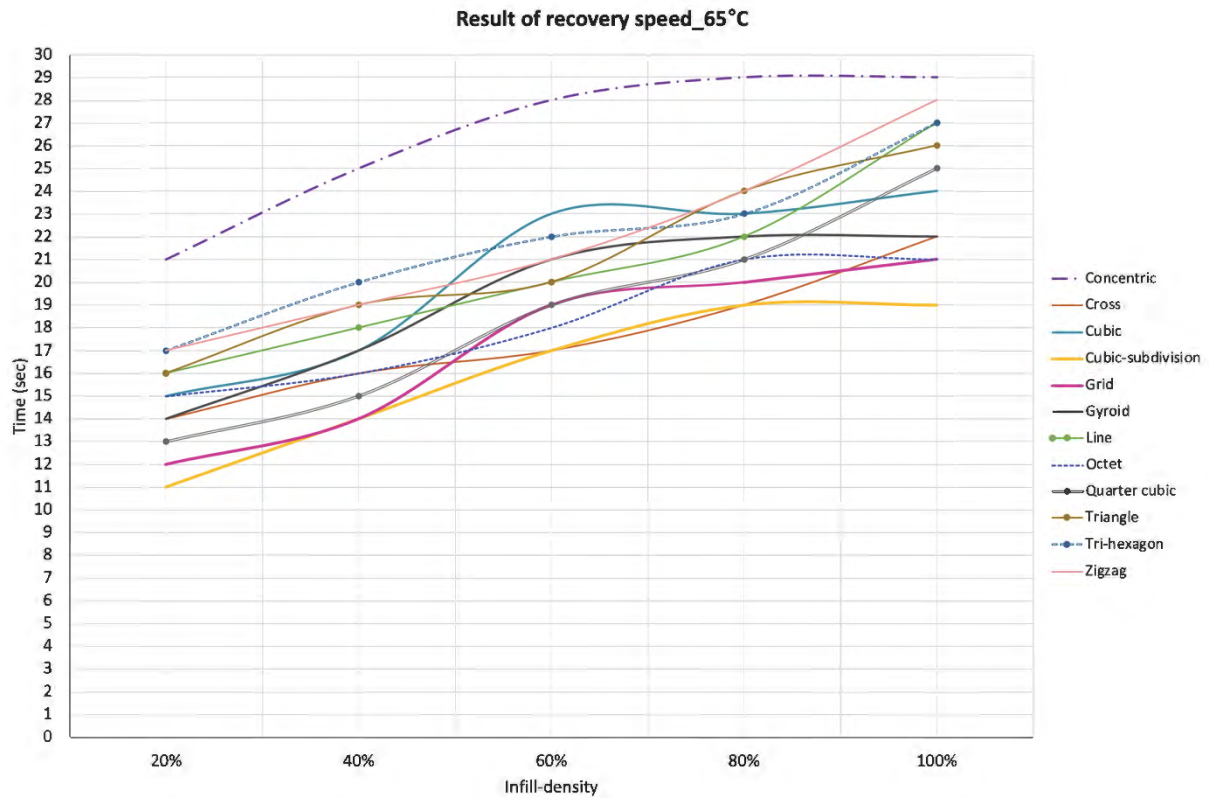


Figure 6-14. The quality recovery rates of the 12 patterns and 5 infill densities at 65 °C, 70 °C, and 75 °C.

Figure 6-15 shows the same shape recovery rate results with a focus on the printing pattern. Each pattern's shape recovery time was clearer than the shape recovery quality. For all patterns, the higher the infill density, the more time was required for the recovery time. Furthermore, the higher the recovery temperature, the quicker the shape recovery time. As shown in Figure 6-14, the rate of shape recovery for non-experimental infill densities was predictable. Therefore, it can be predicted that a concentric pattern with 90% infill density at a shape recovery temperature of 75 °C can achieve a shape recovery time of 23 seconds.



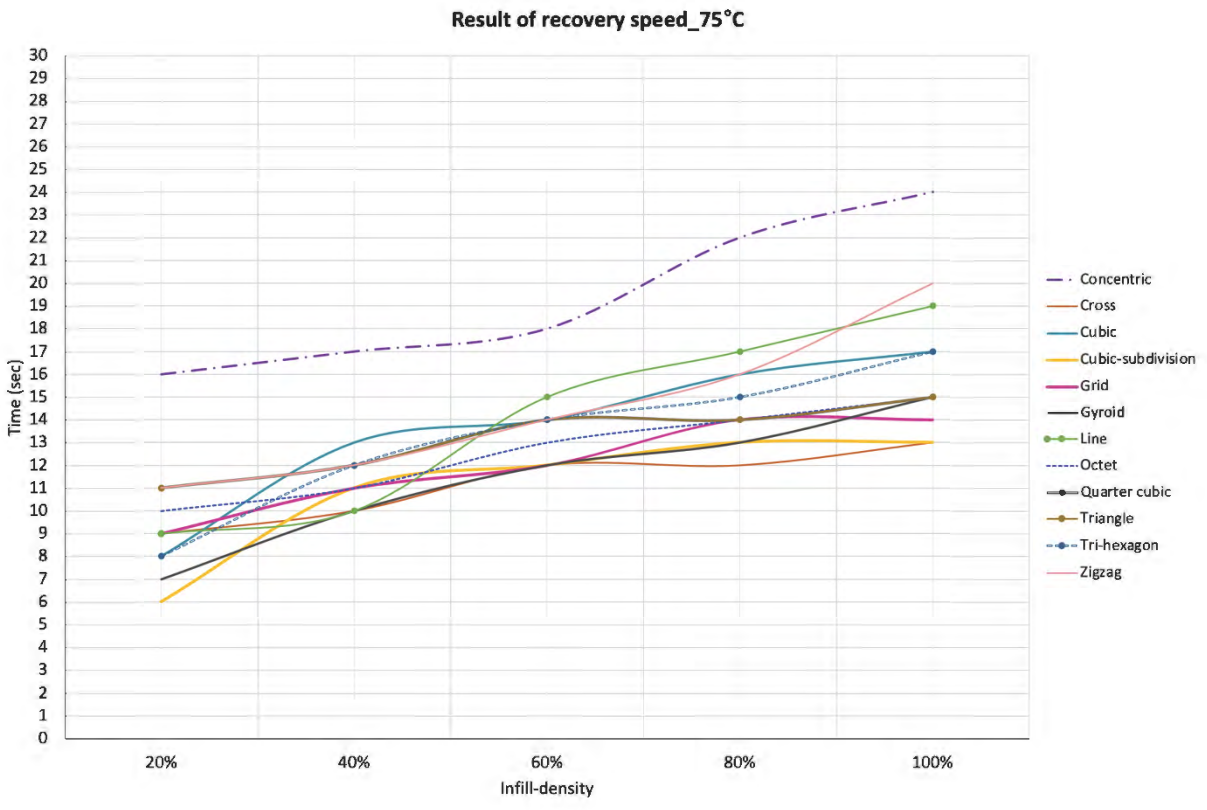
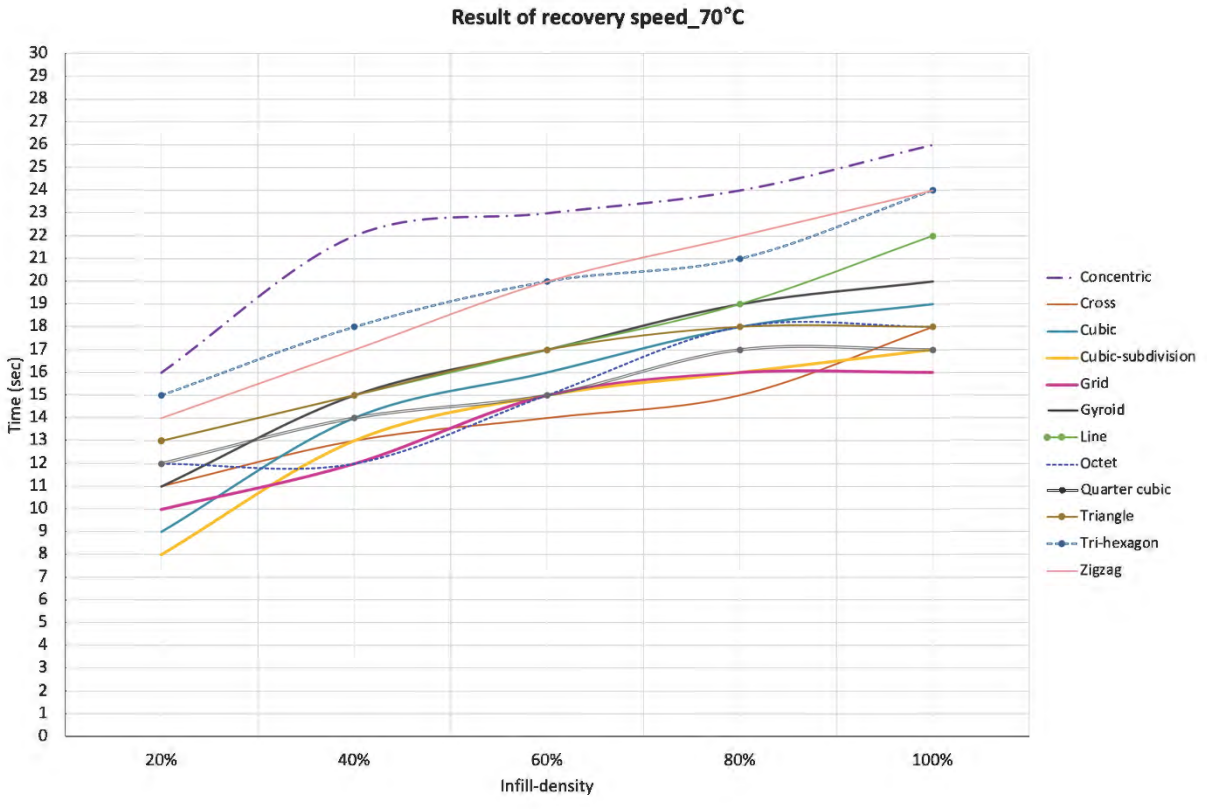


Figure 6-15. The recovery times for the 12 patterns and 5 infill densities at 65 °C, 70 °C, and 75 °C.

Overall, the experimental results show that the octet and quarter-cubic patterns with an infill density of 100% gave the highest recovery grade of 1. These patterns showed good shape recovery at 70 °C and 75 °C but not at 65 °C. Moreover, the lowest recovery result was the grade 9 recovery for the line pattern with a 20% infill density. The line pattern resulted in low recovery across all infill densities and temperatures. The pattern with the shortest recovery time was the cubic subdivision pattern, which recovered its shape in 6 seconds at 20% infill density. The pattern with the longest recovery time was the concentric pattern with 100% infill density, which recorded a recovery time of 29 seconds. Figure 6-16 shows the results derived from this experiment. It generally showed slow shape recovery and low recovery quality at low temperatures. On the other hand, it showed fast shape recovery and high recovery quality at high temperatures. In addition, it showed slow shape recovery and high recovery quality at high infill density, fast shape recovery, and low recovery quality at low infill density. It can be inferred that this result is due to the following effects. Firstly, the pattern impacts the characteristics of different SMEs. Patterns are structured with different masses when printed. This means that applying the same infill density will eventually result in different masses. Therefore, the shape-recovery effect is different depending on the type of pattern. Secondly, the higher the temperature, the faster the shape recovery, so shape recovery is possible. When these parameters are set, the high temperature quickly rubberises the material, thereby accelerating shape recovery and penetrating deeper in order to deliver the shape recovery energy. Thirdly, the higher the infill density, the slower the shape recovery due to taking longer to become ductile the material. Also, the recovery energy from heat can be lower than the mass of the material. This finding is consistent with Yang et al. (2016), who investigated the relationship between part density and extrusion temperature and concluded that dense shape memory polymer (SMP) structures induce greater recovery stress. However, the correlation between infill density and shape recovery has not yet been accurately analysed. Experiments in this study have shown that triangle patterns have low recovery rates when applying the same infill density, and most patterns, including octets, have high recovery rates. This is expected as a result of differences in mass arising from the intrinsic properties of the pattern.

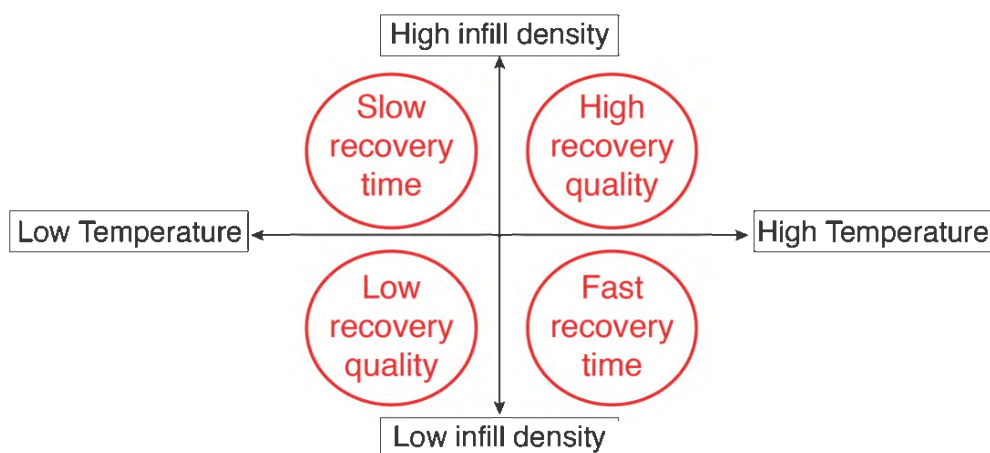


Figure 6-16. Simple results for the experiment on the 12 patterns and five infill densities.

6.2.4 The Results and the Development of a 4DP Tool

The results of this experiment are shown in Figure 6-17, which acts as a single visual reference. As shown at the bottom of Figure 6-17, the distribution was classified according to infill density, temperature, and pattern. Twelve patterns were expressed as numbers from 1 to 12, and the patterns were arranged in alphabetical order: 1 - concentric pattern; 2 - cross line pattern; 3 - cubic pattern; 4 - cubic subdivision pattern; 5 - grid pattern; 6 - gyroid pattern; 7 - line pattern; 8 - octet pattern; 9 - quadrilateral pattern; 10 - triangular pattern; 11 - tri-hexagon pattern; and 12 - zigzag pattern. The X-axis represents shape recovery time, which is the time the part took in seconds to return to its original shape. The Y-axis is the shape recovery grade, which is the rate at which the part returned to its original shape, with lower numbers described as higher shape recovery. The graph shows the distribution and time results for a total of 180 shape recovery results with three recovery temperatures of 65 °C, 70 °C, and 75°C, 5 infill densities, and 12 printing patterns. Those objects with high shape recovery and fast recovery times are displayed in the upper right corner of the matrix. Conversely, poor shape recovery and slow recovery time results are shown in the lower-left corner of the matrix. The shape recovery results are provided for low infill densities and temperatures to high infill densities and temperatures. As a result of the printing parameters, the shape recovery results and times are generally evenly distributed on the graph, as indicated by the centre part. It can be seen that most of the high-grade recovery quality occurs at high infill densities, while high infill densities are distributed in the slow shape recovery time on the left side of the matrix. In addition, it is confirmed that the higher the temperature, the higher the shape recovery and the faster the shape recovery. Except for the line pattern, it can be seen that the high temperature of 75°C is distributed in the high-grade recovery quality. Moreover, the slow shape recovery time is mostly distributed at lower temperatures. Therefore, aside from certain patterns, printing parameters have a significant impact on the quality of shape recovery and recovery time.

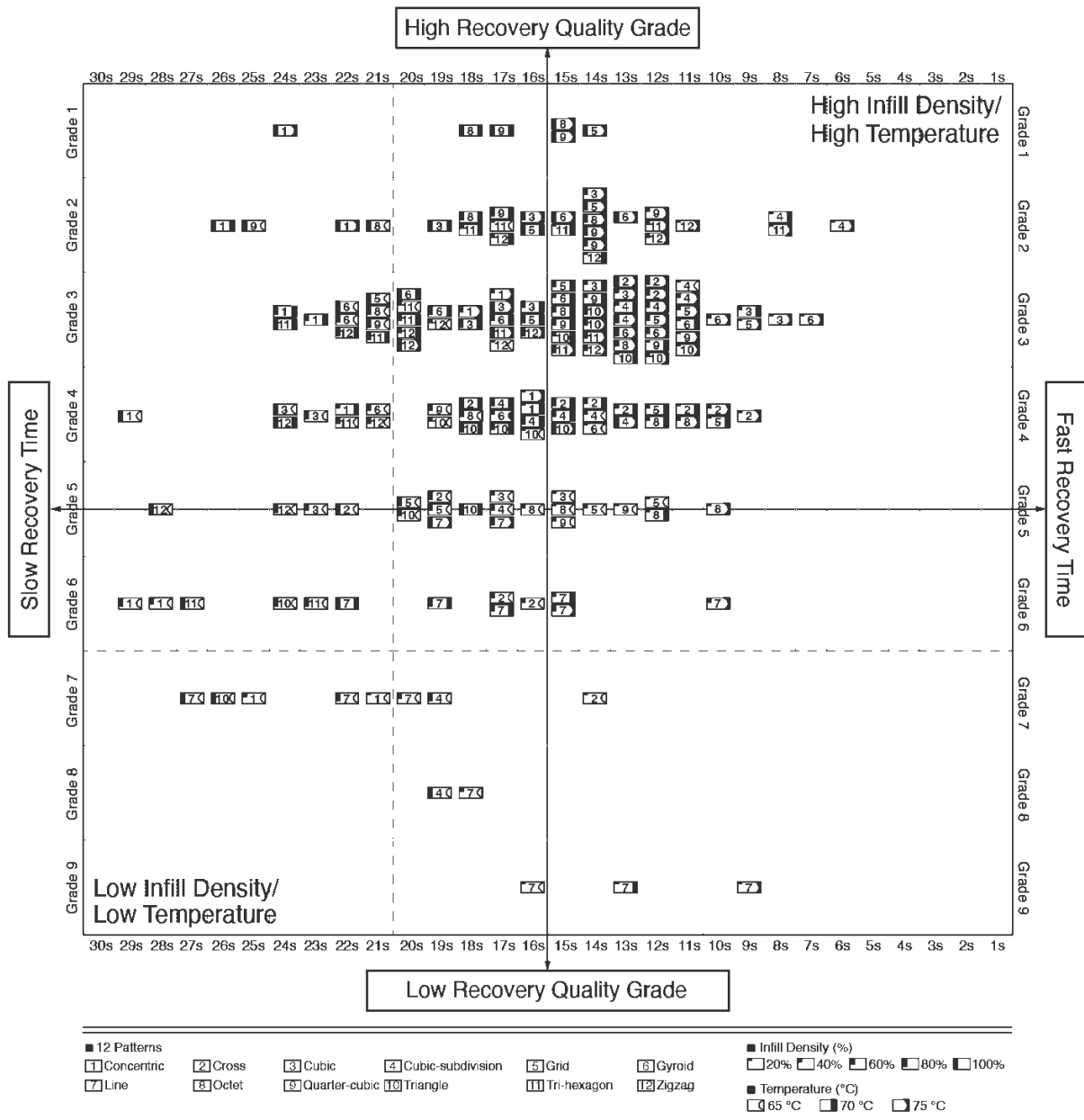


Figure 6-17. The quality of shape recovery and recovery times according to printing parameters.

6.2.5 Repeated experiment

This experiment, 12 repeated experiments were performed using two patterns for N and 5 different infill densities of 20%, 40%, 60%, 80%, and 100%. In this experiment, the same water bath experiment process as the previous experiment was performed. Table 6-6 shows the results of 12 repeated tests on a 3D-printed PLA sample of material N. These 3D printed PLA samples were used to re-evaluate the characteristics of the Octet, which showed the highest recovery grade, and the Line pattern, which showed the lowest recovery grade, and the 5 infill densities. As with previous experiments, the print pattern and infill density were applied to the PLA samples to determine the recovery quality and recovery time. The selected patterns and infill densities were applied in 12 experimental repetitions to produce accurate and comprehensive results. PLA samples were fabricated on the same Qidi X-Pro printer as in the previous

experiment, and the parameters were the same as in the previous experiment. The extruder temperature was set at 210°C, and the print speed at 50 mm/s. , the retraction speed was set to 30 mm/min, and the retraction distance was set to 1.5 mm. Shape recovery experiments were performed using rectangular samples with 80 mm × 6 mm × 3 mm dimensions. A glass transition temperature (T_g) of 80°C was chosen for safe transformation, which is higher than the T_g of each PLA sample. In this experiment, the recovery temperature for the filament test was set to 75°C according to the use of T_g and PLA. All temperatures were held for 2 min to determine the bending rating. SME quality was rated from 1 (highest) to 9 (worst rating). The shape recovery grade was defined as the difference between the original and recovered strains, with a flat shape indicating good recovery quality. As a result, in the previous experiment, the recovery grades of 20%, 40%, 60%, 80%, and 100% of the Octet pattern's infill densities were 5, 4, 3, 2, and 1. The recovery time results showed sequentially 10 seconds, 11 seconds, 13 seconds, 14 seconds, and 15 seconds from 20% to 100% infill density. As a result of 12 re-experiments, the Octet pattern showed the same result. Likewise, the Line pattern showed similar results in recovery grade and time. In previous experiments, the recovery grade results for infill densities of 20%, 40%, 60%, 80%, and 100% of the line pattern showed grades 9, 6, 6, 5, and 5. The recovery time results showed sequentially 9 seconds, 10 seconds, 15 seconds, 17 seconds, and 19 seconds from 20% to 100% infill density. The Octet and Line patterns showed the results of previous experiments and approximations.

Table 6-6. 12 sets repeated SMEs test results.

	Infill density	20 %	40 %	60 %	80 %	100 %
Test Number	Pattern	Time / Result	Time / Result	Time / Result	Time / Result	Time / Result
Set 1	Octet	10 sec / 5	11 sec / 4	13 sec / 3	14 sec / 2	15 sec / 1
	Line	10 sec / 9	11 sec / 6	16 sec / 6	18 sec / 5	20 sec / 5
Set 2	Octet	11 sec / 4	12 sec / 3	14 sec / 2	16 sec / 2	19 sec / 1
	Line	9 sec / 9	11 sec / 6	17 sec / 6	19 sec / 6	20 sec / 5
Set 3	Octet	8 sec / 4	11 sec / 3	13 sec / 2	15 sec / 2	14 sec / 1
	Line	10 sec / 9	12 sec / 6	16 sec / 7	18 sec / 6	19 sec / 5
Set 4	Octet	10 sec / 5	12 sec / 3	13 sec / 2	17 sec / 1	18 sec / 1
	Line	10 sec / 9	12 sec / 6	16 sec / 7	19 sec / 6	23 sec / 6
Set 5	Octet	12 sec / 5	14 sec / 3	15 sec / 2	17 sec / 1	18 sec / 1
	Line	8 sec / 9	10 sec / 7	15 sec / 6	17 sec / 5	20 sec / 6
Set 6	Octet	12 sec / 5	14 sec / 3	15 sec / 2	16 sec / 1	17 sec / 1
	Line	8 sec / 9	10 sec / 7	15 sec / 7	17 sec / 6	20 sec / 5
Set 7	Octet	12 sec / 5	14 sec / 3	15 sec / 3	17 sec / 1	18 sec / 1
	Line	10 sec / 9	12 sec / 7	17 sec / 7	18 sec / 7	20 sec / 6
Set 8	Octet	13 sec / 5	14 sec / 3	15 sec / 3	17 sec / 1	18 sec / 1
	Line	8 sec / 9	11 sec / 7	15 sec / 7	17 sec / 7	29 sec / 6
Set 9	Octet	10 sec / 4	13 sec / 3	15 sec / 2	16 sec / 1	17 sec / 1
	Line	9 sec / 9	11 sec / 7	15 sec / 6	16 sec / 6	18 sec / 6
Set 10	Octet	10 sec / 4	13 sec / 3	15 sec / 2	16 sec / 1	17 sec / 1
	Line	9 sec / 9	11 sec / 7	16 sec / 6	18 sec / 6	19 sec / 6
Set 11	Octet	12 sec / 5	14 sec / 3	15 sec / 2	16 sec / 1	17 sec / 1
	Line	10 sec / 9	12 sec / 7	18 sec / 7	20 sec / 6	22 sec / 5
Set 12	Octet	9 sec / 5	11 sec / 4	13 sec / 3	14 sec / 2	15 sec / 1
	Line	11 sec / 9	12 sec / 6	16 sec / 6	18 sec / 5	20 sec / 5

6.3 Chapter Summary

Chapter 6 focused on the PLA sample experiments that were printed using the parameters that greatly influenced the objects analysed in Chapter 5, including infill density, printing pattern, and temperature (65 °C, 70 °C, and 75 °C), as well as the results derived from the first three experiments. Twelve patterns, five infill densities, and three temperatures were applied to derive the SMEs (recovery quality and time) in all of the cases. The experimental results were compared and analysed through graphs, which were created by converting the recovery rate and time into numerical data. The shape recovery rate and recovery time data derived from the experiment were analysed with a shape control table and a physical version of the 4DP toolkit. In addition, evaluation experiments were performed in order to verify the graphic and toolkit samples as well as the experimental data. The 4DP has two main advantages: Firstly, 4DP parts can be designed and programmed by controlling and selecting temperature, pattern, and fill density; and, secondly, it could potentially be used to diagnose errors in the printed outputs and analyse the interactions between programming elements and AM machines. In the next chapter, the 4DP toolkit is explored by detailing the ways in which the usability and accessibility of the

4DP toolkit can be improved upon in order to maximise its two main advantages. It also explains the web 4DP printing toolkit, which is the advanced form of the 4DP toolkit that consists of graphic layouts.

Chapter 7. Design and Development of Toolkit

7.1 Introduction

The data from the previous chapter were used to develop a four-dimensional printing (4DP) toolkit with graphic layouts in order to improve access to information. The 4DP toolkit was also used to evaluate whether it was possible to control the sample's shape recovery by analysing the shape-recovery effect's recovery quality and recovery time. This evaluation experiment had the repeatability of the previous experiments and was used to determine how approximate the result value can be. As a result, the evaluation experiment that combined the pattern and infill density yielded similar results to the previous experiments. However, the usability and accessibility of the 4DP toolkit created from the data with accuracy needed much improvement. Therefore, this chapter proposes and explains the web 4DP toolkit, which is an advanced form of the 4DP toolkit that is organised as a graphic layout. This chapter will explain the 4DP web toolkit, after which the ways in which to improve the 4DP web toolkit that were determined through a questionnaire will be discussed. The web toolkit provides overall 4DP-related information, such as the definition of 4DP, shape recovery, and the 4DP process, in order to ensure that users expand their knowledge and easily apply the information contained therein. In addition, accessibility, which is the advantage of the internet, is improved, thereby ensuring that more users can easily access and use it.

7.2 A Graphic Representation of the Results

Figure 7-1 has been provided in order to improve access to the quantified results of the experiments. Figure 6-17 shows the distribution of printing parameters according to the shape recovery effect, however Figure 7-1 is the reconstructed result of the shape recovery effect based on the printing parameters distributed in the matrix of Figure 6-17. This is to easily find and apply the numerical results of the shape recovery effect according to the printing parameters. Among the numbers in the middle of the table, the single digits in red are the grades of the shape recoveries. A lower grade indicates better shape recovery, and a higher grade indicates a lower shape recovery. The blue row just below the numbers in red is the number of seconds it took the shape to recover its shape. The top row of the table contains the 12 printing patterns, the five infill densities are included on the left, and the three different shape recovery temperatures are included as the bottom row.

With a grade of 9, the pattern with the lowest recovery rate at 20% infill density was the line pattern, which showed poor results at the recovery temperatures of 65 °C, 70 °C, and 75°C. Similarly, the pattern with the longest recovery time was the concentric pattern at 100% infill density, and it had a shape recovery time of more than 29 seconds at 65 °C. Using this graphic representation, all 180 shape recovery results are provided for the five packing densities, 12 patterns, and three temperatures.

		Pattern												3D Printed PLA sample Bending Recovery Test - Recovery Quality Grade and Time Results																								
Grade Time(s)	Conc-entric	Cross	Cubic	Cubic-subdivision	Grid	Gyroid	Line	Octet	Quarter-cubic	Triangles	Tri-hexagon	Zigzag																										
Infill density	100%	4 29s	2 26s	1 24s	5 22s	4 18s	3 13s	4 24s	2 19s	3 17s	4 13s	8 19s	4 17s	4 13s	3 21s	2 16s	1 14s	3 22s	3 20s	15s	27s	22s	19s	21s	18s	15s	25s	17s	15s	26s	18s	15s	27s	24s	17s	28s	24s	20s
	80%	6 29s	3 24s	2 22s	5 19s	4 15s	3 12s	4 23s	3 18s	2 16s	7 19s	4 16s	3 13s	5 20s	3 16s	2 14s	3 22s	3 19s	3 17s	7 22s	6 19s	5 17s	3 21s	6 18s	5 14s	3 21s	2 17s	2 14s	6 24s	4 18s	3 14s	6 23s	3 21s	3 15s	5 24s	3 22s	16s	
	60%	6 26s	3 23s	3 18s	6 17s	4 14s	3 12s	5 23s	3 16s	2 14s	5 17s	4 15s	3 12s	5 19s	3 15s	3 12s	4 21s	3 17s	3 14s	7 20s	6 17s	6 15s	4 18s	3 15s	3 13s	4 19s	3 15s	2 14s	5 20s	4 17s	3 14s	4 22s	3 20s	14s	21s	20s	14s	
	40%	7 25s	4 22s	3 17s	6 16s	4 13s	4 10s	5 17s	3 14s	3 13s	4 14s	3 13s	3 11s	5 14s	4 12s	3 11s	4 17s	3 15s	3 10s	8 18s	6 15s	6 10s	5 16s	4 12s	4 11s	5 15s	3 14s	2 12s	4 19s	3 15s	3 12s	2 20s	3 18s	2 12s	3 19s	2 17s	12s	
	20%	7 21s	4 16s	4 16s	7 14s	4 11s	4 09s	5 15s	3 09s	3 08s	2 08s	2 08s	5 11s	4 08s	3 06s	3 08s	5 14s	4 11s	3 07s	9 16s	9 13s	9 09s	5 15s	5 12s	5 10s	5 13s	3 12s	3 11s	4 16s	3 13s	3 11s	2 17s	2 15s	2 08s	3 17s	2 14s	11s	
		65 °C	70 °C	75 °C	65 °C	70 °C	75 °C	65 °C	70 °C	75 °C	65 °C	70 °C	75 °C	65 °C	70 °C	75 °C	65 °C	70 °C	75 °C	65 °C	70 °C	75 °C	65 °C	70 °C	75 °C	65 °C	70 °C	75 °C	65 °C	70 °C	75 °C	65 °C	70 °C	75 °C	65 °C	70 °C	75 °C	
		Temperature (°C)																																				

Figure 7-1. The results of the experiment on the impact of the 12 patterns and five infill densities.

The quarter-cubic and octet print patterns had the highest recovery quality, and the line pattern had the lowest recovery quality. In a further analysis, the shape recovery grade, which indicated the quality of the recovery, was divided into three groups so that the 180 listed shape recovery values could be easily identified. Figure 7-2 shows the highest quality recovery, which were the shape recovery grades 1 to 3 that were reflected in the displayed print pattern. Figure 7-3 shows the shape recovery data from grades 4 to 6, which were defined as medium recovery quality grades. Finally, Figure 7-4 shows the shape recovery data from the patterns with grade 7 to 9 recovery rates, which were defined as low recovery quality.

		Pattern												High Recovery Quality Grade 1 to 3																								
Grade Time(s)	Conc-entric	Cross	Cubic	Cubic-subdivision	Grid	Gyroid	Line	Octet	Quarter-cubic	Triangles	Tri-hexagon	Zigzag																										
Infill density	100%	2	1		3		2	3		3	2	1	3	3	2		2	1	1		2	1	1				3	3							3			
	80%	3	2		3		3	2		3	3	3						3	2	2		3	2	2			3	3							3	3		
	60%	3	3		3		3	2		3	3							3	3			3	3				3	3								3	3	
	40%		3				3	3		3	3								3	2			3	3				3	3							3	2	2
	20%						3	3		3	2	2							3	3			3	3				3	3								3	2
		65 °C	70 °C	75 °C	65 °C	70 °C	75 °C	65 °C	70 °C	75 °C	65 °C	70 °C	75 °C	65 °C	70 °C	75 °C	65 °C	70 °C	75 °C	65 °C	70 °C	75 °C	65 °C	70 °C	75 °C	65 °C	70 °C	75 °C	65 °C	70 °C	75 °C	65 °C	70 °C	75 °C	65 °C	70 °C	75 °C	
		Temperature (°C)																																				

Figure 7-2. The patterns with the highest shape recovery rates.

		Pattern												Medium Recovery Quality Grade 4 to 6																							
Grade Time(s)	Conc-entric	Cross	Cubic	Cubic-subdivision	Grid	Gyroid	Line	Octet	Quarter-cubic	Triangles	Tri-hexagon	Zigzag																									
Infill density	100%	4		5	4		4		4	4		4		4	4		6	5		5	4	6		5	4		5	4									
	80%	6		5	4		4		5		4		6	5		4		6	5		6	4	6		5			5									
	60%	6		6	4		5		5		4		6	6	4		4		6	6	4		4		4			4									
	40%	4		6	4	4	5		4		4		6	6	5	4	4	5		6	6	5	4	4	5		4										
	20%	4	4		4	4	5		5	4		4		5	4		4		5	5	5	5		4													
		65 °C	70 °C	75 °C	65 °C	70 °C	75 °C	65 °C	70 °C	75 °C	65 °C	70 °C	75 °C	65 °C	70 °C	75 °C	65 °C	70 °C	75 °C	65 °C	70 °C	75 °C	65 °C	70 °C	75 °C	65 °C	70 °C	75 °C	65 °C	70 °C	75 °C	65 °C	70 °C	75 °C	65 °C	70 °C	75 °C
		Temperature (°C)																																			

Figure 7-3. The patterns with intermediate shape recovery rates.

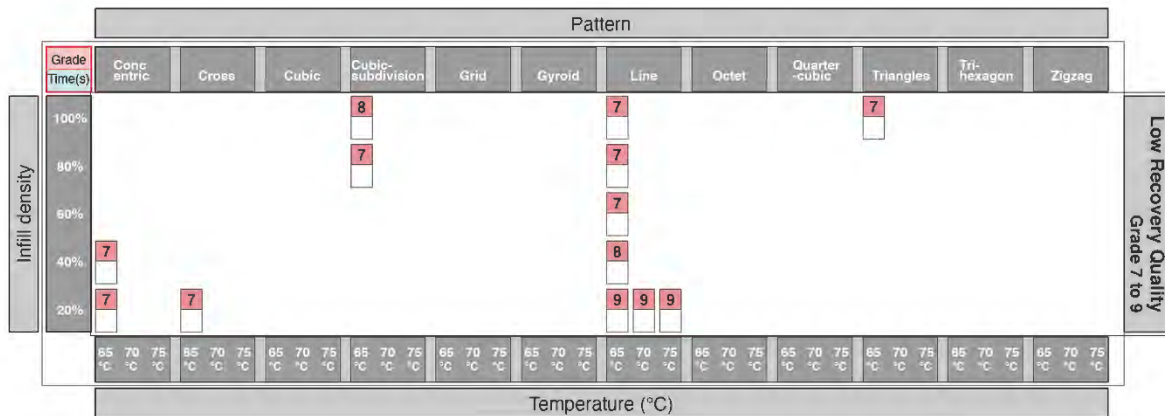


Figure 7-4. The patterns with poor shape recovery rates.

Similarly, the data in Figure 7-1 allows us to apply the same approach as in Figures 7-2 to 7-4 to identify the printing patterns that affect the recovery time of 4DP parts. Numerical data representing the time in seconds for shape recovery were divided into three groups: Figure 7-5 shows the shortest shape recovery time; Figure 7-6 shows the intermediate shape recovery time; and Figure 7-7 shows the longest recovery time. Also, 1–10 seconds represent the fastest recovery time, 11–20 seconds represent the intermediate recovery time, and 21–30 seconds represent the longest recovery time. The shortest recovery times were mainly found for the 20% and 40% infill densities. The intersection, cubic subdivision, lattice, gyroid, line, octet, and triangle patterns were recorded as having the fastest recovery times. Median recovery times accounted for the largest percentage. The slow recovery times were mainly due to the high infill densities of 80% and 100% as well as low temperatures. Therefore, a low infill density at high temperatures significantly shortened recovery time. Conversely, a high infill density at low temperatures resulted in slower recovery times. In conclusion, recovery times are strongly influenced by the pattern, infill density, and temperature.

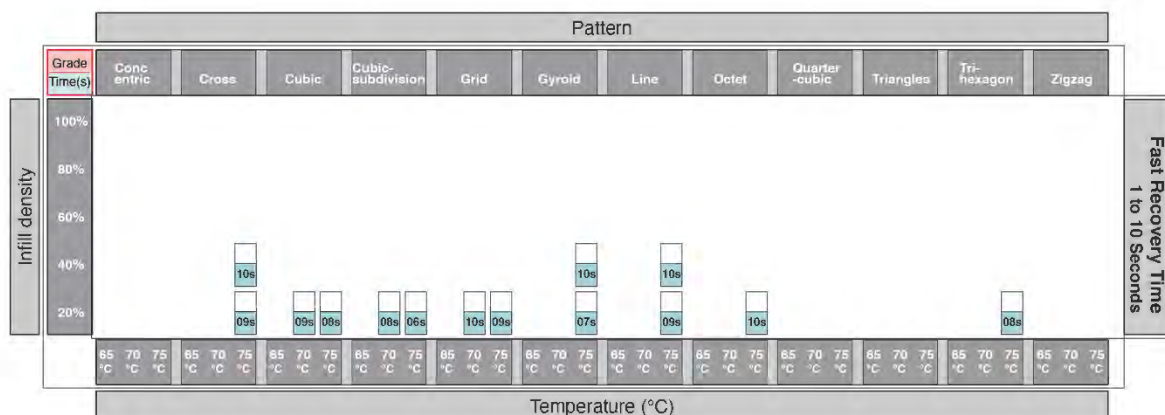


Figure 7-5. The patterns with the shortest recovery times.

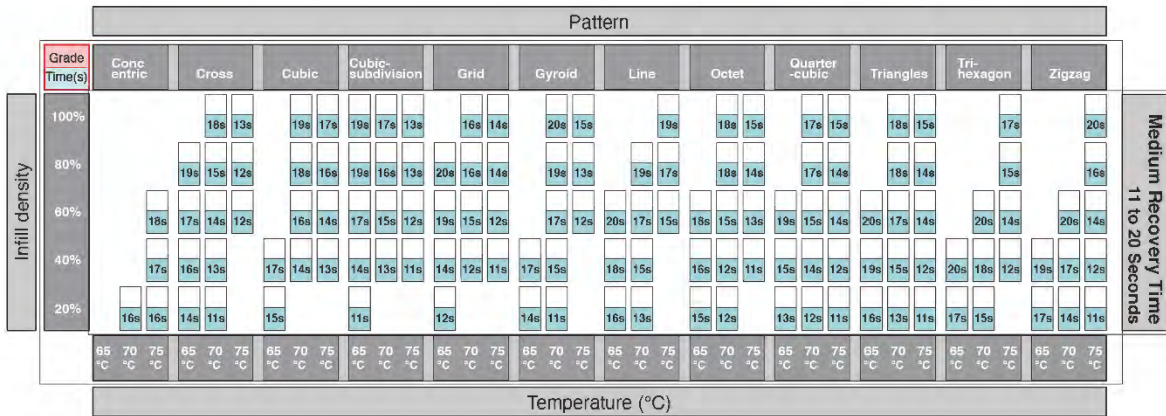


Figure 7-6. The patterns with intermediate recovery times.

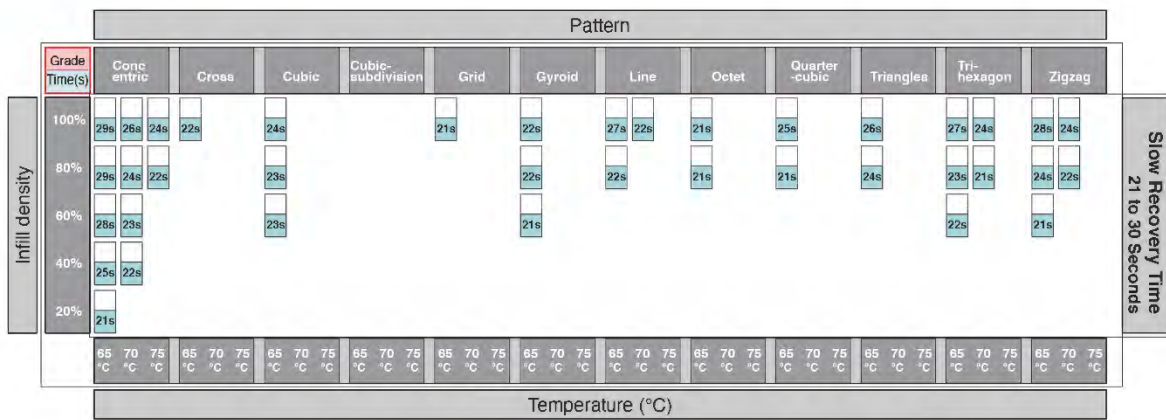


Figure 7-7. The patterns with the longest recovery times.

In the physical version of the 4DP toolkit that was created (see Figure 7-8), Figures 7-2 to 7-7 are printed on a transparent acetate film, so that users can intuitively filter information or identify overlapping areas. This physical version was tested by potential users who provided positive feedback on the toolkit’s accuracy and ease of use. The collected information has been systematised to disseminate research findings and provide results to the research community, so that designers, engineers, and manufacturers can evaluate and implement the feasibility of applying shape-changing behaviours.



Figure 7-8. The physical version of the 4DP toolkit

7.3 The Initial 4DP Web Toolkit

7.3.1 Scenario

Based on 7.2, two separate scenarios are discussed in order to provide a holistic view of the ways in which the toolkit can be used to develop 4D-printed parts. Since the main purpose is to determine whether the 4DP parameters can be applied efficiently, the initial product and sample development process were omitted from the scenario. The first scenario was derived from empirical research, which details the problems that 4DP users may encounter when 4DP without experience or knowledge of the rules related to shape recovery (Figure 7-9). To make a shape recovery sample, users repeated experiments several times through trial and error. However, it is ultimately difficult for new users to determine their desired recovery rates and times. This problem can arise when new users are unaware of the large impact of the printing parameters as well as the specificity of the material. Over a thousand samples were used to collect the data for this study. Thus, it is very difficult to adjust parameter values without prior data.

The second scenario indicates that the user can easily and quickly adjust the desired recovery rate and time using quantified data. This scenario illustrates the usability of the physical toolkit introduced in the previous chapter. Users can achieve their goals with less trial and error by using the physical toolkit to produce their desired 4D-printed parts (Figure 7-10).

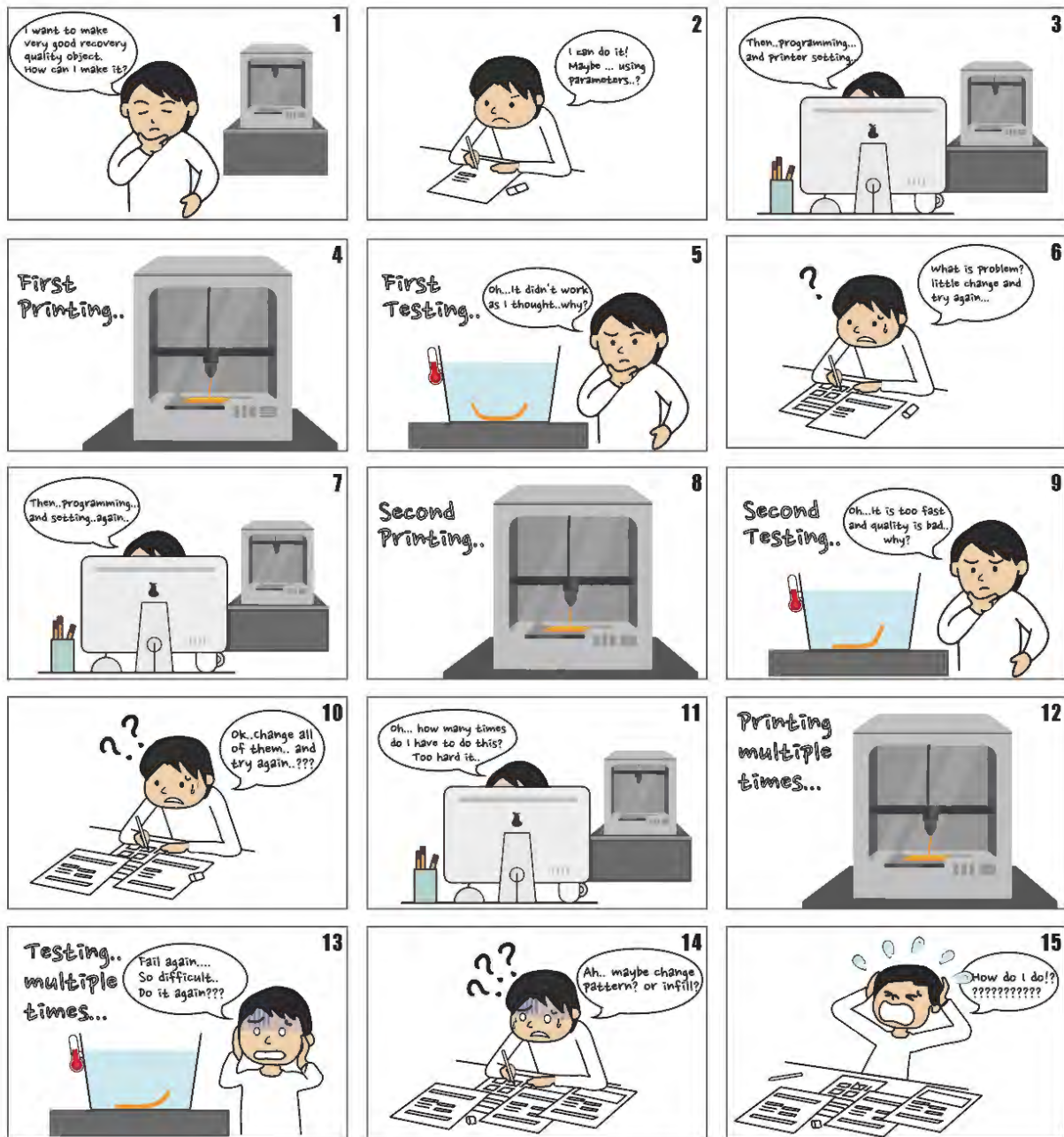


Figure 7-9. Scenario 1: Without using the 4DP toolkit.

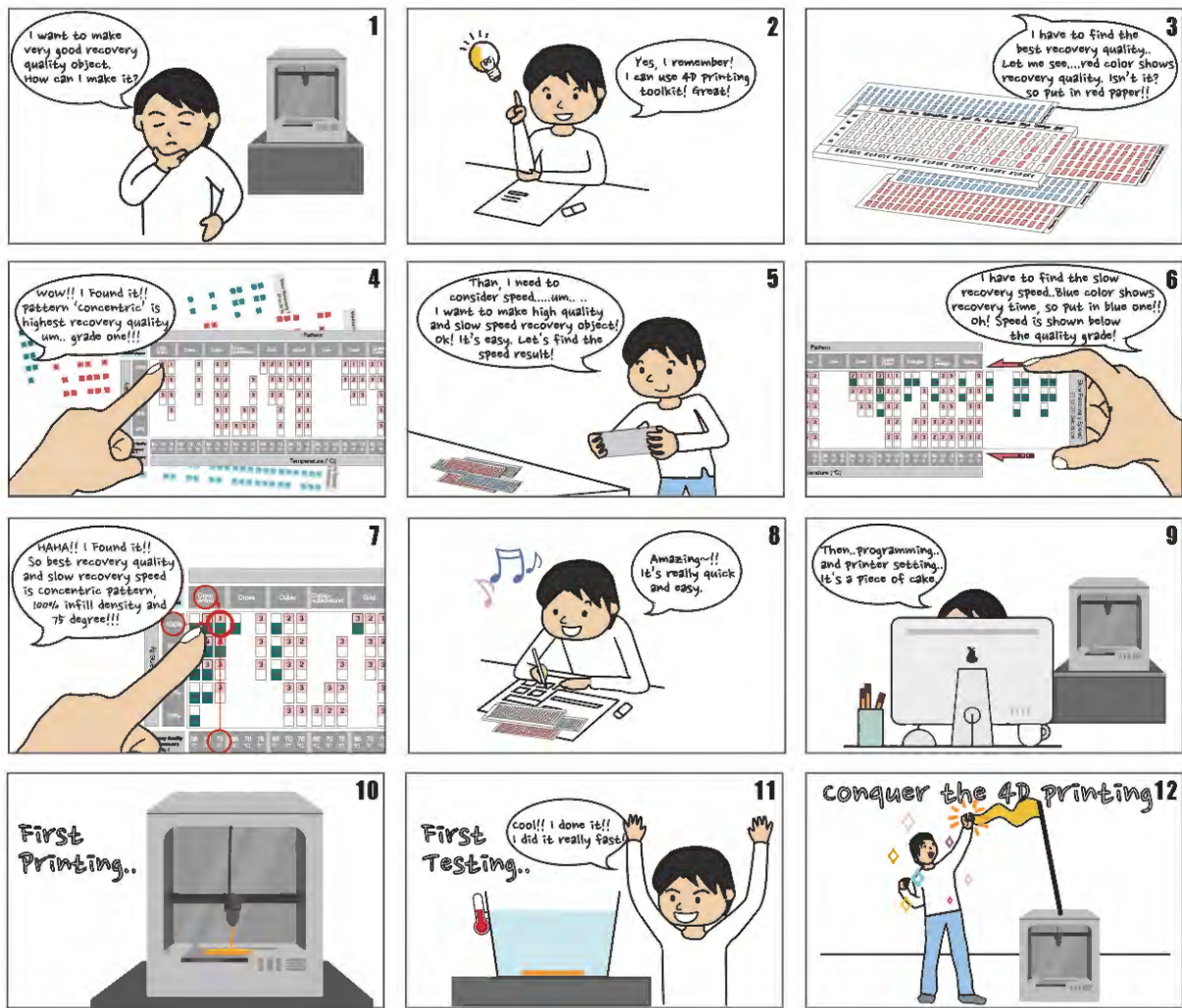


Figure 7-10. Scenario 2: Using the 4DP toolkit.

7.3.2 The 4DP Web Toolkit

Based on the usability of the initial physical toolkit, the web toolkit was proposed (see Figure 7-11). Although the 4D printing toolkit can be accessed using various utilities such as mobile, AR, and VR, it was thought that it would be efficient to use the desktop to implement a lot of information and images for the initial toolkit production. Therefore, a web toolkit using the desktop was applied. It consists of an introduction to the 4DP toolkit, an explanation of the criteria and the basis of the shape recovery grade, and a shape recovery control table that can be used for the collected data. The shape recovery control table shown in Figure 7-11 shows all of the results of the experiments on the 12 printing patterns, the five infill densities, and the three shape recovery temperatures. This table details a total of 180 pieces of numerical data, including recovery grades and times. The numbers contained in the red row are the grades of the shape recovery results, with grade 1 meaning a higher recovery rate. Conversely, higher numbers indicate poor shape recovery rates. The blue rows indicate the time it took for the part to return to its original state. Time was measured to a maximum of 30 seconds. With this recovery control method, all recorded results at the five infill densities, 12 patterns, and three temperatures are detailed, allowing easy control of 4D-printed parts.

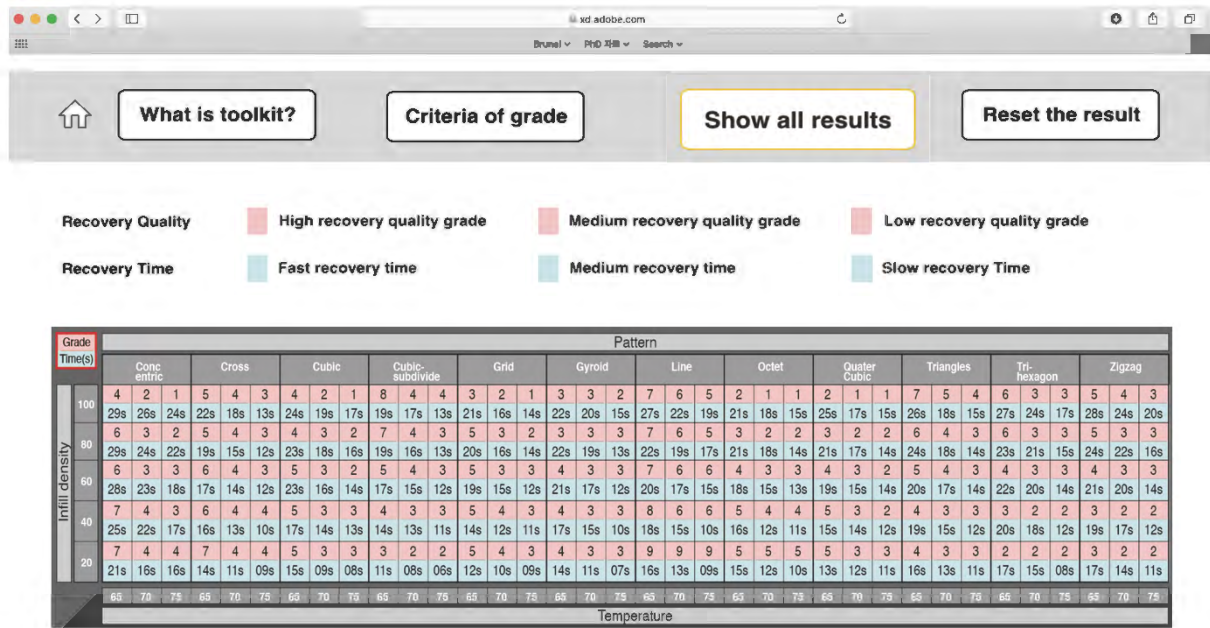


Figure 7-11. The initial version of the 4DP web toolkit.

7.4 The Finalisation of the 4DP Web Toolkit

7.4.1 The Questionnaire

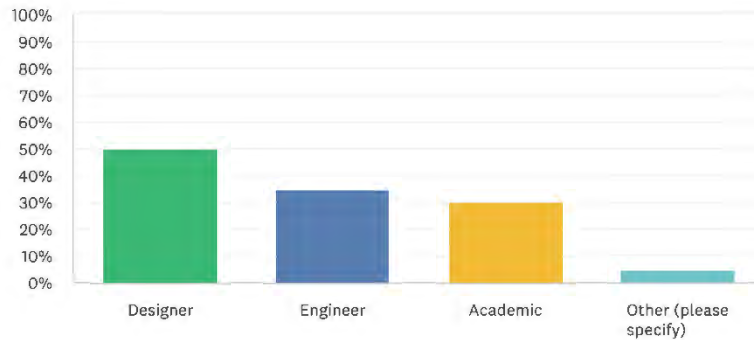
In order to objectively improve the usability of the 4DP web toolkit, questionnaires were used. This investigation was conducted by the Research Ethics Policy of the College of Engineering, Design and Physical Sciences at Brunel University London. The BREO Acceptance Letter can be found in Appendix I. All participants were briefed on the nature of the activity. A Participant Information Sheet can be found in Appendix II. Participants ranged from researchers in the academic area to design students and conducted a survey. Participants' identities and organizations were kept anonymous. The survey took no more than 10 minutes. Twenty-one participants directly used the web toolkit in order to provide suggestions for improving it. The questions were divided into three sections, with 13 questions in total, 10 of which related to the research. Before conducting the survey, the participants were given a description and objectives of this research because the participants were required to use the 4DP web toolkit. Therefore, participants were given sufficient time to use the 4DP web toolkit, so that they could understand the questions about it. The participants were allowed to provide multiple responses to the questions. The first section contained questions 1 to 3, which asked for the participants' information. Because knowledge of 4DP is the basis of this study, designers, engineers, and academics who use 4DP were recruited and were asked about their careers in this area. After this, they were provided with a link to the web toolkit and urged to use it. The second section was designed to elicit the problems the participants experienced with the 4DP web toolkit. The questions were numbered from 4 to 6, and the main aim of the questions was to determine what needs to be improved in the 4DP web toolkit, such as the toolkit's clarity and interface. The third section included questions on the visual elements of the 4DP web toolkit, and the questions were numbered from 7 to 10. These were used to determine the ways in which the graphical shape recovery control table could be improved. Questions on visual investigation

and table comprehension were included because clear visual delivery and understanding are important. Finally, the questionnaire concluded with requesting feedback from the participants.

7.4.2 Results from the Questionnaire

Section 1. Participants information

Q1. Please identify which field you belong to.

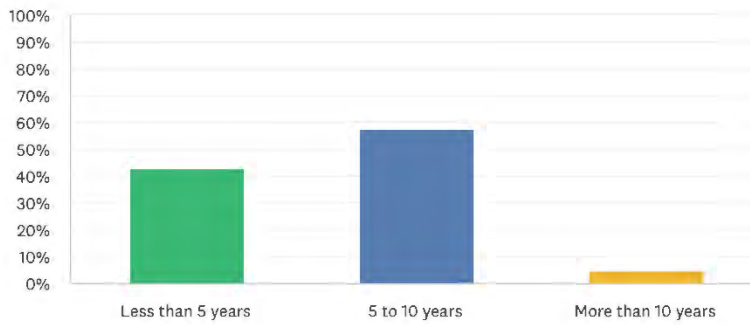


ANSWER CHOICES	RESPONSES
▼ Designer	50.00% 10
▼ Engineer	35.00% 7
▼ Academic	30.00% 6
▼ Other (please specify)	Responses 5.00% 1
Total Respondents: 20	

Figure 7-12. The results for question 1.

Question 1 was a question about the participants' professional fields. In order to ensure ease of understanding and accurate responses, the participants had to have basic knowledge of 4DP. Therefore, this was an important question in the questionnaire. Participants who did not have knowledge of 4DP could have been less objective. 10 people participated in the design field, 6 people in the academic field, 7 people in the engineer field, and 1 person in the public sector. More than 95% of the participants belonged to design and engineering industries, thereby increasing the objectivity of the survey.

Q2. How long have you worked in your field?

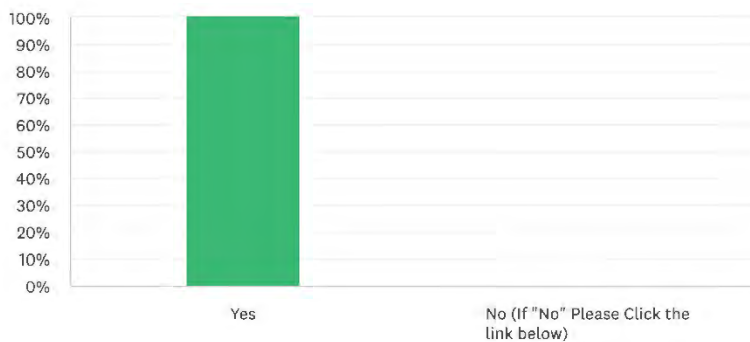


ANSWER CHOICES	RESPONSES	
Less than 5 years	42.86%	9
5 to 10 years	57.14%	12
More than 10 years	4.76%	1
Total Respondents: 21		

Figure 7-13. The results for question 2.

Question 2 requires a high understanding of related knowledge to derive an appropriate answer and objective results. Therefore, it is most important to involve participants with expertise. Consequently, it was structured based on the participants' relevant skills and field experience, and questions were asked to ensure the understanding and objectivity of the questionnaire. The proportion of participants with more than 5 years of pertinent experience exceeded 61%. This means that more accurate responses are obtained. They are experts who already have knowledge of AM and 4DP, and participants who have experience working with AM in their respective fields.

Q3. Did you go through the link above to access the 4DP web toolkit?



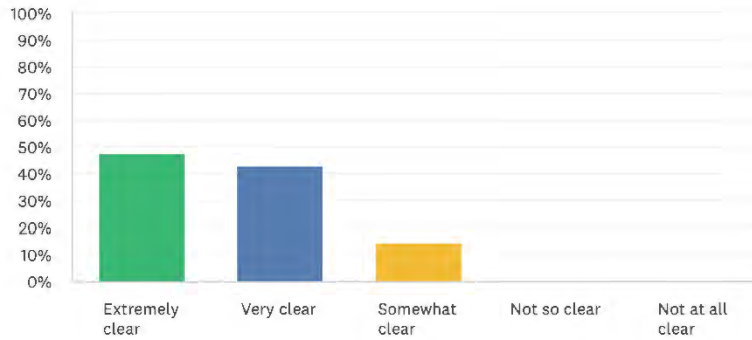
ANSWER CHOICES	RESPONSES	
Yes	100.00%	21
No (If "No" Please Click the link below)	0.00%	0
Total Respondents: 21		

Figure 7-14. The results for question 3.

Question 3 prompted the use of the 4DP web toolkit. Before answering the question, the participants were urged to use the 4DP web toolkit a few times as the use of the toolkit was inevitable, and all of them used it.

Section 2. Usability of web 4D printing toolkit

Q4. How do you rate the clarity of the information provided by the 4DP web toolkit?

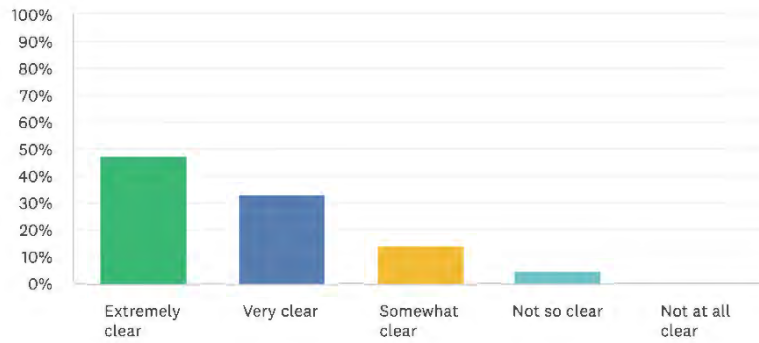


ANSWER CHOICES	RESPONSES	
Extremely clear	47.62%	10
Very clear	42.86%	9
Somewhat clear	14.29%	3
Not so clear	0.00%	0
Not at all clear	0.00%	0
Total Respondents: 21		

Figure 7-15. The results for question 4.

Question 4 was asked so as to determine the clarity of the information for the 4DP web toolkit. Since the goal of the toolkit is to provide a source that users can quickly understand and use, the clarity of the information in the toolkit is very important. Nearly 90% of the participants answered that the information in the 4DP web toolkit was clear.

Q5. How would you rate the usability of the 4DP web toolkit's interface?

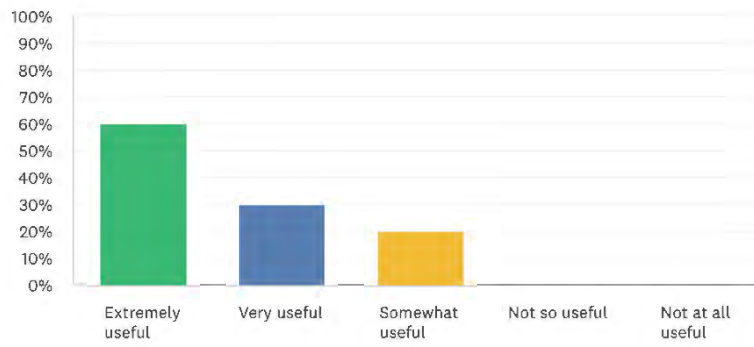


ANSWER CHOICES	RESPONSES
Extremely clear	47.62% 10
Very clear	33.33% 7
Somewhat clear	14.29% 3
Not so clear	4.76% 1
Not at all clear	0.00% 0
Total Respondents: 21	

Figure 7-16. The results for question 5.

Question 5 was related to the usability of the 4DP web toolkit. Although it can be accessed from both desktop and mobile phones, the participants were asked to access the toolkit through their desktop computer in order to ensure reliable transmission. Therefore, all the participants used the toolkit on their desktop computers. The interface denotes the ways in which participants can connect to and select the table of contents of the information provided as well as the ways in which to adjust the shape recovery control tables. The results show that more than 80% of the participants easily understood the interface.

Q6. How do you generally feel about the 4DP web toolkit?



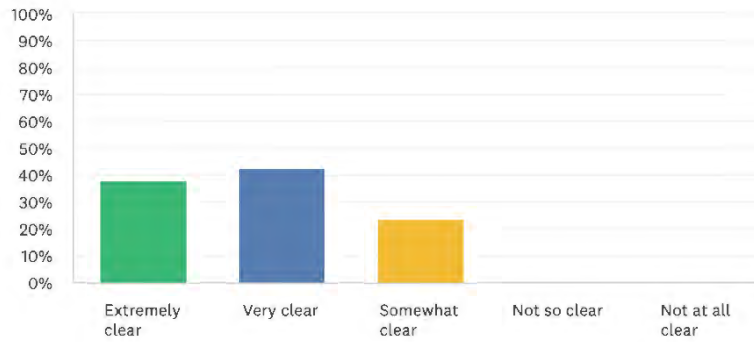
ANSWER CHOICES	RESPONSES	
Extremely useful	60.00%	12
Very useful	30.00%	6
Somewhat useful	20.00%	4
Not so useful	0.00%	0
Not at all useful	0.00%	0
Total Respondents: 20		

Figure 7-17. The results for question 6.

Question 6 focused on the overall need for the 4DP web toolkit by determining whether the participants who used it would be willing to use it again. It was a question in which participants chose useful if they were willing to reuse and not useful if they were not. More than 90% of the participants expressed a desire to reuse the toolkit. This could be the basis for the need for a 4DP web toolkit.

Section 3. Infographic of 4D printing toolkit

Q7. When you look at the graphical 4DP toolkit, what do you think about the size of the toolkit in terms of visibility?

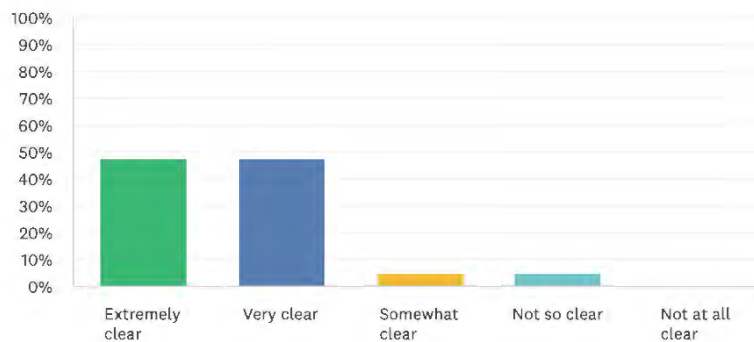


ANSWER CHOICES	RESPONSES
Extremely clear	38.10% 8
Very clear	42.86% 9
Somewhat clear	23.81% 5
Not so clear	0.00% 0
Not at all clear	0.00% 0
Total Respondents: 21	

Figure 7-18. The results for question 7.

Question 7 was related to recognising the information in the shape recovery control table. This table contained the 180 pieces of numerical data. Therefore, the visible aspects, such as the size and font of the text, had to be considered. More than 80% of respondents said they were comfortable with the visual aspect.

Q8. What do you think of the colour that represent recovery quality and recovery time in the graphical 4DP toolkit?

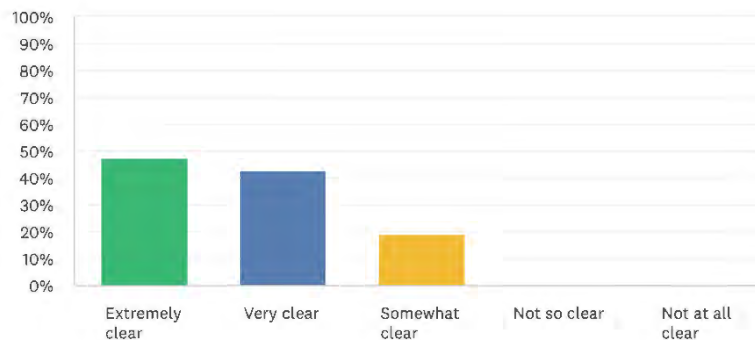


ANSWER CHOICES	RESPONSES
Extremely clear	47.62% 10
Very clear	47.62% 10
Somewhat clear	4.76% 1
Not so clear	4.76% 1
Not at all clear	0.00% 0
Total Respondents: 21	

Figure 7-19. The results for question 8.

Question 8 also considered the visualisation of the 4DP table. Numerical data representing recovery quality and time were not only textual but also coloured. This was to increase the convenience and intuitiveness of the toolkit. Many participants answered that it was clear, but one of participants answered that it was unclear, which was due to the clarity of a single colour being poor.

Q9. How would you rate the clarity and understandability of the data presented in the graphical 4DP toolkit?

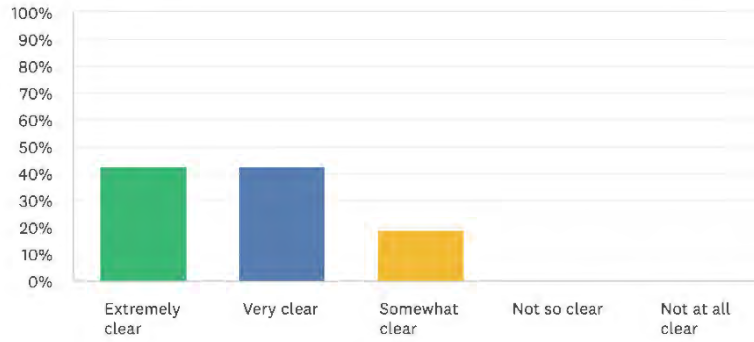


ANSWER CHOICES	RESPONSES
Extremely clear	47.62% 10
Very clear	42.86% 9
Somewhat clear	19.05% 4
Not so clear	0.00% 0
Not at all clear	0.00% 0
Total Respondents: 21	

Figure 7-20. The results for question 9.

Question 9 evaluated whether the users could easily use the transmitted results to control the shape recovery control table. More than 90% of the participants stated that there was no problem using the transmitted results and that the numerical table arrangement was easy to understand.

Q 10. How would you rate using the graphical 4DP toolkit that shows parameters?



ANSWER CHOICES	RESPONSES
Extremely clear	42.86% 9
Very clear	42.86% 9
Somewhat clear	19.05% 4
Not so clear	0.00% 0
Not at all clear	0.00% 0
Total Respondents: 21	

Figure 7-21. The results for question 10.

Question 10 concerned the overall need for a shape recovery control table. This was to determine whether participants who used it were willing to use this table. More than 84% of the participants felt the need to use it and expressed a desire to reuse it. This could be the rationale for the need for a shape recovery control table.

Finally, individual comments and e-mails were requested from the participants in order to improve the scalability of the study and the 4DP web toolkit. The survey was conducted based on the participants' direct experiences with the usability, necessity, and clarity of the toolkit and shape recovery control table. As a result, more than 90% of respondents agreed on the usefulness and reuse of the 4DP Web Toolkit, and they answered that there was a high need for a graphical 4DP table. However, many of the participants responded positively to the question, but improvements still needed to be made. For more useful usability, there was feedback on adding information related to 4DP, such as the background of 4DP and the definition and method of SMEs. In addition, there was feedback from the participants that it may be difficult to distinguish the shape recovery result due to the consistent colour of the graphical 4DP table. Uniform colour coding could have adversely affected clarity and visibility, and the need for expanded information related to 4DP and toolkits also emerged.

7.4.3 Scenario

Figure 7-22 presents scenarios of the ways in which participants used the 4DP web toolkit based on the questionnaire. The processes for using the toolkit and the ways in which to use it are briefly explained through cartoons. In this scenario, the user has the idea of creating a 4D-printed part and designs it. For a comprehensive understanding, the user accesses information about the 4DP web toolkit. By controlling the status window that determines the recovery rate and recovery time, the user can quickly and easily produce the desired result. This

scenario does not focus on the steps taken after using the toolkit as the creation of 4D-printed parts is based on the user's autonomy. The user then emphasises that the 4DP web toolkit can result in easy production of and access to creating desired 4DP products and objects.

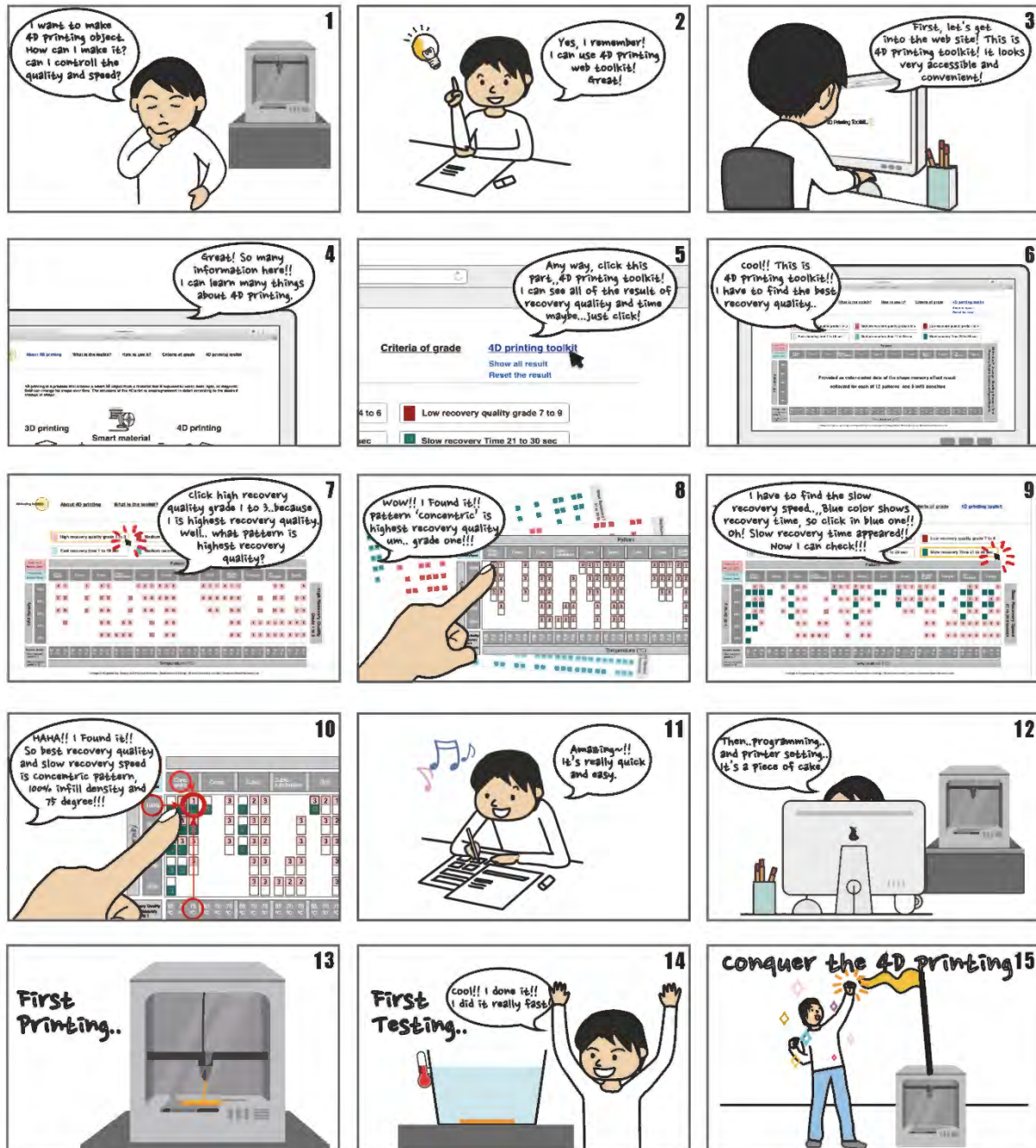
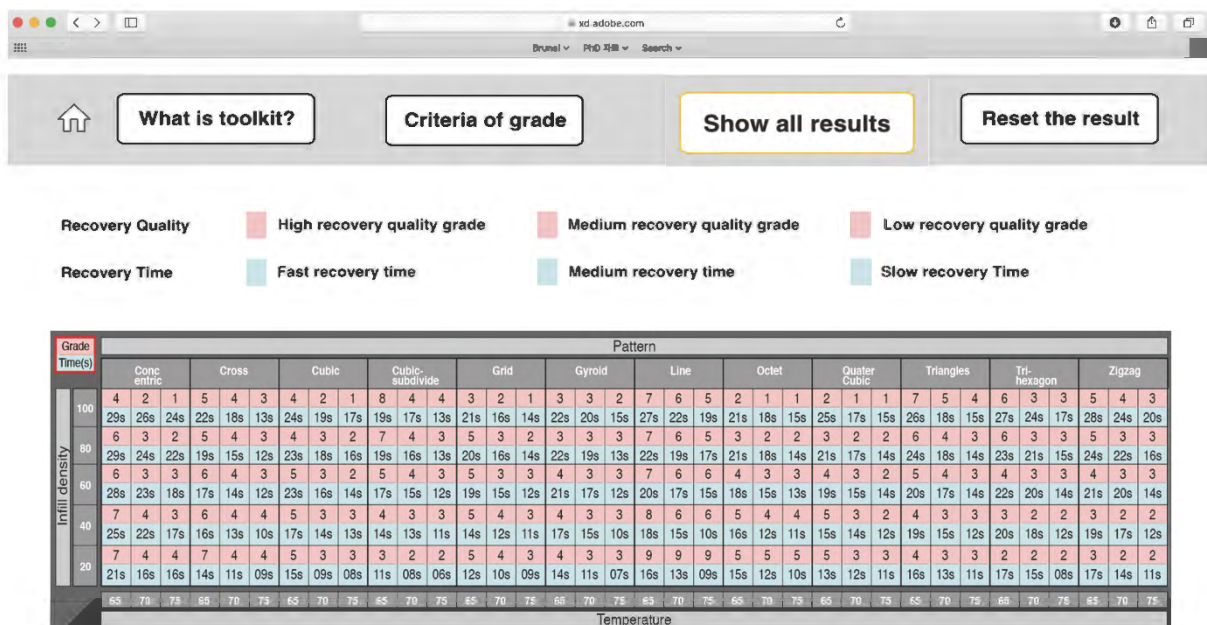


Figure 7-22. Scenario 3: Using the 4DP web toolkit.

7.4.4 The Final 4DP Web Toolkit

The upper image of Figure 7-23 is the same as Figure 7-11. The image is re-attached for easy comparison of the improved 4DP Web Toolkit. An improved form of the 4DP web toolkit is discussed herein, which was created in order to reduce the problems identified in the questionnaire (Figure 7-23). Although a large number of participants responded positively to

the usability and clarity of the toolkit and shape recovery control table, some problems needed to be improved for better understanding and access. These problems include the visibility of the shape recovery control table and the need for expanded information on 4DP and toolkit use. The single colour coding of the initial shape recovery control table has been improved. This was needed as the difference between recovery grade and time was not differentiated, so it was difficult for users to understand how to select the desired data. The three phases of shape recovery grade, colour-coded in red, and the three phases of recovery time, colour-coded in blue, were represented by single curls. This was improved by dividing the shape recovery grade and shape recovery time into three stages in order to provide a clear distinction. This improvement ensures high intuition and clarity as colour coatings are divided according to grades. In addition, in terms of the need for expanded information on 4DP and using the toolkit, an overview of 4DP, related information, and in-depth information on the ways in which to use the shape recovery control table were added in order to enhance the users' understanding. Therefore, 4DP-related information, such as the definition of 4DP and the process and concept of SMEs, was added, and the method and criteria from which the results of SMEs in this experiment were derived were explained. And images of the results of all experiments were attached. In particular, the absence of a method for using the shape recovery control table was a problem that may have confused users. Therefore, providing additional information on how to use the shape recovery control table will shorten the time taken to determine the ways in which to use it.



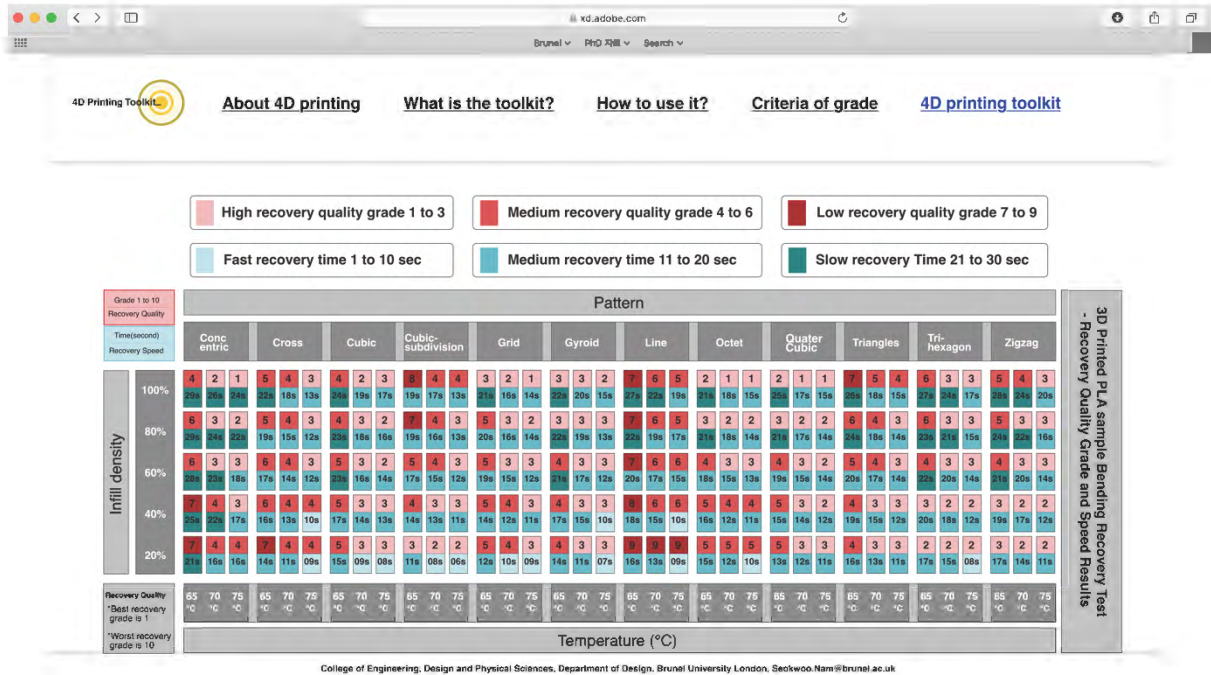


Figure 7-23. The final version of the 4DP web toolkit_ before and after.

7.5 Chapter Summary

The 4DP web toolkit, which is an advanced form of the 4DP toolkit, was discussed in this chapter. This more advanced toolkit was produced by examining the usability based on the participants' experiences that were gathered through the questionnaire. More than 95% belong to the design and engineering industry, and more than 61% participated in the survey of participants who have worked in the professional field for more than five years. Participants used the web 4DP toolkit directly online and participated in the survey. Furthermore, based on their feedback, we improved the Web 4DP Toolkit. Although 21 participants responded positively to the usability and clarity of the toolkit and shape recovery control tables, some issues had to be improved for better understanding and access. There were two major problems with this. The first is the need for expanded information on web toolkits and theoretical knowledge, such as the definition of 4DP and the concept of SMEs. Also included are methods of the derivation of toolkit data and criteria. In order to solve the problem of information expansion of the overall web toolkit, information such as the definition of 4DP and the process and concept of SMEs was added. In addition, in-depth information on how to use the shape recovery control table was added, and the method and criteria for deriving the results of SMEs in this experiment were explained. Moreover, images of the results of all experiments were attached. The second is the issue of visibility of the graphical 4DP toolkit. The initial shape recovery control table was single coding. This needed improvement because there is no distinction between recovery grades and time, making it difficult for users to understand how to select the data they want. The three stages of the shape recovery grade indicated in red and the three stages of the recovery time indicated in blue were marked with different curls. This improvement ensures that the colour coding is graded for high intuition and clarity.

The clarity and efficiency of the experimental data were reconfirmed through the application and testing of the shape recovery sample using the 4DP web toolkit. The ability to control the recovery rate and time of printed samples is the basis for predicting the desired shape recovery rate and time through printing parameters. Based on this research, the ability to control the intended shape recovery rate and recovery time means that further studies on new areas of 4DP can be conducted. The intended shape recovery and recovery time can increase time efficiency by reducing manufacturing time and trial and error of verification and can also lower economic consumption. Therefore, researchers, designers, and engineers can use the results presented in this chapter to discover new industrial development areas and demonstrate their potential application to structural transformations in product and production industries. The next chapter summarises this study and describes the ways in which the research objectives were achieved. It also highlights the contributions of the research, explains the study's limitations, and provides suggestions for future research.

Chapter 8. Conclusion

8.1 Introduction

This final chapter concludes this research. It revisits the research questions and objectives, reiterates the research findings, and discusses the study’s main contributions and its limitations. It also includes recommendations, thereby enabling future research that can overcome the limitations and expand on the knowledge produced by this thesis. This chapter also describes each chapter’s contribution to the knowledge and provides suggestions for future work. Figure 7.1 provides an overview of this chapter.

8.2 Summary of Work to Answer the Research Questions

In this study, four core studies were performed to develop a 4D printing toolkit: 4DP technology, shape change behavior, theoretical knowledge exploration of printing parameters, and quantification of SMEs results. This section provides a summary of the work done to achieve the research objectives, as shown in Table 8.1.

Table 8-1. Research questions and objectives defined for this research.

Research Questions	Research Objectives	Chapter
1) What is the state of 4D Printing using Shape Memory Polymers?	To analyze the present state and technology of 4D Printing through literature review.	2.2 Additive Manufacturing and 4DP
2) What AM processes and materials are suitable for utilizing shape memory polymers to enable 4D printing?	To analyze the present of 4D Printed SMPs through literature review.	2.3 Shape Memory Polymers (SMPs)
3) What type of shape-changing behaviour can be achieved using a 4D printed SMP?	To understand how the shape change behavior can be achieved through printing parameters and to examine and classify the different types of shape change behaviors for 4D Printed parts in the form of a taxonomy.	2.4 Shape change through 4DP
4) What SMP can be suitable for shape-changing behaviour through printing parameters in this research?	To compare the different types of PLA and find suitable PLA and printing parameters for 4D Printed parts through experiment.	4.5 4DP Parameters of the Shape Change Effect
5) How can the shape-memory effect be affected by printing parameters?	To compare and combine different SME experiments by applying controllable printing parameters.	4. Study 1 5. Study 2 6. Evaluation the influence of print pattern and infill
6) How can the printing parameters be controlled for effective 4D printing and shape-changing behaviour?	To propose methods to control suitable shape-changing effects, such as printing parameters, to design effective 4D printed parts.	7. Design and Development of Toolkit

This research started by reviewing the most current literature on four-dimensional printing (4DP), shape memory polymers (SMPs), shape-changing behaviours, and printing parameters. The findings presented in Chapter 2 and Chapter 3 answered research questions 1, 2, and 3. The findings were analysed to identify the appropriate Additive Manufacturing (AM) strategies and finalise a research direction so as to create a taxonomy of shape-changing behaviours. The optimal methods for controlling printing parameters to ensure the widespread use of 4DP were identified and detailed in a design guideline, thereby providing a basis for achieving users' intended shape-changing behaviours and recovery or more complex shape transformations. This research concluded by providing insights into the potential applications and limitations of a 4DP toolkit. The second topic of investigation was the methods and tools used to identify material properties suitable for 4DP, the results of which answered research question 4. The Shape Memory Effects (SMEs) and repeatability of commercial material lists were investigated. In addition, by selecting the materials suitable for research, the conditions for conducting experiments 2 were created. N was selected as the experimental material, which was used to investigate the printing parameters, including temperature, printing direction, printing speed, printing thickness, infill density, and printing pattern. Each printing parameter was used to compare the shape-recovery effect according to the pattern and infill density, the weight results according to the infill density, and the application of various properties (size, thickness, and ratio). The SMEs according to temperature, print pattern, and infill density had a greater influence on SME than other parameters, such as build orientation, print speed, and layer thickness. Next, to secure a large amount of numerical data, the temperature, print pattern, and infill density (which have the greatest effect on the shape-recovery effect) were subdivided and applied to the experiment. Three recovery temperatures of 65° C, 70 °C and 75 °C, 12 patterns provided by the three-dimensional (3D) printer, and five infill densities (20%, 40%, 60%, 80%, 100%) were used for this purpose. Through this investigation, a total of 180 shape-recovery effects were derived as numerical data. Based on these data, a graphical table was created and developed into a 4DP web toolkit. Participants began using the toolkit due to their participation in the survey, and the overall need for the 4DP web toolkit was identified by determining whether participants who used the 4DP web toolkit were willing to use it again, as in questionnaire question 6. Most participants expressed a desire to reuse the 4DP web toolkit. This can predict that the utility of the 4DP web toolkit may increase. All experiments included validation experiments. This is summarised in Figure 8-1.

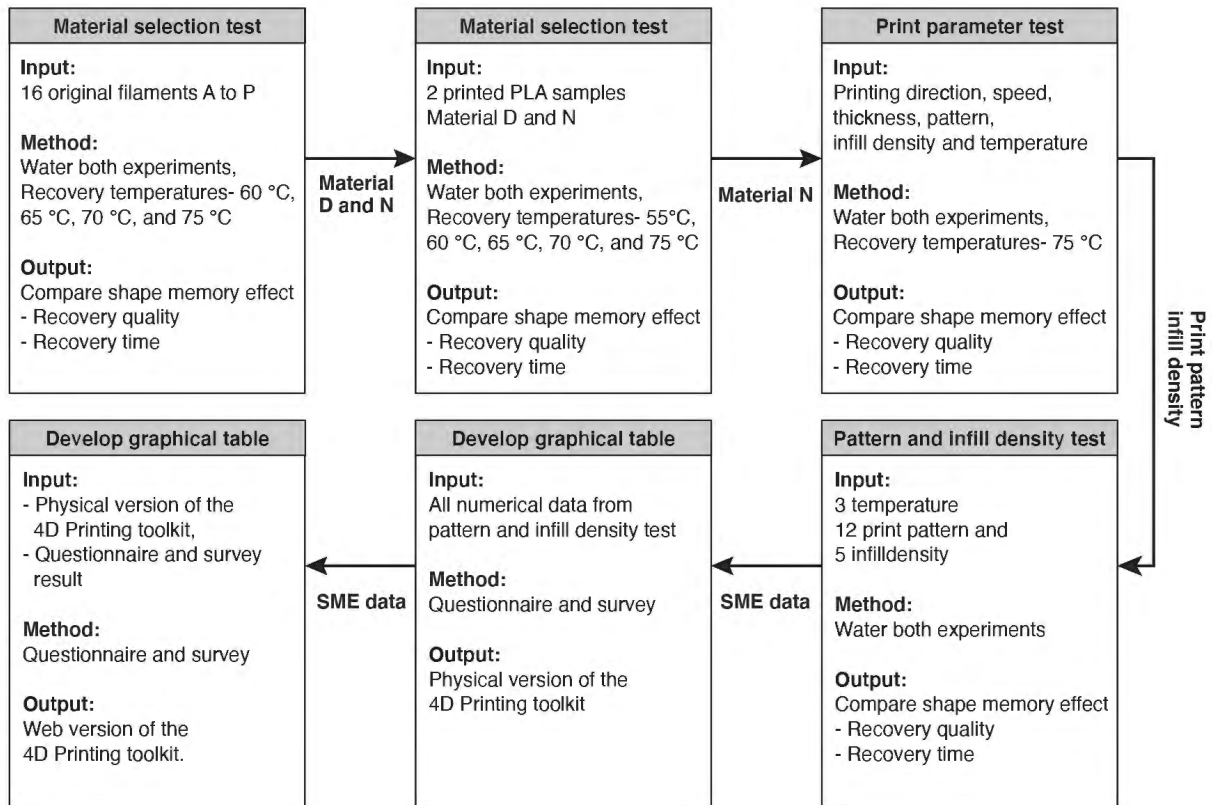


Figure 8-1. A summary of the experiments.

Figure 8-2 documents the entire experimental process of this research. In the input stage, four experiments and in-depth experiments were sequentially performed, and each experiment was performed using the same water bath. Although these experiments provided a fundamental basis for the idea that the pattern and infill density printing parameters affect the shape recovery quality and recovery time, the limitations of this study were that limited polylactic acid (PLA) material was applied, and the size, shape, and shape change behaviour of the applied samples were limited. An extended experiment was attempted due to the lack of evidence related to the data.

This study can provide designers and engineers with an understanding of the potential sculptural behaviours that can be realised using 4DP. This knowledge also enables designers and engineers to implement appropriate design strategies to better control configuration change behaviours through mechanical analysis. It also allows designers to make better 3D modelling and design choices without time-consuming and complex analysis when leveraging AM for rapid prototyping. However, further research is needed so as to more fully validate the data, expand on the basis of this work, and reach accurate conclusions. This will provide a deeper understanding of the 4DP phenomenon.

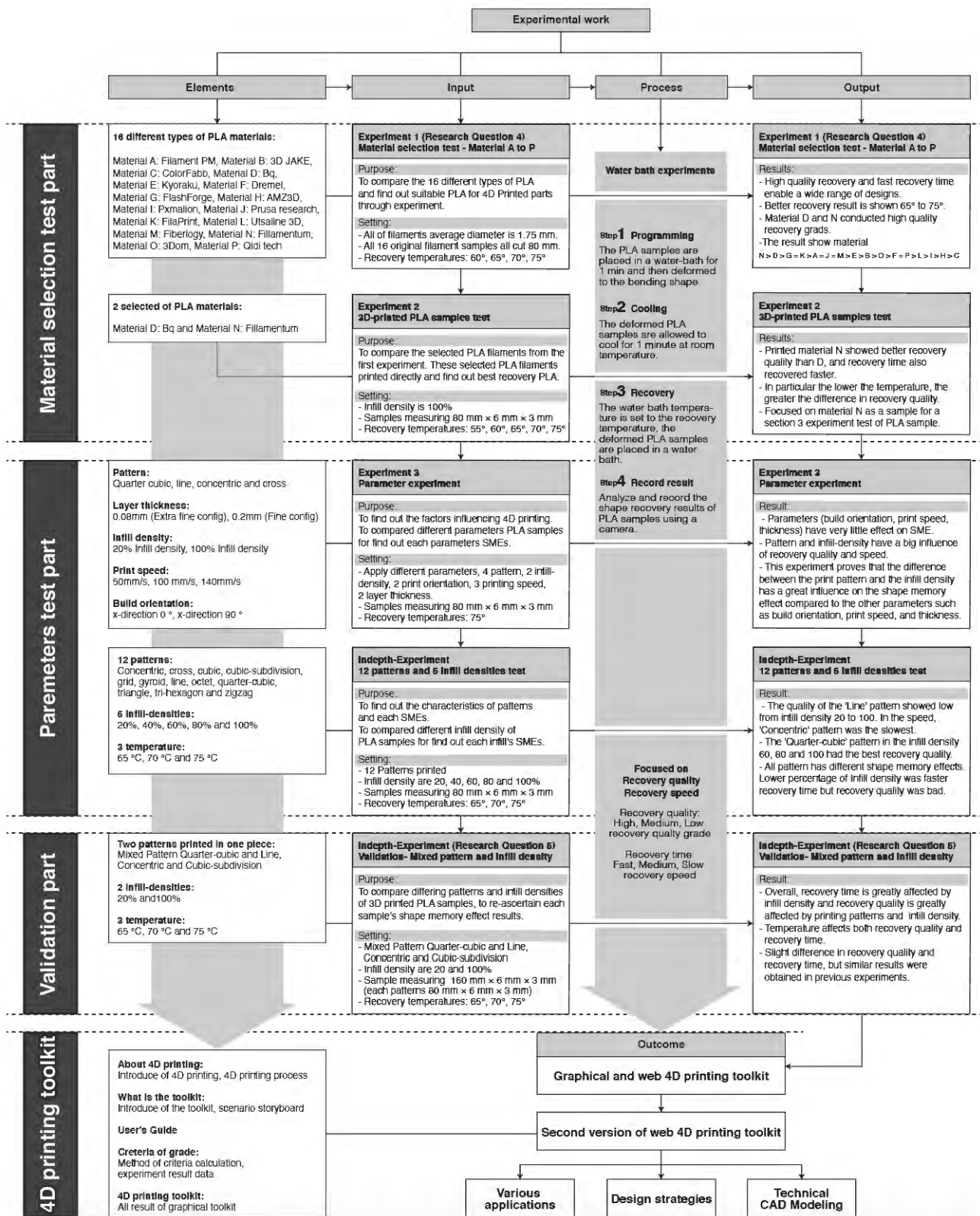


Figure 8-2. The inputs, processes, outputs and outcomes of this research.

8.3 Contributions of the Research

4DP is an emerging technology that needs to be developed. Since most research focuses on scientific theory and technical aspects, research on print control and usability so as to extract effective prints is very limited and fragmented. Additionally, new and established researchers who are interested in this field must invest a great deal of time and effort in accessing and reviewing various sources through a lot of trial and error in order to understand every aspect of the technology. Thus, the results of this thesis may be useful to academic researchers and the engineering and design fields. Researchers and designers with the same interests can use the theoretical knowledge, tools, methods, and results presented in this study to generate new research results or develop new applications and suggest guidelines on the proper use of 4DP in order to save time and costs. It can also be used to educate engineers, designers, and students in industrial design and engineering fields about 4DP and AM. There are several contributions that this research has made.

(1) Theoretical knowledge about 4DP

Academics, researchers, and developers in the 4DP field sift through countless web searches and books to obtain theoretical knowledge on 4DP. Although much knowledge can be obtained, since most theories are based on mechanical experiments that require expertise in the field, users who are new to the field have difficulties acquiring theoretical knowledge. One of the major objectives of this study was to provide easier access to information on the use and control of 4DP. Chapters 1 and 3 discussed the knowledge required to control 4DP, starting with the basic knowledge of how to 4D print. Moreover, it discussed the theoretical knowledge, such as general definitions and descriptions of SMEs, SMMs, and printing parameters required to control 4DP. This theoretical knowledge can inspire interest in 4DP and positively influence its development and theoretical knowledge. This increase in theoretical knowledge will also contribute to education. By conducting a knowledge transfer class on the Product Design Futures Invitational Lecture Series program (2021) at Bournemouth University in the UK, it has provided the opportunity to discuss and analyze the theoretical knowledge and future direction of 4DP with design students (Figure 8.3).



Figure 8-3. Class on the Product Design Futures Invitational Lecture Series program (2021) at Bournemouth University in the UK.

(2) Identification of shape-changing behaviours

Many existing experimental studies, aside from a few, are specialised studies that analyse one type of shape-changing behaviour in-depth and scientifically. The undefined shape-changing behaviours that can be realised with 4DP has resulted in limited research. In Chapter 2, every morphological behaviour identified in the literature was classified into one taxonomy. Thus, the identification of classified and defined shape-changing behaviours can facilitate access to research and development and provide broader ideas. Dimassi et al. (2021) extended further knowledge by describing entities that are deformable over time in terms of shape, function or properties based on shape-changing behaviour (Figure 8-4). He summarized that this represents a view of the transformation process featuring the main transformation functions initiated by the morphological behaviour. It can also help researchers and designers recognise, select, and implement appropriate AM strategies and measures necessary for their intended designs and applications.

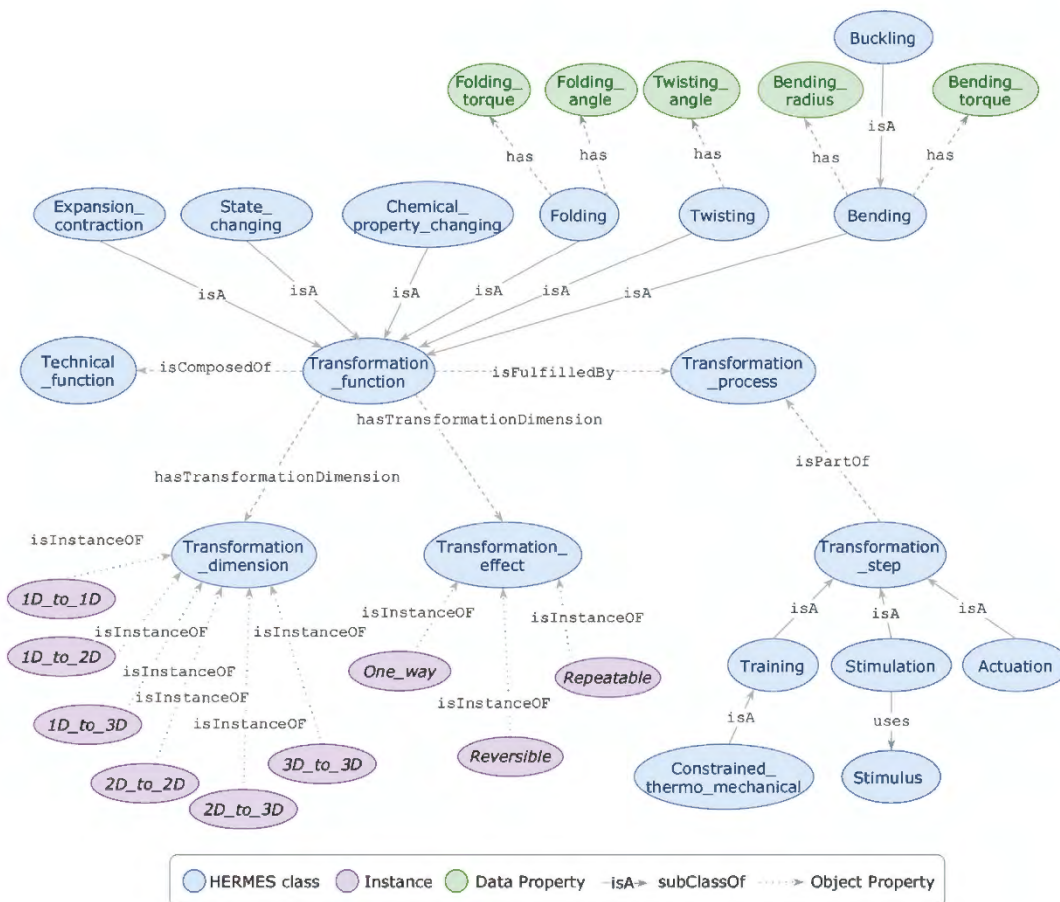


Figure 8-4. Material view with classes and object properties (Dimassi et al., 2021).

(3) Material selection

The materials used in 4DP are countless. Therefore, the material that is selected must be supported by experimental evidence on the material's properties, which can lead to time constraints in research and development. Also, using numerous materials or developing materials is expensive. In Chapter 4, It compared the properties of commercially accessible materials that can be easily obtained by anyone. The data from the comparison of the material

properties can be used to identify the appropriate materials for the users' intended designs and applications. In addition, the criteria for calculating the recovery rate and recovery time can be developed in another study by applying it to various materials.

(4) 4DP guidelines

The main purpose of this study was to propose easy accessibility and effective usability by controlling the parameters of 4DP. The data from Chapter 5 Chapter 6 and Chapter 7 were used to develop 4DP. 4D-printed objects can be developed by applying various SMEs, which are controlled by different parameters and computer modelling designs. Thus, the control of parameters can guide researchers' and designers' intended designs and applications. This research did not derive the SMEs for all of the cases. However, researchers and designers can use the numerical results and guidelines presented in these chapters as a measure to control the shape recovery effects. This could facilitate future research and developments in new areas of 4DP.

8.4 Limitations of the Study

In order to derive the results for the SMEs, many experiments that identified and applied parameters were conducted. However, the shape recovery effect, which is difficult to predict due to the different structural characteristics of alternative patterns, still exists and has not been resolved. Higher infill densities generally result in higher recovery rates. However, in the pattern experiment in Chapter 6, the triangle and zigzag patterns had a pattern that was different from other patterns at a high percentage infill density. This means that shape recovery occurs poorly, even at high percentage infill densities. In future work, additional methods for determining the accuracy and rationale for SMEs need to be identified by analysing the correlation between shape recovery and the structure and mass of the pattern through identifying the granular characteristics of each pattern. In addition, this study focused on the bending that can be realised with 4DP. Countless experiments have been conducted on combining one shape-changing motion and parameters, but it is also necessary to apply other shape-changing motions. Therefore, as in 6.2.5 Repeated experiment, 12 repeated experiments were performed, and the results were almost similar to the previous experiment results. However, 12 repeated experiments of two patterns may still be considered difficult to achieve clear objectivity. Therefore, additional work opportunities must be available to collect data through more repeated experiments. The current findings may not be broadly applicable to potential applications. Therefore, more data is needed on SMEs through printing parameters.

8.5 Recommendations for Further Research

This study has introduced a new method of controlling SMEs through printing parameters. This method allows the user to control the various SMP objects as the rightful SME without trial and error with specific parameters. In addition, this method can serve as a cornerstone for the application of a wider range of AM technologies and SMPs that currently exist. However, although this experiment provided proof that the pattern and infill density printing parameters affect the quality and recovery time of shape recovery, this study can be improved upon. There are several suggestions for further studies.

(1) Applying an expanded material may be necessary. In this research, a method for selecting a specific material and conducting an experiment was carried out. Since it was an experiment that had not yet been attempted, one material that could be suitable for the study was selected in order to create a guideline for the experiment. However, if the shape memory properties of various materials are accumulated, users can apply more diverse materials and contribute to developing manufacturing. In addition, in the material selection experiment in Chapter 4, each pattern's results were derived from the opposite shape-recovery effect. Since the purpose of this thesis was to select a suitable material for use, it was assumed that the materials' different shape recovery results were based on the inherent properties of the material. However, an explanation of the shape recovery results has not been provided. Therefore, the identification of shape recovery effects according to material properties may be needed.

(2) It may be necessary to expand the SMEs according to the shape transformation. Chapter 2 of this study explored various morphological transformations. This study applied bending shape deformation from various shape deformations. However, it is also possible to extract a wider range of shape recovery data by extending it to basic shape-changing behaviours such as folding, rolling, twisting, helixing, buckling, curving, topographical change, expansion and contraction, and complex shape-changing behaviours. Accumulation of shape recovery data following various shape transformations has the potential to control more complex shape changes.

(3) It is necessary to activate and improve the toolkit. The biggest goal of this thesis was to create a method that can help users quickly and easily understand 4DP and effectively create 4D-printed objects. Therefore, Chapter 7 verified the necessity and usability of the 4DP toolkit by suggesting the 4DP web toolkit and encouraging the participants to use it directly. However, this 4DP toolkit still has limitations that need to be studied. This thesis is an initial model that was based on the basic usability of the 4DP toolkit. Therefore, it may be necessary to apply more professional interface fields and develop more diverse access methods that focus on the latest technologies, such as virtual reality and high-tech software. In addition, it is possible to add and share more extensive knowledge beyond the basic 4DP information.

(4) It is necessary to apply 4DP. For example, additional experiments have been performed regarding the size and shape of the sample and the behaviour of different types of shape changes. However, many experiments still need to be conducted. In addition, to verify these data, case studies in which numerically derived results are directly applied are required. This will help designers and engineers better understand the possibilities for manufacturing products using 4DP, and it can also be directly applied to users' products. This is also directly related to the establishment of a computer-aided design (CAD) modelling strategy. It is important to apply CAD modelling to various cases of 4DP programming as it will contribute to creating an effective shape recovery control method that can be applied to various shape change methods.

References

1. Ahmed, A., Arya, S., Gupta, V., Furukawa, H., and Khosla, A. (2021). '4D printing: Fundamentals, materials, applications and challenges'. *Polymer*, 228, 123926. Doi: <https://doi.org/10.1016/j.polymer.2021.123926>.
2. Ahmed, S., Lauff, C., Crivaro, A., McGough, K., Sheridan, R., Frecker, M., and Strzelec, R. (2013). 'Multi-field responsive origami structures: Preliminary modeling and experiments', *International Design Engineering Technical Conferences and Computers and Information in Engineering Conference*. Location and date of conference. American Society of Mechanical Engineers, p. V06BT07A028. Doi: <https://doi.org/10.1115/DETC2013-12405>.
3. Alshebly, Y.S., Nafea, M., Ali, M.S.M. and Almurib, H.A. (2021a). 'Review on recent advances in 4D printing of shape memory polymers', *European Polymer Journal*, 159, 110708. Doi: <https://doi.org/10.1016/j.eurpolymj.2021.110708>.
4. Alshebly, Y.S., Nafea, M., Almurib, H.A., Ali, M.S.M., Faudzi, A.A.M. and Tan, M.T. (2021b). 'Development of 4D printed PLA actuators with an induced internal strain upon printing', *2021 IEEE International Conference on Automatic Control & Intelligent Systems (I2CACIS)*. Location and date of conference. IEEE, pp. 41-45.
5. Ali, M., Abilgazyev, A., and Adair, D. (2019). '4D printing: a critical review of current developments, and future prospects'. *The International Journal of Advanced Manufacturing Technology*, 105(1), 701-717. Doi:10.1007/s00170-019-04258-0.
6. Armon, S., Aharoni, H., Moshe, M., and Sharon, E. (2014). 'Shape selection in chiral ribbons: from seed pods to supramolecular assemblies'. *Soft matter*, 10(16), 2733-2740. Biocode: 2014APS..MARS16008A.
7. ASTM International. (2010). *ASTM F2792-10: standard terminology for additive manufacturing technologies*. Place of publication: ASTM International.
8. Bakarich, S.E., Gorkin R. III, Panhuis, M.I.H. and Spinks, G.M. (2015a). '3D/4D Printing hydrogel composites: a pathway to functional devices', *MRS* 1, pp. 1-6. Doi: <https://doi.org/10.1557/adv.2015.9>.
9. Bakarich, S.E., Gorkin R. III, Panhuis, M.I.H. and Spinks, G.M. (2015b). '4D printing with mechanically robust, thermally actuating hydrogels', *Macromolecular Rapid Communications*, 36 (12), pp. 1211-1217. Doi: <https://doi.org/10.1002/marc.201500079>.
10. Baker, A., Bates, R.G, Llewellyn-Jones, T., Valori, P.B., Dicker, P.M. and Trask, R.S. (2019). '4D printing with robust thermoplastic polyurethane hydrogel-elastomer trilayers', *Materials & Design*, 163, 107544. Doi: <https://doi.org/10.1016/j.matdes.2018.107544>.
11. Bodaghi, M. and Liao, W.H. (2019). '4D printed tunable mechanical metamaterials with shape memory operations', *Smart Materials and Structures*, 28 (4), 045019. Doi: 10.1088/1361-665X/ab0b6b.
12. Boley, J.W., Van Rees, W.M., Lissandrello, C., Horenstein, M.N., Truby, R.L., Kotikian, A., and Mahadevan, L. (2019). 'Shape-shifting structured lattices via multimaterial 4D printing', *Proceedings of the National Academy of Sciences*, 116 (42), pp. 20856-20862. Doi: <https://doi.org/10.1073/pnas.1908806116>.
13. Byun, M., Santangelo, C. and Hayward, R. (2013). 'Swelling-driven rolling and anisotropic expansion of striped gel sheets', *Soft Matter*, 9, pp. 8264-8273. Doi: <https://doi.org/10.1039/C3SM50627D>.
14. Cadete, M. S., Gomes, T. E., Gonçalves, I., and Neto, V. (2022). 'Controlling Morphing Behavior in 4D Printing: A Review About Microstructure and Macrostructure Changes in Polylactic Acid'. *3D Printing and Additive Manufacturing*. Doi: <https://doi.org/10.1089/3dp.2022.0088>.
15. Cendula, P., Kiravittaya, S., Mei, Y., Deneke, C. and Schmidt, O. (2009). 'Bending and wrinkling as competing relaxation pathways for strained free-hanging films', *Phys Rev B*, 79, p. 085429

16. Chen, D., Liu, Q., Han, Z., Zhang, J., Song, H., Wang, K. and Shi, Y. (2020). '4D printing strain self-sensing and temperature self-sensing integrated sensor-actuator with bioinspired gradient gaps', *Advanced Science*, 7 (13), p. 2000584. Doi: <https://doi.org/10.1002/advs.202000584>.
17. Chen, T., Müller, J. and Shea, K. (2016). 'Design and fabrication of a bistable unit actuator with multi-material additive manufacturing', *2016 International Solid Freeform Fabrication Symposium*. University of Texas at Austin, date of symposium. Publisher, page number. Doi: <https://hdl.handle.net/2152/89751>.
18. Choi, J. (2022). 'Investigating the role of infill structures on the shape memory effect of shape memory polymers in additive manufacturing' Doi: <https://doi.org/10.25560/93384>.
19. Chu, H., Yang, W., Sun, L., Cai, S., Yang, R., Liang, W., and Liu, L. (2020). '4D printing: a review on recent progresses'. *Micromachines*, 11(9), 796. Doi: <https://doi.org/10.3390/mi11090796>.
20. Damico, J.S., Oelschlaeger, M. and Simmons-Mackie, N.N. (1999). 'Qualitative methods in aphasia research: Conversation analysis', *Aphasiology*, 13, pp. 667-680. Doi: <https://doi.org/10.1080/026870399401777>.
21. Demaine, E.D. (2001). 'Folding and unfolding linkages, paper, and polyhedra', *Discrete and computational geometry*. Springer, Berlin, pp 113–124.
22. Dimassi, S., Demoly, F., Cruz, C., Qi, H. J., Kim, K. Y., André, J. C., and Gomes, S. (2021). 'An ontology-based framework to formalize and represent 4D printing knowledge in design'. *Computers in Industry*, 126, 103374. Doi: <https://doi.org/10.1016/j.compind.2020.103374>.
23. Erkeçoğlu, S., Sezer, A.D. and Bucak, S. (2016). 'Smart delivery systems with shape memory and self-folding polymers'. *Smart drug delivery system*. Doi: <http://dx.doi.org/10.5772/62199>.
24. Farhang, M., Seyed, M., Xun, L. and Jun N. (2017). 'A review of 4D printing', *Materials & Design*, 112, pp. 42–79.
25. Gao, W., Zhang, Y., Ramanujan, D., Ramani, K., Chen, Y., Williams, C.B., Wang, C.C.L., Shin, Y.C., Zhang, S. and Zavattieri, P.D. (2015). 'The status, challenges, and future of additive manufacturing in engineering', *CAD Comput. Aided Des.* 69, pp. 65–89. Doi: <https://doi.org/10.1016/j.cad.2015.04.001>.
26. Ge, Q., Dunn, C., Qi, H. and Dunn, M. (2014). 'Active origami by 4D printing', *Smart Mater*, 23, 094007. Doi 10.1088/0964-1726/23/9/094007.
27. Ge, Q., Qi, H.J. and Dunn, M.L. (2013). 'Active materials by four-dimension printing', *Appl Phys Lett*, 103, 131901. Doi: <https://doi.org/10.1063/1.4819837>.
28. Ge, Q., Serjouei, A., Qi, H.J. and Dunn, M.L. (2016). 'Thermomechanics of printed anisotropic shape memory elastomeric composites', *International Journal of Solids and Structures*, 102, pp. 186-199. Doi: <https://doi.org/10.1016/j.ijsolstr.2016.10.005>.
29. Gladman, A.S, Matsumoto, E.A, Nuzzo, R.G, Mahadevan, L. and Lewis J.A. (2016). 'Biomimetic 4D printing', *Nature Materials*, 15 (4), pp. 413–418. <https://doi.org/10.1038/nmat4544>.
30. GMI., (2022). 'Shape Memory Polymer Market Share and Statistics – 2030'. <https://www.gminsights.com/industry-analysis/shape-memory-polymer-market#> (accessed 13 October 2022).
31. Goo, B., Hong, C.H. and Park, K. (2020). '4D printing using anisotropic thermal deformation of 3D-printed thermoplastic parts', *Materials & Design*, 188, 108485. Doi: <https://doi.org/10.1016/j.matdes.2020.108485>.
32. Han, D. and Lee, H. (2020). 'Recent advances in multi-material additive manufacturing: Methods and applications', *Current Opinion in Chemical Engineering*, 28, pp. 158-166. Doi: <https://doi.org/10.1016/j.coche.2020.03.004>.
33. Hornat, C.C., Yang, Y. and Urban, M.W. (2017). 'Quantitative predictions of shape-memory effects in polymers', *Advanced Mater*, 29 (7), pp. 1603334. Doi: <https://doi.org/10.1002/adma.201603334>.

34. Hosseinzadeh, M., Ghoreishi, M., & Narooei, K. (2023). 4D printing of shape memory polylactic acid beams: An experimental investigation into FDM additive manufacturing process parameters, mathematical modeling, and optimization. *Journal of Manufacturing Processes*, 85, 774-782. Doi: <https://doi.org/10.1016/j.jmapro.2022.12.006>.
35. Hu, G., Damanpack, A., Bodaghi, M. and Liao, W. (2017). 'Increasing dimension of structures by 4D printing shape memory polymers via fused deposition modeling', *Smart Mater*, 26, 125023. Doi: 10.1088/1361-665X/aa95ec.
36. Huang, W.M., Ding, Z., Wang, C.C., Wei, J., Zhao, Y. and Purnawali, H. (2010). 'Shape memory materials', *Mater Today*, 13(7-8), pp. 54-61. Doi: [https://doi.org/10.1016/S1369-7021\(10\)70128-0](https://doi.org/10.1016/S1369-7021(10)70128-0).
37. ISO/ASTM 52900:2021 Additive manufacturing, <https://www.iso.org/obp/ui/#iso:std:isoastm:52900:ed-2:v1:en>
38. Ionov, L. (2013). '3D microfabrication using stimuli-responsive self-folding polymer films', *Polym Rev*, 53, 92-107. Doi: <https://doi.org/10.1080/15583724.2012.751923>.
39. Janbaz, S., Hedayati, R. and Zadpoor, A.A. (2016). 'Programming the shape-shifting of at soft matter: From self-rolling/self-twisting materials to self-folding origami', *Mater Horiz*, 3, pp. 536-547. Doi: 10.1039/C6MH00195E.
40. Jia, X., Shen, B., Zhang, L. and Zheng, W. (2021). 'Construction of shape-memory carbon foam composites for adjustable EMI shielding under self-fixable mechanical deformation', *Chemical Engineering Journal*, 405, 126927. Doi: <https://doi.org/10.1016/j.cej.2020.126927>.
41. Jian, B., Demoly, F., Zhang, Y., Qi, H. J., André, J. C., & Gomes, S. (2022). Origami-based design for 4D printing of 3D support-free hollow structures. *Engineering*. Doi: <https://doi.org/10.1016/j.eng.2021.06.028>.
42. Kačergis, L., Mitkus, R. and Sinapius, M. (2019). 'Influence of fused deposition modeling process parameters on the transformation of 4D printed morphing structures', *Smart Mater. Struct*, 28, 105042. Doi: 10.1088/1361-665X/ab3d18.
43. Kim, J., Hanna, J., Hayward, R. and Santangelo, C. (2012). 'Thermally responsive rolling of thin gel strips with discrete variations in swelling', *Soft Matter*, 8, pp. 2375-2381. Doi: <https://doi.org/10.1039/C2SM06681E>.
44. Kim, K., Guo, Y., Bae, J., Choi, S., Song, H. Y., Park, S., ... & Ahn, S. K. (2021). 4D printing of hygroscopic liquid crystal elastomer actuators. *Small*, 17(23), 2100910. Doi: <https://doi.org/10.1002/sml.202100910>.
45. Kumar, S., Kolekar, T., Patil, S., Bongale, A., Kotecha, K., Zaguia, A. and Prakash, C. (2022). 'A Low-Cost Multi-Sensor Data Acquisition System for Fault Detection in Fused Deposition Modelling', *Sensors*, 22 (2), pp. 517. Doi: <https://doi.org/10.3390/s22020517>
46. Lan, X., Liu, Y., Lv, H., Wang, X., Leng, J. and Du, S. (2009). 'Fiber reinforced shape-memory polymer composite and its application in a deployable hinge', *Smart Materials and Structures*, 18 (2), pp. 024002.1-024002.6, ISSN 0964-1726. Doi: <https://doi.org/10.1088/0964-1726/18/2/024002>.
47. Lauff, M. and Hofer, R. (1984). 'Proteolytic enzymes in fish development and the importance of dietary enzymes', *Aquaculture*, 37 (4), pp. 335-346. Doi: [https://doi.org/10.1016/0044-8486\(84\)90298-9](https://doi.org/10.1016/0044-8486(84)90298-9).
48. Lee, A., An, J. and Chua, C. (2017a). 'Two-Way 4D Printing: A Review on the Reversibility of 3D-Printed Shape Memory Materials', *Science Direct*, 3(5), pp. 663-674. Doi: <https://doi.org/10.1016/J.ENG.2017.05.014>.
49. Lee, J., An, J. and Chua, C. (2017b). 'Fundamentals and applications of 3D printing for novel materials', *Appl. Mater. Today*, 7, pp. 120-133. Doi: <https://doi.org/10.1016/j.apmt.2017.02.004>.

50. Lei, M., Chen, Z., Lu, H. and Yu, K. (2019). 'Recent progress in shape memory polymer composites: methods, properties, applications and prospects', *Nanotechnol Rev.*, 8, pp. 327–351. Doi: <https://doi.org/10.1515/ntrev-2019-0031>.
51. Leist, S.K. and Zhou, J. (2016). 'Current status of 4D printing technology and the potential of light-reactive smart materials as 4D printable materials', *Virtual and Physical Prototyping*, 11 (4), pp. 249-262. Doi: <https://doi.org/10.1080/17452759.2016.1198630>.
52. Leng, J.S., Lan, X., Liu, Y.J., Du, S.Y. (2011). 'Shape-memory polymers and their composites: Stimuli methods and applications', *Prog Mater Sci*, 56 (7), pp. 1077–1135. Doi: <https://doi.org/10.1016/j.pmatsci.2011.03.001>.
53. Li, Y., Zhang, F., Liu, Y. and Leng, J. (2020). '4D printed shape memory polymers and their structures for biomedical applications', *Science China Technological Sciences*, 63(4), pp. 545-560. Doi: [10.1007/s11431-019-1494-0](https://doi.org/10.1007/s11431-019-1494-0).
54. Liu, Y., Genzer, J. and Dickey, M.D. (2016). "'2D or not 2D': Shape-programming polymer sheets", *Prog Polym Sci*, 52, pp. 79–106. Doi: <https://doi.org/10.1016/j.progpolymsci.2015.09.001>.
55. Li, Z., Li, H., Yin, J., Li, Y., Nie, Z., Li, X., and Hao, L. (2022). 'A Review of Spatter in Laser Powder Bed Fusion Additive Manufacturing: In Situ Detection, Generation, Effects, and Countermeasures'. *Micromachines*, 13(8), 1366. Doi: <https://doi.org/10.3390/mi13081366>.
56. Loh, H. H. (2021). '4D printing of shape-changing thermo-responsive textiles' (Doctoral dissertation, Brunel University London).
57. Lu, H.B., Huang, W.M. and Yao, Y.T. (2013). 'Review of chemo responsive shape change/memory polymers', *Pigm Resin Technol*, 42 (4), pp. 237–46. Doi: <https://doi.org/10.1108/PRT-11-2012-0079>.
58. Mallakpour, S., Tabesh, F., and Hussain, C. M. (2021). '3D and 4D printing: From innovation to evolution'. *Advances in Colloid and Interface Science*, 294, 102482. Doi: <https://doi.org/10.1016/j.cis.2021.102482>.
59. Mao, Y., Yu, K., Isakov, M., Wu, J., Dunn, M. and Qi, H. (2015). 'Sequential self-folding structures by 3D printed digital shape memory polymers', *Sci. Rep.*, 5. Doi: [10.1038/srep13616](https://doi.org/10.1038/srep13616).
60. Mao, Y., Ding, Z., Yuan, C., Ai, S., Isakov, M. and Wu, J. (2016). '3D printed reversible shape changing components with stimuli responsive materials', *Sci Rep*, 6, p. 24761. Doi: [10.1038/srep24761](https://doi.org/10.1038/srep24761).
61. Maraveas, C., Bayer, I. S., & Bartzanas, T. (2022). 4D printing: Perspectives for the production of sustainable plastics for agriculture. *Biotechnology Advances*, 54, 107785. Doi: <https://doi.org/10.1016/j.biotechadv.2021.107785>.
62. Melocchi, A., Uboldi, M., Inverardi, N., Briatico-Vangosa, F., Baldi, F., Pandini, S., ... & Gazzaniga, A. (2019). Expandable drug delivery system for gastric retention based on shape memory polymers: Development via 4D printing and extrusion. *International journal of pharmaceutics*, 571, 118700. Doi: <https://doi.org/10.1016/j.ijpharm.2019.118700>.
63. Meng, H. and Li, G. (2013). 'A review of stimuli-responsive shape memory polymer composites', *Polymer*, 54, pp. 2199–2221. Doi: <https://doi.org/10.1016/j.polymer.2013.02.023>.
64. Miao, S., Zhu, W., Castro, N., Nowicki, M., Zhou, X., Cui, H., Fisher, J. and Zhang, L. (2016). '4D printing smart biomedical scaffolds with novel soybean oil epoxidized acrylate', *Sci Rep*, 6, p. 27226 Doi: <https://doi.org/10.1038/srep27226>.
65. Mitchell, A., Lafont, U., Hołyńska, M., and Semprimoschnig, C. J. A. M. (2018). 'Additive manufacturing—A review of 4D printing and future applications'. *Additive Manufacturing*, 24, 606-626. Doi: <https://doi.org/10.1016/j.addma.2018.10.038>.

66. Mohammad Vaezi, Srisit Chianrabutra, Brian Mellor and Shoufeng Yang (2013). 'Multiple material additive manufacturing – Part 1: a review', *Virtual and Physical Prototyping*, 8:1, 19-50, Doi: 10.1080/17452759.2013.778175.
67. Monzon, M.D., Paz, R., Pei, E., Ortega, F., Suarez, L.A., Ortega, Z., Aleman, M.E., Plucinski, T. and Clow, N. (2017). '4D Printing: Processability and measurement of recovery force in shape memory polymers', *The international Journal of Advanced Manufacturing Technology*, 89 (5-8), pp. 1827-1836. Doi: 10.1007/s00170-016-9233-9.
68. Mu, T., Liu, L., Lan, X., Liu, Y. and Leng, J. (2018). 'Shape memory polymers for composites', *Composites Science and Technology*, 160, pp. 169-198. Doi: <https://doi.org/10.1016/j.compscitech.2018.03.018>.
69. Naficy, S., Spinks, G.M. and Baughman, R.H. (2016). 'Bio-inspired polymer artificial muscles', in eds. Names (eds.) *Bio-inspired Polymers*. Place of publication: Royal Society of Chemistry, pp. 429-459.
70. Nam, S. and Pei, E. (2019). 'A taxonomy of shape-changing behavior for 4D Printed parts using shape-memory polymers', *Progress in Additive Manufacturing Journal*, 4 (2), pp. 167–184. Doi: <https://doi.org/10.1007/s40964-019-00079-5>.
71. Nam, S. and Pei, E. (2020). 'The influence of Shape changing behaviors from 4D printing through material extrusion print patterns and infill densities', *Materials*, 13 (17), p. 3754. Doi: <https://doi.org/10.3390/ma13173754>.
72. Namvar, N., Zolfagharian, A., Vakili-Tahami, F., & Bodaghi, M. (2022). Reversible energy absorption of elasto-plastic auxetic, hexagonal, and AuxHex structures fabricated by FDM 4D printing. *Smart Materials and Structures*, 31(5), 055021. Doi 10.1088/1361-665X/ac6291.
73. Ng, W.L., Lee, J.M., Zhou, M., Chen, Y.W., Lee, K.X.A., Yeong, W.Y. and Shen, Y.F. (2020). 'Vat polymerization-based bioprinting—process, materials, applications and regulatory challenges', *Biofabrication*, 12 (2), p. 022001. Doi 10.1088/1758-5090/ab6034.
74. Nkomo, N. (2018). 'A Review of 4D Printing Technology and Future Trends', *SACAM Conference 2018*, location and date of conference. Publisher: page number.
75. Noroozi, R., Bodaghi, M., Jafari, H., Zolfagharian, A. and Fotouhi, M. (2020). 'Shape-adaptive metastructures with variable bandgap regions by 4D printing', *Polymers*, 12 (3), pp. 519. Doi: <https://doi.org/10.3390/polym12030519>.
76. Pandini, S., Baldi, F., Paderni, K., Messori, M., Toselli, M., Pilati, F., Gianoncelli, A., Brisotto, M., Bontempi, E. and Riccò, T. (2013). 'One-way and two-way shape memory behaviour of semi-crystalline networks based on sol-gel cross-linked poly (ϵ -caprolactone)'. *Polymer*, 54(16), pp.4253-4265. Doi: <https://doi.org/10.1016/j.polymer.2013.06.016>.
77. Pugliese, R., and Regondi, S. (2022). 'Artificial Intelligence-Empowered 3D and 4D Printing Technologies toward Smarter Biomedical Materials and Approaches'. *Polymers*, 14(14), 2794. Doi: <https://doi.org/10.3390/polym14142794>.
78. Queiroz, M.M., Pereira, S.C.F., Telles, R. and Machado, M.C. (2019). 'Industry 4.0 and digital supply chain capabilities: A framework for understanding digitalisation challenges and opportunities', *Benchmarking: an international journal*, vol. number, page number. Doi: <https://doi.org/10.1108/BIJ-12-2018-0435>.
79. Ragin, C.C. (1987). 'The comparative method: moving beyond qualitative and quantitative strategies'. Berkeley: University of California Press. Doi: <https://doi.org/10.1525/9780520957350>.
80. Rastogi, P. and Kandasubramanian, B. (2019). 'Breakthrough in the printing tactics for stimuli-responsive materials: 4D printing', *Chemical Engineering*, 366, pp. 264-304. Doi: <https://doi.org/10.1016/j.cej.2019.02.085>
81. Ratna, D. and Karger-Kocsis, J. (2008). 'Recent advances in shape memory polymers and composites: A review', *J Mater Sci*, 43 (1), pp. 254–69. Doi:10.1007/s10853-007-2176-7.

82. Raviv, D., Zhao, W., McKnelly, C., Papadopoulou, A., Kadambi, A., Shi, B., Hirsch, S., Dikovsky, D., Zyracki, M., Olguin, C., Raskar, R. and Tibbits, S. (2014). 'Active printed materials for complex self-evolving deformations', *Scientific Reports*, 4 (7422). Doi: <https://doi.org/10.1038/srep07422>.
83. Rayate, A., & Jain, P. K. (2018). A review on 4D printing material composites and their applications. *Materials Today: Proceedings*, 5(9), 20474-20484. Doi: <https://doi.org/10.1016/j.matpr.2018.06.424>.
84. Roos, Y. and Karel, M. (1991). 'Plasticizing effect of water on thermal behavior and crystallization of amorphous food models', *J Food Sci*, 56(1), pp. 38–43. Doi: <https://doi.org/10.1111/j.1365-2621.1991.tb07970>.
85. Ryan, K. R., Down, M. P. and Banks, C. E. (2021). 'Future of additive manufacturing: Overview of 4D and 3D printed smart and advanced materials and their applications', *Chemical Engineering Journal*, 403, pp. 126162. Doi: <https://doi.org/10.1016/j.cej.2020.126162>.
86. Ryu, J., D'Amato, M., Cui, X., Long, K.N., Qi, H.J. and Dunn, M.L. (2012). 'Photo-origami—bending and folding polymers with light', *Appl Phys Lett*, 100 (2012), pp. 161908. Doi: <https://doi.org/10.1063/1.3700719>.
87. Senatov, F. S., Niaza, K. V., Zadorozhnyy, M. Y., Maksimkin, A. V., Kaloshkin, S. D., & Estrin, Y. Z. (2016). Mechanical properties and shape memory effect of 3D-printed PLA-based porous scaffolds. *Journal of the mechanical behavior of biomedical materials*, 57, 139-148. Doi: <https://doi.org/10.1016/j.jmbbm.2015.11.036>.
88. Serjouei, A., Yousefi, A., Jenaki, A., Bodaghi, M., & Mehrpouya, M. (2022). 4D printed shape memory sandwich structures: experimental analysis and numerical modeling. *Smart Materials and Structures*, 31(5), 055014. Doi: 10.1088/1361-665X/ac60b5.
89. Scalet, G., Pandini, S., Messori, M., Toselli, M., and Auricchio, F. (2018). 'A one-dimensional phenomenological model for the two-way shape-memory effect in semi-crystalline networks'. *Polymer*, 158, 130-148. Doi: <https://doi.org/10.1016/j.polymer.2018.10.027>.
90. Scalet, G. (2020). 'Two-way and Multiple-way Shape Memory Polymers for Soft Robotics: An Overview', *Actuators*, 9, p. 10. 10.3390/act9010010. Doi: <https://doi.org/10.3390/act9010010>.
91. Shahinpoor, M. (2020). '14 Shape Memory Polymers (SMPs) as Smart Materials'. *Fundamentals of Smart Materials*, 160.
92. Shan, W., Chen, Y., Hu, M., Qin, S. and Peng Liu, P. (2020). '4D printing of shape memory polymer via liquid crystal display (LCD) stereolithographic 3D printing', *Mater. Res. Express*, 7, p. 105305. Doi 10.1088/2053-1591/abbd05.
93. Sharon, E. and Efrati, E. (2010). 'The mechanics of non-Euclidean plates', *Soft Matter*, 6 (22), pp. 5693-5704. Doi: <https://doi.org/10.1039/C0SM00479K>.
94. Sossou, G., Demoly, F., Belkebir, H., Qi, H. J., Gomes, S. and Montavon, G. (2019a). 'Design for 4D printing: Modeling and computation of smart materials distributions', *Materials & Design*, 181, p. 108074. Doi: <https://doi.org/10.1016/j.matdes.2019.108074>.
95. Sossou, G., Demoly, F., Belkebir, H., Qi, H. J., Gomes, S. and Montavon, G. (2019b). 'Design for 4D printing: A voxel-based modeling and simulation of smart materials', *Materials & Design*, 175, p. 107798. Doi: <https://doi.org/10.1016/j.matdes.2019.107798>.
96. Spiegel, C. A., Hackner, M., Bothe, V. P., Spatz, J. P., and Blasco, E. (2022). '4D Printing of Shape Memory Polymers: From Macro to Micro'. *Advanced Functional Materials*, 2110580. Doi: <https://doi.org/10.1002/adfm.202110580>.
97. Strzelec, K., Sienkiewicz, N., and Szmechtyk, T. (2020). 'Classification of shape-memory polymers, polymer blends, and composites'. In *Shape Memory Polymers, Blends and Composites* (pp. 21-52). Springer, Singapore.

98. Subash, A., and Kandasubramanian, B. (2020). '4D printing of shape memory polymers'. *European Polymer Journal*, 134, 109771. Doi: <https://doi.org/10.1016/j.eurpolymj.2020.109771>.
99. Sun, L., Huang, W., Ding, Z., Zhao, Y., Wang, C., Purnawali, H. and Tang, C. (2012). 'Stimulus- responsive shape memory materials: A review', *Mater. Des.*, 33, pp. 577–640. Doi: <https://doi.org/10.1016/j.matdes.2011.04.065>.
100. Tan, L.J., Zhu, W. and Zhou, K. (2020). 'Recent progress on polymer materials for additive manufacturing', *Advanced Functional Materials*, 30 (43), p. 2003062. Doi: <https://doi.org/10.1002/adfm.202003062>.
101. Tanveer, M., Haleem, A., and Suhaib, M. (2019). 'Effect of variable infill density on mechanical behaviour of 3-D printed PLA specimen: an experimental investigation'. *SN Applied Sciences*, 1(12), 1-12. Doi: 10.1007/s42452-019-1744-1.
102. Teoh, J.E.M., Chua, C.K., Liu, Y. and An, J. (2017). '4D printing of customised smart sunshade: A conceptual study', In: da Silva, F.M., Bártolo, H., Bártolo, P., Almendra, R., Roseta, F, Almeida, H.A. et al., (eds.) *Challenges for technology innovation: An agenda for the future*. London: CRC Press, p. 105–108.
103. Teng, X., Zhang, M. and Mujumdar, A.S. (2021). '4D printing: Recent advances and proposals in the food sector', *Trends in Food Science & Technology*, 110, pp. 349–363. Doi: <https://doi.org/10.1016/j.tifs.2021.01.076>.
104. Teunis, M., Shahram, J. and Amir, Z. (2017). 'Programming 2D/3D shape-shifting with hobbyist 3D printers', 4 (6), pp. 935–1202. Doi: 10.1039/C7MH00269F.
105. Tezerjani, S.M.D., Yazdi, M.S. and Hosseinzadeh, M.H. (2022). 'The effect of 3D printing parameters on the shape memory properties of 4D printed polylactic acid circular disks: An experimental investigation and parameters optimization', *Materials Today Communications*, p. 104262. Doi: <https://doi.org/10.1016/j.mtcomm.2022.104262>.
106. Tibbits, S. (2014). '4D Printing: Multi-Material Shape Change', *Architectural Design*, 84 (1), pp. 116–121. Doi: <https://doi.org/10.1002/ad.1710>.
107. Tolley, M. T., Felton, S. M., Miyashita, S., Aukes, D., Rus, D., and Wood, R. J. (2014). 'Self-folding origami: shape memory composites activated by uniform heating'. *Smart Materials and Structures*, 23(9), 094006. Doi: 10.1088/0964-1726/23/9/094006
108. Türk, D.A., Brenni, F., Zogg, M. and Meboldt, M. (2017). 'Mechanical characterization of 3D printed polymers for fiber reinforced polymers processing', *Mater*, 118, pp. 256–265. Doi: <https://doi.org/10.1016/j.matdes.2017.01.050>.
109. Valvez, S., Reis, P.N.B, Susmel, L. and Berto, F. (2021). 'Fused Filament Fabrication-4D-Printed Shape Memory Polymers: A Review', *Polymers*, 13, p. 701. Doi: <https://doi.org/10.3390/polym13050701>.
110. van Manen, T., Janbaz, S. and Zadpoor, A.A. (2017). 'Programming 2D/3D shape-shifting with hobbyist 3D printers', *Mater. Horiz.*, 4, pp. 1064-1069. Doi: 10.1039/C7MH00269F
111. van Manen, T., Janbaz, S. and Zadpoor, A.A. (2018). 'Programming the shape-shifting of flat soft matter', *Materials Today*, 21 (2), pp. 144–163. Doi: <https://doi.org/10.1016/j.mattod.2017.08.026>.
112. Wang, W., Yao, L., Zhang, T., Cheng, C., Levine, D. and Ishii, H. (2017). 'Transformative appetite: shape-changing food transforms from 2D to 3D by water interaction through cooking', In: ACM 978-1-4503-4655-9/417/05. Doi: <https://doi.org/10.1145/3025453.3026019>.
113. Wang, J., Wang, Z., Song, Z., Ren, L., Liu, Q., and Ren, L. (2019). 'Biomimetic Shape–Color Double-Responsive 4D Printing'. *Advanced Materials Technologies*, 4(9), 1900293. Doi: <https://doi.org/10.1002/admt.201900293>.

114. Wang, J., Wang, Z., Song, Z., Ren, L., Liu, Q., and Ren, L. (2019). 'Programming multistage shape memory and variable recovery force with 4D printing parameters'. *Advanced Materials Technologies*, 4(11), 1900535. Doi: <https://doi.org/10.1002/admt.201900535>.
115. Westbrook, K.K., Kao, P.H., Castro, F., Ding, Y. and Qi, H.J. (2011). 'A 3D finite deformation constitutive model for amorphous shape memory polymers: a multi-branch modeling approach for nonequilibrium relaxation processes', *Mechanics of Materials*, 43 (12), pp. 853-869. Doi: <https://doi.org/10.1016/j.mechmat.2011.09.004>.
116. Wu, J., Yuan, C., Ding, Z., Isakov, M., Mao, Y., Wang, T., Dunn, M. and Qi, H. (2016). 'Multi-shape active composites by 3D printing of digital shape memory polymers', *Sci. Rep.*, 6, 24224. Doi: <https://doi.org/10.1038/srep24224>.
117. Wu, J., Zhao, Z., Kuang, X., Hamel, C. M., Fang, D., and Qi, H. J. (2018). 'Reversible shape change structures by grayscale pattern 4D printing'. *Multifunctional Materials*, 1(1), 015002. Doi: 10.1088/2399-7532/aac322.
118. Wu, W., Ye, W., Wu, Z., Geng, P., Wang, Y., and Zhao, J. (2017). 'Influence of layer thickness, raster angle, deformation temperature and recovery temperature on the shape-memory effect of 3D-printed polylactic acid samples'. *Materials*, 10(8), 970. Doi: <https://doi.org/10.3390/ma10080970>.
119. Xia, Y., He, Y., Zhang, F., Liu, Y. and Leng, J. (2021). 'A review of shape memory polymers and composites: mechanisms, materials, and applications', *Advanced Materials*, 33 (6), 2000713. Doi: <https://doi.org/10.1002/adma.202000713>.
120. Xie, T. (2011). 'Recent advances in polymer shape memory'. *Polymer*, 52(22), pp.4985-5000. Doi: <https://doi.org/10.1016/j.polymer.2011.08.003>.
121. Xin, X., Liu, L., Liu, Y., & Leng, J. (2020). Origami-inspired self-deployment 4D printed honeycomb sandwich structure with large shape transformation. *Smart Materials and Structures*, 29(6), 065015. Doi: 10.1088/1361-665X/ab85a4.
122. Xin, X., Liu, L., Liu, Y., & Leng, J. (2022). 4D pixel mechanical metamaterials with programmable and reconfigurable properties. *Advanced Functional Materials*, 32(6), 2107795. Doi: <https://doi.org/10.1002/adfm.202107795>.
123. Yang, Y., Chen, Y., Wei, Y. and Li, Y. (2016). '3D printing of shape memory polymer for functional part fabrication', *Int. J. Adv. Manuf. Technol.*, 84, pp. 2079–2095. Doi: <https://doi.org/10.1007/s00170-015-7843-2>.
124. Yarwindran, M., Sa'aban, N.A., Ibrahim, M. and Periyasamy, R. (2016). 'Thermoplastic elastomer infill pattern impact on mechanical properties 3D printed customized orthotic insole', *ARPN*, 11 (10), ISSN 1819-6608.
125. Yu, K., Dunn, M.L. and Qi, H.J. (2015). 'Digital manufacture of shape changing components', *Extreme Mech Lett*, 4, pp. 9–17. Doi: <https://doi.org/10.1016/j.eml.2015.07.005>.
126. Yu, Y., Liu, H., Qian, K., Yang, H., McGehee, M., Gu, J., Luo, D., Yao, L. and Zhang, Y.J. (2020). 'Material characterization and precise finite element analysis of fiber reinforced thermoplastic composites for 4D printing', *CAD*, 122, 102817. Doi: <https://doi.org/10.1016/j.cad.2020.102817>.
127. Zarek, M., Mansour, N., Shapira, S. and Cohn, D. (2017). '4D printing of shape memory-based personalized endoluminal medical devices', *Macromolecular Rapid Communications*, 38 (2), 1600628. Doi: <https://doi.org/10.1002/marc.201600628>.
128. Zhang, Q., Zhang, K. and Hu, G. (2016). 'Smart three-dimensional lightweight structure triggered from a thin composite sheet via 3D printing technique', *Sci Rep*, 6, 22431. Doi: <https://doi.org/10.1038/srep22431>.
129. Zhang, W., Wang, H., Wang, H., Chan, J., Liu, H., Zhang, B., Zhang, Y., Agarwal, K., Yang, X., Ranganath, A., Low, H., Ge, Q. and Yang, J. (2021). 'Structural multi-colour invisible inks with submicron 4D

printing of shape memory polymers', *Nat Commun*, 12, pp. 112. Doi: <https://doi.org/10.1038/s41467-020-20300-2>.

130. Zhang, W., Zhang, F., Lan, X., Leng, J., Wu, A. S., Bryson, T. M., ... & Chou, T. W. (2018). Shape memory behavior and recovery force of 4D printed textile functional composites. *Composites Science and Technology*, 160, 224-230. Doi: <https://doi.org/10.1016/j.compscitech.2018.03.037>.

131. Zhao, Z., Peng, F., Cavicchi, K.A., Cakmak, M., Weiss, R.A. and Vogt, B.D. (2017a). 'Three-Dimensional Printed Shape Memory Objects Based on an Olefin Ionomer of Zinc-Neutralized Poly(ethylene-co-methacrylic acid)', *ACS Appl. Mater. Interfaces*, 9, pp. 27239–27249. Doi: <https://doi.org/10.1021/acsami.7b07816>.

132. Zhao, Z., Wu, J., Mu, X., Chen, H., Qi, J. and Fang, D. (2017b). 'Origami by frontal photopolymerization', *Science*, 3 (4), e1602326. Doi: 10.1126/sciadv.1602326.

133. Zhao, Z., Wu, J., Mu, X., Chen, H., Qi, H.J. and Fang, D. (2017c). 'Desolvation induced origami of photocurable polymers by digit light processing', *Macromolecular Rapid Communications*, 38 (13), 1600625. Doi: <https://doi.org/10.1002/marc.201600625>.

134. Zheng, Y., Zhang, W., Baca Lopez, D.M. and Ahmad, R. (2021). 'Scientometric analysis and systematic review of multi-material additive manufacturing of polymers', *Polymers*, 13 (12), p. 1957. Doi: <https://doi.org/10.3390/polym13121957>.

135. Zhou, Y., Huang, W. M., Kang, S. F., Wu, X. L., Lu, H. B., Fu, J., & Cui, H. (2015). From 3D to 4D printing: approaches and typical applications. *Journal of Mechanical Science and Technology*, 29, 4281-4288. Doi:10.1007/s12206-015-0925-0.

136. Zhou, J. and Sheiko, S.S. (2016). 'Reversible shape-shifting in polymeric materials', *J. Polym. Sci. B Polym. Phys.*, 54, pp. 1365–1380. Doi: <https://doi.org/10.1002/polb.24014>.

137. Zolfagharian, A., Kaynak, A., Khoo, S.Y. and Kouzani, (2018). 'A pattern-driven 4D printing', *Sensors and Actuators, A: physical*, 274, pp. 231–243, ISSN 0924-4247. Doi: <https://doi.org/10.1016/j.sna.2018.03.034>.

Appendix

Appendix I. BREO Acceptance Letter



College of Engineering, Design and Physical Sciences Research Ethics Committee
Brunel University London
Kingston Lane
Uxbridge
UB8 3PH
United Kingdom
www.brunel.ac.uk

18 February 2021

LETTER OF APPROVAL (CONDITIONAL)

APPROVAL HAS BEEN GRANTED FOR THIS STUDY TO BE CARRIED OUT BETWEEN 18/02/2021 AND 01/04/2021

Applicant (s): Mr. Seokwoo Nam Dr. Eujin Pel

Project Title: 4D printing toolkit for controlling printing parameters

Reference: 29721-MHR-Jan/2021- 30957-1

Dear Mr. Seokwoo Nam

The Research Ethics Committee has considered the above application recently submitted by you.

The Chair, acting under delegated authority has agreed that there is no objection on ethical grounds to the proposed study. Approval is given on the understanding that the conditions of approval set out below are followed:

- Approval is given for remote (online/telephone) research activity only. Face-to-face activity and/or travel will require approval by way of an amendment.
- The agreed protocol must be followed. Any changes to the protocol will require prior approval from the Committee by way of an application for an amendment.
- In addition to the above, please ensure that you monitor and adhere to all up-to-date local and national Government health advice for the duration of your project.
- As per our correspondence on 2/2/21 please ensure all participants remain anonymous, and refer to them only by their job role or a pseudonym if required.

Please add the online consent form to your questionnaire before issue. <https://breo.brunel.ac.uk/Personalisation/DisplayPage/50>

(This can be addressed outside of the BREO system)

Please note that:

- Research Participant Information Sheets and (where relevant) flyers, posters, and consent forms should include a clear statement that research ethics approval has been obtained from the relevant Research Ethics Committee.
- The Research Participant Information Sheets should include a clear statement that queries should be directed, in the first instance, to the Supervisor (where relevant), or the researcher. Complaints, on the other hand, should be directed, in the first instance, to the Chair of the relevant Research Ethics Committee.
- Approval to proceed with the study is granted subject to receipt by the Committee of satisfactory responses to any conditions that may appear above, in addition to any subsequent changes to the protocol.
- The Research Ethics Committee reserves the right to sample and review documentation, including raw data, relevant to the study.
- You may not undertake any research activity if you are not a registered student of Brunel University or if you cease to become registered, including abeyance or temporary withdrawal. As a deregistered student you would not be insured to undertake research activity. Research activity includes the recruitment of participants, undertaking consent procedures and collection of data. Breach of this requirement constitutes research misconduct and is a disciplinary offence.

Professor Hua Zhao

Chair of the College of Engineering, Design and Physical Sciences Research Ethics Committee

Brunel University London

Appendix II. Participation Information Sheet

PARTICIPANT INFORMATION SHEET

Study title: 4D printing toolkit for controlling printing parameters

Invitation Paragraph

Thank you for submitting your valuable feedback. We appreciate your insights to help us improve and build with a better 4D printing toolkit.

All information you provide will be kept confidential. The ethical consent for this project has been sought by the Research Ethics Committee of the College of Engineering, Design and Physical Sciences at Brunel University London.

Please contact Seokwoo.Nam@Brunel.ac.uk for further information, any issues regarding participating in this study or to collaborate on projects.

What is the purpose of the study? Why have been invited to participate?

The purpose of the 4D printing toolkit through in-depth experiment is that can help designers or engineers appropriately apply the desired shape recovery quality and shape recovery time by controlling printing parameters such as pattern, infill density, deformation and recovery temperature when making 4D printing products.

Do I have to take part?

Your participation is completely voluntary.

What will happen to me if I take part? What do I have to do?

You will be asked to answers a number of open questions, which will help the researchers understand your perceptions toward the toolkit, such your perception towards its usability of web 4D printing toolkit and infographic of 4D printing toolkit. If you have any questions, please feel free to clarify them with the researchers.

What are the possible disadvantages and risks of taking part? What are the indemnity arrangements?

The study is considered low risk. It is very unlikely to cause any financial loss/burden to participants. No sensitive and personal question is included. It should take no more than 5 minutes to complete.

What if something goes wrong?

You can decide to leave the study at any point.

Will my taking part in this study be kept confidential?

The information will be used of academic purposes only and treated as highly confidential. All answers will be anonymised. The results will not be publicly published nor made available outside of the university.

What will happen to the results of the research study?

The findings will be presented to the academic staff and the Brunel Design School also use conference or journal paper and doctoral thesis.

Contact for further information and complaints

For further information, please contact Dr Eujin Pei, College of Engineering, Design and Physical Sciences. The contact details are:

Dr Eujin Pei

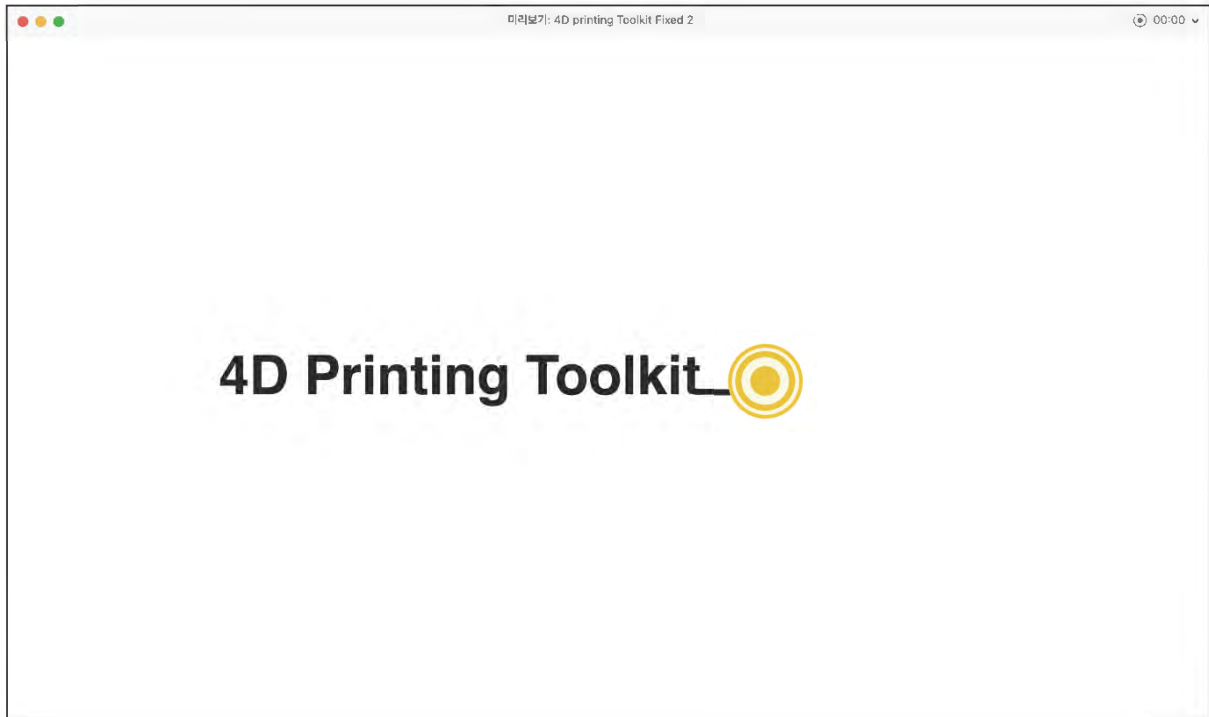
College of Engineering, Design and Physical Sciences

Brunel University, Uxbridge, UB8 3PH

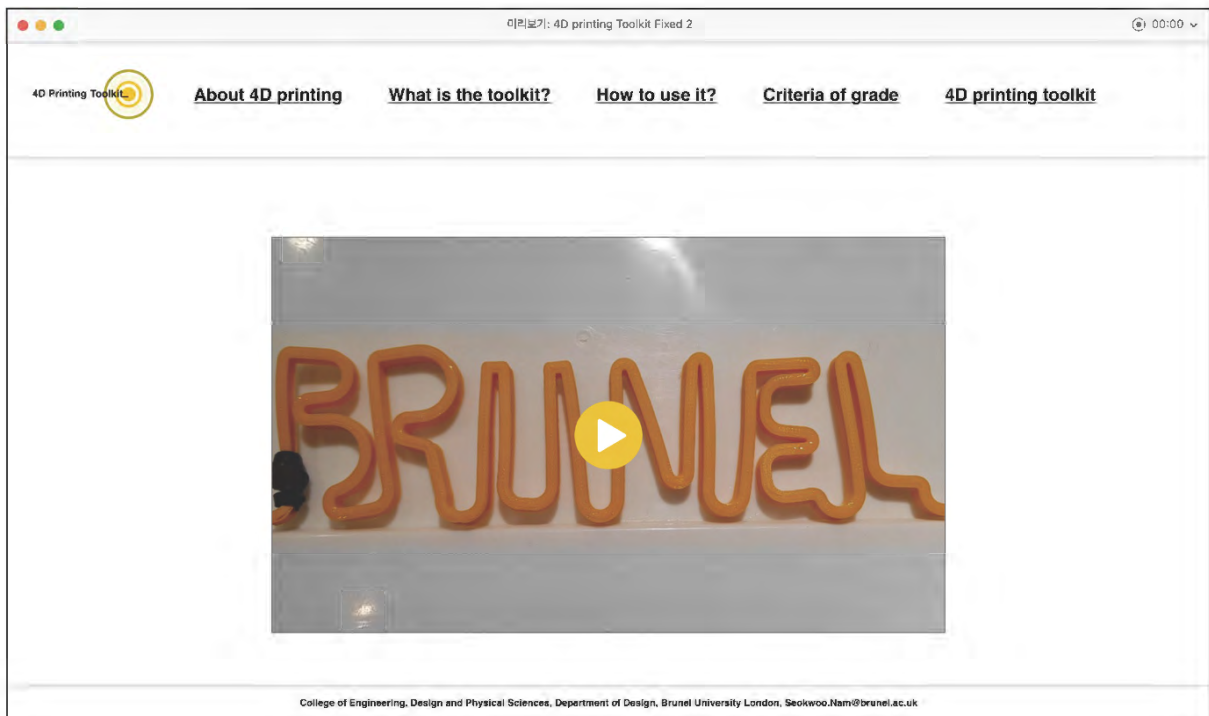
Tel: +44 1895 268055.

Email: eujin.pei@brunel.ac.uk

Appendix III. 4D Printing web toolkit (Final version)



Main page of the 4DP web toolkit



Video of the 4DP web toolkit

이리보기: 4D printing Toolkit Fixed 2 00:00

4D Printing Toolkit [About 4D printing](#) [What is the toolkit?](#) [How to use it?](#) [Criteria of grade](#) [4D printing toolkit](#)

4D printing is a process that creates a smart 3D object from a material that if exposed to water, heat, light, or magnetic field can change its shape over time. The structure of the 4D print is preprogrammed in detail according to the desired change of shape.

3D printing + Smart material + Stimulus = 4D printing

← Previous College of Engineering, Design and Physical Sciences, Department of Design, Brunel University London, Seokwoo.Nam@brunel.ac.uk Next →

Information on 4DP

이리보기: 4D printing Toolkit Fixed 2 00:00

4D Printing Toolkit [About 4D printing](#) [What is the toolkit?](#) [How to use it?](#) [Criteria of grade](#) [4D printing toolkit](#)

Process of shape change effect for 4D printing

Important

The shape memory effect is the result of programming that determines both the extent of the state of change and the desired shape when external stimuli is applied.

The shape memory effect occurs during the shape recovery phase.

← Previous College of Engineering, Design and Physical Sciences, Department of Design, Brunel University London, Seokwoo.Nam@brunel.ac.uk

Information on the shape change effect

4D Printing Toolkit

[About 4D printing](#) [What is the toolkit?](#) [How to use it?](#) [Criteria of grade](#) [4D printing toolkit](#)

Purposes:

The purpose of the toolkit through in-depth experimentation is that can help designers or engineers appropriately apply the desired shape recovery quality and shape recovery time by controlling printing parameters such as pattern, infill density, deformation and recovery temperature when making 4D printing products.

College of Engineering, Design and Physical Sciences, Department of Design, Brunel University London, Seokwoo.Nam@brunel.ac.uk






Next →

Information on the 4DP web toolkit

4D Printing Toolkit

[About 4D printing](#) [What is the toolkit?](#) [How to use it?](#) [Criteria of grade](#) [4D printing toolkit](#)

Key Parameters

12 Patterns	5 Infill densities	3 Recovery temperatures
 Concentric  Cross  Cubic  Cubic-subdivision  Grid  Gyroid  Line  Octet  Quarter-cubic  Triangle  Tri-hexagon  Zigzag	 20% Infill density  40% Infill density  60% Infill density  80% Infill density  100% Infill density	 <p>65°C, 70°C, 75°C</p>

← Previous

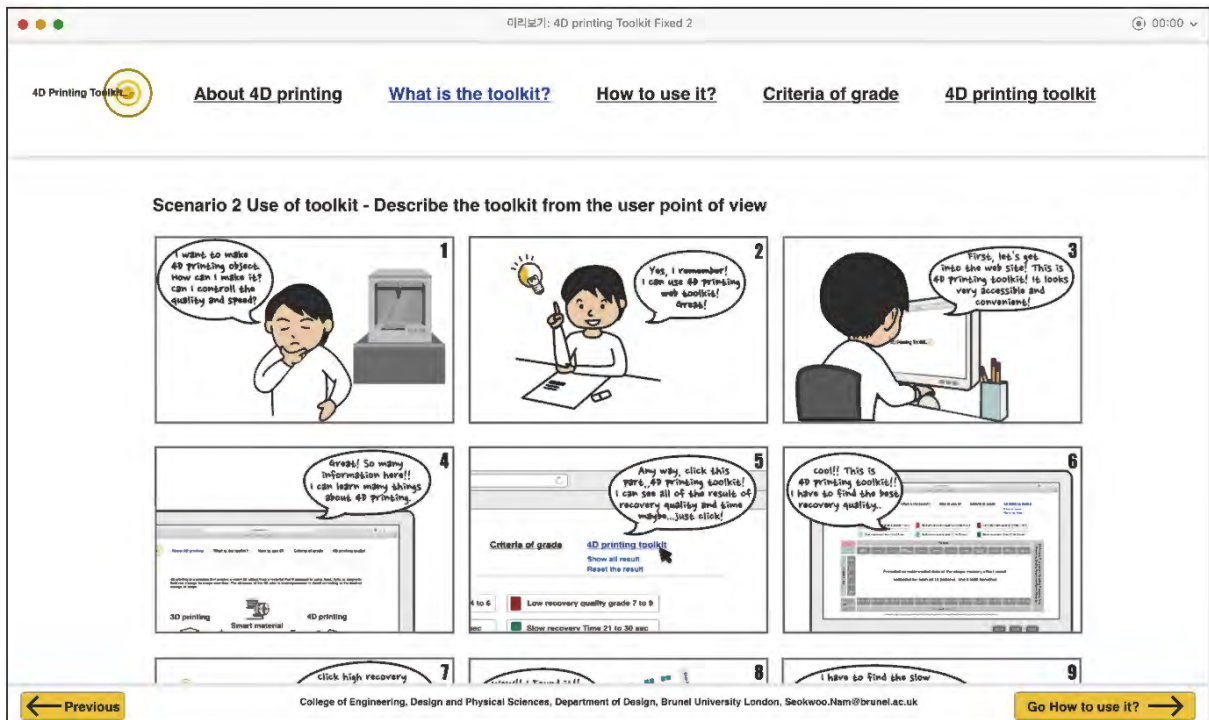
College of Engineering, Design and Physical Sciences, Department of Design, Brunel University London, Seokwoo.Nam@brunel.ac.uk

Next →

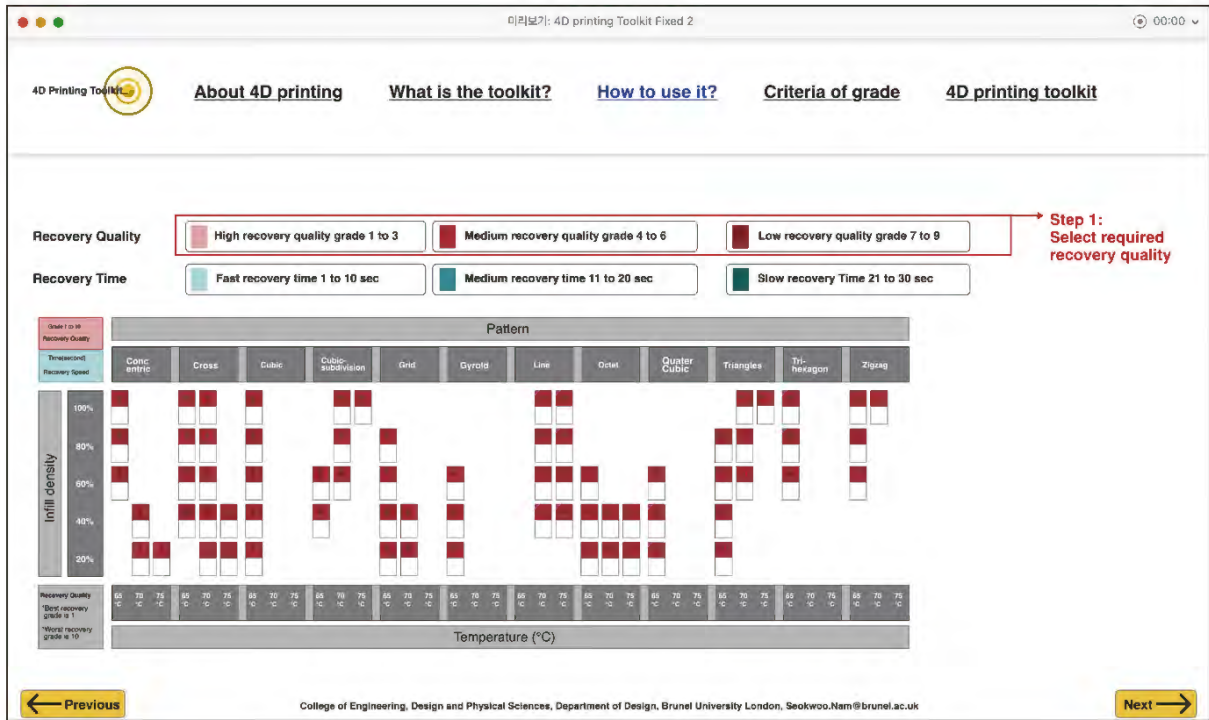
Information on the key parameters



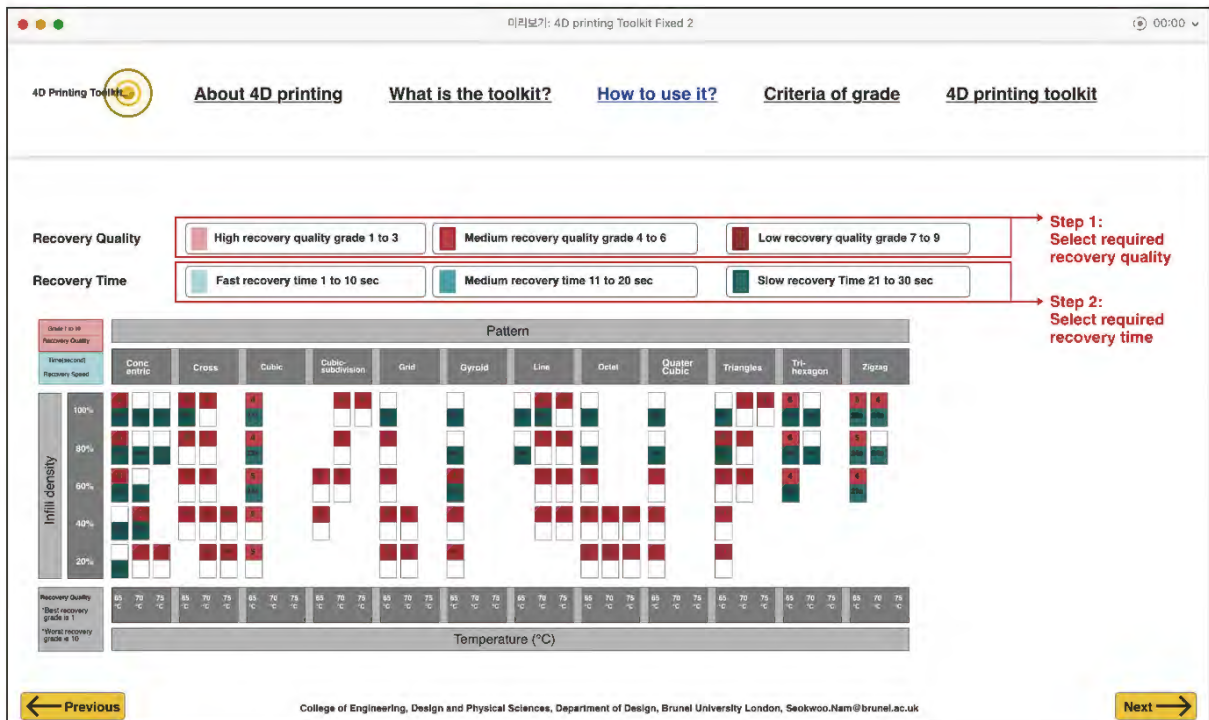
Scenario 1 of the 4DP web toolkit



Scenario 2 of the 4DP web toolkit



User's guide for the 4DP web toolkit 1



User's guide for the 4DP web toolkit 2

4D Printing Toolkit | About 4D printing | What is the toolkit? | How to use it? | Criteria of grade | 4D printing toolkit

Recovery Quality: High recovery quality grade 1 to 3, Medium recovery quality grade 4 to 6, Low recovery quality grade 7 to 9

Recovery Time: Fast recovery time 1 to 10 sec, Medium recovery time 11 to 20 sec, Slow recovery Time 21 to 30 sec

Pattern: Conc. entric, Cross, Cubic, Cubic-subdivision, Grid, Gyroid, Line, Octet, Quarter Cubic, Triangles, Tri-hexagon, Zigzag

Infill density: 100%, 80%, 60%, 40%, 20%

Temperature (°C): 65, 70, 75, 80, 85, 90, 95, 100, 105, 110, 115, 120, 125, 130, 135, 140, 145, 150, 155, 160, 165, 170, 175, 180, 185, 190, 195, 200

Steps:

- Step 1: Select required recovery quality
- Step 2: Select required recovery time
- Step 3: Select and change required recovery quality and time
- Step 4: Identify and record required recovery quality and time

College of Engineering, Design and Physical Sciences, Department of Design, Brunel University London, Seokwoo.Nam@brunel.ac.uk

User's guide for the 4DP web toolkit 3

4D Printing Toolkit | About 4D printing | What is the toolkit? | How to use it? | Criteria of grade | 4D printing toolkit

Recovery Quality: High recovery quality grade 1 to 3, Medium recovery quality grade 4 to 6, Low recovery quality grade 7 to 9

Recovery Time: Fast recovery time 1 to 10 sec, Medium recovery time 11 to 20 sec, Slow recovery Time 21 to 30 sec

Pattern: Conc. entric, Cross, Cubic, Cubic-subdivision, Grid, Gyroid, Line, Octet, Quarter Cubic, Triangles, Tri-hexagon, Zigzag

Infill density: 100%, 80%, 60%, 40%, 20%

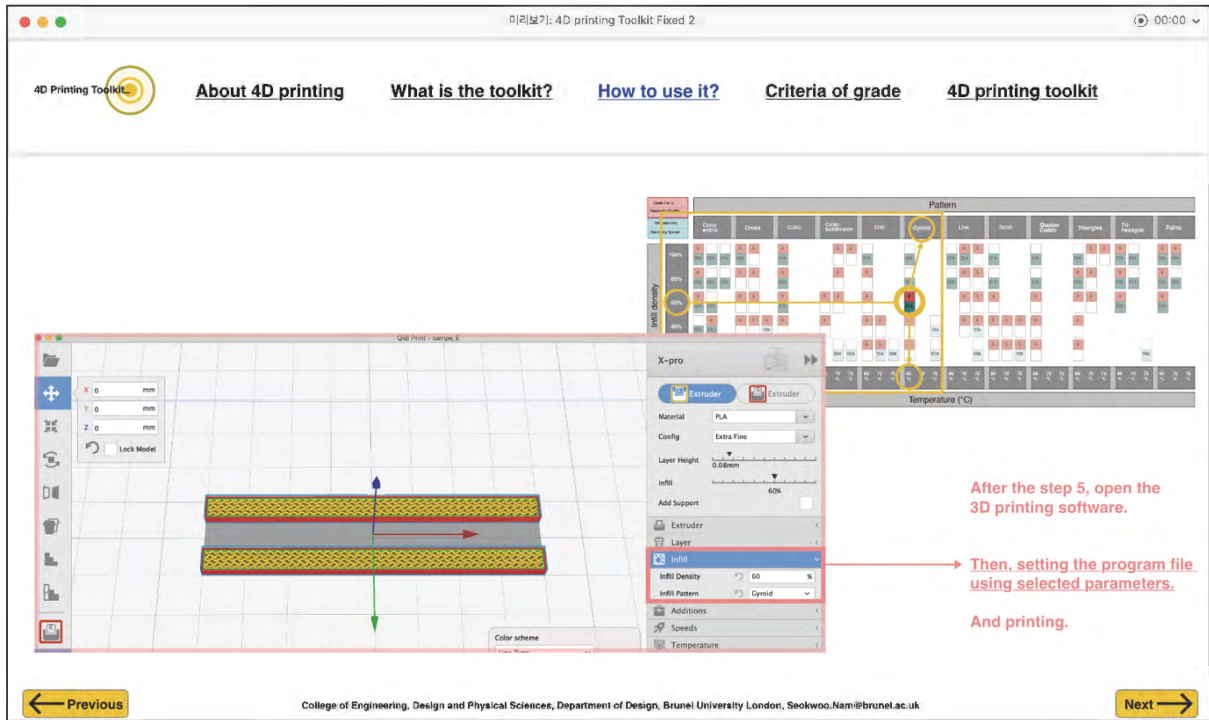
Temperature (°C): 65, 70, 75, 80, 85, 90, 95, 100, 105, 110, 115, 120, 125, 130, 135, 140, 145, 150, 155, 160, 165, 170, 175, 180, 185, 190, 195, 200

Steps:

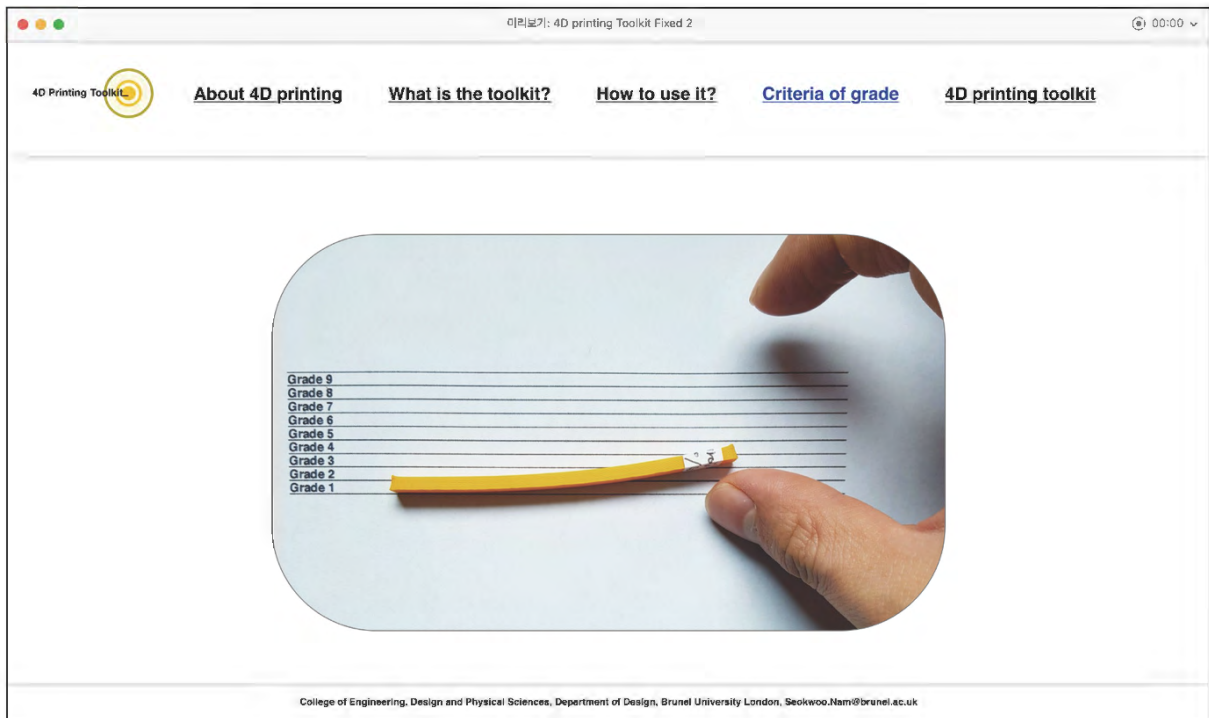
- Step 1: Select required recovery quality
- Step 2: Select required recovery time
- Step 3: Select and change required recovery quality and time
- Step 4: Identify and record required recovery quality and time
- Step 5: Select required recovery result, can check printing parameters; pattern, infill density and temp.

College of Engineering, Design and Physical Sciences, Department of Design, Brunel University London, Seokwoo.Nam@brunel.ac.uk

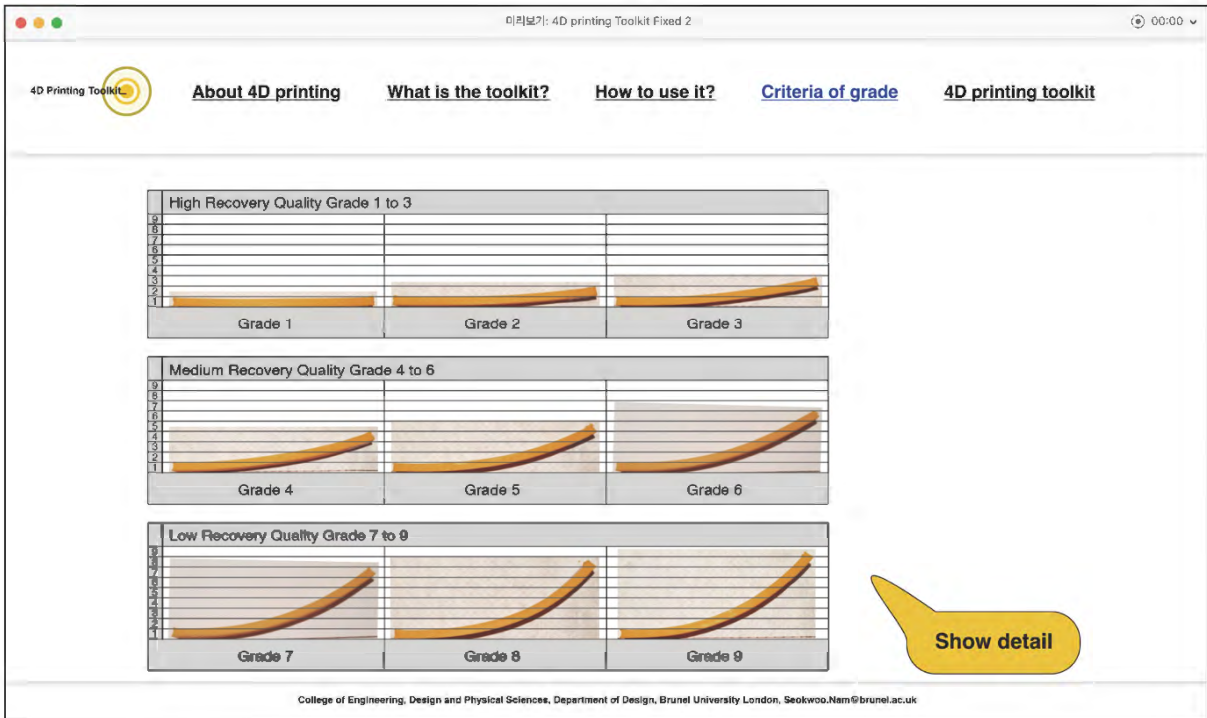
User's guide for the 4DP web toolkit 4



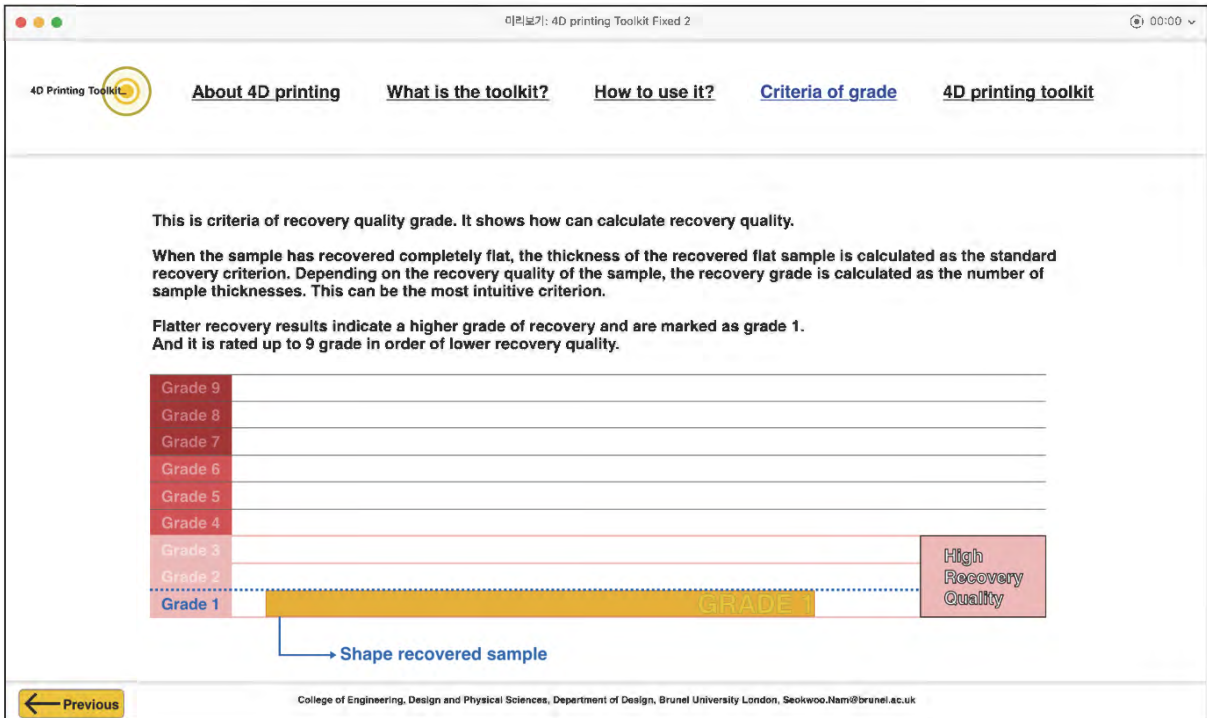
User's guide for the 4DP web toolkit 5



Information on grade 1 criteria



Information on grade 2 criteria



Information on grade 3 criteria

이리보기: 4D printing Toolkit Fixed 2 00:00

4D Printing Toolkit [About 4D printing](#) [What is the toolkit?](#) [How to use it?](#) [Criteria of grade](#) [4D printing toolkit](#)

This is criteria of recovery quality grade. It shows how can calculate recovery quality.

When the sample has recovered completely flat, the thickness of the recovered flat sample is calculated as the standard recovery criterion. Depending on the recovery quality of the sample, the recovery grade is calculated as the number of sample thicknesses. This can be the most intuitive criterion.

Flatter recovery results indicate a higher grade of recovery and are marked as grade 1. And it is rated up to 9 grade in order of lower recovery quality.

← Previous

College of Engineering, Design and Physical Sciences, Department of Design, Brunel University London, Seokwoo.Nam@brunel.ac.uk

Information on grade 4 criteria

이리보기: 4D printing Toolkit Fixed 2 00:00

4D Printing Toolkit [About 4D printing](#) [What is the toolkit?](#) [How to use it?](#) [Criteria of grade](#) [4D printing toolkit](#)

This is criteria of recovery quality grade. It shows how can calculate recovery quality.

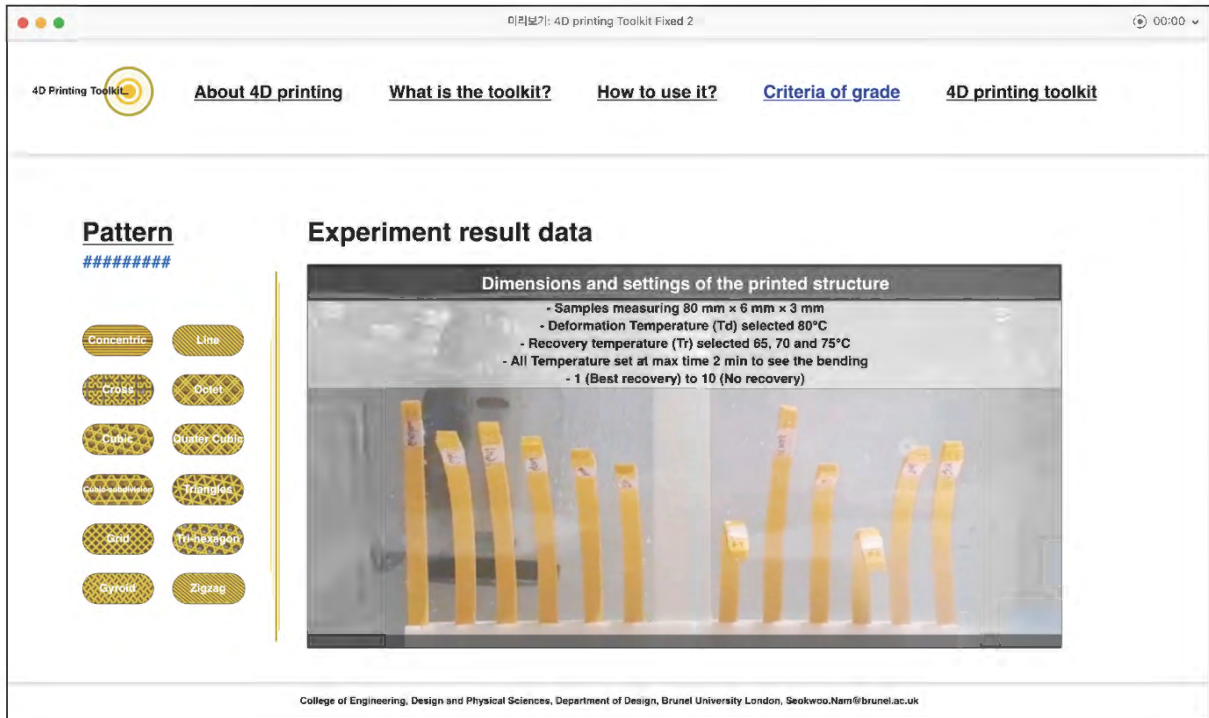
When the sample has recovered completely flat, the thickness of the recovered flat sample is calculated as the standard recovery criterion. Depending on the recovery quality of the sample, the recovery grade is calculated as the number of sample thicknesses. This can be the most intuitive criterion.

Flatter recovery results indicate a higher grade of recovery and are marked as grade 1. And it is rated up to 9 grade in order of lower recovery quality.

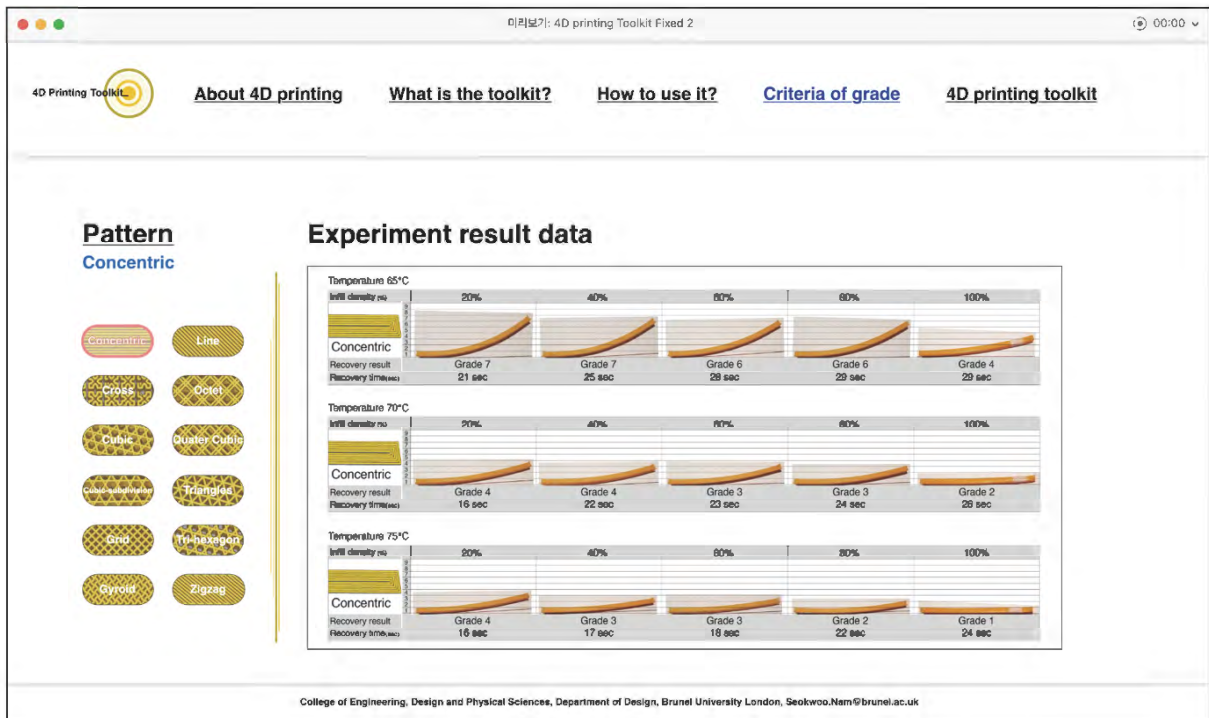
← Previous

College of Engineering, Design and Physical Sciences, Department of Design, Brunel University London, Seokwoo.Nam@brunel.ac.uk

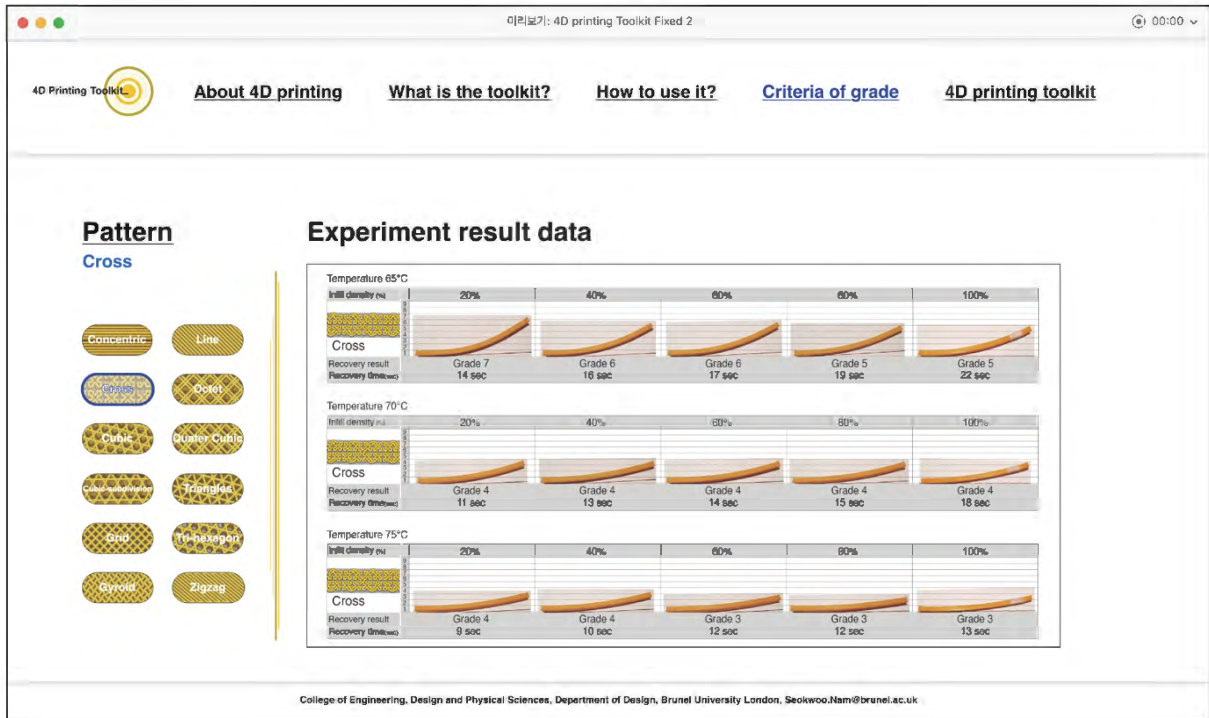
Information on grade 5 criteria



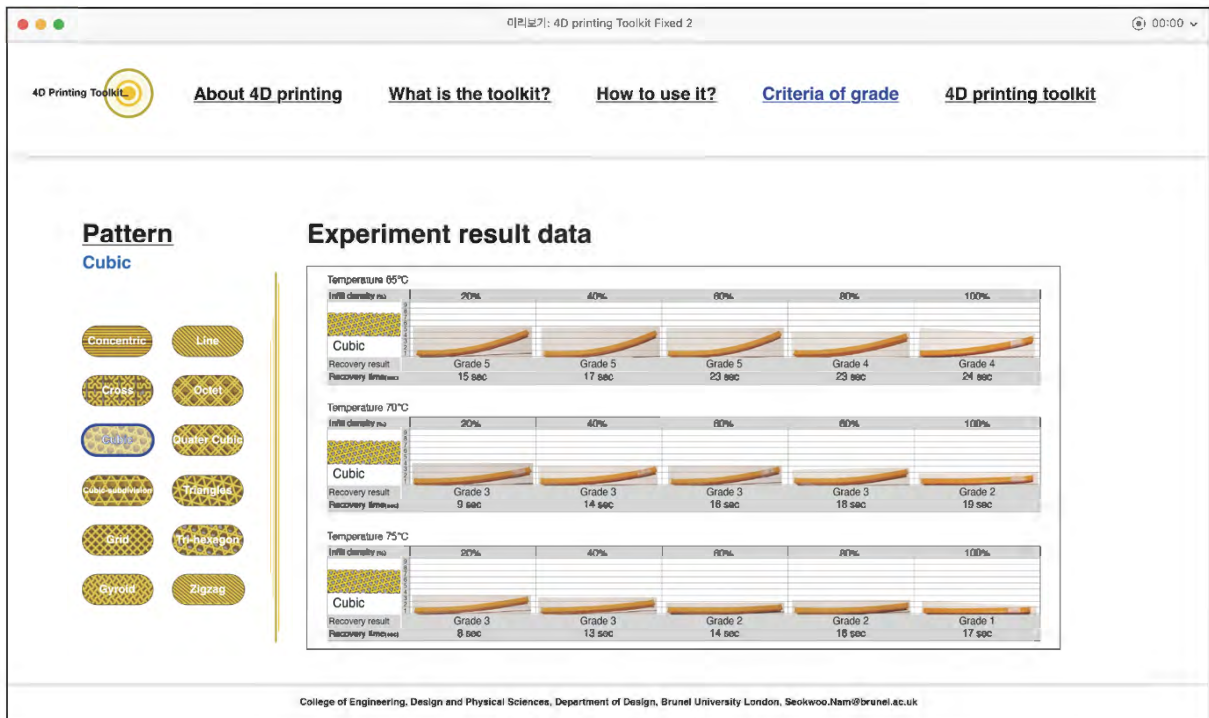
Information on the experiment result data (main page)



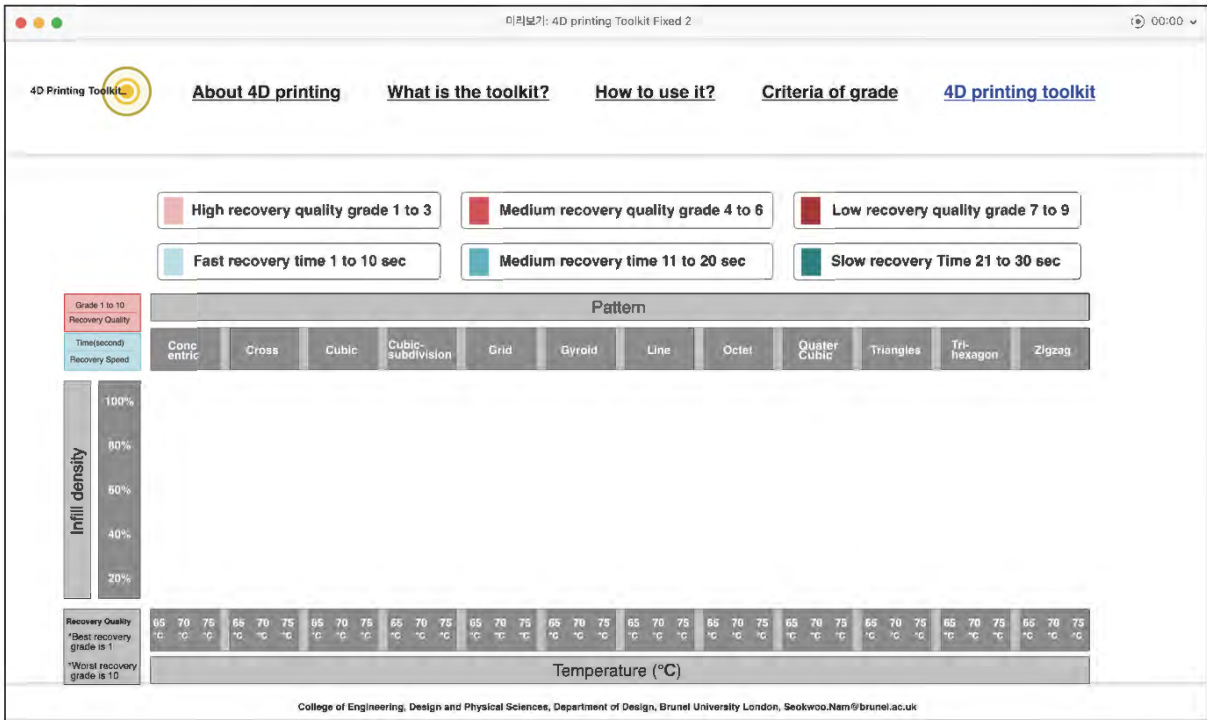
Information on the experiment result data 1



Information on the experiment result data 2



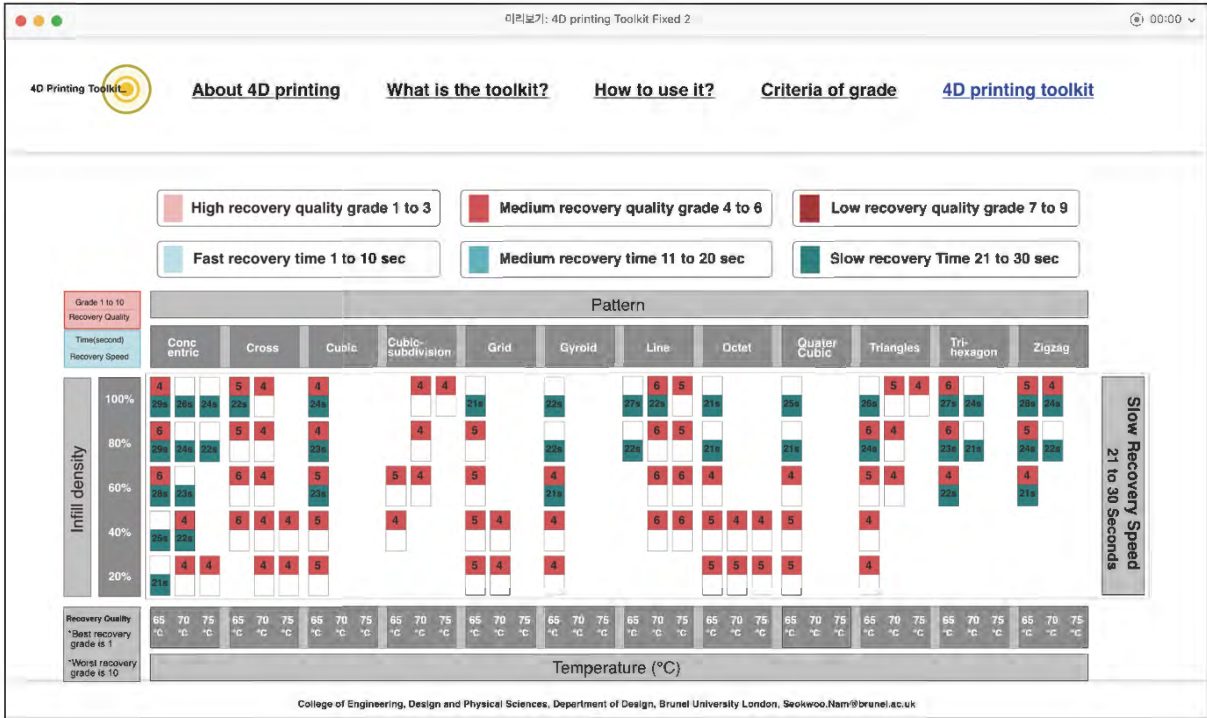
Information on the experiment result data 3



4DP toolkit frame



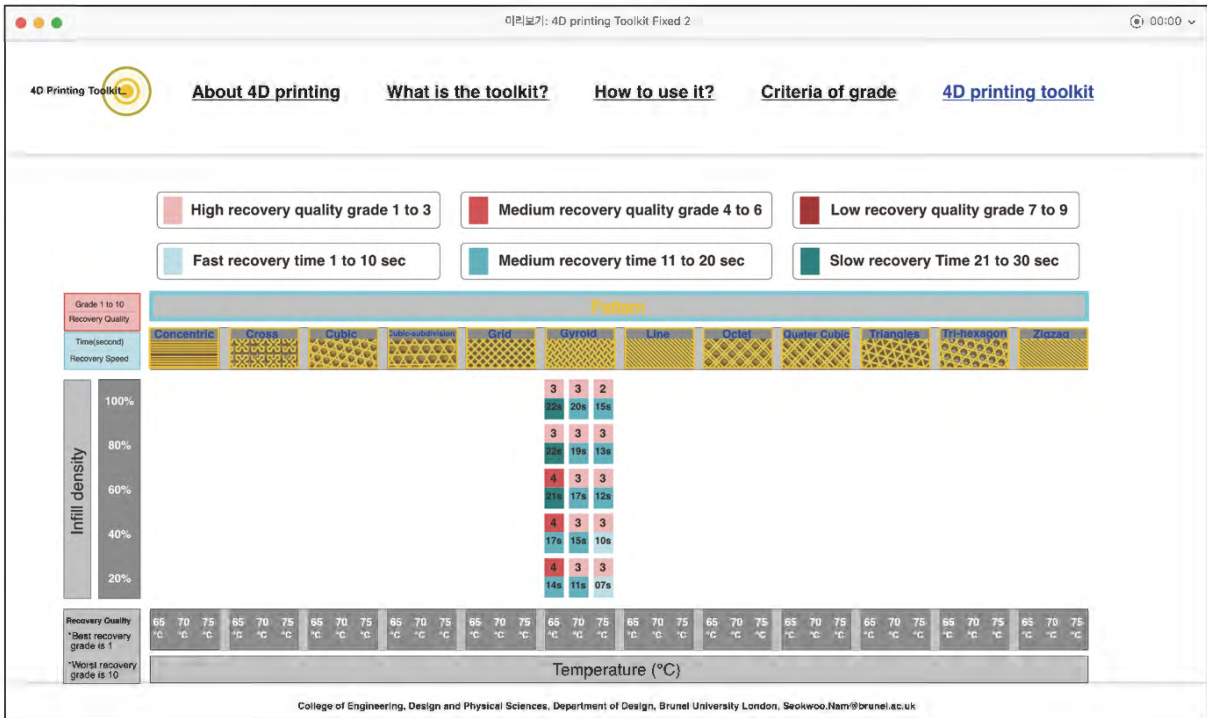
4DP toolkit showing all of the SME results



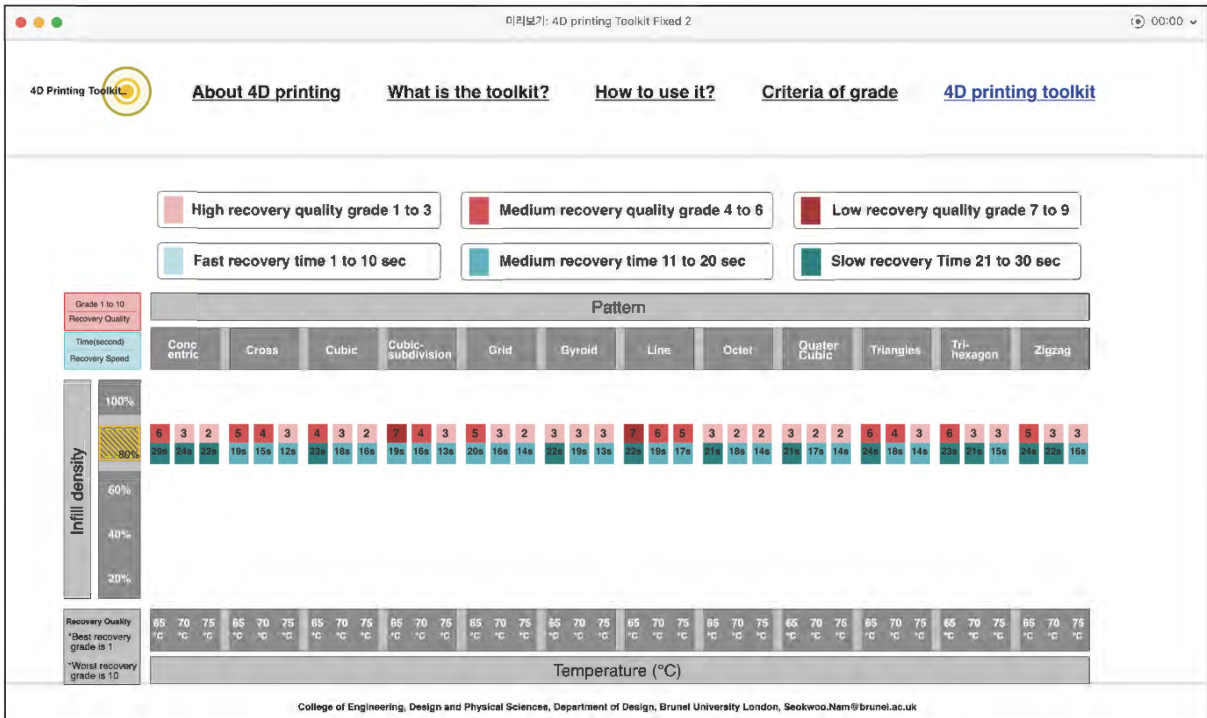
Use of the 4DP toolkit to select the parameter results



Use of the 4DP toolkit to select the temperature results



Use of the 4DP toolkit to select the pattern results



Use of the 4DP toolkit to select the infill density results

Appendix IV. List of Publications

Journal papers

Nam, S. and Pei, E. (2019). 'A taxonomy of shape-changing behavior for 4D printed parts using shape-memory polymers', *Progress in Additive Manufacturing*, 4 (2), pp. 167–184.
<https://doi.org/10.1007/s40964-019-00079-5>.

Pei, E., Loh, G.H. and Nam, S. (2020). 'Concepts and Terminologies in 4D Printing', *Appl. Sci.* 10 (13), p. 4443. <https://doi.org/10.3390/app10134443>.

Nam, S. and Pei, E. (2020). 'The Influence of Shape Changing Behaviors from 4D printing through Material Extrusion Print Patterns and Infill Densities', *Materials*, 13 (17), p. 3754.
<https://doi.org/10.3390/ma13173754>.

Conference papers

Pei E., Loh G.H., Nam S.W. and Azhar E.F. (2019). 'Programming 4D Printed Parts Through Shape-Memory Polymers and Computer-Aided-Design', In: Almeida H., Vasco J. (eds). ProDPM 2019 Conference. https://doi.org/10.1007/978-3-030-29041-2_19.

Conferences

2019 Rapid Design Prototyping and Manufacturing Conference

2019 Progress in Digital and Physical Manufacturing Proceedings of ProDPM'19

2021 ONLINE 4D printing & MetaMaterials Conference

2021 EPSRC DfAM workshop

2021 PRES2021 Conference

Symposiums

2019 Design Doctoral Symposium & Additive Manufacturing

2020 Design Doctoral Symposium & Additive Manufacturing

Teaching experiences (Guest lecturer)

Senior Lecturer & Programme Leader at Bournemouth University

Series of guest lectures for Product Design Futures